Vinicius Queiroz Araújo

Diversidade, isolamento e função fisiológica dos celomócitos de Echinodermata: utilização de equinóides como modelo

São Paulo
2020

Vinicius Queiroz Araújo

Diversidade, isolamento e função fisiológica dos celomócitos de Echinodermata: utilização de equinóides como modelo.

Diversity, isolation and physiological function of Echinodermata coelomocytes: use of echinoids as model organisms

Tese apresentada ao Instituto de Biociências da Universidade de São Paulo, para a obtenção de Título de Doutor em Ciências, na Área de Fisiologia Geral.

Orientador: Prof. Dr. Márcio Reis Custódio

São Paulo
2020

FICHA CATALOGRÁFICA

Queiroz, Vinicius
Diversidade, isolamento e função fisiológica dos celomócitos de Echinodermata: utilização de equinoides como modelo. / Vinicius Queiroz; Orientador Márcio reis Custódio. -- São Paulo, 2020
177 páginas.

Tese (Doutorado) – Instituto de Biociências da Universidade de São Paulo, Departamento de Fisiologia.

1. Celomócitos 2. Echinoidea 3. Função fisiológica. Instituto de Biociências da Universidade de São Paulo. Departamento de Fisiologia Geral.

Comissão Julgadora:

_____

Prof(a). Dr(a)

_____

Prof(a). Dr(a).

_____

Prof(a). Dr(a).

_____

Prof. Dr. Márcio Reis Custódio

Orientador

“Aos meus pais, Djalma e Marinlava, e a Licia Sales, minha companheira em todos os momentos... fossem eles bons ou ruins”

“O acaso só favorece os espíritos predispostos.”

(Loius Pasteur)

Um cavalheiro deveria saber um pouco de zoologia dos invertebrados, assim como ele deve conhecer algo sobre pintura e música e sobre as ervas do seu jardim

(adaptado de Martin Well, Lower invertebrates, 1968)

Agradecimentos

Primeiramente agradeço a Deus, por me manter vivo, com saúde e força para que fizesse o que sempre gostei. Agradeço também a minha mãe Yemanjá e ao Dr. Zé Pilintra, por me concederem perfeitos dias de coleta, ótimas condições de maré (mesmo quando não parecia que o seria) e fizeram as coisas darem certo quando tudo parecia que iria dar errado.

Ao meu orientador Prof. Márcio Reis Custódio, por todo o apoio, paciência, conversas e muitos ensinamentos. Agradeço também pelas várias perguntas singulares, e inusitadas, que desde o mestrado me fizeram estar mais atentos para outras possibilidades não "equinodérmicas". Agradeço também pela disponibilidade do CEBIMÁRCIO, sempre disponível para as coletas e procedimentos de campo!

Aos meus pais, Djalma Fernandes Araújo e Marinalva Queiroz Araújo, pelo apoio, incentivo e pelas palavras amigas e reconfortantes na hora do desespero. Agradeço também a minha noiva Licia Sales, que sempre me apoiou, entendeu e não me deixou abater, mesmo nas horas que isso parecia inevitável. Agradeço tudo que vc tem feito por mim. MUITO OBRIGADO.

Ao Vagner Alberto, que sempre me socorreu quando precisei de ajuda com os reagentes ou aparelhos, e com os seus famosos "ajustes técnicos" que sempre salvam o dia de pós-graduando. Agradeço também pelas conversas, que sempre me alegravam quando as coisas não iam tão bem.

Aos colegas de laboratório, que sempre tornaram os meus "dias de bancada" menos sofridos, e os dias de coleta mais alegres e divertidos. Sem vcs o toda a caminhada teria sido muito mais difícil.

Aos Profs. Dr. Vincenzo Arizza e Dra. Mirella Vazzana, da Universidade de Palermo (Itália), com sua hospitalidade e muito boa recepção, que me me ajudaram com todas as dificuldades e me fizeram sentir mais "em casa", mesmo estando numa terra estranha.

Ao Professores Dr. Alberto Ribeiro, Dra. Renata Guimarães, Dr. Álvaro Migoto, Dr. Federico Bronw e Dr. José Eduardo Marian, pela disponibilidade de sua infraestrutura e/ou sugestões de ótima qualidade.

Aos técnicos Waldir Caldeira, Márcio Cruz, Sheilla Shumidt (LME - IB-USP) pelo uso dos equipamentos e apoio com a microscopia eletrônica, parte extremamente importante do meu trabalho.

Agradeço a FAPESP pela conceção da bolsa de doutorado e de BEPE, sem as quais grande parte deste trabalho não teria sido realizado.

Aos funcionários do Cebimar, Instituto de Biociências e do Departamento de Fisiologia, sem eles muitas coisas não existitiriam.

Enfim, agradeço a todos que torceram por mim, mesmo sem eu saber, e àqueles que porventura não tenham sido aqui mencionados.

RESUMO GERAL

Para os vertebrados, o sistema circulatório pode ser visto como um sistema integrador. Entre os papéis desempenhados diretamente por ele, através do sangue e seus componentes, um dos mais importantes é a identificação de partículas e/ou substâncias estranhas. Nesse contexto, as células sanguíneas (especificamente os leucócitos) são responsáveis por cumprir essa missão. Nos invertebrados, dentro de suas restrições, o sistema circulatório também desempenha funções semelhantes realizadas por suas células circulantes. Dependendo do grupo, essas células são denominadas hemócitos de coelomócitos. Para os equinodermos, os celomócitos (as células livre circulantes na cavidade celelômica) estão envolvidas na maioria das reações imunes, sendo os principais responsáveis pela luta contra corpos e substâncias estranhas. No entanto, diferentemente dos vertebrados, o nível de conhecimento sobre os efetores imunes dos equinodermos é consideravelmente menor. Mesmo para o Echinoidea – o grupo mais bem estudado em Echinodermata – os aspectos básicos ainda precisam ser mais detalhados. Perguntas básicas como a diversidade de células da classe Echinoidea, o número real de subpopulações de células em ouriços do mar e o papel fisiológico de algumas subpopulações (*e.g.* esferulócitos e células vibráteis), ainda permanecem sem respostas. Nesse contexto, este estudo tem como objetivo investigar a diversidade e a função fisiológica dos coelomócitos dos equinodermos, utilizando equinóides como organismos modelo. Cinco tipos principais de células foram encontrados, compreendendo 14 subpopulações, um número significativamente diferente do indicado na literatura geral. As células dos ouriços-do-mar de *Paracentrotus* foram estudadas, um dos modelos mais importantes na pesquisa de equinodermos (*i.e. P. lividus*), revelando novos tipos de células para as espécies do gênero. Além disso, fornecemos um modelo que explica a sequência de maturação dos esferulócitos de *Paracentrotus*. Ainda, uma caracterização detalhada das células vibráteis de *Eucidaris tribuloides* foi feita e à luz desses novos dados, uma discussão sobre a função desta célula é fornecida. Por meio de uma técnica recente de citometria de fluxo (citometria de fluxo por imagem - IFC), obtivemos pela primeira vez *gates* com subpopulações celômicas isoladas, e através de experimentos de infecção bcteriana, analisados pelo IFC, observamos o envolvimento de células vibráteis nas reações imunes. Por fim, elucidamos como os esferulócitos vermelhos liberam o equinocromo-A, um mecanismo completamente diferente do especulado na literatura, e relatamos um estudo de caso em que alterações

fisiológicas em um ouriço-do-mar pareciam ser causadas por um briozoário, durante uma associação simbiótica. Assim, os resultados obtidos neste estudo lançam luz sobre alguns aspectos cruciais da fisiologia e imunobiologia dos equinodermos, fornecendo os primeiros passos para a resolução destas questões.

Palavras Chave: Citometria de fluxo, degranulação, esferulócito vermelho, ouriço-do-mar, sistema imune.

ABSTRACT

To vertebrates, the circulatory system may be seen as an important system that integrates the organism. Among the roles performed directly by it, through the blood and its components, one of the most important ones is to patrol the body for foreign particles and/or substances. In this context, the blood cells (specifically the leukocytes), are responsible to accomplish this mission. In the invertebrates, within your restrictions, the circulatory system also performs similar functions accomplished by its circulating cells. Depending on the group, these cells have been named hemocytes of coelomocytes. To the echinoderms, the cells in their coelomic cavity (coelomocytes) are involved in most of the immune reactions, being the main effectors responsible to fight against foreign bodies and substances. However, differently from the vertebrates, the level of knowledge about the echinoderm immune effectors is considerably lower. Even to the Echinoidea – the best-studied group in Echinodermata – the basic aspects still needs further studies. Basic questions, such as the diversity of cells in the class Echinoidea, the real number of cell subpopulations in sea urchins, and the physiological role of the less studied cells (e.g. spherulocytes and vibratile cells) remain unsolved. In this context, this study aims to investigate the diversity and the physiological function of echinoderm coelomocytes, using echinoids as model organisms. We found five main cell types, comprising 14 subpopulations, a number significantly different from the pointed out in the general literature (three and four, respectively). The cells of *Paracentrotus* sea urchins were studied, one of the most important models in echinoderm research (*i.e. P. lividus*), revealing new cell types to these species. Additionally, we provided a model that explains the maturation sequence of the spherulocytes of *Paraaacentrotus*. Still, a detailed characterization of *Eucidaris tribuloides* vibratile cells' was made, and on the light of these new data, a discussion on the function of the vibratile cell is provided. Through an unusual flow cytometric technic (*i.e.* image flow cytometry - IFC), we obtained for the first time gates with isolated coelomocyte subpopulation, and through infection experiments analyzed by IFC, we observed the involvement of vibratile cells in immune reactions. Lastly, we elucidate how red spherulocytes release the echinochrome-A, which is a mechanism completely different from the speculated in the literature, and reported a study case where physiological alterations in a sea urchin seemed to be caused by a bryozoan during a symbiotic association. Thus, the results obtained in this study shed light on

some crucial aspects of echinoderm physiology and immunobiology, providing the first steps on these important questions.

Keywords: Degranulation, flow cytometry, immune system, red spherulocyte, sea urchin.

Introdução Geral

INTRODUÇÃO GERAL

Nos vertebrados, o sangue possui funções diversas, executadas por tipos celulares distintos e sobre os quais o nível de conhecimento é muito elevado, principalmente nos mamíferos. De maneira geral, as células do tecido sanguíneo dos vertebrados, tais como os trombócitos, os eritrócitos e os leucócitos são responsáveis pela execução de processos muito importantes na manutenção da homeostase, como, por exemplo, coagulação, transporte de gases e resposta imune, respectivamente (Snyder & Sheafor, 1999; Tavares-Dias & Oliveira, 2009; Zimmerman et al., 2010). Sabem-se detalhes sobre as características básicas, tais como morfologia (Azwai et al., 2007), ultraestrutura (Williams et al., 2009), mecanismos moleculares e funções fisiológicas (Falanga et al., 2000). Além disso, os órgãos ou tecidos de origem destas células (Palis, 2014) e seus processos de diferenciação e maturação (Yang et al., 2013) são bem definidos. Mesmo para os vertebrados mais basais, o estado do conhecimento é avançado (Old & Huveneers, 2006; Arikan & Çiçek, 2014) e isso pode ser constatado pelo fato de que até patologias apresentadas pelas células sanguíneas destes animais são conhecidas (Maciel et al., 2011; Sailasuta et al., 2011). Este cenário, no entanto, não é o mesmo para a maioria dos invertebrados.

Invertebrados também possuem células circulantes com características funcionais similares às encontradas nos vertebrados, embora recebendo nomes distintos devido às diferentes organizações corporais. Nos grupos mais basais, tais como Porifera, Cnidaria e Platyhelminthes, os quais não apresentam uma cavidade corporal preenchida por fluido, estas células são comumente denominadas de amebócitos, células intersticiais ou neoblastos (Frank et al., 2004). Nos mais derivados como os Mollusca, Arthropopda, ou Echinodermata, os quais possuem uma cavidade preenchida com fluido denominda de hemocele ou celoma, as células livre-circulantes são denominadas coletivamente de hemócitos e/ou celomócitos respectivamente (Tahseen, 2009).

Dentre os grupos que apresentam celoma, temos os Echinodermata. Este filo é composto por deuterostômios (Figura 1) exclusivamente marinhos, que apresentam como características distintivas um endoesqueleto de carbonato de cálcio na forma de calcita, um sistema vascular aquífero e uma conspícua simetria radial pentâmera quando adultos (Pawson, 2007). As 7000 espécies de equinodermos (Pawson, 2007) são agrupadas em cinco classes bem distintas (Crinoidea, Asteroidea, Ophiuroidea, Echinoidea e Holothuroidea), cujo relacionamento filogênético ainda encontra-se sob

debate (Pisani et al., 2012; Reich et al., 2015). Duas hipóteses são atualmente aceitas para explicar as relações dentro de Echinodermata (*i.e.* Asterozoa e Cryptosyringida), e o ponto contrastante reside no posicionamento da classe Ophiuroidea (Figura 2). Na hipótese Aterozoa, Ophiuroidea e Asteroidea formam um grupo monofilético (Asterozoa), que é grupo-irmão de Echinozoa (Echinoidea + Holothuroidea). Por outro lado, a segunda hypótese pontua que Ophiuroidea seria o grupo irmão de Echinozoa, formando o clado Cryptosyringida (Ophiuroidea + (Echinoidea + Holothuroidea) (Figura 2). Embora ambas as hipóteses sejam constatemente pontuadas, a hypótese Asterozoa vem ganhnado cada vez mais suporte (Telford et al., 2014; Reich et al., 2015).

Do ponto de vista fisiológico, os equinodermos são desprovidos de sistemas respiratórios e circulatórios especializados, como visto nos deuterostômios mais derivados (*e.g.* Vertebrata), contudo, o fluido celomático e seus componentes celulares (celomócitos) têm sido pontuados por desempenhar diversas das funções fisiológicas fundamentais, tais como nutrição e imunidade (Boolotian, 1966; Smith et al., 2010). Tradicionalmente, estes celomócitos são identificados por características morfológicas superficiais e divididos em seis categorias principais: fagócitos ou amebócitos, hemócitos, células cristal, células progenitoras, células vibráteis e esferulócitos (Chia & Xing, 1996). No entanto, estes tipos celulares não se distribuem igualmente entre os grupos internos de Echinodermata. Em Asteróides, por exemplo, fagócitos são constantemente pontuados como o principal (ou o único) tipo celular existente (Kaneshiro & Karp, 1980; Coteur et al., 2002), enquanto que em Holothuroidea, as seis grandes categorias são comumente descritas (Xing et al., 2008).

Para os Echinoidea, o grupo mais conhecido de equinodermos, quatro tipos celulares têm sido comumente mencionados: fagócitos, células vibráteis, e os esferulócitos vermelho e transparente (Smith et al., 2006; 2018). No entanto, estes tipos são característicos dos equinóides regulares (*i.e.* ouriços-do-mar), e alguns trabalhos chegam a pontuar que estes são os únicos tipos celulares presentes na classe Echinóidea (Karp & Cofaro, 1982; Cavey & Märkel, 1994). Contudo, embora equinoides regulares possam ser os equinoides mais conhecidos, echinóides irregulares (*i.e.* bolachas-do-mar e ouriços cordiformes) formam um grupo bem consistente e diverso denominado Irregularia (Figura 3), que contém uma maior diversidade de espécies que entre os ouriços regulares (Kroh & Mooi, 2019). Estudos abordando as células dos equinoides irregulares são escassos e restritos geralmente a descrição dos tipos celulares existentes

(Kawaguti & Yamasu, 1976), com pouquíssimos trabalhos abordando aspectos fisiológicos nestes animais (Bookhout & Greenburg, 1940).

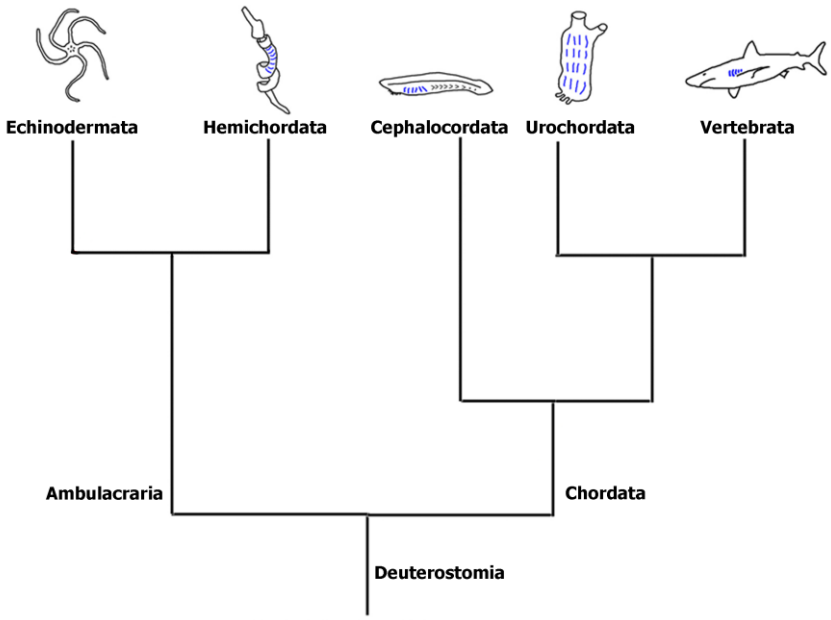

Figura 1 – Filogenia dos Deuterostomia, destacando a posição dos equinodermos e sua relação com os outros deuterostomados. Adaptado de Grahan & Richardson, 2012.

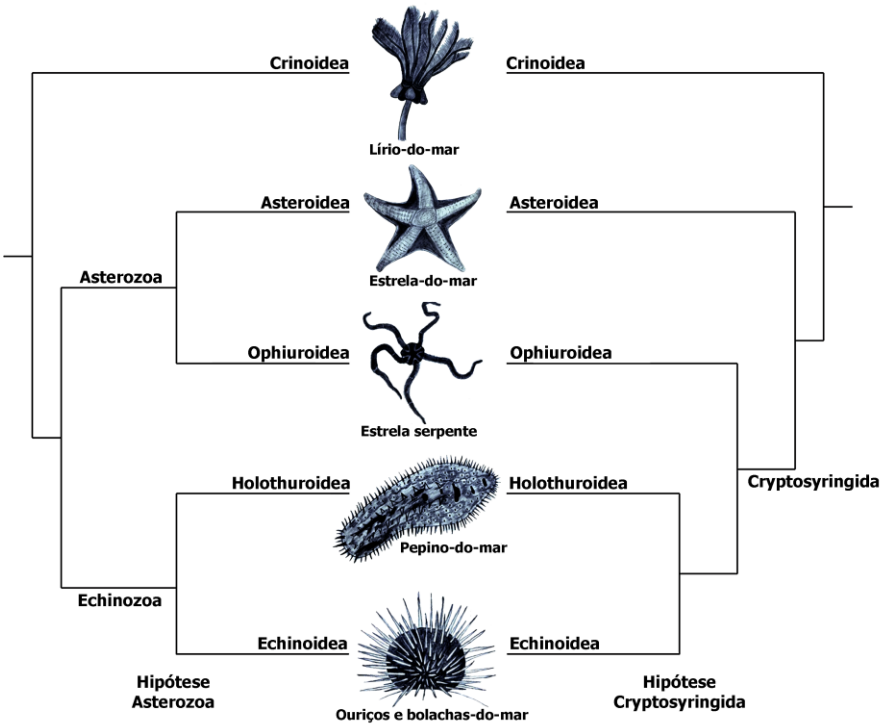

Figura 2 – Hipóteses concorrentes das relações filogenéticas entre os equinodermos existentes. Adaptado de Reich et al., 2015.

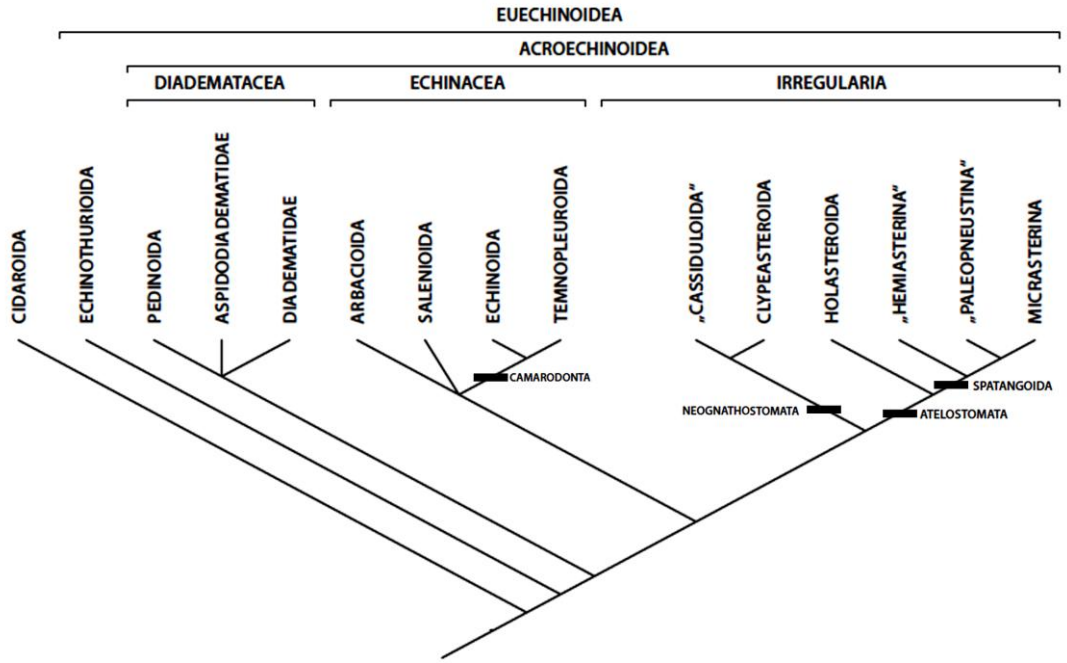

Figura 3 – Entendimento atual das relações filogenéticas dentro da classe Echinoidea. Adaptado de Ziegler et al., 2009.

Apesar do papel fundamental que os celomócitos desempenham na fisiologia dos Echinodermata, e consequentemente dos Echinoidea, e do alto nível de conhecimento em relação às células celômicas dos equinoides, estudos investigando as grandes questões envolvendo estas células ainda são necessários (Chia & Xing, 1996). Por exemplo, com relação aos tipos celulares presente na classe Echinoidea, é notório que a grande maioria dos dados provém de estudos com ouriços regulares (Smith et al., 2006; 2010; 2018). No entanto, exceto para os fagócitos, que têm sido bem estudados tanto em relação à quantidade de subpopulações quanto em relação às respectivas morfologias (Edds, 1993), existe uma carência de informação para os outros tipos. Para os esferulócitos, existem informações conflitantes sobre a quantidade real de tipos existentes, onde tem sido descrito que a quantidade pode variar entre duas a quatro (Chien et al., 1970; Vethamany & Fung, 1972). De fato, um trabalho recente fez uma caracterização morfológica detalhada dos esferulócitos de *Eucidaris tribuloides*, mostrando que, pelo menos para esta espécie, existem três subpopulações de esferulócitos (Queiroz & Custódio, 2015). Para a célula vibrátil, trabalhos mais detalhados ainda se fazem necessários.

Outra questão interessante pode ser vista em relação à natureza química das inclusões citoplasmáticas dos esferulócitos e da célula vibrátil. Dentre os esferulócitos, apenas o conteúdo de um tipo é relativamente bem conhecido: o *esferulócito vermelho*.

Este celomócito contém Equinocromo-A (Service & Wardlaw, 1984; Ageenko et al., 2011), uma naftoquinona que dá a cor avermelhada característica desta célula e é dita por possuir função antioxidante, antibacteriana e antifúngica, antitumoral ou como tendo participação em reações imunes (Koltsova et al., 1981; Ageenko et al., 2011). Para os outros esferulócitos e a célula vibrátil, as informações são mais gerais, frutos de análises citoquímicas (Liebman, 1950; Johnson, 1969b; Queiroz & Custódio, 2015). Observaram-se mucopolissacarídeos e proteínas respectivamente, no conteúdo das esférulas citoplasmáticas dos esferulócitos transparente e granular de *Euciddaris tribulóides* (Queiroz & Custódio, 2015). Para a célula vibrátil, sabe-se que as esférulas são preenchidas com glicosaminoglicanos (Johnson, 1969b).

Uma questão crucial no estudo dos celomócitos de Echinodermata, e que ainda parece estar longe de ser resolvida, é o isolamento/separação das frações celulares (Chia & Xing, 1996). Independente do objetivo do estudo, os trabalhos que abordam os celomócitos utilizam duas abordagens principais: uma suspensão de células contendo todas as subpopulações celulares (Johnsson, 1969a), ou uma suspensão enriquecida, contendo um tipo celular predominante (Arizza et al., 2007). Embora algumas frações possam ter um alto grau pureza (*e.g.*esferulócitos vermelhos – Arizza et al., 2007), as técnicas usualmente empregadas ainda não permitiram o isolamente completo dos tipos celulares (Chia & Xing, 1996). Mesmo, técnicas mais avançadas, como por exemplo, a citmoetria de fluxo, têm se mostrado pouco eficientes na resolução desta questão (McCaughey & Bodnar, 2012).

Para as funções fisiológicas dos celomócitos dos Echinodermata, o principal modelo de estudo tem sido os Echinoidea, com um alto nível de conhecimento para estes animais (Smith et al., 2018), se comparado com os outros grupos de equinodermos (Ramírez-Gómez & García-Arrarás, 2010). Sabe-se que os fagócitos são os principais efetores imunes, estando envolvidos em uma ampla variedade de funções, tais como fagocitose, regeneração, encapsulamento, rejeição de enxerto, dentre outras (Smith et al., 2006). Para os esferulócitos vermelho e transparente, sabe-se do seu ativo envolvimento com atividade bactericida e citotáxica, respectivamente (Arriza et al., 2007; Coates et al., 2018). Para a célula vibrátil, a função ainda continua sob debate, mas duas hipóteses são atualmente aceitas: envolvimento na movimentação do fluido celômico e/ou coagulação (Smith et al., 2010). Para o recén descrito esferulócito granular de *E. tribulóides*, não há dados de função.

Outro ponto de relevância acerca dos celomócitos de Echinodermata, e consequentemente dos Echinoidea, é em relação a onde estas células são formadas. A pergunta consiste especificamente em saber o local onde os celomócitos se originam, e existem duas hipóteses acerca deste aspecto (Matranga, 2005). A primeira propõe a existência de um órgão celomopoiético, que no caso dos Echinoidea seria o órgão axial, de onde as subpopulações celomócitos seriam originadas (Millott 1969; Bachmann & Goldschmid 1978). A segunda hipótese propõe a existência de uma célula multipotente livre no fluído celômico (*i.e.* célula progenitora) capaz de originar as demais subpopulações (Smith, 1981). Por fim, outra questão extremamente relacionada à origem das células, mas pouco abordada, é a existência de um processo de maturação para os celomócitos. Embora existam evidências de maturação, tanto a para células formadas em um possível órgão celomopoiético (Bachmann & Goldschmid, 1978), como para céluals originandas a partir de uma célula progenitora (Fontaine & Hall, 1981; Queiroz and Custódio, 2015), o assunto ainda necessita ser abordado adequadamente para rresposnder esta questão.

Isso mostra que mesmo para equinóides regulares, que são os principais modelos de estudo dentro dos Echinodermata, pontos chave ainda necessitam de elucidação. Neste sentido, este trabalho se dispôs a investigar alguns destes pontos básicos, que ainda permanecem em aberto. Dentre as questões abordadas aqui, tentamos responder as seguintes perguntas: Quantos tipos celulares ocorrem nos Echinoidea? Como se dá a sua distribuição entre os equinoides regulares e irregulares? Quais as funções fisiológicas dos esferulócitos e da célula vibrátil? Estas células cooperam durante um desafio imune?

OBJETIVOS

O objetivo geral deste trabalho é investigar a diversidasde e a função fisiológica dos celomócitos de Echinodermata, utilizando equinóides como modelo. Especificamente, este trabalho aborda as seguintes questões:

1 – Qual a diversidade celular na classe Echinoidea, e como estas células estão distribuídas entre equinoides regulares e irregulares?

2 – Quantos tipos celulares existem nos ouriços regulares?

3 – Qual a função fisiológica dos esferulócitos e da célula vibrátil?

4 – Qual a dinâmica dos celomócitos sob diferentes condições de estresse?

ORGANIZAÇÃO DA TESE

Além dos tópicos *Introdução Geral* e *Considerações Finais*, esta tese tem mais seis capítulos escritos em inglês sob a forma de manuscritos que estão sendo submetidos para publicação. Antes de cada um, se encontra uma página detalhando a motivação pela qual aquele capítulo foi escrito. A formatação de cada um dos textos está de acordo com a revista a qual se pretende submetê-los.

O capítulo 1, intitulado "Diversidade de celomócitos em Echinoidea" traz o manuscrito "Diversity of coelomic cells in Echinoidea: a morphological and comparative approach", que apresenta a caracterização dos celomócitos da classe Echinoidea, utilizando uma abordagem morfológica, baseado em observações diretas e levantamento bibliográfico. As células de sete espécies foram analisadas por meio da observação da morfologia de células vivas em suspensão e de preparações citoquímicas. Além disso, uma compilação de dados da literatura foi realizado, e o padrão de distribuição das células nos diferentes grupos de equinoides é comentada, sob uma perspectiva evolutiva.

O capítulo 2, intitulado "Célomócitos das espécies do gênero *Paracentrotus* (Echinoidea)" traz o artigo "Coelomic cells of *Paracentrotus* sea urchins (Echinodermata): a comparative approach". Este manuscrito caracteriza as células dos ouriços do gênero *Paracentrotus* (*P. gaimardi* e *P. lividus*), utilizando uma abordagem integrativa, sob uma perspectiva comparativa. Neste capítulo, os celomócitos são analisados de uma forma bem detalhada, por meio da utilização integrada de várias técnicas (*e.g.* células vivas, preparações citoquímicas e microscopia eletrônica de transmisão). Além disso, propõe-se um modelo que explica o processo de maturação dos esferulócitos.

O capítulo 3, intitulado "Células vibráteis de *Eucidaris tribuloides* (Echinoidea: Cidaroida)" trás o manuscrito "Ultrastructure and energy-dispersive X-ray spectroscopy profile of the vibratile cell of *Eucidaris tribuloides* (Echinoidea: Cidaroida)", que apresenta a caracterização da célula vibrátil da espécie *E. tribuloides*, também utilizando uma abordagem integrativa. Neste capítulo, a célula vibrátil é caracterizada de forma bastante detalhada, um possível processo de maturação é proposto, além da obtenção de dados químicos do conteúdo das esférulas desta célula. Por fim, as hipóteses de função da célula vibrátil são discutidas à luz destes novos dados.

O capítulo 4, intitulado "Isolamento e função fisiológica dos celomócitos de *Arbacia lixula* and *Lythechinus variegatus* (Echinoidea: Camarodonta)" traz o manuscrito "Comparative study of coelomocytes from *Arbacia lixula* and *Lythechinus variegatus*: cell characterization and evidences of physiological functions". Este manuscrito apresenta a caracterização dos celomócitos das espécies *A. lixula* e *L. variegatus*, utilizando citometria de fluxo por imagem. Com esta técnica, foi possível obter *gates* com populações isoladas, para ambas as espécies. Além disso, avaliou-se a possibilidade da utilização desta técnica na análise da dinâmica das populações de celomócitos durante uma infecção bacteriana.

O capítulo 5, intitulado "Mecanismo de liberação de equinocromo-A pelo esferulócito vermelho de *Paracentrotus lividus*" trás o manuscrito **"**To degranulate, or not to degranulate, that's the question: Mechanism of echinochrome-A release in *Paracentrotus lividus* red spherulocytes stimulated by lipopolysaccharide" descreve o mecanismo cellular e subcelulr de liberação do equinocromo-A pelo esferulócito vermelho. Além disso, observou-se que este o processo é dependente de sódio, mas não de potássio.

O capítulo 6, intitulado "O estado de saúde de ouriços-do-mar durante associações biológicas: um estudo de caso com *Echinometra lucunter* (Echinoidea)" traz o manuscrito "Taxonomical and biological aspects of the epibiotic association between *Schizoporella errata* (Bryozoa) and the sea urchin *Echinometra lucunter"*. Aqui um estudo de caso é apresentado, relatando um evento bastante incomum: um briozoário vivendo fixada a carapaça de um equinoide. Neste trabalho, a espécie *S errata* foi encontrada vivendo sobre a carapaça de *E. lucunter*. Além das informações de cunho taxonômico relativos a associação, o trabalho também traz informações fisiológicas, sugerindo que o ouriço pode ter sido negativamente afetado, durante o período em que o briozoário estava fixado.

Capítulo 1

Diversidade de celomócitos na classe Echinoidea

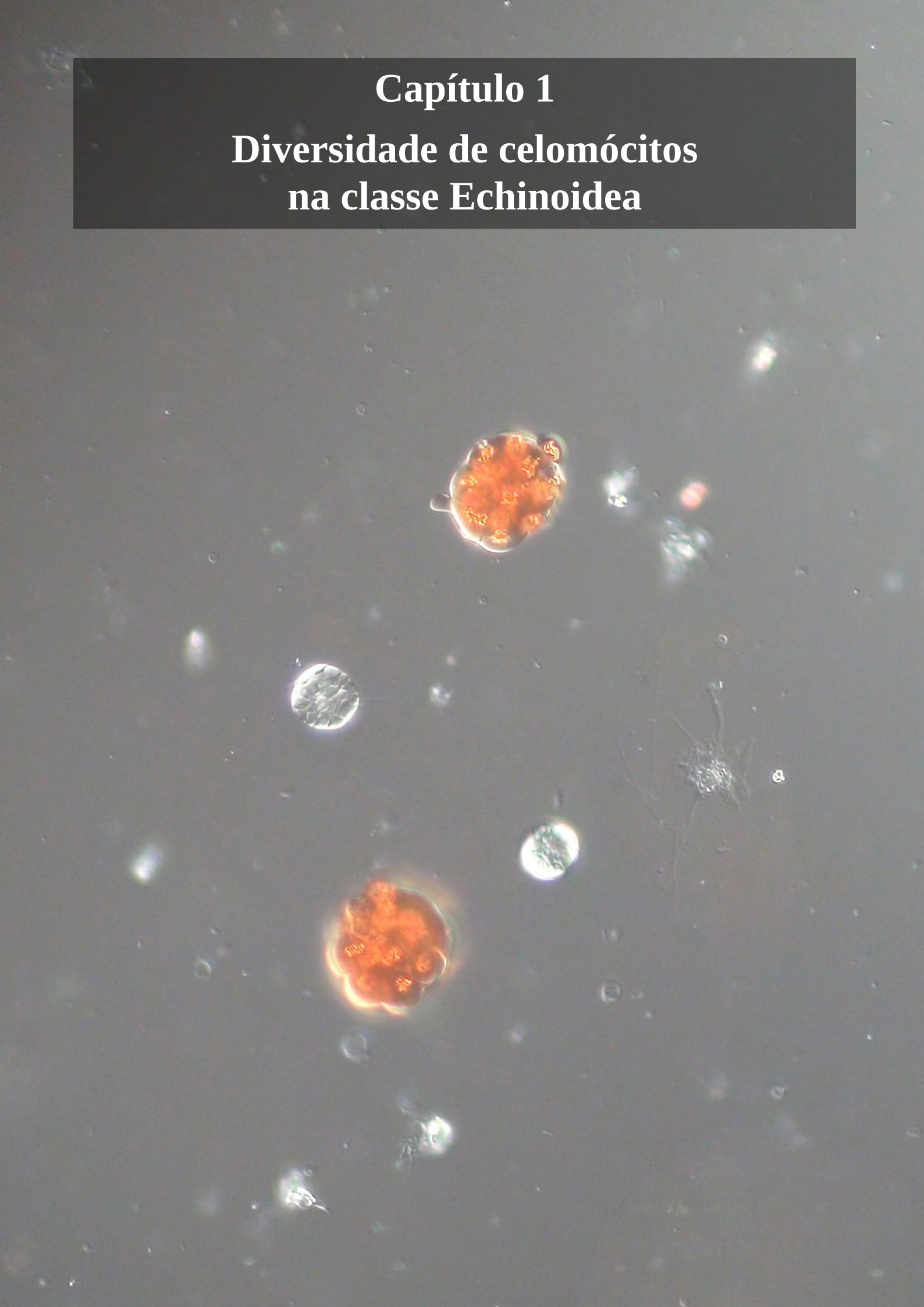

Justificativa

Dentre todos os grandes grupos de equinodermos, os Echinoidea têm sido o mais estudado com relação às células celômicas. É amplamente conhecido que quatro subpopulações celômicas são comumente encontradas nos equinóides: fagócitos, células vibráteis, esferulócitos vermelhos e os transparentes. No entanto, a esmagadora maioria dos trabalhos utiliza equinóides regulares (ouriços-do-mar) como modelo de estudo, extrapolando para toda a classe o padrão encontrado nestes organismos. Trabalhos que abordam as células celômicas dos ouriços irregulares (bolachas-do-mar e ouriços cordiformes) são pontuais e geralmente restritos à descrição dos tipos celulares existentes. Neste contexto, o presente capítulo aborda a diversidade de células presentes nos Echinoidea, considerando os grandes grupos detro desta classe. Uma abordagem comparativa é realizada, utilizando a morfologia das células vivas em suspensão e fixadas em preparações citoquímicas, além da compilação de dados bibliográficos. Todos os resultados são interpretados sob uma perspectiva evolutiva**.**

Diversity of coelomic cells in Echinoidea: a morphological and comparative approach

Vinicius Queiroz and Márcio R. Custódio

To be subbmited to the Journal of Morphology

Departamento de Fisiologia Geral, Instituto de Biociências and Núcleo de Apoio à Pesquisa

– Centro de Biologia Marinha (NAP–CEBIMar), Universidade de São Paulo, São Paulo, Brazil

Abstract: Echinoidea is by far the most known echinoderm group regarding the coelomic cells and their functions. Most knowledge about the morphology and physiological roles of the coelomocytes in Echinodermata has been based on echinoids. However, careful analyses show that these data deal with regular echinoids (sea urchins), leaving a gap regarding the irregular species, (*i.e.* Clypeasteroidea = sand dollars, and Spatangoidea = heart urchins). To this latter group, only descriptive studies are available and even the number of cell types is poorly known. Thus, the present study aims to investigate the diversity of cell types in Echinoidea under an evolutionary perspective, trying to answer two main questions: 1 – What are the most common coelomocytes populations in basal echinoids? 2 – Do basal and derived echinoids share the same coelomic populations? We find six coelomic subpopulations in basal echinoids (cidaroid sea urchins), which also are present in the most derived regular sea urchins. Regarding the irregular species, we find an interesting pattern: in general, spatangoid species showed the same basic cell types observed in regular species, while a very huge diversity of cell types, mainly sperulocytes (*viz*. eight subpopulations) were observed in Clypeasteroidea. Thus, our work shows that the diversity of cellular subpopulations is still underestimated and the generalization should be avoided. Still, the lack of data on irregular echinoids impairs the understanding of their physiology.

Keywords: Clypeasteroidea, evolution, immune cells, physiology,

Correspondence: V. Queiroz, Departamento de Fisiologia Geral, Instituto de Biociências, Universidade de São Paulo, Rua do Matão, nº 321, Cidade Universitária, São Paulo (SP), Brazil. CEP: 05508-090. Tel: +55113091-7522. Fax: +55113091-8095. Email: vinicius_ufba@yahoo.com.br

INTRODUCTION

In physiology, the evolution of biological structures may be described in terms of more or less specialized, instead basal and derived, and such specializations may be observed in all main physiological systems. A remarkable example may be seen in the evolution of the digestive system (Yonge, 1937). It is possible to see since animals with no digestive system, and a completely intracellular digestion (*e.g.* sponges – Godefroy et al., 2019); going through the emergence of a rudimentary digestive cavity (Cnidaria and Platyhelminthes - van Praet, 1985), and the beginning of a extracellular digestion (Cnidaria – Yonge, 1937); until the sophisticated digestive system of the mammals (Furness et al., 2015). In this latter, we can see a remarkable specialization of gut regions as well as accurate control of the system (Withers, 1992), making the digestive process more efficient.

The same reasoning can be applied to the evolution of blood cells, in which we can see evidence of specializations towards both pathways: increase of cell types and specificity of its functions. In the basal groups, such as Porifera, archeocytes are the main cell types moving in the inner layers (Hartenstein, 2006) and performing different functions such as phagocytosis and collagen synthesis, besides serving as stem cells (Simpson, 1984). Contrarily, a huge amount of cell types with very specific roles has been described to vertebrates (Rowley et al., 1988).

In Echinodermata, a group of deuterostomes that comprise marine invertebrates with a pentarradial symmetry during adult life (Pawson, 2007), the number of "blood cells" is relatively high. For these animals, in which the main circulatory media is called coelomic fluid, the free circulating cells are named coelomocytes (Chia, 1996). Echinoderms have been said to have six groups of coelomocytes: phagocytes, spherulocytes, vibratile cells, crystal cells, progenitor cells, and haemocytes. However, these coelomic populations are not present in all classes. All are relatively common in the major groups of Holothuroidea (Endean, 1958; Xing et al., 2008). For echinoids,

three main types have been described, while only phagocytes are commonly described to Asteroidea (Jangoux and Vanden Bossche, 1975; Coteur et al., 2002).

Echinoids comprise species with a spherical or flatten calcareous test covered with spines. These organisms have been commonly known as *regular* (sea urchins) and *irregular* (sand dollars and heart urchins), although only the irregular ones are monophyletic (Irregularia – Koch et al., 2018). Regarding the state of knowledge of their coelomocytes, Echinoidea is the taxon with the highest level of information (Smith et al., 2006; 2018). Phagocytes, vibratile cells, as well as two subpopulations of spherulocytes (*i.e.* the red and colorless spherulocytes), have been commonly stated as the main cell subpopulations (Smith et al., 2006). Phagocytes are involved with phagocytosis and encapsulation (Gross et al., 2000; Clow et al., 2004), while red and colorless spherulocytes perform antibacterial and cytotoxic activities (Arizza et al., 2007; Coates et al., 2018). Regarding vibratile cells, their physiological roles are not fully understood yet, but it has been proposed that they are involved in the agitation of coelomic fluid or clotting (Bertheussen and Seljelid, 1978).

Despite all knowledge obtained to Echinoids regarding the cell types and their specific functions, almost all data are based on the cells of derived regular echinoids (Smith et al., 2006; 2010; 2018). Still, data on cells of irregular echinoids have been punctual and restricted to descriptive works (Kawaguti and Yaimasu, 1954), while comparative studies under an evolutionary perspective are nonexistent. Thus, the aim of this work is to examine the diversity of coelomocytes from Echinoidea, under an evolutionary perspective. To do this, direct observations of coelomic populations from basal and derived species, combined with data from the literature, were used to address the diversity of cell types. In this context, we intend to answer two main questions: 1 – What are the most common coelomocytes populations in basal echinoids (*i.e.* Cidaroida sea urchins)? 2 – Do basal and derived echinoids share the same coelomic populations?

MATERIAL AND METHODS

Animals, coelomic fluid collection and comparative approach

The coelomocytes of seven regular (*Eucidaris tribuloides*, *Arbacia lixula*, *Lytechinus variegatus*, *Echinometra lucunter*, *and Paracentrotus gaimardi*) and irregular echinoids (*Encope emarginata* and *Clypeaster subdepressus*) were analyzed.

Three to five individuals of each species were collected in the São Sebastião Channel (Brazil) and maintained at 23 °C in marine aquaria at the Instituto de Biociências – Universidade de São Paulo (IB-USP) or at the Centro de Biologia Marinha da Universidade de São Paulo (CEBIMAR).

The coelomic fluid of all specimens was collected by inserting a syringe needle preloaded with 1.5 ml of isosmotic anticoagulant solution (20 mM ethylenediamine tetraacetic acid (EDTA), sodium chloride 460 mM, sodium sulfate 7 mM, potassium chloride 10 mM, 4-(2-hydroxyethyl)-1-piperazineethanesulfonic acid (HEPES) 10 mM, pH 8.2; Dunham and Weissman, 1986) into the peristomial membrane. An equal volume of coelomic fluid was collected, and density was adjusted to 10^6 cells/mL using a Neubauer chamber and anticoagulant solution. After this, the cells were processed following specific protocols described below.

Due to its basal phylogenetic position among echinoids (Lessios et al., 1999), we decided to use the cidaroid sea urchin *E. tribuloides* as the main model in our direct observations. The cells of this basal species were carefully studied using an integrative approach, consisting of live cells in suspension, cytological preparations through cytospin slides as well as scanning and transmission electron microscopy. For the remaining species, only live cells and cytological preparations were considered.

Morphological analyses

Cell types were determined based on morphological parameters, such as the overall shape, and features of the nucleus and cytoplasm inclusions. This information was compared with the main descriptions in the literature (*e.g.* Liebman 1950; Holland et al. 1965; Johnson 1969b; Queiroz and Custódio, 2015).

For living cells, drops of a solution containing cells in suspension were placed in glass slides immediately after being collected and covered with a coverslip. The cells were photographed using a digital imaging system (Leica). Cytological preparations were done using a cytocentrifuge (FANEN 248 - 80 μL per spot, 80 × g/5 min) to attach freshly collected cells to a microscope slide. After, the slides were fixed for 45 min in formaldehyde sublimate and stained with toluidine blue (TB) or Mallory's trichrome (MT) (Martoja & Martoja 1967; Behmer et al. 1976).

Ultrastructural details were obtained using scanning and transmission electron microscopy. For scanning electron microscopy (SEM), cells were cytospun on round coverslips (10 mm) as described above, and washed once in Mili-Q water for 20 minutes. Afterward, the coverslips were dried in a laminar flow hood at room temperature, dehydrated under vacuum (6-12 h) and then stored at room temperature in an enclosed container containing silica gel. Finally, the coverslips were attached on stubs, sputter-coated with a 40-60 nm thick layer of gold and photographed in a scanning electron microscope (Sigma VP, Zeiss). For transmission electron microscopy (TEM), cells were directly fixed in 2.5% glutaraldehyde in natural filtered (0.22 µm) seawater by 4 h and prepared following Taupin's (2008) method. Briefly, the coelomocytes were embedded in agar 2.5%, centrifuged for 5 min (800 rpm) and postfixed in osmium tetroxide (1%) with cacodylate buffer at pH 7.4 for 2 h at 4°C. The coelomocytes were then dehydrated in a graded ethanol series (50, 70, 90 e 100%) and embedded in resin (Embed-812, Electron Microscopy Science). Ultrathin sections were stained with uranyl acetate and lead citrate (30 and 5 min, respectively) and examined under a Zeiss EM900 electron microscope.

Literature survey

Lastly, we did an extensive literature survey about the diversity of coelomocytes in Echinoidea the most common cell types found in these animals, how many species were already analyzed and compared with our results from direct observations. The bibliographic survey consisted of published literature that directly or indirectly dealt with coelomocytes. However, the main requirement to consider a specific publication was that these studies should obligatorily describe, illustrate or at least mention all or most cell types, found in the species analyzed. Studies using inaccurate identifications such as "coelomocytes" or "amoebocytes", which do not provide a description of the cell types were not considered. In this sense, older literature about Echinoidea was used (*e.g.* Geddes, 1880; Kindred, 1924; Boolotian, 1962), as well as recent studies dealing with physiological/immune aspects that mentioned the cell types found (*e.g.* Jellet et al., 1988; Borges et al., 2002). Based on this, we provide a list with all species already analyzed and their coelomic populations, as well as a description of the main coelomocytes observed in Echinoidea. Here, data from literature and direct observations are considered together.

RESULTS

Coelomocytes of Eucidaris tribuloides

For this basal species, four main categories of coelomocytes were observed in all techniques employed (Fig. 1): phagocytes, spherulocytes, vibratile and progenitor cells. For phagocytes, two different types were observed: filopodial and petaloid, as well as three spherulocyte subpopulations: red, colorless and granular.

Phagocytes – Live cells in suspension presented two morphologies: petaloid and filopodial. Both showed a large cell body, with large round cytoplasmic expansions in the first (Fig. 1A), and long filiform cytoplasmic processes in the second. After 10 minutes resting on microscopic slides, most petaloid and filopodial forms disappear and three different morphologies may be seen, named: discoidal and polygonal cells and small phagocytes (not shown). In cytological preparations, the most common morphology was a cell with a very flatten and vacuolated cytoplasm, a large nucleus and no specific affinity to TB or MT (Fig. 1G and M). Petaloid forms were also observed, however they were scarce in cytological preparations. In TEM preparations, phagocytes showed a large central to subcentral nucleus, and one round to oval cytoplasm. The latter is highly vacuolated and sometimes filled with inclusions from phagocytized material. It was common to see many vacuoles/cytoplasm projections next to the cytoplasmic membrane (Fig. 1S). Scanning electron microscopy showed cells with a large and thicker nucleus, surrounded by a flattening vacuolized cytoplasm and a pronounced nucleus (Fig. 1Y).

Vibratile cells: Live cells are unusual coelomocytes, with a round spherulous cell body, nucleus generally central and a long flagellum by which the cell moves (Fig. 1B). Differently from other cell types, vibratile cells do not show amoeboid movements. In cytological preparations vibratile cells show a very flatten cytoplasm, with a central to subcentral nucleus and large round cytoplasmic spherules that stain purple with TB, indicating ß-metachromasia (Fig. 1H, 1N, and 1N *inset*). In TEM preparations, vibratile cells showed a round to oval shape, large cytoplasmic spherules filled with a sparse material and a large central nucleus (Fig. 1T). SEM analyses showed a very flatten cell with a very spread cytoplasm, in which it is possible to discern the spherules' outline, and a notable central to subcentral nucleus. The flagellum is remarkable, sometimes can be absent (Fig. 1Z).

Progenitor cells – This cell type was scarce in the collected coelomic fluid. In live suspensions, progenitor cells are small and can be easily confused with debris in freshly collected samples (Fig. 1C). After five to ten minutes on the slides, these cells spread and it is possible to see the large and central nucleus surrounded by a very thin layer of cytoplasm (Fig. 1I and O). In TEM analysis, the very large nucleus and its nuclear membrane are remarkable, as well as its condensed chromatin. No visible nucleolus was present. In the cytoplasm, a few scattered mitochondria can be seen (Fig. 1U). In SEM preparations, progenitor cells seem very flat, with a large nucleus surrounded by a very thin layer of cytoplasm (Fig. 1AA).

Spherulocytes – Three subpopulations of spherulocytes were found in *E. tribuloides*: red colorless and granular spherulocytes. Live red and granular spherulocytes are small cells with small homogeneous spherules, with a red content in the first and a colorless one in the second (Fig. 1D and F). On the other hand, colorless spherulocytes have large and heterogeneous spherules (Fig. 1E). In cytochemical preparations, red spherulocytes shows central to subcentral nucleus and small homogeneous spherules, with a brown color when stained with MT (Fig. 1J) or dark blue in TB slides (Fig. 1P). In colorless spherulocytes, the nucleus is usually small and peripheral, and the large heterogeneous spherules stain light blue with MT, or it blue with TB (Fig. 1K and Q). In the center of the spherules, it is possible to see a darker mass. Granular spherulocytes show a remarkable large nucleus and round cytoplasmic spherules that stain pinkish with MT and bluish-gray with TB (Fig. 1L and R).

Electron microscopy analyses (TEM and SEM) showed conspicuous differences among the spherulocytes (Fig. 1V-X and AB-AD). Red spherulocytes showed a large nucleus, with a cytoplasm filled with spherules of variable sizes, bearing a slight electron-dense material (Fig. 1V). TEM analyses show a cell with small homogeneous spherules (Fig. 1A and B). Colorless spherulocytes have a small peripheral nucleus and spherules with variable sizes. The periphery of the spherules seems to be empty, but there is an electron-dense material in the center, corresponding to the dark mass observed in the cytochemical preparations (Fig. 1W). In SEM analyses, the spherules are heterogeneous, as observed in live cells (Fig. 1AC). Granular spherulocytes show large nucleus In TEM, and large round vacuoles, filled with an electron-dense material (Fig. 1X). Cells in SEM preparations show larger spherules, with more homogeneous sizes (Fig. 1AD).

Coelomocytes of regular echinoids

The same coelomocyte subpopulations observed in *E. tribuloides* were also observed in all derived regular sea urchin species analyzed directly (*A. lixula*, *L. variegatus*, *E. lucunter, and P. gaimardi*). Phagocytes, vibratile cells, red, colorless and granular spherulocytes were the most common cell types and were observed in live suspensions (Fig. 2), and in cytochemical preparations (Fig. 3). Progenitor cells were also observed, mainly in live suspensions, but they were very rare. This fact hindered a correct characterization of this cell population in the derived regular sea urchins. The coelomic populations observed in these derived sea urchins were quite similar to that described to *E. tribuloides*, in both morphological and cytochemical features.

Coelomocytes of irregular echinoids

For the two irregular echinoids analyzed, there were consistent differences regarding the cell types observed. The differences were among both regular and irregular species, as well as between the irregular species themselves. For *C. subdepressus*, phagocytes, vibratile cells as well as yellowish-green, iridescent and bluish-green spherulocytes were found, while phagocytes, reddish vesicular, red, colorless and brown spherulocytes were the main types in *E. emarginata* (Fig. 4). Phagocytes and vibratile cells from *C. subdepressus* as well as phagocytes, red and colorless spherulocytes from *E. emarginata* were morphologically and cytochemically similar to coelomocytes observed in *E. tribuloides* and other regular species. On the other hand, the yellowish-green, iridescent and bluish-green spherulocytes from *C. subdepressus* and the brow and the reddish vesicular spherulocytes of *E. emarginata* were completely different and are characterized bellow.

Yellowish-green spherulocyte – Live cells are filled with homogeneous spherules ranging from olive green to golden-brownish (Fig. 4C). In cytochemical preparations, the nucleus is usually peripheral and it is common to find cells with brownish color in MT and bluish color in TB (Fig. 4H and M), similar to the red spherulocyte.

Iridescent spherulocyte – Live cells show large, lightly heterogeneous orange-reddish iridescent spherules and a peripheral nucleus (Fig. 4D). In cytochemical preparations, the heterogeneous spherules are more visible and stain bluish with MT, and blue with TB (Fig. 4I and N). Stained cells are very similar to colorless spherulocytes.

Bluish-green spherulocytes – Live cells show homogeneous bluish-green spherules and a subcentral to peripheral nucleus (Fig. 4E). Stained cells show homogeneous pink-orange spherules in MT preparations, while cells stained with TB show a grayish-blue coloration. (Fig. 4J and O). These cells were cytochemically similar to granular spherulocytes.

Large spherical cells – Live cells are large coelomocytes with a remarkable vacuole filled with reddish content, few small spherules, and a peripheral nucleus. However, in individuals kept longer times in aquaria, this cell becomes bright red, vacuolated and with large granules inside the vacuoles (Fig. 4Q). In cytochemical preparations, the reddish vesicular spherulocyte shows a large vacuolated cytoplasm, apparently empty, and with dark blue granules in TB and brownish in MT (Fig. 4V and AA). The characteristics of live and stained cells suggest that this subpopulation may contain echinochrome.

Brown spherulocyte – Live cells are very similar to red spherulocytes, having small homogeneous vacuoles, but with brown coloration and elongated shape (Fig. 4T). In MT preparations, brown spherulocytes showed brown spherules with an elongated profile (Fig. 4Y). In TB slides, these cells were not found. Cytochemical features also suggest that this cell may contain some pigment similar to echinochrome.

Coelomocytes in Echinoidea – Literature survey

Altogether, data from 55 echinoids, belonging to six orders and 19 families were obtained (Table 1), based on a literature survey and direct observations. Specifically, 40 regular sea urchins, nine sand dollars and six heart urchins were considered in this analysis. The literature survey showed us that more than 20 different cell types were already recorded in Echinoidea. However, based on descriptions and pictures of the previously studied coelomocytes, and the features of live cells found in the specimens directly analyzed, we observed overlapping of cell types. Thus, we are considering only 14 different subpopulations (Fig. 5), which were grouped in the five main cell types:

Phagocytes – We defined phagocytes as a heterogeneous group, composed of cells with a translucent cytoplasm, which have large cytoplasmic expansions, a large and visible nucleus as well as a cytoplasm without spherules. In this context, three different

subpopulations were observed. *Petaloid phagocytes* (Fig. 5A): cells with a central to subcentral nucleus, large cell body, and huge bladder-like cytoplasmic expansions; *Filopodial phagocytes* (Fig. 5B): cells with a central to subcentral nucleus, a large cell body, and elongated branched pseudopodia; *Large vesicular cells* (Fig. 5C): large cells composed by a huge bladder-like inclusion with very few or without very small vacuoles and a peripherical nucleus.

Fusiform cells (Fig. 5D) - Small but elongated cells with a usually central body, a remarkable nucleus and thin projections in opposite directions;

Progenitor cells (Fig. 5E) – Small cells bearing a very large nucleus in relation to the tiny cytoplasm surrounding it.

Vibratile cells (Fig. 5F) – Small spherule-filled round cell, with a central to subcentral nucleus. The cytoplasm is crowded with small homogeneously colorless spherules. The flagellum is the most remarkable feature of this cell, which is able to swim.

Spherulocytes – Spherulocytes or spherule cells comprise coelomocytes crowded with cytoplasmic vacuoles (spherules), and filled with the most diverse kind of substances. Eight distinct subpopulations were observed:

- *Colorless spherulocytes* (Fig. 5G): Usually oval to a little elongated cell with a subcentral nucleus and a spherule-filled cytoplasm crowded of heterogeneous-sized colorless spherules;

- *Red spherulocyte* (Fig. 5H): Round to elongated coelomocyte, with a subcentral nucleus and cytoplasm filled with remarkably homogeneous red spherules;

- *Granular spherulocyte* (Fig. 5I): Round cell, filled with large round homogeneous colorless spherules and a subcentral nucleus;

- *Brownish spherulocyte* (Fig. 5J): Round to oval cell, peripheral nucleus and a cytoplasm filled with brownish homogeneous spherules;

- *Yellowish-green spherulocyte* (Fig. 5K): Round to elongated cell, filled with yellowish-green spherules;

- *Iridescent spherulocyte* (Fig. 5L): Round to oval cell, with a colorless cytoplasm background and large heterogeneous greenish spherules;

- *Bluish-green spherulocyte* (Fig. 5M): Round to oval spherule-filled cell, with a peripheral nucleus, a bluish-green color that sometimes can be very light, and a so discrete cytoplasm compartmentalization that sometimes does not seem to have spherules**;**

- *Reddish vesicular spherulocyte* (Fig. 5N): cells filled with small granules/vacuoles with a visible Brownian movement and a light cytoplasm background. On some occasions, this cell can show a very bright red coloration and large vacuoles.

Quantitative data about the distribution of Echinoidea coelomocytes showed interesting patterns, and two main aspects deserve to be highlighted: (I) the frequency of specific cell types among echinoids, and (II) the frequency of specific cell types among the different groups of echinoids (*i. e.* sea urchins, sand dollars and heart urchin). At first glance, it is possible to see that all main cell types considered here (*i.e.* phagocytes, fusiform, progenitor and vibratile cells, as well as spherulocytes) are relatively common in echinoids (Table 1 and Fig. 6A). However, the distribution of the subpopulations was different. Phagocytes vibratile cells, red and colorless spherulocytes were the most common cell types, occurring in more the 50% of the analyzed species (Table 1 and Fig. 6A). Fusiform and progenitor cells occurred in 40 and 30% of the species, respectively, while the occurrence of the remaining spherulocyte subpopulations was very low, with a maximum of 21.82% in the yellow-green spherulocyte (Table 1 and Fig. 6A).

The distribution of cell types among the main groups of echinoids showed even more interesting patterns (Fig. 6B and 7). In general, regular echinoids and spatangoids present similar patterns of coelomic types, while some subpopulations were restricted to sand dollars (Fig. 7). Phagocytes were present in all echinoids (Table 1 and Fig. 6B and 7), while fusiform and progenitor cells showed low frequencies. To fusiform cells, the highest frequency of occurrence was observed in sea urchins (45%), followed by heart urchins (33.33%) and sand dollars (22.22%). On the other hand, the occurrence of progenitor cells was similar in all echinoid groups (Fig. 6B). Vibratile cells were common in sea urchins (77.50%) and heart urchins (83.33%), but not in sand dollars, being found only in *C. subdepressus* (11.11%). Spherulocytes showed the most interesting pattern: red and colorless spherulocytes were observed in 100% of sea urchins and heart urchins, but they were observed only 55.56 and 77.78%, respectively, of sand dollars (Fig. 6B). Granular spherulocytes were not observed in sand dollars, while yellowish-green spherulocytes were more frequent in irregular species, occurring

in only 10% of sea urchins analyzed (Fig. 6B). Lastly, brown, iridescent, bluish-green and reddish vesicular spherulocytes were restricted to irregular echinoids, and except to iridescent spherulocytes that were observed in *E. cordatum*, these subpopulations were specific of sand dollars (Fig. 6B).

DISCUSSION

Diversity and distribution of coelomic cells in Echinoidea

Echinoderms have been pointed out to have six main cell types in their coelomic fluid (Chia and Xing, 1996), but these types are not equally distributed among the main groups. Crinoidea and Ophiuroidea have been the less investigated (Endean, 1966), and due to the low number of studied species, general conclusions have been impaired (for review see Endean, 1966; Smith 1981). On the other hand, Asteroidea, Holothuroidea, and Echinoidea have been by far the most studied groups. Although nine coelomic subpopulations have already been recorded to sea stars (Kanungo, 1994), phagocytes seem to be the most common cell type, while other subpopulations seem to be sporadically found (Kanungo, 1994). In fact, sometimes phagocytes were the only cell type descried to Asteroids (Kaneshiro and Karp, 1980; Coteur et al., 2002). Holothuroidea is the order with the highest diversity of coelomic cells (Endean, 1966). For these echinoderms, phagocytes, spherulocytes, vibratile cells, crystal cells, progenitor cells, and haemocytes have been constantly recorded (Endean, 1958; Xing et al., 2008), and even new subpopulations were recently described (Ramírez-Gómez et al., 2010).

Echinoidea is the best-known group regarding the coelomic cells (Smith et al., 2006; 2010; 2018), and most of the available information is based on regular echinoids. Thereby, phagocytes, vibratile cells, as well as red and colorless spherulocytes were sometimes pointed out as the only coelomic subpopulations (Karp and Cofaro, 1982; Cavey and Märkel, 1994). However, our study shows two interesting points: (1) a remarkable diversity of cell types in the coelomic fluid of echinoids, and (2) an intriguing pattern of occurrence among echinoid groups.

Here, we found a high diversity of cell types in Echinoidea (*Cf.* Fig. 5). Altogether, 14 types of coelomocytes were considered in this study, most of them phagocytes and spherulocytes. These cell types comprise three and eight subpopulations

respectively, and this can be an indicator of their importance in echinoid physiology. Although some studies have argued that some coelomic populations may be involved with other physiological functions unrelated to immune response (*e.g.* nutrition or oxygen transport – Endean, 1966; Smith et al., 2010), there are few studies corroborating this idea. Actually, at least to sea urchins, all cell populations really seem to be engaged with the immune responses (Smith et al., 2018).

Phagocytes are one of the most widespread cell types in the coelomic fluid of echinoderms (Endean, 1966), and this is also true to Echinoidea. As seen in our results, phagocytes were observed in all echinoid analyzed (*Cf.* Table 1). Filopodial and petaloid phagocytes were the most common subpopulations in both directly analyzed species and in the literature survey. As described in the literature (Smith et al., 2006; 2010), and seen in the species directly analyzed, filopodial and petaloid always show high cell counts. These cells have been linked with many immune functions, such as encapsulation, clotting, graft rejection, opsonization and phagocytosis (Smith et al., 2006; 2010). Actually, filopodial and petaloid phagocytes seem to be the main effector cells in these processes. On the other hand, large vesicular cells were observed only in *Peronella japonica*, *Clypeaster japonicus*, and *C. subdepressus*. Although this cell type is here considered a phagocyte, this assumption was based on morphological criteria, and there is no evidence if it can be ontogenetically or functionally related to phagocytes.

Fusiform and progenitor cells were observed in all main groups of echinoids (*Cf.* Table 1), although they were not so widespread among them. They were observed in all species analyzed directly, from the basal *E. tribuloides* to the sand dollars. Still, data from literature showed that both cell types are found in the main families of regular sea urchins and in some spatangoid echinoids. Differently from Holothuroidea, in which fusiform and progenitor cells have been documented (Xing et al., 2008; Vazzana et al. 2015), and considered as a usual cell type in coelomic fluid (although fusiform cells show very low frequencies), both cell types seem not so common in echinoids. Despite found in all species directly analyzed, their frequency was low and, it was difficult to find fusiform and progenitor cells, as well as their observations, were sporadic. The low number may answer why these cells were scarcely reported in previous works. Regarding their functions, it is unanimous that progenitor may be a pluripotent cell in echinoderms (for review see Smith, 1981). There is no information about the

physiological function of fusiform cells in sea urchins; however, it is believed that in *Antedon rosacea* (Crinoidea), *Gorgonocephalus euneumis* (Ophiuroidea), *Caudina chilensis* and *Cucumaria plankii* (Holothuroidea), this cell may be progenitor cells undergoing maturation (Smith, 1981). Thus, it is possible that both cell types may represent usual populations, but their very low frequency may have hindered their observation in previous studies.

Vibratile cells are the most intriguing coelomic population in Echinodermata. Although already been found in Ophiuroidea and Holothuroidea, it seems to be typical of echinoids (Endean, 1966). In our study, vibratile cells were observed in most regular sea urchins, and heart urchins. On the other hand, in clypeasteroid echinoids, vibratile cells were observed only in *C. subdepressus*. The metachromatic reaction with TB enabled accurate identification of this cell type in cytological preparations. During our study, we observed that the movement of vibratile cells was impaired in samples obtained using the anticoagulant solution. This was probably due to the chelating effect of EDTA and makes difficult an accurate distinction between vibratile cells, colorless and granular spherulocytes. Additionally, the handling of coelomic fluid solution (vigorous agitation using pipets) may break the flagellum, making them more similar to colorless or granular spherulocytes. Thus, these two procedures may explain why this apparently widespread and characteristic coelomic population in Echinoidea was not found in the sea urchins previously studied (*Cf.* Table 1).

Our data reveal an interesting pattern about the distribution of vibratile cells, showing that it seems to be related to species possessing large coelomic cavities, and this may be related to its physiological function. There are two hypotheses dealing with the function of vibratile cells: coelomic fluid circulation or clotting. The first one advocates that the movement of the flagellum is able to move the coelomic fluid (Cuénot 1981), while according to the second one, vibratile cells may be involved with immune functions by promoting/cooperate in clotting reaction. The first hypothesis seems quite attractive, but two main points argue against it: cells able to move fluids need to be attached to any substrate (*e.g.* choanocytes from sponges or flame cells from Platyhelminthes – Leys and Eerkes-Medrano, 2006; Kieneke et al., 2008). Still, "*in hanging drops vibratile cells, though they jostle other cells during their constant movement, do not radically change the position of other cells nor cause major mixing of the fluid*" (Johnsson, 1969a). On the other hand, there is some evidence corroborating

its involvement during clotting events. Two studies did *in vivo* observations on *Strogylocentrotus* sea urchins (Johnsson, 1969a; Bertheussen and Seljelid, 1978), and they observed that coagulation started with a mucous substance secreted from vibratile cells. Additionally, a recent study based on experimental procedures (*Cf. chapter 3/4*) seems to corroborate the involvement of this coelomocyte in immune reactions.

Spherulocytes are by far the most diverse coelomic population in Echinoidea, comprising eight different subpopulations (*Cf.* Table 1 and Fig. 5). Red and colorless spherulocytes were the most widespread subpopulations in Echinoidea. They were present in all sea urchins and heart urchins and in more than half sand dollars (*Cf.* Fig. 6). On the other hand, granular spherulocytes were found only in sea urchins and heart urchins. These cells have very characteristics morphological features that enable their identification in any echinoid. Live red and granular spherulocytes have small homogeneous spherules with red coloration in red spherulocytes and colorless in granular ones. However, these cells display remarkable characteristics in stained preparations: Red spherulocytes shows a brown coloration, while the granular is reddish/pinkish color in MT preparations. On the other hand, live colorless spherulocytes have heterogeneous colorless spherules, which stain blue in MT preparations.

Live red and colorless spherulocytes were observed in all analyzed species (*Cf.* Table 1), but cytochemical features were observed only in those directly observed, and in few previous works (Liebman, 1950; Johnson, 1969b). Granular spherulocytes were properly described recently (Queiroz and Custódio, 2015), although some previous works have recorded cells with similar morphological, cytochemical or ultrastructural features (Kawaguti, and Yaimasu, 1954; Seargant, 1964; Vethamany and Fung, 1972). Regarding the spherules, it is known that red spherulocytes contain the naphthoquinone Echinochrome-A (Service and Wardlaw, 1984). For the colorless and granular, our cytochemical data indicate that their spherules probably contain mucopolysaccharides and peptides, respectively (Queiroz and Custódio, 2015).

Red and colorless spherulocytes have been associated with the immune system. The first has been related to bactericidal activity and only recently the mechanism was unraveled. It was shown that red spherulocytes release echinochrome-A, decreasing or even stopping bacterial growth by chelating the iron necessary to bacterial growth (Coates, 2018). On the other hand, the colorless spherulocytes seems to contain

molecules able to lysate eucaryotic cells. Arizza and coworkers (Arrizza et al., 2007) found that colorless spherulocytes suffer morphological alterations when in contact with foreign cells, releasing cytolytic compounds. For the granular spherulocytes, only morphological information is available (Queiroz and Custódio, 2015), and there are no data on the physiological function. However, its presence in the main orders of sea urchins, and its distribution in most of the analyzed families may suggest a wide distribution among sea urchins.

Yellowish-green spherulocytes were more common in irregular echinoids than in sea urchins (*Cf.* Fig. 6B). However, differently from other spherulocytes addressed here in both morphological and cytochemical approaches, the criteria adopted to consider it as a different type was completely based on live cells. Thus, this makes it the more problematic category considered here. A good example as this criteria can be flawed, was seen during our direct observation on *Arbacia lixula*. In this species, we found a very rare type of spherulocyte, bearing small homogeneous yellowish spherules in live suspension (*Cf.* Fig. 6K), but with no correspondence in cytochemical preparations. However, in the literature review, we saw that a morphologically similar spherulocyte, named green spherulocyte, was recorded in the same species (Seargeant, 1964), and in *A. punctulata* (Liebman, 1950). According to Seargeant (1964), "*these cells are the same size as the red spherule amoebocytes; the spherules are 1-2 micra in diameter, and are bright yellowish-green in colour*", and Liebman (1950) reported that green spherulocytes stain reddish with MT. Except for the color of live cells, both descriptions fit perfectly the characterization of granular spherulocytes. Green spherulocytes, as described by Seargeant (1964), were also found in *Echinocardium cordatum*, *Spatangus purpureus,* and *Brissopsis lyrifera*, suggesting the presence of granular spherulocytes in these organisms.

On the other hand, the yellowish-green spherulocytes of *C. subdepressus* were completely different from those observed in *A. lixula* (*Cf.* Fig. 5), fitting the pattern described by Kawaguti and Yamasu (1976). They found this cell type in the irregular echinoids *C. japonicus*, *E. cordatum*, and *Lovenia elongata*, and characterized it as a spherical cell, measuring 10-20 µm in diameter, and filled with yellowish-green brilliant granules (Kawaguti and Yamasu, 1976). The live yellowish-green spherulocytes of *C. subdepressus* fits this pattern. However, cytochemically it resembles red spherulocytes, due to its brown color in MT and the blue color in TB. Red spherulocytes are filled with

the naphthoquinone Echinochrome-A, however, that is not the only type of naphthoquinone present in echinoids (Hou et al., 2018). Thus, our data show that yellowish-green spherulocytes deserve accurate studies to solve the question about its existence: are they two distinct coelomic populations or they comprise only one cell type? Apparently, the first hypothesis seems more likely.

The remaining spherulocyte subpopulations (*i.e.* brown, iridescent, bluish-green and reddish-vesicular) showed very interesting morphological and cytochemical features. For instance, live brown and reddish-vesicular spherulocytes have a coloration resembling echinochrome pigments. Still, in MT preparations, brown spherulocytes show elongated brownish spherules, while reddish-vesicular spherulocytes show large and apparently empty vacuoles containing small brownish granules. The color and appearance of this brownish material are similar to the content of red spherulocytes (*Cf.* Fig. 5). On the other hand, although live iridescent and bluish-green spherulocytes do not resemble other subpopulations, they were cytochemically similar to colorless and granular spherulocytes respectively. In cytochemical slides, iridescent spherulocytes stain bluish with MT and dark blue with TB, while bluish-green coelomocytes stain orange-reddish with MT and grayish-blue with TB. These specific colorations with MT were characteristics from colorless and granular spherulocytes. Regarding the physiological functions of these spherulocytes, there is no available information. However, considering cytochemical data, it is possible that brown and reddish-vesicular may be involved in antibacterial activity, while iridescent and bluish-green cells may perform similar functions to colorless and granular spherulocytes.

Regarding the distribution of these subpopulations, except for the iridescent spherulocyte found in the heart urchin *E. cordatum*, all others were restricted to clypeasteroid echinoids. However, the distribution of these cells among the main groups of sand dollars was intriguing. For example, brown spherulocytes were observed only in Mellitidae, while reddish-vesicular spherulocytes were found in Mellitidae and Scutellidae sand dollars (*Cf.* Table 1). On the other hand, bluish-green and iridescent spherulocytes were found in Laganidae, Astriclypeidae and Clypeasteridae sand dollars (*i.e. Peronella japonica*, *Astriclypeus mannii*, *Clypeaster japonicus*, *Clypeaster subdepressus* respectively). Considering the sand dollars analyzed in this work, most species belong to suborder Scutellina, while only *C. japonicus and C. subdepressus* belong to Clypeasterina. These two *Clypeaster* species showed an interesting set of

coelomocytes: no red, colorless or granular spherulocytes, but three cells that have strong cytochemical similarity with them (*i.e.* yellowish-green, iridescent and bluish-green spherulocytes respectively).

In summary, this study made an extensive characterization of live and stained coelomocytes of several Echinoidea species, in addition, to bring a systematic bibliographic survey dealing with the cell types already recorded. Altogether, based on direct observations and literature survey, we collected information of 55 species and interesting patterns were observed regarding the distribution of cell types. Phagocytes were the most widespread cell type, occurring in all species analyzed. The same pattern was observed to red and colorless spherulocytes, found in most of the studied species. Their role in echinoderm physiology (*i.e.* antibacterial and cytotoxic activities), also shows how these cells seem to be important, supporting their wide occurrence. Vibratile cells also showed an interesting distribution. Except for the sand dollars, this cell was recorded in most sea urchins and heart urchins. This shows that this cell type seems to be related to echinoderms possessing large coelomic cavities, reinforcing the hypothesis about the clotting function. Considering that echinoids have a hard testis and there is no musculature to close possible wounds and avoid liquid loss and bacterial entrance, as already seen in Holothuroidea (Vazzana et al., 2015), a motile cell able to detect, and access the injured site may be an interesting strategy to deal with wounds.

Regarding the uncommon types, fusiform and progenitor cells, as well as granular spherulocytes showed a similar occurrence, except by the fact that the latter was not found in sand dollars. These cells occurred in 30 to 40% of the species. However, this percentage may be explained by the fact that fusiform and progenitor cells are rare, while live granular spherulocytes may be confused with vibratile cells or colorless spherulocytes, being accurately identified only in cytochemical preparations. The frequency and characteristics of yellowish-green spherulocytes also show an interesting pattern. Apparently, these cells may be two different populations, depending on the group considered: granular spherulocytes in sea urchins and heart urchins and an echinochrome-bearing spherulocyte in sand dollars. Lastly, brown, iridescent, bluish-green and reddish vesicular cells deserve more studies, not only related to their physiological function but also regarding their occurrence in sand dollars.

As a general conclusion, one can notice that the diversity of cellular subpopulations is still underestimated and their physiological roles poorly understood in

both regular and irregular echinoids. At the end of this study, we are able to answer the main questions that have derived this work, as well as the new ones which aroused during its course. Regarding the first question about the most common coelomocytes populations in basal echinoids, we observed that phagocytes, vibratile cells, red and colorless spherulocytes were found in all Cidaroida. Considering the second question, if basal and derived echinoids share the same coelomic populations, we also saw that both possess the same set of coelomocytes and that these cells are similar to that of heart urchins. On the other hand, sand dollars showed the highest diversity of cell types. Of course, more irregular species need to be investigated, but the pattern observed here seems consistent. Lastly, some interesting questions came to our mind after finished this work: which evolutionary pressures could be driven by the diversification of coelomocytes in Echinoidea? How do these cells have diversified? What is the physiological function of these cells? Why sand dollars seem to have more cell types? This study shows that this field is far from being solved and new questions that deserve further attention.

ACKNOWLEDGMENTS

The authors are indebted to Prof. Renata Guimarães Moreira, Prof. José Eduardo A. R. Marian (IB-USP), and Prof. Álvaro Migoto (CEBIMAR-USP), for support with light microscopy photographs. We also thank Prof. Dr. Alberto Ribeiro and the technicians Sheilla Shumidt and Marcio Cruz for support with electron microscopy imaging. This work was supported by FAPESP (Proc. 2015/21460-5 and 2018/14497-8) and Coordenação de Aperfeiçoamento de Pessoal de Nível Superior (CAPES).

REFERENCES

Abraham M. 1963. Etude morphologique sur les coelomocytes des echinides reguliers, Israel Journal of Zoology, 12:1-4, 101-116

Arizza V, Giaramita F, Parrinello D. 2007. Cell cooperation in coelomocyte cytotoxic activity of *Paracentrotus lividus* coelomocytes. Comp. Biochem. Physiol. A, 147:389-394.

Behmer OA, Tolosa EMC, Freitas-Neto AG. 1976. Manual de técnicas de histologia normal e patológica. São Paulo: EDART/EDUSP.

Behre E. 1932. A preliminary notice on the histology of the body fluid of *Mellita quinquiesperforata* Anat.Rec., 54, (suppl.) 92.

Bertheussen K, Seljelid R. 1978. Echinoid phagocytes in vitro. Exp Cell Res 111:401–412.

Boliek MI. 1935. Syncytial structures in sponge larvae and lymph plasmodia of sea urchins. Journal of the Elisha Mitchell Scientific Society, 51(2), 252-288.

Bookhout CG, Greenburg ND. 1940. Cell types and clotting reactions in the echinoid, *Mellita quinquiesperforata*. The Biological Bulletin, 79(2): 309-320.

Boolootian RA, Giese AG. 1958. Coelomic corpuscles of echinoderms. Biol.Bull., Wood's Hole, 115, 53-63.

Boolootian RA. 1962. The perivisceral elements of echinoderm coelomic fluid. American Zoologist, 2, 275-284

Borges J, Porto-Neto L, Mangiaterra M, Jensch-Junior BE, Silva JRMC. 2002. Phagocytosis in vitro and in vivo in the Antarctic sea urchin *Sterechinus neumayeri* at 0°C. Polar Biol 25: 891-897.

Borges JC, Jensch-Junior BE, Garrido PA, Mangiaterra MB, Silva JR. 2005. Phagocytic amoebocyte subpopulations in the perivisceral coelom of the sea urchin *Lytechinus variegatus* (Lamarck, 1816). Journal Of Experimental Zoology 303A:241–248

Brockton V, Henson JH, Raftos DA, Majeske AJ, Kim YO, Smith LC. 2008. Localization and diversity of 185/333 proteins from the purple sea urchin–unexpected protein-size range and protein expression in a new coelomocyte type. Journal of Cell Science, 121(3), 339-348.

Burton MPM. 1996. Echinoid coelomic cells. Nature 211: 1095–1096.

Cavey MJ and Märkel, K. 1994. Echinoidea. In: Harrison, F. W. & Chia, F. S. (Eds.). Microscopic Anatomy of Invertebrates, Enchinodermata (Vol. 14). Wiley-Liss. (pp. 345-400).

Chia F, Xing J. 1995. Echinoderm Coelomocytes. Zoological Studies 35(4):231-254.

Clow LA, Raftos DA, Gross PS, Smith LC. 2004. The sea urchin complement homologue, SpC3, functions as an opsonin. J. Exp. Biol. 207: 2147-2155.

Coates CJ, McCulloch C, Betts J, Whalley T. 2018. Echinochrome A release by red spherule cells is an iron-withholding strategy of sea urchin innate immunity. Journal of innate immunity, 10(2), 119-130.

Coteur G, DeBecker G, Warnau M, Jangoux M, Dubois P. 2002. Differentiation of immune cells challenged by bacteria in the common European starfish, *Asterias rubens* (Echinodermata). Eur. J. Cell Biol. 81: 413-418.

Cuénot L. 1891. Etudes sur les sang et les glandes lymphatiques dans la sériee animale (2° partie: Invértebés). Arch. Zool. Exptl. Gén (Sér. 2), 9, 13-90, 365-475, 593-670.

Cuénot L. 1891. Études sur le sang et les glandes lymphatiques, Invertébrés. Arch. Zool. exp. gen., 9, 565-475, 595-670.

Cuénot L. 1897. Les globules sanguins et les organes lymphoides des Invertébrés. Arch.Anat.micr., 1, 155-192.

Davidson E. 1953. Clotting of the perivisceral fluid of the sand dollar, Echinarachnius parma. Biol.Bull.,Wood's Hole, 105, 372.

Deveci R, Şener E, İzzetoğlu S. 2015. Morphological and ultrastructural characterization of sea urchin immune cells. Journal of morphology, 276(5), 583-588.

Dunham P, Weissman G. 1986. Aggregation of marine sponge cells induced by Ca pulses, Ca ionophores, and phorbol esters proceed in the absence of external Ca. Biochemical and Biophysical Research Communications 134:1319–1326. doi:10.1016/0006-291X(86)90394-3.

Endean R. 1958. The coelomocytes of *Holothuria leucospilota*. Journal of Cell Science, 3(45), 47-60.

Endean R. 1966. The coelomocytes and coelomic fluid. In: Boolootian, R. A. (Ed.). Physiology of Echinodermata (pp.301-328). New York: Interscience Publishers.

Faria MT, Silva JRMC 2008. Innate immune response in the sea urchin *Echinometra lucunter* (Echinodermata). Journal of invertebrate pathology, 98(1), 58-62.

Fauré-Premiet E. 1927. Les amibocytes des invertébrés à l'état quiescent et a l'état actif. Arch. Anat.micr. 23, 99-173.

Furness JB, Cottrell JJ, Bravo DM. 2015. Comparative gut physiology symposium: comparative physiology of digestion. Journal of animal science, 93(2), 485-491.

Geddes P. 1880. On the coalescence of amoeboid cells into plasmodia and on the so-called coagulation of invertebrate fluids. Proc.roy.Soc., Ser.B., 30, 252-255

Godefroy N, Le Goff E, Martinand-Mari C, Belkhir K, Vacelet J, Baghdiguian S. 2019. Sponge digestive system diversity and evolution: filter feeding to carnivory. Cell and tissue research, 1-11.

Gross PS, Clow LA, Smith LC. 2000. SpC3, the complement homologue from the purple sea urchin, *Strongylocentrotus purpuratus*, is expressed in two subpopulations of the phagocytic coelomocytes. Immunogenetics 51: 1034-1044.

Gross PS, Clow LA, Smith LC. 2000. SpC3, the complement homologue from the purple sea urchin, *Strongylocentrotus purpuratus*, is expressed in two subpopulations of the phagocytic coelomocytes. Immunogenetics, 51(12):1034-1044.

Hartenstein V. 2006. Blood cells and blood cell development in the animal kingdom. Annu. Rev. Cell Dev. Biol., 22, 677-712.

Henri V. I906. Etude du liquide perivisceral dês oursins. C. Rend. Soc. Biol., Paris, 880-882.

Holland ND, Phillips JH, Giese AC. 1965. An autoradiographic investigation of coelomocyte production in the purple sea urchin (*Strongylocentrous purpuratus*). Biological Bulletin 128:259–270. doi:10.2307/1539554.

Holland ND, Phillips JH, Giese AC. 1965. An autoradiographic investigation of coelomocyte production in the purple sea urchin (Strongylocentrous purpuratus). Biological Bulletin 128:259–270. doi:10.2307/1539554.

Hou Y, Vasileva EA, Carne A, McConnell M, Bekhit AEDA, Mishchenko NP. 2018. Naphthoquinones of the spinochrome class: occurrence, isolation, biosynthesis and biomedical applications. RSC advances, 8(57), 32637-32650.

Jacobson FW, Millott N. 1953. Phenolases and Melanogenesis in the Coelomic Fluid of the Echinoid *Diadema antillarum* Phillippi. Proc. R. Soc. Lond. B 1953 141, 231-247.

Jangoux M,Vanden Bossche JP. 1975. Morphology and dynamics of the coelomocytes of Asterias rubens L. (Echinodermata, Asteroidea). Forma Functio 8, 191 ± 208.

Jellett JF, Wardlaw AC, Scheibling RE. 1988. Experimental infection of the echinoid Strongylocentrotus droebachiensis with Paramoeba invadens: quantitative changes in the coelomic fluid. Dis Aquat Org, 4, 149-157

Johnson PT. 1969a. The coelomic elements of sea urchins (Strongylocentrotus). I. The normal coelomocytes; their morphology and dynamics in hanging drops. Journal of Invertebrate Pathology 13:25–41. doi:10.1016/0022-2011(69)90236-5.

Johnson PT. 1969b. The coelomic elements of sea urchins (Strongylocentrotus) II. Cytochemistry of the Coelomocytes. Histochemie 17:213–231. doi:10.1007/BF00309866.

Jones GM, Herbda AJ, SCHEIBLING RE, Miller RJ. 1985. Histopathology of the disease causing mass mortality of sea urchins (Strongylocentrotus droebachiensis) in Nova Scotia. J. Invertebr. Pathol. 45: 260–271.

Kaneshiro ES, Karp RD. 1980. The ultrastructure of coelomocytes of the sea star Dermasterias imbricate. Biol. Bull., 159: 295-310.

Kanungo K. 1984. The Coelomocytes of Asteroid Echinoderms. In: Cheng T.C. (Ed) Invertebrate Blood. Comparative Pathobiology, vol 6. Springer, Boston, MA

Karp RD, Coffaro KA. 1982. Cellular Defense Systems of the Echinodermata. In: Cohen N., Sigel M.M. (Eds) Phylogeny and Ontogeny. Springer, Boston, MA.

Kawaguti S, Yaimasu T. 1954. Pigment cells in the perivisceral fluid of the Echinoidea. Biological journal of Okayama University, 1: 249-264

Kieneke A, Ahlrichs WH, Arbizu PM, Bartolomaeus T. 2008. Ultrastructure of protonephridia in Xenotrichula carolinensis syltensis and *Chaetonotus maximus* (Gastrotricha: Chaetonotida): comparative evaluation of the gastrotrich excretory organs. Zoomorphology 127:1–20.

Kindred J. 1921. Phagocytosis and clotting in theperivisceral fluid of echinoderms. Biol.Bull.,Wood's Hole, 41, 144-152.

Kindred, J., 1924 The cellular elements in the perivisceral fluid of echinoderms. Biol.Bull.,Wood's Hole, 4§, 228-251.

Kindred J. 1926. A study of the genetic relationship of the amoebocytes with spherules in *Arbacia*. Biol.Bull. , Wood's Hole, 147-154.

Koch NM, Coppard SE, Lessios HA, Briggs DE, Mooi R, Rouse GW. 2018. A phylogenomic resolution of the sea urchin tree of life. *BMC evolutionary biology*, *18*(1), 189.

Kuhl VJ. 1957. Die Zellelemente in der Lieheshohlenflussigkeit der Seeigel *Psaimechinus miliaris* und iht Bewegung physiologisches Verhalten. Z.Zellforsch. 27, 1-15.

Laughlin JD. 1989. Coelomocytes of the Urchin Lytechinus pictus (Echinoidea). Journal of invertebrate pathology 54, 404-405

Lessios HA, Kessing BD, Robertson DR, Paulay G. 1999. Phylogeography of the pantropical sea urchin Eucidaris in relation to land barriers and ocean currents. Evolution, 53(3), 806-817.

Leys SP, Eerkes-Medrano DI. 2006. Feeding in a Calcareous Sponge: Particle Uptake by Pseudopodia. Biol Bull 211: 157-171.

Liebman E. 1950. The leucocytes of *Arbacia punctulata*. Biological Bulletin 98:46–59. doi:10.2307/1538598.

Lin W, Grant S, Beck G. 2007. Generation of monoclonal antibodies to coelomocytes of the purple sea urchin *Arbacia punctulata*: characterization and phenotyping. *Developmental & Comparative Immunology*, *31*(5), 465-475.

Mangiaterra MBBCD, Silva JRMC. 2001. Induced inflammatory process in the sea urchin *Lytechinus variegates*. Invertebrate Biology 120(2): 178-184.

Matranga V, Bonaventura R (2002) Sea urchin coelomocytes, the progenitors of vertebrate immune effectors, as bio-indicators of stress and pollution. In: Yokota Y, Matranga V, Smolenicka Z (eds) The sea urchin: from basic biology to aquaculture. Swets and Zeitlinger, Lisse, The Netherlands, pp 161–176

Ohuye T. 1936. On the coelomic corpuscles in the body fluid of some invertebrates 5, Reaction of the coelomic corpuscles of an echinid, Temnopleurus Hardwickii to vital dyes and some chemical reagents. Sci.Rep.Tohoku Univ., Biol., 11, 223-238.

Pawson DL. 2007. Phylum Echinodermata. Zootaxa, 1668: 749-764.

Piryaei F, Mostafavi PG, Shahbazzadeh D, Bagheri KP. 2018. Cytological study of Echinometra mathaei (Echinoidea: Camarodonta: Echinometra) the Persian Gulf sea urchin. International Journal of Aquatic Science, 9(2): 77-84.

Prouho H. 1887. Recherches sur le *Dorocidaris papillata* et quelques autres échinides de La Mediterranee. Arch.Zool.exp.gén., ser.2, 5, 214-380.

Queiroz V, Custódio MR. 2015. Characterisation of the spherulocyte subpopulations in Eucidaris tribuloides (Cidaroida: Echinoidea). Italian Journal of Zoology, *82*(3): 338-348.

Ramírez-Gómez F, Aponte-Rivera F, Méndez-Castaner L, García-Arrarás JE. 2010. Changes in holothurian coelomocyte populations following immune stimulation with different molecular patterns. Fish & shellfish immunology, 29(2), 175-185.

Ratcliffe NS, DA Millar. 1988. Comparative aspects and possible phylogenetic affinities of vertebrate and invertebrate blood cells. In AF Rowley, NA Ratcliffe, eds. Vertebrate blood cells. New York: Cambridge University Press, pp. 1-17.

Rowley AF, Rowley AF, Ratcliffe NA. 1988. Vertebrate blood cells. CUP Archive.

Saergant MPM. 1964. Studies on the coelomic cells and haemal system op some echinoids. Thesis Submitted for the Degree of Doctor of Philosophy Bedford College, University of London. 291 p.

Schinke H. 1950. Bildung und Ersatz der Zellelemente der Leibeshöhlenflüssigkeit von *Psammechinus miliaris* (Echinoidea). Zeitschrift Für Zellforschung Und Mikroskopische Anatomie, 35(3-4), 311–331.

Service M, Wardlaw AC. 1984. Echinochrome-A as a bactericidal substance in the coelomic fluid of *Echinus esculentus* (L.). Comp Biochem Physiol B Comp Biochem 1984; 79: 161–165.

Smith CL, Ghosh J, Buckley KM, Clow LA, Dheilly NM, Huag T, Henson JH, ChengMan Lun CL, Majeske AJ, Matranga V, Nair SV, Rast JP, Raftos DA, Roth M, Sacchi S, Schrankel CS, Stensvag K. 2010. Echinoderm immunity. *In*: Söderhäll K, editor. Invertebrate immunity. New York, NY: Landes Bioscience and Springer Science BusinessMedia. pp. 260–301.

Smith LC, Arizza V, Hudgell MAB, Barone G, Bodnar AG, Buckley KM, Furukawa R. 2018. Echinodermata: the complex immune system in echinoderms. *In*: Cooper L. (Ed). Advances in comparative immunology (pp. 409-501). Springer, Cham.

Smith LC, Britten RJ, Davidson EH (1992) SpCoel1: a sea urchin profilin gene expressed specifically in coelomocytes in response to injury. Mol Biol Cel 3:403–414

Smith LC, Rast JP, Brockton V, Terwilliger DP, Nair SV, Buckley KM, Majeske AJ. 2006. The sea urchin immune system. Invertebrate Survival Journal 3:25–39.

Smith VJ 1981. The echinoderms. *In*: Ratcliffe NA, Rowley AF, (Eds). Invertebrate blood cells. New York, NY: Academic Press. 513–562.

Taupin P. 2008. Electron microscopy of cell suspension. Annals of Microscopy 8:19–21.

Theél H. 1896. Remarks on the activity of amoeboid cells in the echinoderms. Zoologiska Studier, Festskrift Wilhelm Lilljeborg, Upsala, 47-58.

Theél H. 1919. Om amoebocyter och andra kroppar i perivisceralhalan hos echinodermer. Ark. Zool., 12, 14, 1-48.

Van Praet M. 1985. Nutrition of sea anemones. Adv. Mar. Biol. 22:65–69.

Vazzana M, Siragusa T, Arizza V, Buscaino G, Celi M. 2015. Cellular responses and HSP70 expression during wound healing in *Holothuria tubulosa* (Gmelin, 1788). Fish & shellfish immunology, 42(2): 306-315.

Vethamany VG, Fung M. 1972. The fine structure of coelomocytes of the sea urchin, Strongylocentrotus dröbachiensis (Müllier O.F.). Canadian Journal of Zoology 50:77–81. doi:10.1139/z72-014.

Withers PC. 1992. Digestion. Comparative animal physiology, 892-949.

Xing K, Yang HS, Chen MY. 2008. Morphological and ultrastructural characterization of the coelomocytes in *Apostichopus japonicus*. Aquatic Biology, 2(1): 85-92.

Yonge CM. 1937. Evolution and adaptation in the digestive system of the metazoa. Biological Reviews, 12(1): 87–114.

Ziegler A, Faber C, Bartolomaeus T. 2009. Comparative morphology of the axial complex and interdependence of internal organ systems in sea urchins (Echinodermata: Echinoidea). *Frontiers in Zoology*, *6*(1), 10.

Figures, Tables, and Captions

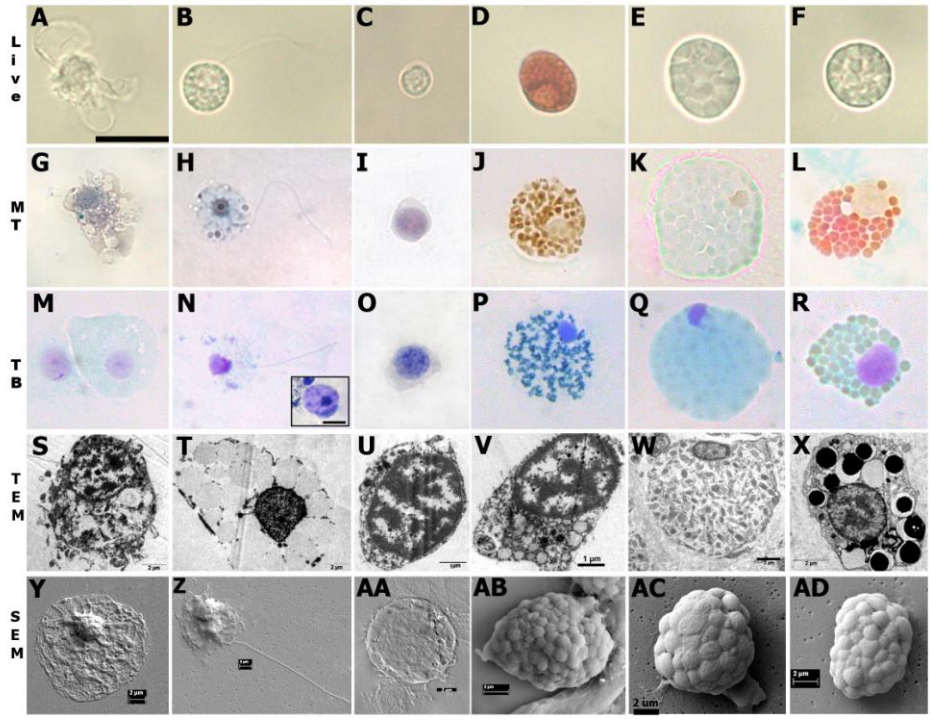

Figure 1 – Coelomocytes of the basal sea urchin *Eucidaris tribuloides* in different approaches. A-F – Live cells; G-R cytochemistry; G-L – Mallory trichrome; M-R – Toluidine blue; S-X – Transmission electron microscopy; Y-AD – Scanning electron microscopy.

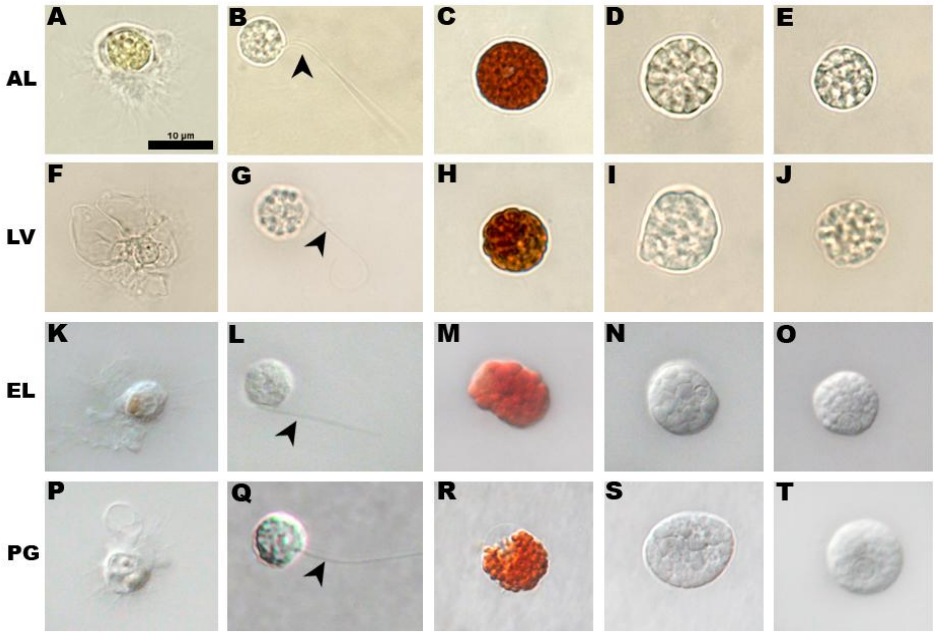

Figure 2 – Live coelomocytes of the derived sea urchins. A-E – *Arbacia lixula*; F-J – *Lytechinus variegatus*; K-O – *Echinometra lucunter*; P-T – *Paracentrotus gaimardi*. A, F, K, P – Phagocytes; B, G, L, Q – Vibratile cell; C, H, M, R – Red spherulocytes; D, I, N, S – Colorless spherulocyte; E, J, O, T – Granular spherulocyte.

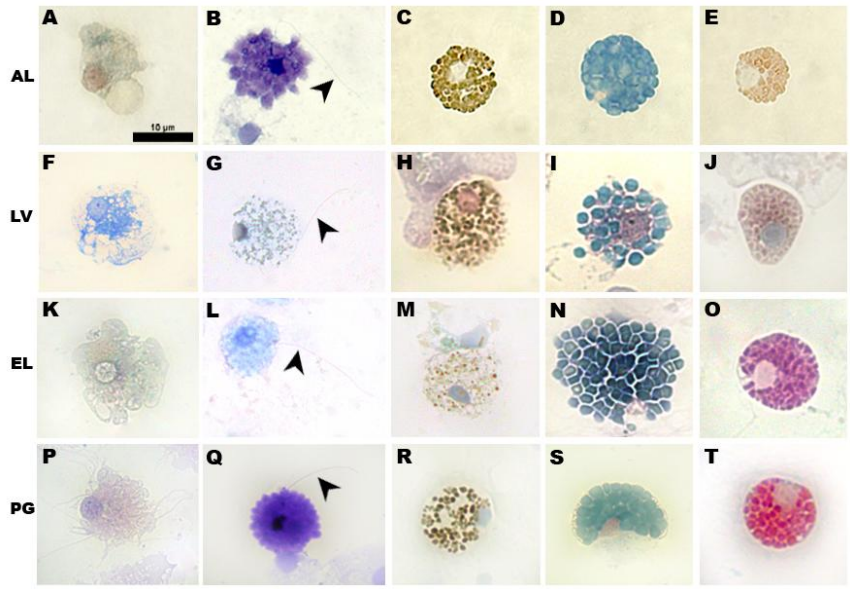

Figure 3 – Stained coelomocytes of the derived sea urchins. A-E – *Arbacia lixula*; F-J – *Lytechinus variegatus*; K-O – *Echinometra lucunter*; P-T – *Paracentrotus gaimardi*. A, F, K, P – Phagocytes; B, G, L, Q – Vibratile cell; C, H, M, R – Red spherulocytes; D, I, N, S – Colorless spherulocytes; E, J, O, T – Granular spherulocytes.

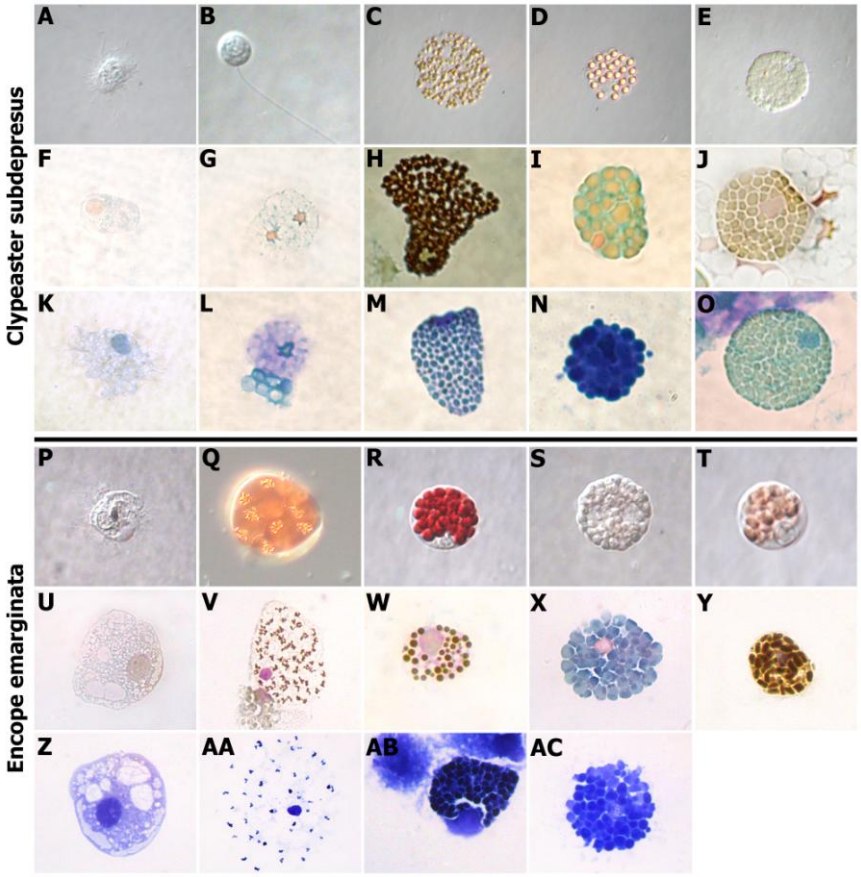

Figure 4 – Live and stained coelomocytes of *Clypeaster subdepressus* (A-O) and *Encope emarginata* (P-AC). A, F, K, P, U, Z – Phagocytes; B, G, L – Vibratile cells; C, H, M – Yellowish-green spherulocyte; D, I, N – Iridescent spherulocyte; E, J, O – Bluish-green spherulocyte; Q, V, AA – Reddish vesicular spherulocyte; R, W, AB – Red spherulocyte; S, X, AC – Colorless spherulocyte; T, Y – Brownish spherulocyte. A-E and P-T – Live cells (Differential interference contrast – DIC); F-J and U-Y – Mallory trichrome; K-O and Z-AC – Toluidine blue.

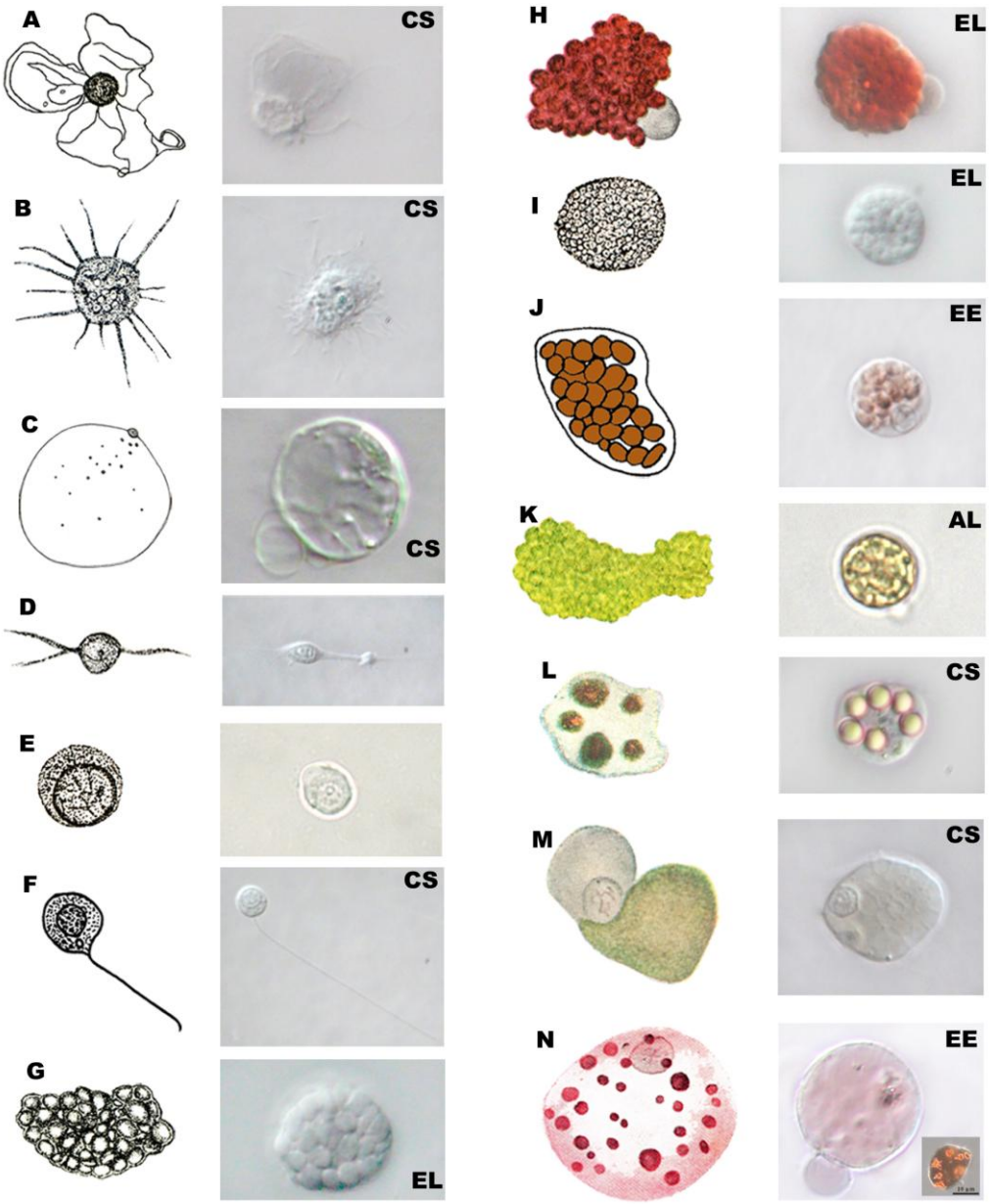

Figure 5 – Main cell types already observed in Echinoidea: A-C – Phagocytes; D – Fusiform cell; E – Progenitor cell; F – Vibratile cell; G-N – Spherulocytes. A – Petaloid phagocyte; B – Filiform phagocyte; C – Large vesicular cells; D – Fusiform cell; E – Progenotor cell; F – Vibratile cell; G – Colorless spherulocyte; H – Red spherulocyte; I – Granular spherulocyte; J - Brownish spherulocyte; K – Yellowish-green spherulocyte; L – Iridescent spherulocyte; M – Bluish-green spherulocyte; N – Reddish vesicular spherulocyte. Drawings: A-E, G-I, and K-N = Adapted from Kawaguti and Yamasu, 1976; F = Kindred, 1921; J = Bookhout and Greenburg, 1940. Pictures from author = A-D, F, L, M = *Clypeaster subdepresus*; E = *Eucidaris tribuloides*; G-I = *Echinometra lucunter*; J and N = *Encope emarginata*; K = *Arbacia lixula*. Drawings and photos are not in scale.

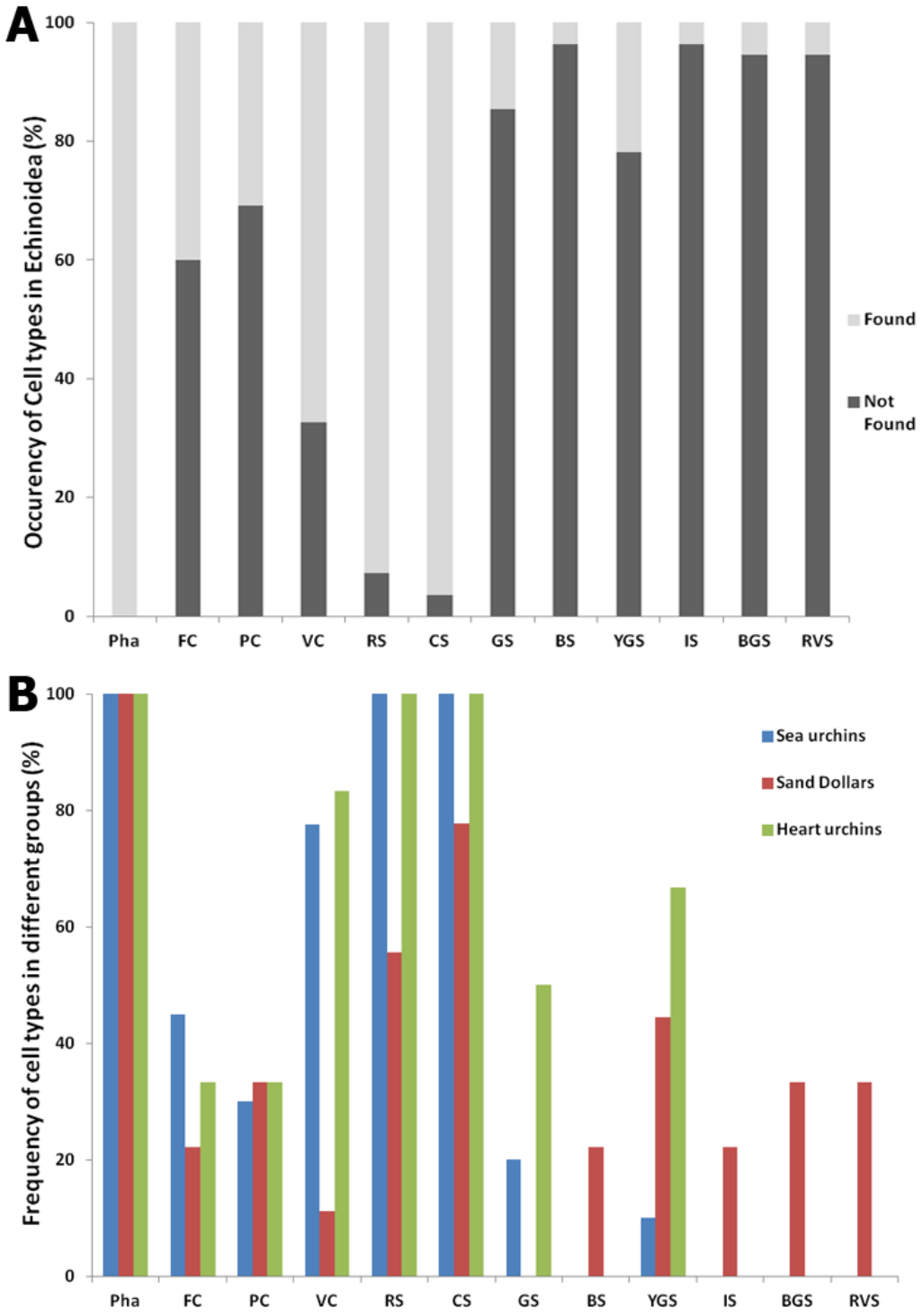

Figura 6 – Cell types recorded in the class Echinoidea. A – Percentage of presence and absence of the cell types in the class Echinoidea. B – Percentage of the presence of the different cell types in the three main groups of Echinoidea. Legend: Pha = Phagocytes, FC = Fusiform cell; VC = Vibratile cell; RS = Red spherulocyte; CS = Colorless spherulocytes; GS = Granular spherulocyte; BS = Brown spherulocyte; YGS = Yellowish-green spherulocyte; IS = Iridescent spherulocyte; BGS = Bluish-green spherulocyte; RVS = Redish vesicular spherulocyte.

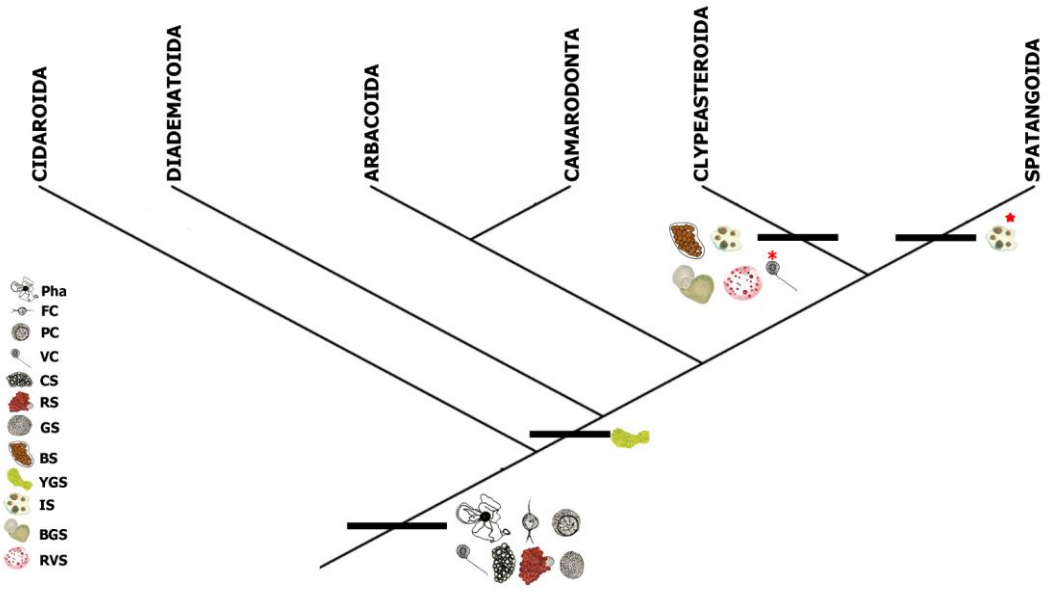

Figure 7 – Graphic representation of cell distribution among the orders of Echinoidea analyzed in the present study (Adapted from Ziegler et al., 2009). Legend: Pha = Phagocytes, FC = Fusiform cell; VC = Vibratile cell; RS = Red spherulocyte; CS = Colorless spherulocytes; GS = Granular spherulocyte; BS = Brown spherulocyte; YGS = Yellowish-green spherulocyte; IS = Iridescent spherulocyte; BGS = Bluish-green spherulocyte; RVS = Redish vesicular spherulocyte; Red asterisk = Lost: found only in *Clypeaster subdepressus*. Red star = Gain: found only in *Echinocardium cordatum*.

Table 1 – List of analyzed species and cell types found in the class Echinoidea, based on literature survey and direct observations. Legend: Pha = Phagocytes, FC = Fusiform cell; VC = Vibratile cell; RS = Red spherulocyte; CS = Colorless spherulocytes; GS = Granular spherulocyte; BS = Brown spherulocyte; YGS = Yellowish-green spherulocyte; IS = Iridescent spherulocyte; BGS = Bluish-green spherulocyte; RVS = Redish vesicular spherulocyte; DO = Direct observations; ? = need confirmation.

	Order	Family	Species	Most common cell types												Reference
				Pha	FC	PC	VC	RS	CS	GS	BS	YGS	IS	BGS	RVS	
Regular	Cidaroida	Cidaridae	***Eucidaris tribuloides***	**x**	**x**	**x**	**x**	**x**	**x**	**x**						DO, 37
			Cidaris cidaris	x			x	x	x							7, 8, 24
			Stylocidaris affinis	x			x	x	x							1
	Arbacioida	Arbaciidae	***Arbacia lixula***	**x**	**x**	**x**	**x**	**x**	**x**	**x**		**x**				**DO**, 1, 25
			Arbacia punctulata	x			x	x	x	x		x				17, 19, 22, 45
	Diadematoida	Diadematidae	*Diadema antillarum*	x			x	x	x	x		x				6, 25, 30
			Diadema savignii	x	x		x	x	x							4
			Diadema setosum	x				x	x							16
			Centrostephanus longispinus	x			x	x	x							1
			Echinothrix diadema	x	x		x	x	x							4
			Echinothrix calamaris	x	x	x	x	x	x	x						4, 16
	Camarodonta	Toxopneustidae	***Lytechinus variegatus***	**x**	**x**	**x**	**x**	**x**	**x**	**x**		**x**				**DO**, 2, 32, 35
			Lytechinus pictus	x			x	x	x							21
			Sphaerechinus granularis	x	x		x	x	x							1, 11
			Toxopneustes pileolus	x				x	x							16
			Tripneustes gratilla	x				x	x	X						16
		Parachinidae	*Paracentrotus lividus*	x	x	x	x	x	x	x						1, 7, 8, 10, 13, 25, 39, 43
			Paracentrotus gaimardi	**x**	**x**	**x**	**x**	**x**	**x**	**x**						**DO**
			Psammechinus microtuberculatus	x			x	x	x							7, 8
			Psammechinus miliaris	x			x	x	x							6, 20, 26, 27, 31
		Strongylocentrotidae	*Strongylocentrotus purpuratus*	x			x	x	x	?						3, 4, 34, 36, 40, 42
			Strongyloncentrotus fragilis	x	x		x	x	x							3, 4
			Strongylocentrotus droebachiensis	x			x	x	x	x						14, 15, 18, 38, 41
			Pseudocentrotus depressus	x		x		x	x							16
			Hemicentrotus pulcherrimus	x		x		x	x							16
			Mesocentrotus franciscanus	x	x		x	x	x							3, 4
			Heliocidaris crassispina	x		x		x	x							16
		Echinometridae	***Echinometra lucunter***	**x**	**x**	**x**	**x**	**x**	**x**	**x**						**DO**, 33
			Echinometra mathaei	x	x	x	x	x	x	x						4, 16, 44
			Echinometra oblonga	x	x		x	x	x							4
			Echinometra vanbrunti	x	x		x	x	x							4
			Echinostrephus aciculatus	x	x		x	x	x							4
			Heterocentrotus trigonarius	x	x		x	x	x							4
			Heterocentrotus mamilatus	x	x		x	x	x							4
		Echinidae	*Echinus sculentus*	x		x	x	x	x							12, 31
			Gracilechinus acutus	x			x	x	x							7, 8
			Sterechinus neumayeri	x			x	x	x							5
		Temnopleuridae	*Temnopleurus toreumaticus*	x				x	x	?						16
			Temnopleurus hardwickii	x				x	x	x						16, 23
			Mespilia globulus	x				x	x							16
Irregular	Clypeasteroida	Mellitidae	***Encope emarginata***	**x**	**x**	**x**		**x**	**x**		**x**				**x**	**DO**
			Mellita quinquiesperforata	x				x	x		x				x	28, 29
		Dendrasteridae	*Dendraster excentricus*	x				x	x			x		?		3, 4, 18
		Echinarachniidae	*Echinarachnius parma*	x				x	x							9
		Scutellidae	*Scaphechinus mirabilis*	x				x	x						x	16
		Laganidae	*Peronella japonica*	x					x				x			16
		Astriclypeidae	*Astriclypeus mannii*	x					x			x	x	x		16
		Clypeasteridae	*Clypeaster japonicus*	x		x						x	x	x		16
			Clypeaster subdepressus	x	x	x	x					x	x	x		**DO**
	Spatangoida	Brissidae	*Brissus latecarinatus*	x	x		x	x	x							3
			Rhynobrissus sp.	x	x		x	x	x							3
		Loveniidae	*Brissopsis lyrifera*	x			x	x	x	x		x				25
			Lovenia elongata	x		x		x	x			x				16
		Spatangidae	*Echinocardium cordatum*	x		x	x	x	x	x		x	x			16, 25
			Spatangus purpureus	x			x	x	x	x		x				12, 25

List of references - 1 – Abraham, 1963 **2** – Boliek, 1935; **3** – Boolootian and Giese, 1958; **4** – Boolootian, 1962; **5** – Borges et al., 2002; **6** – Burton, 1996; **7** – Cuénot, 1891; **8** – Cuénot, 1897; **9** – Davidson; 1953; **10** – Deveci et al., 2015; **11 -** Fauré-Premiet, 1927; **12** – Geddes, 1880; **13** – Henri, 1906; **14** – Jellett et al., 1988; **15** – Jones et al., 1985; **16** – Kawaguti and Yaimasu, 1954; **17** – Kindred, 1921; **18** – Kindred, 1924; **19** – Kindred, 1926; **20** – Kuhl, 1957; **21** – Laughlin, 1989; **22** – Liebman, 1950; **23** – Ohuye, 1936; **24** – Prouho, 1887; **25** – Saergant, 1964; **26** – Schinke, 1950; **27** – Theél, 1919; **28** – Behre, 1932; **29** – Bookhout et al., 1940; **30** – Jacobson and Millott, 1953; **31** – Theél, 1896; **32** – Mangiaterra and Silva, 2001; **33** – Faria and Silva, 2008; **34** – Gross et al., 2000; **35** – Borges et al., 2005; **36** – Brockton et al., 2008; **37** – Queiroz and Custódio, 2015; **38** – Vethamany and Fung, 1972; **39** – Arizza et al., 2007; **40** – Holland et al., 1965; **41** – Bertheussen and Seljelid, 1978; **42** – Smith et al., 1992; **43** – Matranga and Bonaventura, 2002; **44** – Piryaei et al., 2018; **45** – Lin et al., 2007.

Capítulo 2
Celomócitos das espécies do gênero *Paracentrotus* (Echinoidea)

Justificativa

Paracentrotus (Lamarck, 1816), é um gênero de equinóides regulares conhecidos pelo seu polimorfismo cromático, sendo composto por apenas duas espécies: *P. gaimardi* e *P. lividus*. A primeira têm sido pouquíssima estudada, enquanto a segunda é um dos principais modelos de estudo dentro dos Echinoidea. *Paracentrotus lividus* vem sendo utilizada nas mais diversas áreas, desde embriologia e biologia celular até genética de populações e aquicultura. Em imunologia, esta espécie também é um importante modelo, tendo seus mecanismos imunes moleculares e celulares bem estudados. Para os celomócitos, existem vários estudos caracterizando os tipos celulares de *P. lividus*, que são os seus principais efetores imunes. No entanto, durante a caracterização dos celomócitos de *P. gaimardi*, alguns, além dos tipos celulares comuns a *P. lividus* (*i.e.* fagócitos, células vibráteis e os esferulócitos vermelhos e transparentes), dois tipos adicionais foram observados: o esferulócito granular e um tipo de célula cristal. Ainda para todas as subpopulações de esferulócitos encontradas em *P. gaimardi*, foi observado um continuum de células, que emboram fossem bastante similares em linhas gerais, apresentavam algumas diferenças em relação ao tamanho do núcleo e organização do citoplasma, que possibilitavam a sua organização em uma sequência. Assim, o presente capítulo apresenta a caracterização dos celomócitos de *P. gaimardi* e *P. lividus*, usando uma abordagem morfológica (*e.g.* células vivas em suspensão, preparações citoquímicas e microscopia eletrônica de varredura), nun contexto comparativo, visando analisar se os tipos novos observados em *P. gaimardi* poderiam ser encontrados em *P. lividus*. Além da caracterização, apresentamos uma hipótese de maturação dos esferulócitos, a qual explica a variação morfológica dentro de uma mesma subpopulação.

Coelomic cells of *Paracentrotus* sea urchins (Echinodermata): a comparative approach

Vinicius Queiroz[1, 2], Vincenzo Arizza[2], Mirella Vazzana[2] and Márcio R. Custódio[1]

To be subbmited to the Journal Zoologischer Anzeiger

1 – Departamento de Fisiologia Geral, Instituto de Biociências and Núcleo de Apoio à Pesquisa – Centro de Biologia Marinha (NAP–CEBIMar), Universidade de São Paulo, São Paulo, Brazil

2 – Dipartimento Scienze e Tecnologie Biologiche Chimiche e Farmaceutiche (STEBICEF), Università degli Studi di Palermo, Palermo, Italy

Abstract: The genus *Paracentrotus* comprises two species: *P. lividus* and *P. gaimardi*. The first one is one of the most studied sea urchins in the world, while the second is poorly known. Even basic aspects, such as the types of cells circulating in the coelomic fluid are unknown for *P. gaimardi*. Thus, this works aims to characterize the coelomic cells of *Paracentrotus* sea urchins, from a comparative perspective, using an integrative approach. Seven different coelomic subpopulations were found in *Paracentrotus* sea urchins. Phagocytes, vibratile cells, red, colorless and granular spherulocytes were common to both species, while crystal cells were specific to *P. gaimardi* and progenitor cells were found only in *P. lividus*. For all spherulocyte subpopulations, a set of morphologically similar cells were observed in both cytological preparations and scanning electron microscopy analyses, being interpreted as a putative maturation sequence. Based on morphological and morphometric data (nucleus and cytoplasm diameter as well as nucleus/cytoplasm ratio), this sequence may be organized in different stages: Early, Intermediate and Final. Lastly, we propose a model that describes how spherulocytes maturate. Thus, in addition to important questions raised in this paper for *Paracentrotus* sea urchins, our results also show that after to find a new coelomic subpopulation in *P. lividus,* one of the most studied sea urchin species of the world, the basics aspects of sea urchin physiology/immunology need to (re)visited.

Keywords: Coelomocytes cytology, granular spherulocyte, maturation process.

Running title: Coelomic cells of *Paracentrotus* sea urchins

*Corresponding author: V. Queiroz, Departamento de Fisiologia Geral, Instituto de Biociências, Universidade de São Paulo, Rua do Matão, nº 321, Cidade Universitária, São Paulo (SP), Brazil. CEP: 05508-090. Tel: +55113091-7522. Email: vinicius_ufba@yahoo.com.br

INTRODUCTION

The genus *Paracentrotus* comprises only two sea urchin species: *P. gaimardi* and *P. lividus* (Calderon et al., 2009). *Paracentrotus gaimardi* is a little-known species from the South Atlantic Ocean, found only in some places of African and Brazilian coasts (Mortensen, 1943; Calderon et al., 2010). In Brazil, its distribution is restricted to the south-southern region, ranging from Rio de Janeiro to Santa Catarina states (Mortensen 1943; Lopes and Ventura, 2012). This sea urchin presents an astonishing and intriguing color polymorphism (*e.g.* black, brown, gray, green, or pink), characteristic which has guided most studies about it (Calderon et al. 2010; Lopes and Ventura 2012; Duarte et al. 2016). Studies addressing its biology are scarce (Boudouresque and Yoneshigue 1987; Villaça and Yoneshigue 1987) and information about the physiological and/or immunological aspects of *P. gaimardi* are unavailable.

On the other hand, the Mediterranean sea urchin *Paracentrotus lividus* (Lamarck, 1816) is a well-known species. It is a North-Eastern Atlantic echinoid with a wide distribution, ranging from Scotland and Ireland to Southern Morocco and the Canary Islands, including all Mediterranean Sea (Boudoresque & Verlaque 2007; 2013; Pantazis, 2009; Soliman et al. 2015; Yeruham et al., 2015). Its main biological aspects are well-understood, not only due to its commercial significance (Gianguzza et al., 2008), but also because it has been used in basic and applied researches (Telford et al., 2014; Schillaci et al., 2014). In fact, this species has been a model in the most diverse areas, such as developmental biology (Gildor et al., 2016), physiology (Arizza et al., 2013), cellular and molecular biology (Cervello et al., 1994) and immunology (Arizza et al., 2007).

Similarly to vertebrates, the sea urchin immune system also consists of humoral and cellular responses, with the latter considered as the first line of defense (Chiaramonte and Russo, 2015). The immune aspects of *P. lividus* are relatively well understood, mainly regarding the coelomocytes, the circulating cells in the coelomic fluid. The main cell populations have been identified (Matranga et al., 2005), as well as their morphology properly depicted in light and transmission electron microscopy (Devecy et al., 2015). It has been shown that *P. lividus*' phagocytes are also responsible for removal of foreign particles (Smith et al., 2010, Arizza et al., 20013), while red and colorless spherulocytes are linked to bacterial growth inhibition (Gerardi et a., 1990) and cytotoxicity (Arizza et al., 2007), respectively. Still, that pathogen-associated molecular patterns (PAMPs), toxic metals and nanoparticles are able to modulate coelomocyte activity (Pagliara and Stabili, 2012; Pinsino et al., 2015; Romero et al., 2016). On the other hand, even the basic aspects of coelomocytes and the immune system of *P. gaimardi* are still unknown.

In this context, this works aims to characterize the coelomic cells of *Paracentrotus* sea urchins, from a comparative perspective. Using morphological and morphometric data, the coelomocytes of the poorly known sea urchin *P. gaimardi* and the well-know *P. lividus* were thoroughly studied. Data from light microscopy of living and stained cells, as well as scanning electron microscopy, were used to address the coelomocytes of these two sea urchins, showing unknown cell types in both species. Additionally, based on morphological and morphometric parameters, we propose a model that explains how the spherulocyte subpopulations maturate.

MATERIAL AND METHODS

Animals, bleeding procedure and cell counts

Specimens of *P. gaimardi* (n=6) were collected by free diving at Praia Grande, São Sebastião, SE Brazil (23°49'24" S, 45°25'01" W), while specimens of *P. lividus* (n=6) were collected in the Gulf of Palermo (38°06.00′ N; 13°30.00′ E), Palermo, SW Italy. For both species, coelomic fluid was collected with a syringe needle preloaded with 0.5 ml of isosmotic anticoagulant solution (20 mM ethylenediamine tetraacetic acid (EDTA), sodium chloride 460 mM, sodium sulfate 7 mM, potassium chloride 10 mM, 4-(2-hydroxyethyl)-1-piperazineethanesulfonic acid (HEPES) 10 mM, pH 8.2 –

Dunham and Weissman, 1986), inserted into the peristomial membrane and the same volume of coelomic fluid was withdrawn from each sea urchin. Total cell counts (TCC) were made using a Neubauer chamber just after coelomic fluid collection, and the results adjusted to compensate initial dilution. For differential cell counts (DCC), cell density was adjusted to $1x10^6$ cells/ml using an anticoagulant solution, and the proportion of main cell types, *viz.* phagocytes, vibratile cells, red and colorless spherulocytes, were recorded under a light microscope. In this procedure, due to the delay in finding typical colorless and granular spherulocytes during differential cell counts, and the fact that this delay is able to affect the analysis, these two populations were considered together. Cell viability was determined by the Trypan Blue assay (0.4%) and was higher than 95% in all samples.

Morphological and morphometric analysis

Live cells in suspension were observed just after being collected, as described in Queiroz and Custódio (2015) and 20 cells of each type were measured, except for the rare crystal and progenitor cells, in which only five were measured. For cytological analyses, live cells were deposited on a slide using a cytocentrifuge (FANEN 248, 6 $x10^4$ cells per spot, 80 × g / 5 min), fixed for 45 min in formaldehyde sublimate (Custódio et al. 2004; Queiroz and Custódio, 2015) and stained with toluidine blue (TB) or Mallory's trichrome (MT) (Behmer et al., 1976). For scanning electron microscopy (SEM), live cells were deposited on round coverslips using the cytocentrifuge and fixed with formaldehyde sublimate, as described before. After, the coverslips were washed once in Milli-Q water for 40 minutes, air-dried and stored at room temperature in a closed container with silica gel. Finally, the coverslips were sputter-coated with a 40-60 nm thick layer of gold and photographed in a scanning electron microscope Sigma VP (Zeiss). For morphological descriptions, we will use the terms *flat* and *spread* with different practical meanings. *Flat/flatten* will be used to cells in which it is possible to see the cytoplasm outline (*e.g.* phagocytes), while *spread* will be used to cells in which the cytoplasm is so thin that is difficult to see the boundary between the cell and the substrate (*e.g.* vibratile cells).

For the spherulocytes, three putative differentiation stages - early, intermediate and final - were defined, based on nucleus and spherule diameter as well as cytoplasm organization, as previously observed to *Eucidaris tribuloides* (Queiroz and Custódio,

2015). Measurements of nucleus and cytoplasm of 30 cells in each maturation stage (n= 90 cells for each species) were made using the ImageJ software, and the nucleus/cytoplasm ratio calculated dividing the nucleus diameter by the cytoplasm length of the same cell. Measurements of three spherules per cell from 15 cells per maturation stage were also obtained (n=45 spherules per species). Values are presented as mean ± standard deviation (Table 1 and 2), or maximum-minimum (Table 3). One-way analysis of variance (ANOVA) was used to test differences among nucleus, cytoplasm and spherules diameters, as well as the nucleus/cytoplasm ratio (NCR) of different maturation stages. Student t-test was used to analyze differences in cell type measurements between species. To analyze the relation between spherule size and the stage of maturation, the spherule diameter was tested against the nucleus diameter of the same cell using a Pearson correlation. The GraphPad Prism software v. 5.01 was used to perform all statistical analyses.

RESULTS

Five cell types, phagocytes (Ph), vibratile cells (VC), red, colorless and granular spherulocytes (RS, CS, and GS, respectively) were found in both species (Fig. 1 and 2). Crystal cells (CC), small cells bearing a crystal-like structure in the cytoplasm, were found only in *P. gaimardi*. Meanwhile, progenitor cells (PC), coelomocytes with a disproportionally large nucleus, were found in *P. lividus*. For all spherulocyte subpopulations, a set of morphologically similar cells were observed and interpreted as a putative maturation sequence. These cells can be organized in different stages based on their nuclear size and cytoplasmic characteristics, named Early, Intermediate and Final, (Fig. 3 and 4). Spherulocytes in the early stage have a large nucleus and a homogeneous or lacy cytoplasm. In the intermediate stage, the nucleus becomes smaller and more condensed and the spherules more evident. In the final stage, the cells have the smallest nucleus diameter in comparison to other coelomocytes and a completely spherule-filled cytoplasm. Ultrastructural analyses confirm the pattern observed in cytochemical preparations (Fig. 4).

Total and Differential Cell Counts (TCC and DCC)

The total cell count in the coelomic fluid was similar for both species ($p > 0.05$) (Table 1). Except for the red spherulocyte, there was no significant difference in the cell percentage among the species. Phagocytes were the most frequent subpopulation in both, but the prevalence of the other populations differed (Table 1). For *P. gaimardi*, red spherulocytes were more frequent than colorless/granular and vibratile cells. On the other hand, vibratile cells were the second most frequent type in *P. lividus*, followed by colorless/granular and red spherulocytes. Crystal cells from *P. gaimardi* and progenitor cells from *P. lividus* were rare, accounting for less than 1%.

Morphology of living and stained mature coelomocytes

Live phagocytes were the largest cells (Table 2), usually with many filiform or bladder-like cytoplasmic expansions (Fig. 1A and M). Stained phagocytes were large round to oval flatten cells, with large central to subcentral nucleus (Table 2), and an irregularly vacuolated cytoplasm (Fig. 1G and S). Vibratile cells were round and translucent, with a conspicuous flagellum (Fig. 1B and N). In cytospin preparations, these cells are round spread cells, filled with spherules containing proteoglycans, as indicated by the metachromasia in TB preparations (Fig. 1S and T). We also observed two uncommon cell types: the crystal cell of *P. gaimardi* and the progenitor cell of *P. lividus*. Live crystal cells were small (Table 2), with a prominent translucent green crystal-like structure in its cytoplasm (Fig. 1C). In cytological preparations, this spread cell showed no specific affinity to TB (Fig. 1I) or MT, but the intracellular crystal became darker with both stains. No nucleus could be detected in both preparations. Live progenitor cells showed a round to oval shape, with a relatively large nucleus (Table 2 and Fig. 1O) and the exact morphology can be seen in cytological preparations (Fig. 1U). The nucleus/cytoplasm ratio of this cell (0.77 ± 0.07) is very high in comparison with other cell types.

Live RS and GS were usually round, with round uniform spherules (Fig. 1D, F, P, and R). The colorless spherulocyte (CS) showed an elongated profile, with spherules of various sizes and shapes (Fig. 1E and Q). In RS, the spherules contained echinochrome, as indicated by the red color, and hyaline substances in GS and CS (Fig. 1D-F and P-R). In cytochemical preparations, typical mature red spherulocytes were

very difficult to find, mainly in *P. lividus* RS were very flattened cells tending sometimes to spread, with homogeneous round spherules which stain brownish in MT preparations (Fig. 1J and V *inset*) and dark blue in TB (Fig. 1V). However, mainly in *P. lividus* the most common morphology of mature RS in cytochemical preparations is an almost spread cell with round homogeneous empty vacuoles (Fig. 3D and P). Colorless spherulocytes showed large round to elongated spherules, light blue with MT (Fig. 1K and W) and dark blue in TB slides. Granular spherulocytes showed small round homogeneous spherules, similar in size to that of RS. The GS stain reddish/pinkish with MT (Fig. 1L and X), but not with TB, showing a grayish-blue color.

Morphology of mature coelomocytes in SEM

Phagocytes showed a quite flat and vacuolated cytoplasm, with filiform or bladder-like cytoplasmic expansions and a large nucleus (Fig. 2A and G). Vibratile cells had a pronounced and usually central nucleus and a very spread cytoplasm. Different from the other cells with spherules, vibratile cells seem to be much fragile, losing its spherule integrity and becoming much spread (Fig. 2B and H). Sometimes it is possible to observe the flagellum (Fig. 2B), but it is easily lost during preparations/analysis (Fig. 2H). Crystal cells showed a very spread cytoplasm, with no visible nucleus and a remarkable cubic crystalloid beneath a thin layer of cell membrane (Fig. 2C). Progenitor cells are flat and round, with a large central nucleus surrounded by a thin layer of cytoplasm (Fig. 2I).

Red spherulocyte showed a remarkable thicker nucleus and a very flatten cytoplasm (almost spread), composed by a lattice of large and uniform spaces that contained the spherules (Fig. 2D and J). Although very difficult to find, typical mature RS showed the round regular-sized spherules loosely grouped (Fig. 2D *inset*). On the other hand, CS and GS showed a comparatively thicker cell, with well-delimited spherules of irregular sizes and shapes in CS (Fig. 2E and K), or regular sizes and shapes in GS (Fig. 2F and L).

Spherulocyte morphology during the maturation process

For all spherulocyte subpopulations of both species, a set of morphologically and cytochemically similar cells were found (Fig. 3 and 4), and we interpreted them as a

putative maturation process. In the early stage, RS is a compact cell with a prominent peripheral nucleus. The cytoplasm is composed of a large amount of an unorganized and apparently empty mesh, composed of small granules (Fig. 3A and M; Fig. 4A and J). The CS and GS also showed a large nucleus, but differently from the RS, they have a uniformly homogeneous cytoplasm with a quite finely granular appearance (Fig. 3E, I, Q and U). However, in SEM it is possible to observe that the cytoplasm is formed by discrete divisions, which seem the formation of the spherules (Fig. 4D, G, M, and P). Still, in GS clear spots are common (Fig. 3I, U) that can be seen as empty spaces in SEM (Fig. 4P).

Cells in the intermediate stage showed more evident characteristics. In RS, the nucleus continues remarkable, but the lattice in the cytoplasm becomes more organized than in the previous stage, being composed of a mix of large and small spaces (Fig. 3B, C, N, O and Fig. 4B and K). However, although not so common, sometimes it may be difficult to see this organization in some RS of *P. gaimardi* because the cytoplasm may be covered by a granular material with a brownish coloration in MT preparations (Fig. 3B and C *insets* and Fig. 4B *inset*). In the CS and GS, the homogeneous cytoplasm becomes more subdivided and the spherule outline becomes more and more evident (Fig. 3F, G, J, K, R, S, V, X). In this stage, the heterogeneous spherules of CS are visible (Fig. 4E and N), as well as the homogeneous spherules of GS (Fig. 4H and Q).

In the final stage, for all spherulocytes, the nucleus is condensed and it is possible to completely differentiate the spherules. The RS show a lattice with large and more regular round inclusions (Fig. 3D and P; Fig. 4C and L), that may be covered with a granular material in *P. gaimardi* (Fig. 3D *inset*). The CS and GS present quite evident spherules, with heterogeneous shapes and sizes in CS, and more round and uniform-sized in GS (Fig. 3H, L, T, Z, and Fig. 4F, I, O, and R).

Spherulocyte morphometry during maturation

The measurements show that while nucleus diameter and the Nucleus/Cytoplasm Ratio decreased along the maturation process, the cytoplasm size was stable (Fig. 5 and Table 3). Early RS nuclei were larger, decreasing during the maturation, with the smaller values in the final stage (Fig. 5A). Except for the intermediate stage, there were no differences in nucleus diameter between species (Fig. 5A). The cytoplasm of the red

spherulocyte showed a uniform size along the maturation process (Fig. 5B). Except for the intermediate stage, there was no difference between *P. gaimardi* and *P. lividus* cytoplasm diameter. Considering the Nucleus/Cytoplasm Ratio, the highest values were found in the early stage, which decreased in the final stage. There were differences between early and final stages for both species, but not between species (Fig. 5C).

The CS followed the same general pattern seen in RS (Fig. 5D): the nucleus was larger in the early stage and smaller in the final stage, with significant differences between the early and final stages. Significant differences between species were seen only in the early stage (Fig. 5D). Cytoplasm diameter was similar among all categories, and except for the final stage, there was no difference between the *P. gaimardi* and *P. lividus* (Fig. 5E). Nucleus/Cytoplasm Ratio followed the same tendency observed to RS: highest values in the early stage and smallest ones in the final. The ratio was significantly different between the early and final stages in both species, but interspecific differences were seen only in early and intermediate stages (Fig. 5F), except for the final.

The GS showed interspecific differences in nucleus and cytoplasm diameters since *P. gaimardi* has higher values than *P. lividus* (Fig. 5G-I). The nucleus was significantly larger in the early stage than in the final (Fig. 5G), but the cytoplasm diameter showed similar values among the stages (Fig. 5H). However, interspecies comparisons showed that the measures of *P. gaimardi's* GS cytoplasm were significantly higher than *P. lividus'* (Fig. 5H). Regarding the NCR, cells in the early stage showed higher values than the final stages, and except for the early stage, interspecies differences were statistically significant (Fig. 5I).

The spherule content of RS is very sensitive to cytological procedures, which makes difficult to find typical mature RS (Fig. 1J and V). However, this fact was more frequent in *P. lividus* than in *P. gaimardi*. It was common to find RS in both species completely empty, but with a peculiar cytoplasmic organization, ranging from small to large cytoplasmic reticules (Fig. 3A-D and M-P). After careful analyses, we observed that different spherule diameters could be related to the maturation sequence. There is a strong negative correlation between spherule diameter and nucleus size (*P. gaimardi*: $r = -0.742$, $p = 0.0001$; *P. lividus*: $r = -0.715$; $p < 0.0001$), indicating that the spherules increase while nucleus become more condensed (Fig. 6A and B). Additionally, the spherule diameters of each spherulocyte population differ along the maturation process

(Fig. 6C). The RS in the early stage (Fig. 3M) showed a reticulated and unorganized cytoplasm with very small spherules (0.58 ± 0.13 µm in *P. gaimardi*; 0.64 ± 0.12 µm in *P. lividus*), while there was a mix of organized and unorganized areas with heterogeneously-sized spherules in the intermediate stages (Fig. 3B-C and N-O), measuring 0.95 ± 0.25 µm in *P. gaimardi* and 1.05 ± 0.13 µm in *P. lividus* (Fig. 6C). In the final stage, the cytoplasm of RS showed a uniformly organized lattice composed by large round-shaped spaces (Fig. 4D and P), whose diameter is 1.61 ± 0.30 µm in *P. gaimardi* 1.5 ± 0.31 µm in *P. lividus*. These differences were significant among maturation stages in the same species, but not between species (Fig. 6C).

DISCUSSION

The main biological aspects of *P. lividus* have been well-known since it is widely used as an animal model (Cervello et al., 1994; Arizza et al., 2007). In an immunological perspective, although there are works addressing the dissolved molecules in the coelomic fluid (Stabili et al., 1996; Drago et al., 2009), the coelomic cells have been the main target (Cervello *et al*., 1994; Stabili et al., 1996; Arizza et al., 2007; Giaramita et al., 2008). These studies, in addition to contributing to the knowledge of *P. lividus* physiology, increased significantly the understanding of the immune aspects of Echinoidea as a whole (Smith et al., 2010; 2018). On the other hand, the knowledge on these aspects on the South Atlantic congener *P. gaimardi* is completely absent, and even basic data such as the number of coelomic subpopulations or their proportions are yet unknown.

Total and differential cell counts of *P. lividus* were similar to that of *P. gaimardi* and fitted the pattern previously described for echinoids in the literature (Bertheussen and Seljelid, 1978; Smith et al., 2010; Coates et al., 2017). Even for the red spherulocytes, that showed a higher percentage in *P. gaimardi*, the proportions are in accordance with *P. lividus* and other sea urchins (Smith et al., 2010; Coates et al., 2017). Some factors have been pointed out as influencing physiological or immune parameters, such as gender or age (Arizza et al., 2013; McCaughey and Bodnar, 2012), the last one also affecting cell counts (McCaughey and Bodnar, 2012). Thus, it is possible that the difference observed in the RS percentage can be related to factors other than the interspecific differences.

Both species presented six cell types, (*cf.* Fig. 1, 2), and not only the four usual coelomocytes commonly described in the literature (*i.e.* phagocytes, vibratile cells, and red and colorless spherulocytes - Deveci et al., 2015; Smith et al., 2010; 2018). Petaloid and filopodial phagocytes were the most common morphologies observed in the fresh coelomic fluid. However, they not represent the real subpopulation of phagocytes (Edds 1993, Gross et al., 2000). In fact, petaloid and filopodial forms have been pointed out as transitory stages of the same cell type (Eliseikina and Magarlamov, 2002; Matranga et al., 2005). In cytochemical preparations, phagocytes are quite remarkable, and both morphologies can be seen. They are flattened large cells, with a large and poorly condensed nucleus, many filiform or bladder-like expansions and a vacuolated cytoplasm. All these features make this cell type unmistakable, and the same features were already recorded to *P. lividus* (Deveci et al., 2015).

Vibratile cells are a very intriguing subpopulation of coelomocytes. Live cells show a round outline, vacuolated cytoplasm and a remarkable flagellum, which is its main distinctive characteristic (Johnson, 1969). However, these cells are very sensitive to handling/fixation, easily losing the flagellum. Nevertheless, vibratile cells can be promptly identified in cytological preparations by using TB stain, even after losing the flagellum (*cf.* Fig. 1). In TB preparations, vibratile cells show a usual central to subcentral nucleus and a very spread cytoplasm composed by homogeneous spherules that stain purple. Among the sea urchin coelomocytes, vibratile cells are the only cell type that stains purple in TB preparations. This color means a weak metachromasy (ß – metachromasia; Sridharan and Shankar, 2012) provided by its glycosaminoglycan reserves (Volpi and Maccary, 2002). This reaction was seen here for both *Paracentrotus* species and an apparently purple coloration was previously seen in *P. lividus* (Deveci et al., 2015) and *Strongylocentrous purpuratus* (Holland et al. 1965).

Crystal cells were already recorded in holothuroids, ophiuroids and asteroids (Andrew, 1962; Johnson and Beeson, 1966; Smith, 1981), but this is the first record in sea urchins. The crystalloid in CC from holothurians, which are the most known model, dissolve under the slight osmotic stress or staining procedures (Hetzel, 1963). On the other hand, the one from *P. gaimardi*'*s* cells is resistant to staining and SEM procedures (*cf.* Fig.s 1 and 2). These characteristics suggest that, although the CC of *P. gaimardi* also has a crystal in its cytoplasm, probably it is not the same cell found in holothuroids. Progenitor cells found in *P. lividus* were morphologically similar to the small cells

described by Deveci et al. (2015), with a large nucleus, a thin cytoplasm and a very low percentage in the coelomic fluid suggesting that they are the same cell type. Lastly, although CC and PC have been specific to *P. gaimardi* and *P. lividus* respectively, we cannot discard the possibility of their widespread presence in this genus. These cells were very rare in the coelomic fluid, and we may have failed to find them in the studied samples.

Red and colorless spherulocytes have been traditionally studied as live cells, being easily identified according to the spherule content (Deveci et al., 2015; Queiroz and Custódio, 2015). However, these two subpopulations can also be easily distinguished in cytochemical preparations, according to their morphology and stain affinity (Queiroz and Custódio, 2015). The RS and CS of *P. gaimardi* and *P. lividus* followed exactly the same pattern observed in *E. tribuloides* (Queiroz and Custódio, 2015), but CS morphology differed from that previously illustrated to *P. lividus*. Actually, the stained cell illustrated as colorless spherulocytes by Deveci et al. (2015) is very similar in morphology to the empty RS depicted here (*Cf.* Fig. 3O and P), or the degranulated RS of *P. lividus* depicted by Coates et al. (2017 – Fig. 3). Still, the large subcentral nucleus and cytoplasmic organization of *P. lividus* CS depicted by Deveci et al. (2015) resembles in some aspects the red spherulocyte of *E. tribuloides* (Queiroz and Custódio, 2015 – Fig. 4).

In addition to the spherulocyte subpopulations usually observed in sea urchins, we found a little-known subtype: the granular spherulocyte. This newly-described cell (Queiroz and Custódio, 2015) was found in *P. gaimardi* and in *P. lividus* and is quite similar to that of *E. tribuloides*. Despite all similarity, live granular spherulocytes in *Paracentrotus* species were not brown as in *E. tribuloides*. However, Jacobson and Millot (1953) suggest that all spherule cells are colorless in the coelomic fluid, and the red coloration of the red spherulocyte is due to some unknown chemical reaction of its content when exposed to the air. Clearly, this is not true to the RS but explains properly why only a few live brown granular spherulocytes were found in *E. tribuloides* (Queiroz and Custódio, 2015), and only colorless cells were found in *Paracentrotus* species.

Works addressing echinoderm coelomocytes through SEM are scarce and only sea stars and sea cucumber were already studied (Kaneshiro and Karp, 1980; Silva and Peck, 2000; Xing et al., 2008). These works used different methods to fix the cells and/or attach them on stubs, which hinder morphological comparisons. However, in this

study we used SEM analysis to obtain structural details for *Paracentrotus* coelomocytes, confirming all morphological features observed in cytological preparations. Morphological characteristics were quite specific, allowing accurate identification and based on these characteristics, coelomocytes could be divided into non-spherulous and spherulous cells. Phagocytes, crystal, and progenitor cells are in the first group. Phagocytes and progenitor cells have a flattened appearance, but the analysis of the very heterogeneous cytoplasm with a filiform or blader-like expansion of the phagocytes and the remarkably large nucleus surrounded by a thin layer of cytoplasm of the progenitor cell is enough to accurate identification. Crystal cells are non-spherulous cells with a very spread cytoplasm and a conspicuous crystalloid. Regarding spherulous cells, they can be divided into two subgroups: cells with flattened or spread cytoplasm and a thicker nucleus; or cells with thicker cytoplasm and depressed nucleus. Although vibratile cells and RS share the characteristics of the first subgroup, the very spread cytoplasm of vibratile cells and the apparently empty reticulated cytoplasm in RS provide characteristics to accurate identification. Colorless and GS are in the second subgroup and can be differed according to their cytoplasmic spherules, large and heterogeneous in CS and smaller and homogeneous in GS.

For vertebrates, the main aspects of blood cells have already long been unraveled (Turgeon, 2012; Campbell, 2015), including the identification of specific markers to differentiate maturation stages (Terstappen et al., 1990). However, the situation for invertebrate is quite different and except for insects, the study of their "blood cells" is comparatively less usual. Molecular or fluorescent markers are limited, and unable to differentiate cell types (Dyrynda et al., 1997), which is also true to echinoderms (Lin et al. 2007; Li et al. 2010). Thus, most studies with invertebrates still use morphological features to examine hemocyte/coelomocyte maturation (Battison et al., 2003; Rebelo et al. 2013).

Morphological and cytochemical data were clearly useful for our understanding of the set of spherulocytes bearing similar features. Since each subpopulation showed a continuous set of specific features, we observed that these cells could be organized in a sequence. Based on the nucleus and cytoplasm modifications, we propose a model that describes how spherulocytes maturate (Fig. 7). Immature cells show a large nucleus, a homogeneous cytoplasm filled by small spherules and present a high NCR. During maturation, the nucleus becomes more condensed, the spherules

become larger, and the NRC decreases; culminating in mature cells, which have the smallest nuclear diameter, a cytoplasm completely organized and filled with spherules as well as the lowest NCR value.

The changes in the nucleus size along the maturation suggest an intense RNA transcription in immature cells (Sato et al. 1994; Schmidt & Schibler 1995; Webster et al. 2009), which seems to be reduced in mature spherulocytes. In immature spherulocytes, the spherule outline is tenuous and the content is homogeneous, but these characteristics change during maturation, and the spherules can be easily distinguished in mature stages. This fact was also observed in the early GS of *E. tribuloides*, in which the cytoplasm is filled with tiny structures, which seem to fuse, originating the large spherules in mature cells (*cf.* Queiroz and Custódio, 2015 - Fig. 8). A similar situation was observed here mainly in RS, in which immature cells showed smaller vacuoles than mature ones. Thus, we hypothesize that immature spherulocytes with a large nucleus and small vacuoles would be actively transcribing to produce their contents. Along with the maturation the RNA transcription is reduced, the nucleus starts to condense and the tiny spherules fuse, originating mature cells with a smaller nucleus and larger spherules (Fig. 8).

The maturation process of *Paracentrotus* spherulocytes hypothesized here follows the pattern observed for other invertebrate circulating cells bearing vacuoles. Hemocytes from the mollusks *Crassostrea rhizophorae* and *Bulinus truncate*, and the crustacean *Homarus americanus* increased the number and/or the size of cytoplasmic spherules. For the last two species, the chromatin was more condensed and organized in mature cells (Cheng and Guida 1980; Battison et al., 2003; Rebelo et al., 2013), and the NCR was also high in immature hemocytes of *H. americanus* (Battison et al., 2003). Similar changes in the nuclei were also observed in mammalian blood cells (Moras et al., 2017, Arpitha et al., 2005; Pethig et al., 2010), and related to the levels of transcriptional activity (Efroni et al., 2008).

There has long been a consensus that echinoids present only four main types of circulating cells in the coelomic fluid (Smith, 1981; Smith et al., 2010; 2018), although new subpopulations have recently been identified (Queiroz and Custódio, 2015). Here, using an integrative approach combining live cells in suspension, cytology and scanning electron microscopy, we characterize sea urchin coelomocytes for the first time in a completely comparative approach. This is also the first study dealing with

Paracentrotus cells and seven coelomic subpopulations were found in their coelomic fluid, including the newly-described granular spherulocyte and the crystal and progenitor cells. Lastly, we propose a model to explain how spherulocytes maturate in sea urchins, based on evidence of *Paracentrotus* species.

Thus, the results in this paper arise some important questions about sea urchin coelomocytes that can guide future researches: would the same coelomic subpopulations and the maturation process be found in other sea urchin species? What are the physiological functions of the granular spherulocyte and the crystal cell? Are progenitor cells really pluripotent cells for sea urchins? Does *Paracentrotus gaimardi* show the same physiological/immunological responses already observed in *P. lividus?* We found a new coelomic subpopulation in *P. lividus,* one of the most studied sea urchin species of the world, and this makes clear that even the basics aspects of sea urchin physiology/immunology need to (re)visited.

ACKNOWLEDGMENTS

The authors are indebted to Prof. Renata Guimarães Moreira, Prof. José Eduardo A. R. Marian (IB-USP), and Prof. Álvaro Migoto (CEBIMAR-USP), for support with light microscopy photographs. We also thank Prof. Dr. Alberto Ribeiro and the technicians Sheilla Shumidt and Marcio Cruz for support with electron microscopy imaging. This work was supported by FAPESP (Proc. 2015/21460-5 and 2018/14497-8) and Coordenação de Aperfeiçoamento de Pessoal de Nível Superior (CAPES).

REFERENCES

Abdel-Hamid, M. E., Mona, M. H., Shoukr, F. A., Self, A. I., Eissa, S. H. (1993). The blood cells of a sea urchin from Abou-Kir coast Alexandria, Egypt. Qatar Univ. Sci. J., 13(1): 92- 100.

Andrew, W. (1962). Cells of the blood and coelomic fluids of tunicates and echinoderms. American Zoologist, 2:285-297.

Arizza, V., Giaramita, F., Parrinello, D., Cammarata, M., Parrinello, N. (2007). Cell cooperation in coelomocyte cytotoxic activity of *Paracentrotus lividus* coelomocytes. Comparative Biochemistry and Physiology Part A: Molecular & Integrative Physiology 147:389–394. doi:10.1016/j.cbpa.2007.01.022.

Arizza, V., Vazzana, M., Schillaci, D., Russo, D., Giaramita, F. T., Parrinello N. (2013). Gender differences in the immune system activities of the sea urchin *Paracentrotus lividus*. Comparative Biochemistry and Physiology, Part A, 164: 447–455.

Arpitha, P., Prajna, N. V., Srinivasan, M., Muthukkaruppan, V., (2005). High expression of p63 combined with a large N/C ratio defines a subset of human limbal epithelial cells: implications on epithelial stem cells. Invest. Ophthalmol. Vis.Sci. 46 (10), 3631–3636.

Battison, A., Cawthorn, R., Horney, B. (2003). Classification of *Homarus americanus* hemocytes and the use of differential hemocyte counts in lobsters infected with *Aerococcus viridans* var. *homari* (Gaffkemia). J Invertebr Pathol. 84(3):177-97.

Bertheussen, K., Seljelid, R. (1978). Echlnoid phagocytes in vitro. Expl Cell Res. 11 1: 401-412

Boudouresque, C. F. & Yoneshigue Y. (1987). Données preliminaires sur les peuplementes phytobenthiques et sur les echinides herbivores de la région de Cabo Frio (Bresil). Nerítica, 2: 65-106.

Calderón, IVentura C. R. R., Turon X., H. A. Lessios. (2010). Genetic divergence and assortative mating between color morphs of the sea urchin *Paracentrotus gaimardi*. Mol. Ecol., 19: 484-493.

Calderón, I., Turon X. Lessios H.A. (2009). Characterization of the sperm molecule binding in the sea urchin genus *Paracentrotus*. J. Mol. Evol., 68: 366-376.

Campbell, T. W. (2015). Exotic Animal Hematology and Cytology. Fourth Edition. Wiley-Blackwell 424 pp.

Cervello, M., Arizza, V., Lattuca, G., Parrinello, N., Matranga, V. (1994). Detection of vitellogenin in a subpopulation of sea urchin coelomocytes. European Journal of Cell Biology, 64(2):314-9.

Cheng, T. C., Guida, V. G., (1980). Hemocytes of *Bulinus truncates rohlfsi* (Mollusca: Gastropoda). J Invertebr Pathol 35:158–167.

Chiaramonte, M., Russo, R. (2015). The echinoderm innate humoral immune response, Italian Journal of Zoology, 82:3, 300-308, DOI: 10.1080/11250003.2015.1061615

Collard, M., Laitat, K., Moulin, L., Catarino, A. I., Grosjean, P., Dubois, P. (2013). Buffer capacity of the coelomic fluid in echinoderms. Comparative Biochemistry and Physiology, Part A 166 (2013) 199–206.

Drago, F., Malagoli, D., Pezzino, F. M., D'Urso, V., Sammartano, F. (2009). Presence of a low molecular weight lectin in the coelomic fluid of the sea urchin *Paracentrotus lividus*. Invertebrate Survival Journal 6: 15-20.

Duarte, M., Ventura, C., Silva, E. (2016). Genetic variation in color morphs of the endangered species, *Paracentrotus gaimardi* (Echinoidea: Echinidae). Lat. Am. J. Aquat. Res, 44(1): 46-55.

Dyrynda EA, Pipe RK, Ratcliffe NA (1997) Sub-populations of hemocytes in the adult and developing marine mussel, *Mytilus edulis*, identified by use of monoclonal antibodies. Cell Tissue Res 289:527–536.

Edds, K. T. (1993). Cell biology of echinoid coelomocytes. I. Diversity and characterization of cell types. J. Invert. Biol. 61: 173-178.

Efroni, S., Duttagupta, R., Cheng, J., Dehghani, H., Hoeppner, D. J., Dash, C., Bazett-Jones, D. P., Le Grice, S., McKay, R. D., Buetow, K. H., Gingeras, T. R., Misteli, T., … Meshorer, E. (2008). Global transcription in pluripotent embryonic stem cells. Cell stem cell, 2(5), 437-47.

Eliseikina, M. G., Magarlamov, T. Y. (2002). Coelomocyte morphology in the Holothurians *Apostichopus japonicus* (Aspidochirota: Stichopodidae) and *Cucumaria japonica* (Dendrochirota: Cucumariidae). Russian Journal of Marine Biology, 28:197–202.

Fontaine, A. R., Hall, B. D. (1981). The haemocyte of the holothurians *Eupentacta quinquesemita*: Ultrastructure and maturation. Canadian Journal of Zoology 59:1884–1891. doi:10.1139/

Gerardi, G., Lassegues, M., Canicattì, C., (1990). Cellular distribution of sea urchin antibacterial activity. Biol. Cell 120, 161–165.

Gianguzza, P., Badalamenti, F., Gianguzza, F., Bonaviri, C., Riggio, S. (2008). The operational sex ratio of the sea urchin *Paracentrotus lividus* populations: the case of the Mediterranean marine protected area of Ustica Island (Tyrrhenian Sea, Italy). Marine Ecology – AN Evolutionary Perspective 30:125–132.

Giaramita, F. T., Vizzini, A., Parrinello, D., Mansueto, V., Salerno, G., Arizza, V. (2008). Effetti del cadmio sulle attività cellulari dell'echinoderma *Paracentrotus lividus* (Echinoidea). Biologia Marina Mediterranea, 15 (1): 420-421.

Gildor, T., Malik, A., Sher, N., Avraham, L., Ben-Tabou de-Leon, S. (2016). Quantitative developmental transcriptomes of the Mediterranean sea urchin *Paracentrotus lividus*. Mar Genomics, 25:89-94.

Gross, P. S., Clow L. A., Smith L. C. (2000). SpC3, the complement homologue from the purple sea urchin, *Strongylocentrotus purpuratus*, is expressed in two subpopulations of the phagocytic coelomocytes. Immunogenetics 51: 1034-1044.

Hetzel, H. R. (1963) Studies on holothurian coelomocytes. I. A survey of coelomocyte types. Biol Bull 125:289–301

Holland, N. D., Phillips, J. H., Giese, A. C. (1965). An Autoradiographic Investigation of Coelomocyte Production in the Purple Sea Urchin (*Strongylocentrous purpuratus*). Biol Bull 128(2):259–270.

Johnson, P.T., Beesan, R.J. (1966). In vitro studies on *Patira miniata* (Brandt) coelomocytes, with remarks on revolving cysts. Life Sciences, 5: 1641-1666.

Kaneshiro ES, Karp RD. 1980. The ultrastructure of coelomocytes of the sea star *Dermasterias imbricata*. Biol. Bull. 159: 295-310.

Lemee, R., Boudouresque, C.F., Gobert, J., Pascale M., Mari X., Meinesz A., Menager, V., Ruitton, S. (1996). Feeding behavior of *Paracentrotus lividus* in the presence of *Caulerpa taxifolia* introduced in the Mediterranean Sea. Oceanologica Acta 19(3–4), 245–53.

Lopes, E.M., Ventura, C.R.R. (2012). Morphology and gametic compatibility of color morphs of *Paracentrotus gaimardi* (Echinodermata: Echinoidea). Invertebrate Biology 131(3): 224–234.

Matranga, V., Pinsino, A., Celi, M., Natoli, A., Bonaventura, R., Schröder, H. C, Müller, W. E. (2005). Monitoring chemical and physical stress using sea urchin immune cells. Progress in Molecular and Subcellular Biology 39:85–110.

McCaughey, C., & Bodnar, A. (2012). Investigating the sea urchin immune system: Implications for disease resistance and aging. Journal of Young Investigator, 23: 25-33.

Moras, M., Lefevre, S. D., Ostuni, M. A. (2017). From Erythroblasts to Mature Red Blood Cells: Organelle Clearance in Mammals. Frontiers in physiology, 8, 1076. doi:10.3389/fphys.2017.01076.

Mortensen, T. H. (1943). Monograph of the Echinoidea. III, 3. Camarodonta. II. Echinidae, Strongylocentrotidae, Parasaleniidae, Echinometridae. C.A. Reitzel, Copenhagen, 446 pp.

Ozlem C. A., Hatice P. (2008). Effects of bisphenol A on the embryonic development of sea urchin (*Paracentrotus lividus*). Environmental Toxicology, 23(3):387-92.

Pagliara P. & Stabili L. (2012). Zinc effect on the sea urchin *Paracentrotus lividus* immunological competence. Chemosphere, 89(5): 563-568.

Pantazis, P.A. (2009). The culture potential of *Paracentrotus lividus* (Lamarck 1816) in Greece: a preliminary report. Aquaculture International, 17: 545. https://doi.org/10.1007/s10499-008-9223-5

Pethig, R., Menachery, A., Pells, S., De Sousa, P., (2010). Dielectrophoresis: a review of applications for stem cell research. J. Biomed. Biotechnol. 2010, 182581.

Pétinay, S., Chataigner, C., Basuyaux, O. (2009). Standardization of larval development of the sea urchin, *Paracentrotus lividus*, as a tool for the assessment of seawater quality. Compets Rendus Biologies, 332(12):1104-1114.

Pinsino, A., Russo, R., Bonaventura, R., Brunelli, A., Marcomini, A., Matranga, A. (2015). Titanium dioxide nanoparticles stimulate sea urchin immune cell phagocytic activity involving TLR/p38 MAPK-mediated signaling pathway. Scientific Reports. DOI: 10.1038/srep14492

Ramirez-Gomez, F., Aponte-Rivera F., Mendez-Castaner L., Garcia-Arraras, J. E. (2010). Changes in holothurian coelomocyte populations following immune stimulation with different molecular patterns. Fish Shellfish Immunol. 29: 175-185.

Ramírez-Gómez, F. & García-Arrarás, J.E. (2010). Echinoderm immunity. ISJ 7: 211-220.

Rebelo M.dF., Figueiredo E.dS., Mariante R.M., Nóbrega A., de Barros C.M., Allodi S. 2013. New Insights from the Oyster *Crassostrea rhizophorae* on Bivalve Circulating Hemocytes. PLoS ONE 8(2): e57384.

Schillaci, D., Cusimano, M.G., Spinello, A., Barone, G., Russo, D., Vitale, M., Parrinello, D., Arizza, V. (2014). Paracentrin 1, a synthetic antimicrobial peptide from the sea-urchin *Paracentrotus lividus*, interferes with staphylococcal and *Pseudomonas aeruginosa* biofilm formation. AMB Express, 4, 78. doi:10.1186/s13568-014-0078-z

Silva JRMC, Peck L. 2000. Induced in vitro phagocytosis of the Antarctic starfish *Odontaster validus* (Koehler 1906) at 0°C. Polar Biology 23: 225±230

Smith L.C., Hawley T.S., Henson J.H., Majeske A.J., Oren M., Rosental B. (2019). Methods for collection, handling, and analysis of sea urchin coelomocytes. In: Methods in Cell Biology, ISSN 0091-679X, https://doi.org/10.1016/bs.mcb.2018.11.009

Smith, V.J. (1981). Invertebrate blood cells. In: Ratcliffe NA, Riowley AF (eds), The echinoderms, Academic Press, New York, pp 513-562.

Stabili, L., Pagliara, P., Roch, P. (1996). Antibacterial activity in the coelomocytes of the sea urchin *Paracentrotus lividus*. Comparative Biochemistry and Physiology Part B: Biochemistry and Molecular Biology, 113(3): 639-644.

Telford, M.J., Lowe, C.J., Cameron, C. B., Ortega-Martinez, O., Aronowicz, J., Oliveri, P., Copley, R.R. (2014) Phylogenomic analysis of echinoderm class relationships supports Asterozoa. Proc. R. Soc. B 281: 20140479. http://dx.doi.org/10.1098/rspb.2014.0479

Terstappen, L.W., Safford, M., Loken, M. R. (1990). Flow cytometric analysis of human bone marrow. III. Neutrophil maturation. Leukemia, 4(9):657-663.

Tyler, R.D., Cowell, R.L., 1998. Bone marrow. In: Cowell, R.L. (Ed.), Diagnostic Cytology of the Dog and Cat. Mosby, St. Louis., pp. 99–119.

Turgeon, M.L. (2012). Clinical hematology: theory and procedures. Lippincott Williams & Wilkins.

Turon, X., Giribet, G., Lopez, S., Palacin, C. (1995). Growth and population structure of *Paracentrotus lividus* (Echinodermata: Echinoidea) in two contrasting habitats. Marine Ecology Progress Series. 122: 193-204.

Villaça, R.C. & Yoneshigue Y. (1987). Données préliminaires sur le comportment alimentaire de *Paracentrotus gaimardii* dans la région de Cabo-Frio (Bresil). In: C.F. Boudouresque (ed.). Colloque International sur *Paracentrotus lividus* et les oursins comestibles, GIS Posidoinie publ, Marseille, pp. 125-138.

Volpi, N., & Maccary F. (2002). Detection of submicrogram quantities of glycosaminoglycans on agarose gels by sequential staining with toluidine blue and Stain-All. Electrophoresis, 23(24): 4060-4066.

Weinstein, P.P. (2006). Morphological differentiation and function of the coelomocytes in the parasitic stages of *Nippostrongylus brasiliensis*. J Parasitol, 92(5):894-917.

Xavier, L.A.R. (2010). Checklist of Echinodermata in Santa Catarina State, Brazil. Braz. J. Aquat. Sci. Technol. 14(2): 73-78.

Xing J, H.S. Yang, M.Y. Chen, Morphological and ultrastructural characterization of the coelomocytes in *Apostichopus japonicus*, Aquat. Biol. 2 (2008) 85–92.

Yeruham, E., Rilov, G., Shpigel, M., Abelson, A. (2015). Collapse of the echinoid *Paracentrotus lividus* populations in the Eastern Mediterranean—result of climate change? Scientific Reports. 2015;5:13479. doi:10.1038/srep13479.

Figures, Tables, and Captions

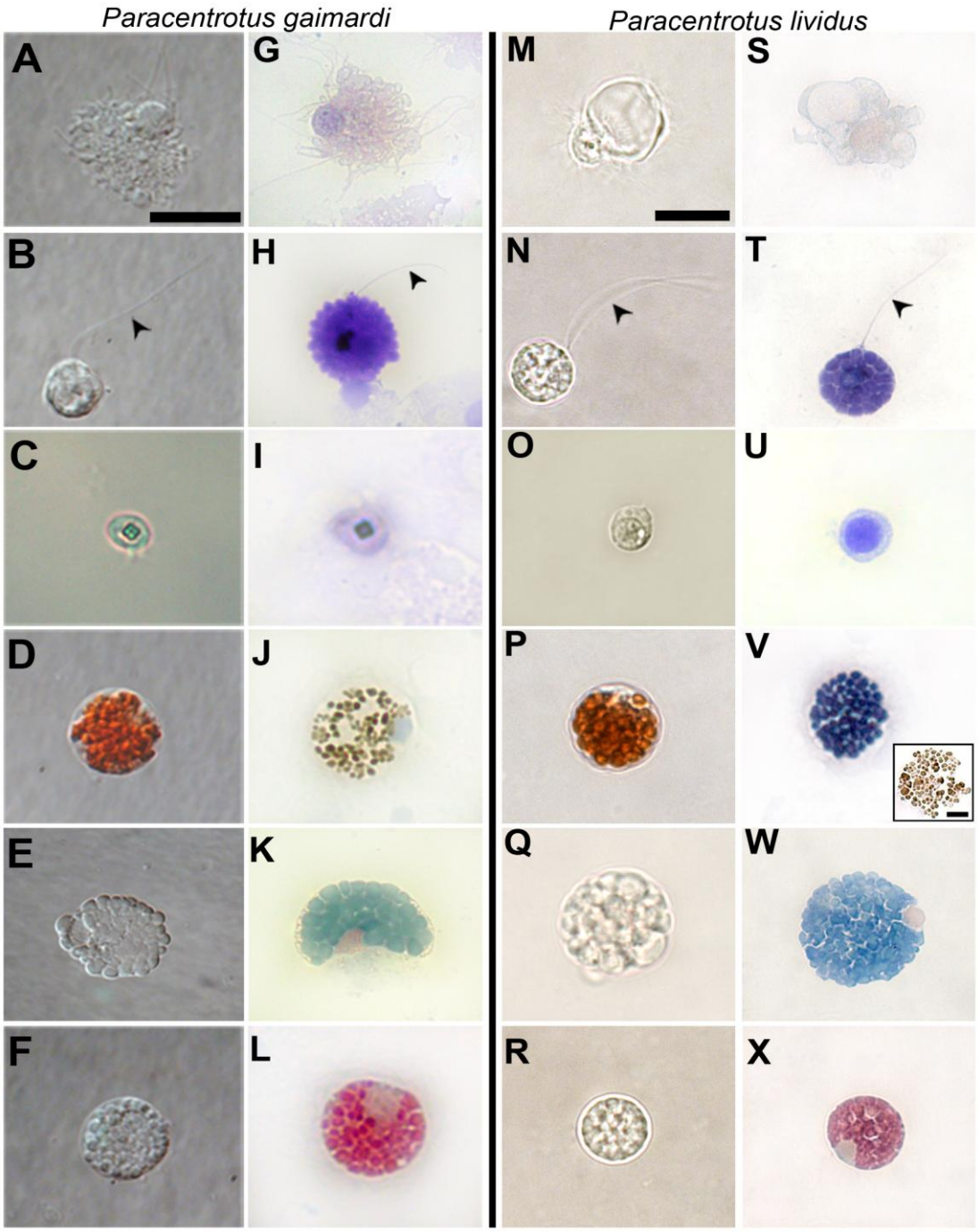

Figure 1 – Live and stained mature coelomocytes of *Paracentrotus* sea urchins. A-L – coelomocytes of *Paracentrotus gaimardi*; M-X – coelomocytes of *Paracentrotus lividus*. A, G, M, and S – Phagocytes; B, H, N, and T – Vibratile cell; C and I – Crystal cell; O and U – Progenitor cell; D, J, P, and V – Red spherulocyte; E, K, Q, and W – Colorless spherulocyte; F, L, R and X – Granular spherulocyte. A-F and M-R – Live cells; G-L and S-X – Stained cells; A-B and D-F – Differential interference contrast; C and M-R – Light microscopy; G, J-L, S, V *inset*, W and X – Mallory's trichrome; H-I, T-V – Toluidine blue. Legend: Arrowhead = Flagellum. Scale: 10 µm.

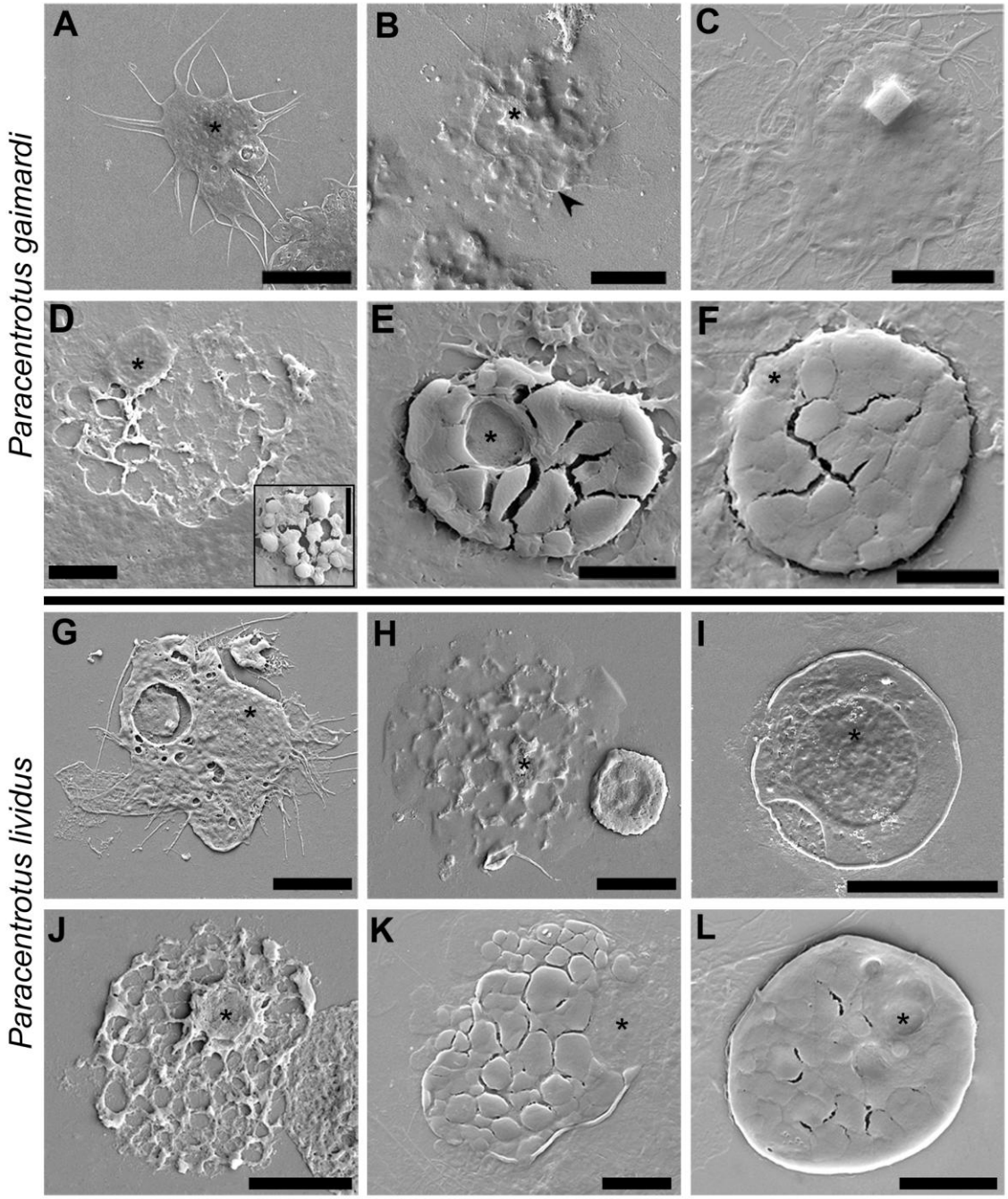

Figure 2 – Scanning electron transmission of mature coelomocytes of *Paracentrotus* sea urchins. A-F – coelomocytes of *P. gaimardi*; G-L – coelomocytes of *P. lividus*. A and G– Phagocyte; B and H – Vibratile cell; C – Crystal cell; I – Progenitor cell; D and J – Red spherulocyte; D *inset* – Typical mature Red spherulocyte; E and K – Colorless spherulocyte; F and L – Granular spherulocyte. Legend: Arrowhead = Flagellum; Asterisk = nucleus. Scale: A = 10 µm; B-L = 5 µm.

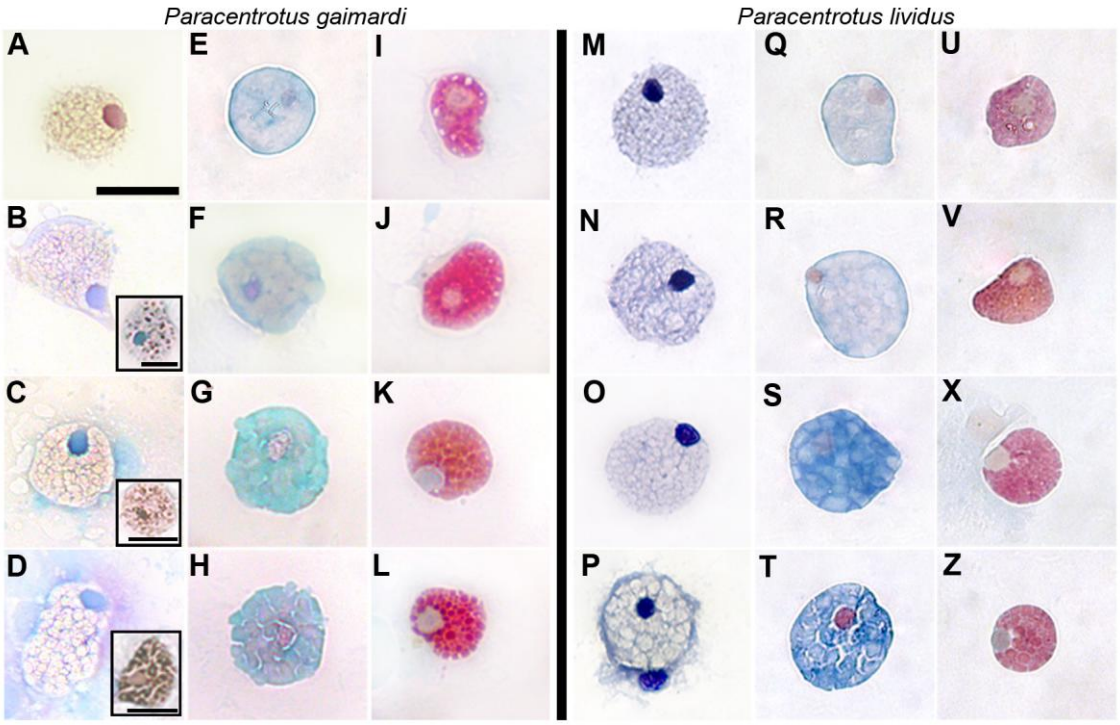

Figure 3 – Stained spherulocytes of *Paracentrotus* sea urchins in different stages of maturation. A-L – Spherulocytes of *P. gaimardi*; M-Z – Spherulocytes of *P. lividus*. A-D and M-P – Red spherulocyte; E-H and Q-T – Colorless spherulocyte; I-L and U-Z – Granular spherulocyte. A, E, I, M, Q, and U – Early stage; B-C, F-G, J-K, N-O, R-S, V-X – Intermediate stage; D, H, L, P, T, Z – Final stage. A-L and Q-Z – Mallory trichrome; M-P – Toluidine blue. Scale: 10 µm.

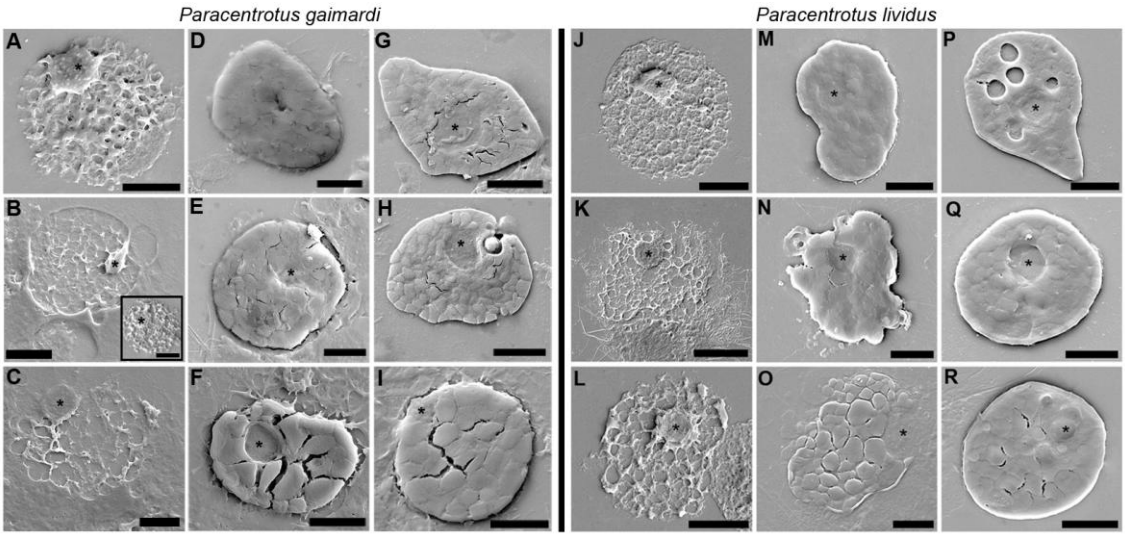

Figure 4 – Scanning electron microscopy of *Paracentrotus* sea urchins spherulocytes in different stages of maturation. A-I – Spherulocytes of *P. gaimardi*; J-R – Spherulocytes of *P. lividus*. A-C and J-L – Red spherulocyte; D-F and M-O – Colorless spherulocyte; G-I and U-Z – Granular spherulocyte. A, D, G, J, M, and P – Early stage; B, E, H, K, N, and Q – Intermediate stage; C, F, I, L, O, and R – Final stage. Scale: A-J and L-R = 5 µm; K = 10 µm.

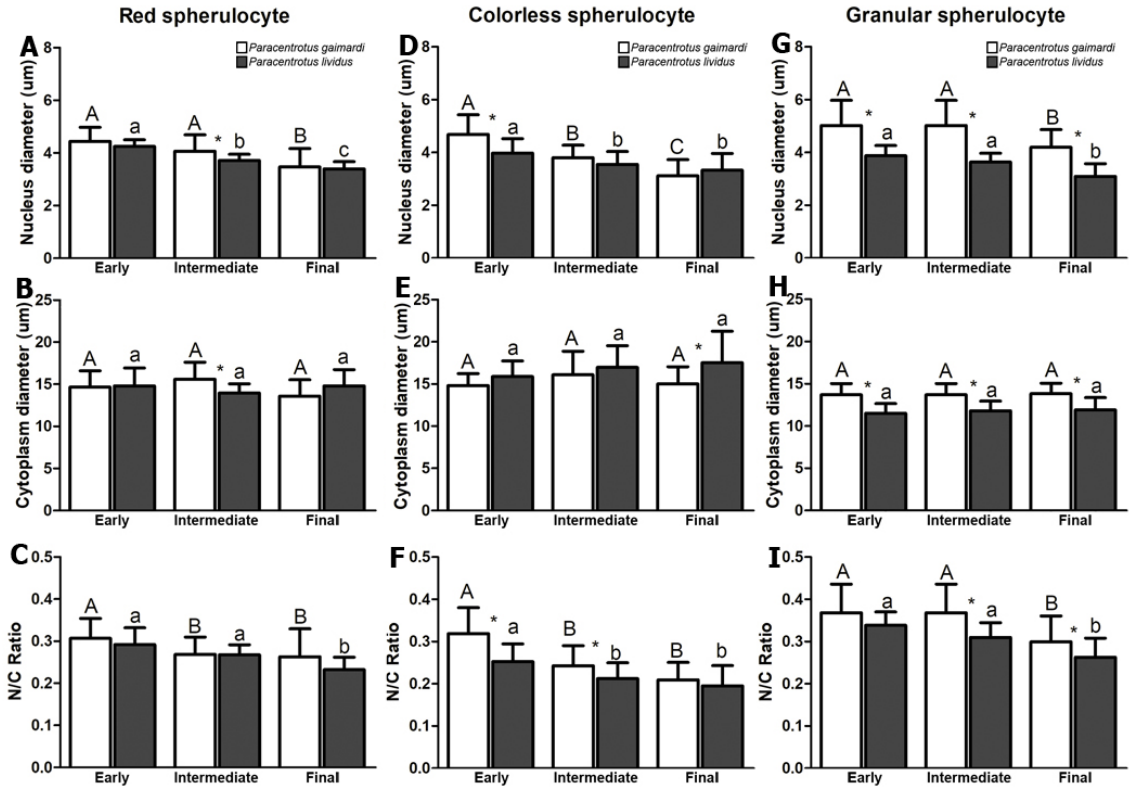

Figure 5 – Morphometric characteristics of *Paracentrotus gaimardi* and *Paracentrotus lividus* spherulocytes. A-C – Nucleus diameter; D-F – Cytoplasm diameter; G-I – Nucleus/Cytoplasm Ratio. Capital letters – *P. gaimardi*, Small letters – *P. lividus*. For each parameter, distinct letters show significant differences among stages ($p < 0.05$); asterisk (*) shows significant differences between species ($p < 0.05$).

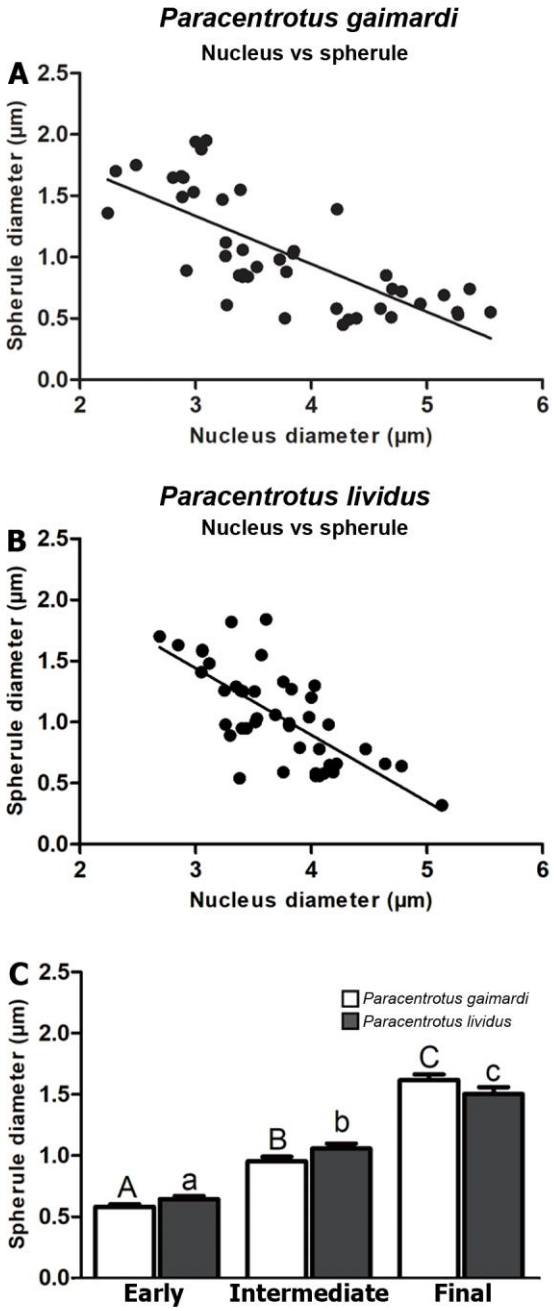

Figure 6 – Spherule diameter of red spherulocytes in *Paracentrotus gaimardi* and *Paracentrotus lividus*. A and B – Pearson correlation between nucleus diameter and spherule diameter in *P. gaimardi* and *P. lividus* respectively. C – Comparison of spherule diameter in different maturation stages in *P. gaimardi* and *P. lividus*. Capital letters – *P. gaimardi*, Small letters – *P. lividus*. Distinct letters show significant differences among maturation stages ($p < 0.05$).

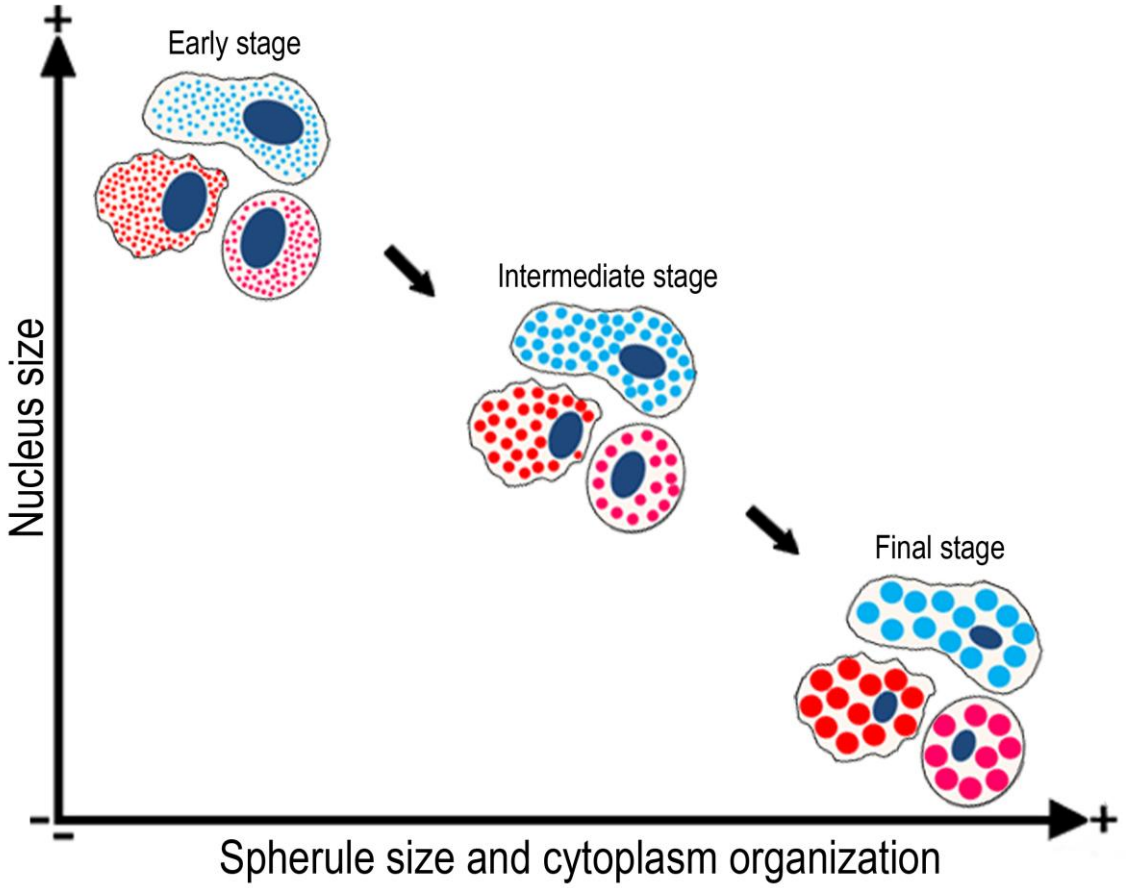

Figure 7 – Proposed model for spherulocytes maturation, as seen by morphological and morphometric features. In the early stage, spherulocytes present a large nucleus and an unorganized cytoplasm filled with small spherules. During the maturation, the nucleus decrease in diameter and the tiny cytoplasmic spherules fuse, becoming larger. In the final state, these coelomocytes show the smaller nucleus diameter and the cytoplasm is filled with large spherules. The colors and the shapes in the picture refer to the remarkable color and morphology of the spherulocytes, either live or stained with Mallory's Trichrome. Legend: Red = Red spherulocyte; Blue = colorless spherulocyte; Pink = granular spherulocytes.

Tables

Table 1 – Total and differential cell counts of *Paracentrotus* sea urchins

	Paracentrotus gaimardi	***Paracentrotus lividus***
Total cell count (cell/mL)	$5.53 \times 10^6 \pm 5 \times 10^5$	$5.35 \times 10^6 \pm 5.75 \times 10^5$
Differentia cell count (%)		
Phagocytes	77.8 ± 1.8%	81.9 ± 4.1%
Vibratile cells	5.8 ± 1.46	7.74 ± 2.47
Red spherulocyte	10 ± 0.45 [a]	5.03 ± 1.34
Colorless spherulocyte	6.39 ± 0.85	5.33 ± 0.91
Crystal cell	>1	-
Progenitor cell	-	>1

a = Significant differences in T-student test ($p < 0.05$)

Table 2 – Cytoplasm and nucleus diameter from coelomocytes of *Paracentrotus* sea urchins.

	Paracentrotus gaimardi				*Paracentrotus lividus*			
	Live		**Stained**		**Live**		**Stained**	
	Cytoplasm	**Nucleus**	**Cytoplasm**	**Nucleus**	**Cytoplasm**	**Nucleus**	**Cytoplasm**	**Nucleus**
Phagocytes	17.6 ± 4.81	4.49 ± 0.66	21.95 ± 4.48	6.95 ± 0.54	24.54 ± 4.01	5.71 ± 1,72	17.78 ± 5.29	5.21 ± 0.83
Vibratile cells	7.62 ± 1.03	4.11 ± 0.47	13.71 ± 0.73	4.31 ± 0.50	9.38 ± 0.59	3.92 ± 0.59	14.31 ± 0.80	4.50 ± 0.42
Crystal cell	5.08 ± 0.32	a	6.03 ± 0.34	a	b	b	b	b
Progenitor cell	b	b	b	b	6.51 ± 0.67	4.43 ± 0.39	5.85 ± 0.30	4.48 ± 0.54
Red spherulocyte [c]	9.47 ± 0.86	3.61 ± 0.57	13.60 ± 1.92	3.46 ± 0.70	10.66 ± 1.31	3.36 ±0.21	14.79 ± 1.95	3.39 ± 0.27
Colorless spherulocyte [c]	11.69 ± 1.5	4.21 ± 0.30	15.01 ± 2.04	3.11 ± 0.60	13.95 ± 1.35	5.08 ± 0.73	17.53 ± 3.73	3.32 ± 0.63
Granular spherulocyte [c]	8.96 ± 0.84	3.95 ± 0.45	13.85 ± 1.25	4.20 ± 0.67	9.30 ± 0.93	3.36 ± 0.52	11.90 ± 1.46	3.09 ± 0.48

Measurements are expressed as mean ± standard deviation. a = nucleus not observed; b = cell not found; c = measures of cells in the final stage.

Table 3 – Morphometric data from *Paracentrotus* sea urchins spherulocytes during maturation process.

Paracentrotus gaimardi	**Red spherulocyte**			**Colorless spherulocyte**			**Granular spherulocyte**		
	Nucleus (µm)	**Cytoplasm (µm)**	**NCR**	**Nucleus (µm)**	**Cytoplasm (µm)**	**NCR**	**Nucleus (µm)**	**Cytoplasm (µm)**	**NCR**
Early	5.65 – 3.61	18.05 – 11.22	0.41 – 0.23	5.91 – 3.01	18.11 – 12.82	0.44 – 0.20	7.39 – 3.91	15.92 – 11.62	0.51 – 0.29
Intermediate	5.11 – 3.26	18.68 – 11.48	0.34 – 0.19	4.80 – 3.10	22.30 – 11.67	0.34 – 0.14	4.70 – 2.52	17.07 – 9.07	0.39 – 0.24
Final	4.93 – 1.82	16.62 – 9.80	0.44 – 0.14	4.04 – 2.09	19.33 – 11.71	0.29 – 0.14	5.90 – 3.37	16.39 – 11.58	0.47 – 0.21
Paracentrotus lividus	**Red spherulocyte**			**Colorless spherulocyte**			**Granular spherulocyte**		
	Nucleus (µm)	**Cytoplasm (µm)**	**NCR**	**Nucleus (µm)**	**Cytoplasm (µm)**	**NCR**	**Nucleus (µm)**	**Cytoplasm (µm)**	**NCR**
Early	4.71 – 3.80	17.96 – 10.86	0.40 – 0.23	5.83 – 3.31	20.63 – 13.19	0.34 – 0.18	4.98 – 3.22	13.13 – 9.03	0.40 – 0.28
Intermediate	4.11 – 3.18	15.83 – 11.65	0.30 – 0.23	4.50 – 2.56	21.61 – 12.93	0.30 – 0.15	4.12 – 3.06	14.58 – 9.31	0.40 – 0.27
Final	3.83 – 2.77	19.91 – 12.52	0.29 – 0.18	4.59 – 1.69	26.44 – 11.37	0.31 – 0.11	3.83 – 2.34	14.78 – 9.01	0.35 – 0.18

Values are placed as maximum and minimum (Max – Min).

Capítulo 3

Células vibráteis de *Eucidaris tribuloides* (Echinoidea: Cidaroida)

Justificativa

Dentre os equinodermos, os Echinoidea têm sido tradicionalmente o grupo mais bem estudado com relação às células celomáticas, em especial os equinóides regulares. Sabe-se que estes organismos possuem quatro subpopulações celulares no fluido celômico, que são os fagócitos, os esferulócitos vermelho e transparente e as células vibráteis. Os fagócitos e os esferulócitos vermelho são os tipos mais bem estudados, tanto do ponto de vista morfológico quanto funcional, exercendo funções como fagocitose e atividade bactericida. Para os esferulócitos transparentes, sabe-se que sua função esta relacionada com atividade citotóxica. No entanto, para a intrigante célula vibrátil, cujo nome deriva da presença de um flagelo responsável pelo movimento da célula, muito pouco é conhecido e mesmo as características morfológicas têm sido pouco observadas. Com relação à possível função desta célula, que ainda está em debate, as principais hipóteses destacam: a movimentação do fluido celômico por meio do movimento flagelar, ou a participação desta célula no evento de coagulação, devido a liberação do conteúdo cytoplasmático. Neste contexto, este capítulo se propõe a preencher uma das lacunas no conhecimento da célula vibrátil: o entendimento detalhado da sua morfologia. Assim, o objetivo foi fazer uma caracterização morfológica detalhada da célula vibrátil, utilizando uma abordagem integrativa. Para isso, foram utilizados dados de células vivas em suspensão, preparações citoquímicas, microscopia eletrônica de transmissão e varredura, além da análise química do conteúdo da célula por meio de espectroscopia de raios-X. Com isso, foi possível fazer uma caracterização detalhada da morfologia da célula vibrátil e obter informações sobre o conteúdo das esférulas citoplasmáticas, além de informações sobre um possível processo de maturação deste celomócito. Por fim, a função fisiológica desta célula é discutida, à luz dos novos dados obtidos aqui.

Ultrastructure and energy-dispersive X-ray spectroscopy profile of the vibratile cell of *Eucidaris tribuloides* (Echinoidea: Cidaroida)

Vinicius Queiroz[1]*, Enrique Rozas[2], Márcio Reis Custódio[1]

To be subbmited to the Journal Zoological Studies

1- Departamento de Fisiologia Geral, Instituto de Biociências and Núcleo de Apoio à Pesquisa – Centro de Biologia Marinha (NAP–CEBIMar), Universidade de São Paulo, São Paulo, Brazil. E-mail: mcust@usp.br

2- Departamento de Engenharia Química. Escola Politécnica. Universidade de São Paulo. São Paulo, Brazil. E-mail: isoquir@gmail.com

Vinicius Queiroz, Enrique Rozas, and Márcio R. Custódio (2020) The main coelomic cell types currently recognized in echinoids (sea urchins) are phagocytes, spherulocytes, and vibratile cells. The latter is poorly studied, and the scarcely available data have been obtained through either live cell suspensions or transmission electron microscopy. In this study, we provide a detailed characterization of the vibratile cell of the cidaroid sea urchin *Eucidaris tribuloides* using an integrative approach based on live cells, cytochemistry, scanning, and transmission electron microscopy and energy-dispersive X-ray spectroscopy (EDS). Cytochemical preparations using toluidine blue showed different putative maturation stages characterized by a decrease of cytoplasm diameter, an increase of metachromasy, roughness of the cytoplasm and Nucleus-Cytoplasm Ratio, which were confirmed by SEM examination. In TEM analyses, cytoplasmic spherules of similar size filled with a cotton-like material were remarkable. The chemical composition obtained in EDS analyses showed very low levels of nitrogen, which supports the cytochemical results. A profile of this cell is provided and its role as progenitor cell is discussed. The results indicate that this cell subpopulation is not homogenous, but shows different stages of development in the coelomic fluid.

Keywords: Coelomocytes, cell physiology, Echinodermata, integrative approach, maturation process.

***** Correspondence: E-mail: vinicius_ufba@yahoo.com.br

BACKGROUND

Echinoids (sea urchins) have been the most commonly employed model in works addressing echinoderm coelomocytes (Matranga et al. 2000; 2002; 2005; Ramírez-Gómez and García-Arrarás 2010; Smith et al. 2010; Branco et al. 2013; 2014; Stabili and Pagliara 2015; Romero et al. 2016; Manzo et al. 2017). Based on these studies, three different coelomocyte populations are usually recognized in echinoid coelomic fluid: phagocytes, spherulocytes (red and colorless) and the poorly known vibratile cell (Chia and Xing 1995; Smith et al. 2006; 2010; Ramírez-Gómez and García-Arrarás 2010; Silva 2013; Deveci et al. 2015). The latter is characterized by its rounded outline, spherulous cytoplasm, and a prominent flagellum.

Such flagellated cells were also reported in the coelomic fluid of Ophiuroidea, Asteroidea, and Holothuroidea (Kindred 1924; Johnson and Beesan 1966; Kanungo 1979; Xing et al. 2008). Echinodermata seems to be the only metazoan group known to have constitutive free-circulating flagellated cells in the coelomic cavity (Kanungo 1979; Smith 1981). On the other hand, flagellated protozoans have been commonly recorded living inside the digestive tract of arthropods (Kitade 2004; Ohkuma 2008; Berlanga, et al. 2009; Ohkuma et al. 2009; Duarte et al. 2017). For example, many species of flagellated protozoa have been described as symbionts in termites (Isopoda: Insecta) and cockroaches (Blattaria: Insecta), where these organisms help with cellulose digestion (Yoshimura et al. 1993; Pester and Brune 2007; Ni and Tokuda 2013). This kind of relationship involving flagellated protozoans has not been reported in echinoderms. Even so, symbiotic protozoans from other groups (*e.g.* ciliates) have been commonly found within sea urchins (Beers 1948; Berger 1964; Xu et al. 2008; Wells 2013), and the vibratile cells had already been considered as an endoparasitic protozoan (Cuénot 1912).

Nowadays, the vibratile cell is widely accepted as a constitutive sea urchin cell, though its real physiological role is still unknown. The most accepted functions are related to clotting or mixing of coelomic fluid (Bertheussen and Seljelid 1978; Ramírez-Gómez and García-Arrarás 2010; Smith et al. 2010; Deveci et al. 2015), but some authors have hypothesized that they could actually represent a progenitor line (Liebman 1950; Isaeva 1994; Eliseikina and Magarlamov 2002). The few works addressing the vibratile cell have used either light (Johnson 1969a; Bertheussen and Seljelid 1978; Laughlin 1989; Deveci et al. 2015) or transmission electron microscopy (TEM – Chien

et al. 1970; Vethamany and Fung 1972; Deveci et al. 2015). Still, except for Johnson (1969b), most studies do not bring any further specific detail (Liebman 1950; Holland et al. 1965; Deveci et al. 2015).

Recent works addressing bivalve and sea urchin blood cells (Rebelo et al. 2013; Queiroz and Custódio 2015) demonstrated that the use of different methods in an integrated way can reveal highly relevant information. In this context, we provide an extensive characterization of this poorly known coelomocyte, the vibratile cell of *Eucidaris tribuloides*, using an integrative approach including suspension of live cells, cytology, and electron microscopy (scanning and transmission). Based on morphological features, a putative maturation sequence was proposed. To complement the cytochemical analyses, this cell was analyzed by energy-dispersive X-ray spectroscopy (EDS) in order to determine the elemental profile and investigate the presence of non-usual (inorganic) compounds. The diagnostic features of the vibratile cells are provided, and their role as a progenitor lineage is discussed, including the description of a possible alternative for this role. Using these techniques we were able to describe the cellular ultrastructure and verify that this cell subpopulation is not homogenous, but present different stages of development in the coelomic fluid.

MATERIAL AND METHODS

Animals and coelomocytes collection

Ten specimens of *Eucidaris tribuloides* were collected in the São Sebastião Channel and maintained at room temperature in marine aquaria at the Laboratório de Biologia Celular de Invertebrados Marinhos (IB-USP). Coelomocytes were extracted with a syringe preloaded with isosmotic anticoagulant solution (20 mM ethylenediamine tetraacetic acid (EDTA), sodium chloride 460 mM, sodium sulfate 7 mM, potassium chloride 10 mM, 4-(2-hydroxyethyl)-1-piperazineethanesulfonic acid (HEPES) 10 mM, pH 8.2; Dunham and Weissman 1986) in the peristomial membrane, and withdrawing the coelomic fluid up to a final dilution of 1:1 (Borges et al. 2005; Queiroz and Custódio 2015). The density of the cell suspension was calculated with the aid of a Neubauer chamber and adjusted afterward to $1x10^6$ cells/ml with the anticoagulant solution.

Light microscopy

Live cells were observed immediately after extraction. Measurements were obtained from 25 cells of each type using a digital imaging system (Opton). Cytological procedures included the preparation of microscopy slides using two different methods: (*i*) live cells were deposited on slides using a cytocentrifuge. This method uses low-centrifugal force to deposit and flatten isolated cells on microscopy slides. The coelomic cell suspension was spun (FANEN 248, 8 x10^4 cells per spot, 80 × g/5 min – Custódio et al. 2004) and fixed for 45 min in a closed vial containing some drops of formalin (formaldehyde 37%) on gauze swabs (formaldehyde sublimate - Martoja and Martoja 1967) or (*ii*) cells were collected directly in anticoagulant solution with glutaraldehyde 2.5% (final concentration), fixed for 4h at 4°C and cytospun in the same way. The slides were stained with hematoxylin and eosin (H&E), Mallory's Trichrome (MT) or Toluidine Blue (TB) following standard methods (Martoja and Martoja 1967; Behmer et al. 1976), and mounted with non-aqueous synthetic medium (Entellan, Merck). Cells were characterized according to overall shape, nuclear characteristics and cytoplasmic affinity to stains, following descriptions in the literature (*e.g.* Liebman 1950; Holland et al. 1965; Johnson 1969b). Putative maturation stages were determined according to cytochemical and structural differences of nuclei and cytoplasm content, following the sequence and general morphological features provided by Fontaine and Hall (1981). Measurements were also taken in the slides from 25 cells of each maturation stage (and from 25 putative progenitor cells), using the same digital imaging system as above.

Electron microscopy

For scanning electron microscopy (SEM), fixed cells were cytospun on coverslips (FANEN 248, 8 x10^4 cells per spot, 80 × g/5 min) and washed once in Milli-Q water for 20 minutes. Afterward, the coverslips were air-dried in a laminar flow cabinet at room temperature, dehydrated under vacuum (6-12 h) and then stored at room temperature in a closed container with silica gel. Finally, the coverslips were attached on stubs, sputter-coated with a 40-60 nm thick layer of gold and photographed in a scanning electron microscope (Sigma VP, Zeiss). For transmission electron microscopy (TEM), cells directly fixed in 2.5% glutaraldehyde by 4 hours were prepared following Taupin's (2008) method. Briefly, the coelomocytes were embedded in agar 2.5%, postfixed in osmium tetroxide (1%) with 0.1 M sodium cacodylate buffer at pH 7.4 for

2 h at 4°C, dehydrated in a graded ethanol series (50-100%) and embedded in resin (EMbed-812, Electron Microscopy Science). Ultrathin sections were stained with uranyl acetate and lead citrate (30 and 5 min, respectively) and examined in a Zeiss EM900 electron microscope.

Energy-dispersive X-ray spectroscopy (EDS)

Analysis of the cytoplasmic elemental composition of vibratile cells was carried out with the aid of an energy-dispersive X-ray spectroscopy (EDS) coupled to a scanning electron microscope (Phenom World). Cells were collected as described above in SEM procedures. After fixation, they were pelleted and washed twice by centrifugation in anticoagulant solution. Subsequently, they were cytospun on coverslips and attached on stubs. Ten vibratile cells in the medium stage of maturation were analyzed and nuclear and cytoplasmic elemental composition of at least two spots on each region was obtained. The elemental composition of spots on the glass coverslip (control) was also analyzed. Results were normalized and the values express elemental mass percentage in each spot. The values of some elements recorded during the analyses (oxygen, magnesium, aluminum, and silicon) were omitted from the results because they were very variable in all samples (oxygen) or did not belong to the sample itself (glass constituents – magnesium, aluminum, and silicon). The following parameters were used during analyses: Accelerating Voltage of 20-25 keV, Working Distance of 10 mm, Spot Size (as a percentage given by the equipment) of 60%.

Statistical analyses

Data on the nucleus and cytoplasm diameter of live and stained vibratile cells are presented as mean value ± standard deviation. To the putative progenitor cells, only measurements of stained cells are provided. Nucleus-Cytoplasm Ratio (NCR) was calculated from the nucleus and cytoplasm diameter for both coelomocytes. One-way analysis of variance (ANOVA; GraphPad InStat Statistical Software v. 3.0) was used to test differences among nucleus and cytoplasm diameters and the NCR of different maturation stages in the vibratile cells.

RESULTS

Light microscopy

Live cells: In fresh preparations, vibratile cells swim actively by moving their flagellum. These coelomocytes are spherical to subspherical, 7.7 ± 0.39 µm in diameter, ranging from 8.08 to 6.84 µm; their nucleus is rarely visible and the cytoplasm is filled with opalescent spherules ~1 µm in diameter (Fig. 1A). These cells have a long and evident flagellum, easily lost during handling and fixation, whose length ranges from 22.6 to 34.6 µm (Fig. 1A).

Cytospins: In cytological preparations, the vibratile cells showed 10.85 ± 1.9 µm in diameter, with a slightly condensed, subcentral nucleus. The nuclear diameter was 4.5 ± 0.7 µm and a nucleolus was sometimes visible in H&E and Mallory's Trichrome. Cells prepared with these stains presented a lacy aspect in which the vacuoles were apparently empty and the cytoplasm showed a slight affinity to Methyl Blue present in Mallory's Trichrome formulation. On the other hand, the cells showed an apparently filled cytoplasm with variable shades of metachromasy when stained with Toluidine Blue (Fig. 1 D-F). According to the cytoplasm roughness and TB affinity, a possible maturation sequence could be observed and roughly divided into three stages: *lower* (cells with a smooth cytoplasm, large diameter, quite spread in the cytospins, low NCR, and low metachromasy), *medium* (cytoplasm diameter decreases and becomes more granular whereas the NCR increases) and *higher* (cells have smaller cytoplasm diameter, visibly granular, less spread and present high NCR) (Fig. 1D-F and 2). Cells in all three stages could be observed in the same preparation (Fig. 3) and therefore are not a result of the sample processing. Cytoplasm diameter was statistically different in the higher stage of maturation (Fig. 2A) but the nucleus diameter was similar in all maturation stages ($p = 0.0744$), although with a slight tendency to increase from the initial to later stages. The NCR among the three categories was 0.35 (lower), 0.40 (medium) and 0.50 (higher), differing significantly among stages ($p<0.0001$) (Fig. 2C).

Electron microscopy

Scanning (SEM): The same putative maturation stages observed in light microscopy were observed (Fig. 4A-C), in which cells in lower maturation stages had the smoothest and flattest cytoplasm (Fig. 4A). Throughout the maturation process,

vibratile cells in medium stages presented a rough and less flat cytoplasm, with visible cytoplasmic spherules (Fig. 4B and E), culminating in a very rough and slightly flattened cell in the higher maturation stages (Fig. 4C). In all these stages, spherical masses were detected in the cytoplasm, usually associated with cytoplasmic spherules (Fig. 4A-C and E). A single flagellum is present (Fig. 4D-F) and its insertion seems to be directly in the cellular body (Fig. 4G). The diameter is constant along its all extension (0.216 ± 0.011 µm), except in the terminal region, which has a smaller diameter (0.09 ± 0.008 µm. Fig. 4F).

Transmission (TEM): Ultrastructural analyses showed that the vibratile cells are usually spherical, and the nucleus has an irregular outline, being generally central. Chromatin is mostly granular (Fig. 5A and B), and a lobed nucleus was sometimes visible (Fig. 5C). A prominent nucleolus was not observed. The cytoplasm is packed with spherules of similar size (Fig. 5A-F), each filled with a cotton-like material (Fig. 5A-F) and a more electron-dense eccentric sphere containing a granular core (Fig. 5C-F).

Energy-dispersive X-ray spectroscopy (EDS)

The EDS analyses (Fig. 6A-B) show that the values of all elements were always higher in the nucleus than in the cytoplasm, though less than 5%. The most representative elements in the cell nucleus were carbon (3.16 ± 1.1 %), nitrogen (3.72 ± 0.9 %) and calcium (2.16 ± 1.0 %). Phosphorus and sulfur had the lowest values (0.8 ± 0.6 and 0.37 ± 0.3% respectively). In the cytoplasm, the pattern was similar, but the values were lower: carbon (0.97 ± 0.4 %), nitrogen (3.13 ± 0.2 %) and calcium (1.57 ± 0.3 %). Phosphorus and sulfur were not detected in the cytoplasm.

Possible progenitor cell

Cell types that could correspond to a progenitor line were observed in cytospins and TEM preparations (Fig. 7A-C) and presented a uniform morphology. In cytospins, they have round to oval shape (7.53 ± 1.37 µm), with a large condensed nucleus (5.63 ± 0.97 µm) and reduced cytoplasm. The NCR was very high (0.75 ± 0.06) compared to the vibratile cells. In transmission electron microscopy, nucleus, nuclear

membrane, and its condensed chromatin were remarkable. No visible nucleolus was present (Fig. 7A).

DISCUSSION

Similarly to other echinoderm coelomocytes (*e.g.* spherulocytes), the vibratile cells have received various names such as: "vibratile corpuscles" (Kindred 1921; Boolootian and Geise 1958); "vibratile globules" (Kindred 1924), "flagellated phagocytes" or "flagellated cells" (Liebman 1950; MCrae 1959; Burton 1966). Currently, "vibratile cell" is the accepted and frequent term (Smith et al. 2010; McCaughey and Bodnar 2012; Deveci et al. 2015; Romero et al. 2016), with the flagellum as its main distinctive characteristic.

The general morphological and cytochemical aspects of the vibratile cells of *Eucidaris tribuloides* are similar to those of *Strongylocentrotus droebachiensis*, *S. purpuratus*, *S. franciscanus Paracentrotus lividus* and *Lytechinus pictus* (Liebman 1950; Holland et al. 1965; Johnson 1969a; 1969b; Vethamany and Fung 1972; Bertheussen and Seljelid 1978; Laughlin 1989; Deveci et al. 2015). Previous studies have pointed out complex mucopolysaccharides in the spherules (Holland et al. 1965; Johnson 1969b; Vethamany and Fung 1972; Deveci et al. 2015), and toluidine blue metachromasia indicates the same in *E. tribuloides*.

A putative maturation sequence was observed, with changes according to cytoplasm morphology and the content of the spherules. Immature cells had apparently empty spherules and weak metachromasy (lower maturation levels), and those more differentiated presented stronger metachromasy (higher maturation levels). Despite not having described it in detail, Holland et al. (1965) were the only to remark such differences. They noted that in the vibratile cells of *S. purpuratus*, the cytoplasm ranged from violet to purple, corresponding respectively to our lower and higher maturation stages. Additionally, similar morphological features interpreted as different stages of maturation were seen in *Eupentacta quinquesemita*'s coelomocytes (Fontaine and Hall 1981). However, as stated by Fontaine and Hall (1981), we also know that this categorization is only an attempt to address the maturation process of the vibratile cell and specific studies should be conducted.

In addition to morphological features, cell measurements corroborate our hypothesis on the maturation sequence. Cells in the lower maturation stage had lower NCRs, with smaller nuclei and larger cytoplasm. On the other hand, those in higher maturation stage showed a slightly larger nucleus, a smaller cytoplasm and higher NCR ($p<0.05$). This is the opposite of the observed in spherulocytes (Queiroz and Custódio 2015), in which the decrease of the nucleus size follows the maturation sequence. The vibratile cell seems to maintain the nucleus size during maturation, but the cytoplasm becomes denser and therefore less spread in the cytospins, which is consistent with the suggested functions of this coelomocyte (Ramírez-Gómez and García-Arrarás 2010; Smith et al. 2010). The maintenance of constant nuclear size in both lower and higher maturation stages is consistent with continuous RNA transcription, as described to cells from other taxa (Cheng and Guida 1980; Sato et al. 1994; Schmidt and Schibler 1995; Webster et al. 2009). This can indicate that this cell could indeed be involved in continuous production/release of substances (for clotting?), as described by Johnson (1969a) and Bertheussen and Seljelid (1978) in *Strongylocentrotus* sea urchins.

The knowledge on vertebrate blood cells is quite advanced, with data obtained using a vast array of techniques from cytochemistry to metabolomics (*e.g.* Darghouth et al. 2011; Arizza et al. 2014; Palis 2014). This holds true for the maturation process in these organisms, since that main aspect, such as morphological changes (Thiele et al. 1990; Sohn et al. 1993) regulatory mechanisms (Tebbi et al. 1980; Raghavachar et al. 1987) as well as the expression of specific markers (Andreesen et al. 1986; Elghetany et al. 2004) are well-known. On the other hand, except for insects (especially *Drosophila melanogaster*), in which the knowledge is higher (Nakahara et al. 2010; Minakhina et al. 2011; Vlisidou and Wood 2015; Letourneau et al. 2016), studies with invertebrate circulating cells are scarce. To invertebrates, the maturation process of coelomocytes has usually been inferred through morphological changes (Cheng and Guida 1980; Weinstein 2006; Rebelo et al. 2013), and this is also true for Echinodermata (Fontaine and Hall 1981; Queiroz and Custódio 2015). To this latter, although some fluorescent markers are available (Lin et al. 2007; Li et al. 2010), their use to identify distinct cell lines is unusual. Similarly, *in vitro* studies are scarcer since the maintenance of cultured coelomocytes is a real obstacle (Chia and Xing 1995). Until now, the morphological approach seems to be the most successful way (or the only one) to study the maturation

process in invertebrate immune cells (Cheng and Guida 1980; Fontaine and Hall 1981; Rebelo et al. 2013; Queiroz and Custódio 2015), showing interesting results.

Few studies have analyzed echinoderm coelomic cells under SEM (Kaneshiro and Karp 1980; Fontaine and Hall 1981; Silva and Peck 2000; Xing et al. 2008; Grand et al. 2014). However, morphological studies using this technique can complement TEM analyses. For instance, cytoplasmic spherules, the flagellum and the electron-dense region of vibratile cells can be observed with both techniques. Ultrastructural features observed in light microscopy, such as the border of the spherules and their electron-dense eccentric sphere, are represented in the membrane when the cell is flattened in cytospins and can be detected in SEM (*cf.* Fig. 1 (insets) and Fig. 5A-C). In scanning electron microscopy, the cytoplasmic spherules appear as regular polygonal objects, each with a spherical mass in the periphery, corresponding to the electron-dense region seen in TEM (*cf.* Fig. 4B and 5E). Similar features were also observed in *S. franciscanus* and *S. droebachiensis* (Chien et al. 1970; Vethamany and Fung 1972), described as "*parallel rows of granular material*" and attributed to the conversion of material from one zone to the other, *i.e* our ES to GC regions. Vethamany and Fung (1972) suggest that this structure could be a less hydrated region, and we also found this electron-dense sphere with its highly electron-dense core (*cf.* Fig. 5E). In addition, a region in a putative early dehydration stage was found (*cf.* Fig. 5F), as stated in previous works (Chien et al. 1970; Vethamany and Fung 1972).

Without the presence of the flagella, vibratile cells could be mistaken with spherulocytes in TEM analyses, due to a large number of vacuoles found in both (Queiroz and Custódio 2015). Two particular features of the former can be used to avoid any potential confusion: the large, irregular and commonly centralized nucleus, with condensed chromatin; and vacuoles filled with a cotton-like material, sometimes with an electron-dense region in its periphery containing a darker core. In contrast, in SEM using cytospun cells, vibratile cells can look similar to phagocytes (*cf.* Fig. 4A). Even so, they have a more homogeneous cytoplasm, even in higher maturation stages, the nucleus is more central, less distinct, and the cells themselves are usually more spread than the phagocytes (*cf.* Fig. 4A and D). This set of morphological features can thus be used to avoid misidentification in both transmission and scanning electron microscopy approaches.

Except for studies addressing vanadium in ascidian blood cells (Botte et al. 1979; Tullius et al. 1980; Pirie and Bell 1984; Michibata et al. 1986; Frank et al. 1995; Michibata 1996), few works using X-ray spectroscopy to access invertebrate coelomocytes have been carried out. Those are focused mainly on the toxic effect of nanoparticles (Falugi et al. 2012; van der Ploeg et al. 2014; Bouallegui et al. 2017). The elements identified in the vibratile cells were C, N, Ca, P and S, and their levels were very low (less than 5% regardless of the location. Fig. 6B) when compared with other coelomocytes with inclusions analyzed during this work, *e.g.* colorless (C = 14.11%, N = 5.25%, Ca = 1.79%, P = 0.22%, S = 0.65%) and granular spherulocytes (C = 10.25%, N = 9.28%, Ca = 1.15%, P = 0.12%, S = 3.56%). Different from other studies, in which X-ray microanalyses were able to find atypical chemical elements in invertebrates, such as vanadium, bromide, chromium or arsenic (Michibata et al. 1986; Gleeson et al. 1993; Araújo et al. 2003; Gilbert and Avenant-Oldewage 2017), only the usual cellular constituents were detected in our analyses. However, special attention should be given to the low concentration of nitrogen detected in the cytoplasm. The vibratile cell shows no affinity to acid fuchsin in the Mallory's Trichrome, used to stain protein content (Nielsen et al. 1998), but some metachromasy was revealed by Toluidine Blue. Therefore, the lower concentration of nitrogen in the cytoplasm (3.13%), in comparison with spherulocytes, can be attributed to structural proteins rather than cytoplasmic spherule content, corroborating the idea of a non-peptide rich moiety in vibratile cell vacuoles.

Currently, three main hypotheses on the role of vibratile cells have been considered (Isaeva 1994; Eliseikina and Magarlamov 2002; Ramírez-Gómez and García-Arrarás 2010; Smith et al. 2010). Some authors had already pointed out a stem function and, according to this idea, these cells could serve as a precursor to other coelomocytes (Liebman 1950; Isaeva 1994; Eliseikina and Magarlamov 2002). Such functions are commonly ascribed to progenitor cells, another coelomocyte characterized by a small spherical shape and high Nucleus–Cytoplasm ratio (Fontaine and Lambert 1977; Smith 1981). Similar features are found in cells with differentiative capacity in other taxa, from sponges (as *polybasts* Simpson 1984) to annelids (*neoblasts* Sugio et al. 2008; 2012) and arthropods (*prohaemocytes* Lavine and Strand 2002; Perveen and Ahmad 2017). In echinoids, they were recorded in *Echinus esculentus* (Smith, 1981), and had their ultrastructure detailed in the sea cucumber *Cucumaria normani* (Smith

1981). In our study, we also found coelomocytes similar to *C. normani* progenitor cells in both TEM and cytospin preparations (*cf*. Fig. 7). The morphology of the vibratile cell differs completely from that expected for a cell involved with stem functions, *i.e.* large nucleus, high NCR and a very thin cytoplasm, characteristics found in our putative progenitor cell. Furthermore, results using tritiated thymidine have indicated that vibratile cells do not synthesize DNA (Holland et al. 1965) and therefore probably some proliferating cell type must be differentiating into vibratile cells.

The other possibility is that vibratile cells could be involved in coelomic fluid mixing (Cuénot 1981). However, flagellated or ciliated cells intended to move fluids (*e.g.* sponge choanocytes, protonephidial cells or ciliated peritoneum) are usually found attached to some matrix or tissue (Grimmer and Holland 1979; Leys and Eerkes-Medrano 2006; Kieneke et al. 2008). This attachment is necessary to perform such mechanical function. As said by Johnsson (1969a) "*In hanging drops vibratile cells, though they jostle other cells during their constant movement, do not radically change the position of other cells nor cause major mixing of the fluid*".

The last hypothesis advocates clotting as the main function. According to *in vivo* observations of Johnsson (1969a) and Bertheussen and Seljelid (1978), coagulation started with a mucous substance secreted from vibratile cells. Previous studies, using cytochemical and ultrastructural approach, have shown the presence of such substances inside cytoplasmic granules (Liebman 1950; Holland et al. 1965; Johnsson 1969b; Chien et al. 1970; Vethamany and Fung 1972; Deveci et al. 2015). Another important characteristic is the highly specialized morphology of the vibratile cell, which suggests that these cells might, in fact, be involved in the clotting process.

CONCLUSIONS

Despite the growing increase in the understanding of echinoderm coelomic cells and their biological roles, the vibratile cell is yet one of the most poorly studied coelomocytes. Here we provide relevant information about its morphology and chemistry, as well as a proposal of a putative maturation process, highlighting as an integrative approach can be useful. Although the specific function of this coelomocyte has not been confirmed yet, it seems to be involved in coagulation events. In view of the contrasting morphology from the putative progenitor and the vibratile cell, we believe

that the latter does not fit the requirements to perform a stem cell role. Likewise, its location in the sea urchin body and its highly specialized morphology do not meet the requirements to assume a coelomic fluid movement function.

ACKNOWLEDGMENTS

The authors thank Dr. Alberto de Freitas Ribeiro and the technicians Waldir Caldeira, Marcio V. Cruz and Sheilla Schuindt (LME, Laboratório de Microscopia Eletrônica–IB-USP) for providing equipment and support with electron microscopy and the staff of CEBIMar (USP) for the provision of laboratory facilities and technical support during field trips. We also are indebted to Dr. Jorge Tenorio (Larex, PQI-USP) for providing equipment and support during Energy-dispersive X-ray spectroscopy analyses. This work was supported by CAPES and FAPESP (Proc. 13/50218-2 and 15/21460-5). The authors declare no competing interests exist.

REFERENCES

Andreesen R, Bross KJ, Osterholz J, Emmrich F. 1986. Human macrophage maturation and heterogeneity: analysis with a newly generated set of monoclonal antibodies to differentiation antigens. Blood, 67(5):1257-64.

Araújo MF, Conceição A, Barbosa T, Lopes MT, Humanes M. 2003. Elemental composition of marine sponges from the Berlengas Natural Park, Western Portuguese Coast. X-Ray Spectrom 32:428–433.

Arizza V, Russo D, Marrone F, Sacco F, Arculeo M. 2014. Morphological characterization of the blood cells in the endangered Sicilian endemic pond turtle, *Emys trinacris* (Testudines: Emydidae). Ital J Zool 81(3):344–353.

Beers CD. 1948. The ciliates of *Strongylocentrotus dröbachiensis*: incidence, distribution in the host, and division. Biol Bull 94:99–112.

Behmer OA, Tolosa EMC, Freitas-Neto AG. 1976. Manual de técnicas de histologia normal e patológica. EDART/EDUSP, São Paulo.

Berger J. 1964. Entocommensal ciliates from oceanic Echinoids. J Protozool 11(Suppl): 28–29.

Berlanga M, Paster BJ, Guerrero R. 2009. The taxophysiological paradox: changes in the intestinal microbiota of the xylophagous cockroach *Cryptocercus punctulatus* depending on the physiological state of the host. Inter Microbiol 12: 227–236.

Bertheussen K, Seljelid R. 1978. Echinoid phagocytes in vitro. Exp Cell Res 111:401–412.

Boolootian RA, Geise CA. 1958. Coelomic corpuscles of echinoderms. Biol Bull 15:53–56.

Borges JCS, Jensch-Junior BE, Garrido P, Mangiaterra MBBCD, Silva JRMC. 2005. Phagocytic amoebocyte subpopulations in the perivisceral coelom of the sea urchin *Lytechinus variegatus* (Lamarck, 1816). J Exp Zool 303A:241–248.

Botte L, Scippa S, de Vincentiis M. 1979. Ultrastructural localization of vanadium in the blood cells of Ascidiacea. Experientia 35:1228–1230.

Bouallegui Y, Younes RB, Turki F, Oueslati R. 2017. Impact of exposure time, particle size and uptake pathway on silver nanoparticle effects on circulating immune cells in *Mytilus galloprovincialis*, J Immunotoxicol, 14:1, 116-124

Branco PC, Borges JCS, Santos MF, Jensch Junior BE, Silva JRMC. 2013. The impact of rising sea temperature on innate immune parameters in the tropical subtidal sea urchin *Lytechinus variegatus* and the intertidal sea urchin *Echinometra lucunter*. Mar Envir Res 92:95–101.

Branco PC, Figueiredo DSL, da Silva JRMC. 2014. New insights into the innate immune system of sea urchin: Coelomocytes as biosensors for environmental stress. OA Biol 2:2.

Cheng, T.C., Guida, V.G., 1980. Hemocytes of *Bulinus truncates rohlfsi* (Mollusca: Gastropoda). J Invertebr Pathol 35:158–167.

Chia F, Xing J. 1995. Echinoderm Coelomocytes. Zool Stud 35(4):231–254.

Chien PK, Johnson PT, Holland ND, Chapman FA. 1970. The Coelomic Elements of Sea Urchins (*Strongylocentrotus*) IV. Ultrastructure of the Coelomocytes. Protoplasma 71:419–442.

Cuénot, L. 1912. Contribution a la faune du Bassin d'Arcachon. V. Echinodermes. Bull Stn Biol Arcachon 14:17–116.

Cuénot, L. 1891. Etudes sur les sang et les glandes lymphatiques dans la sériee animale (2° partie: Invértebés). Arch. Zool. Exptl. Gén (Sér. 2), 9, 13-90, 365-475, 593-670.

Custódio MR, Hajdu E, Muricy G 2004. Cellular dynamics of in vitro allogeneic reactions of *Hymeniacidon heliophila* (Demospongiae, Halichondrida). Mar Biol 144(5):999-1010.

Darghouth D, Koehl B, Heilier JF, Madalinski G, Bovee P, Bosman G, Delaunay J, Junot C, Roméo P-H. 2011. Alterations of red blood cell metabolome in overhydrated hereditary stomatocytosis. Haematologica 96(12):1861–1865.

Deveci R, Sener E, Izzetoglu S. 2015. Morphological and Ultrastructural Characterization of Sea Urchin Immune Cells. J Morphol 276(5):583–588.

Duarte, S., L. Nunes, P.A.V. Borges, C.G. Fossdal & T. Nobre 2017. Living inside termites: an overview of symbiotic interactions, with emphasis on flagellate protists. Arquipelago. Life Mar Sci 34:21-43.

Elghetany MT, Ge Y, Patel J, Martinez J, Uhrova H. 2004. Flow cytometric study of neutrophilic granulopoiesis in normal bone marrow using an expanded panel of antibodies: correlation with morphologic assessments. J Clin Lab Anal, 18(1):36-41.

Eliseikina MG, Magarlamov TY. 2002. Coelomocyte Morphology in the Holothurians *Apostichopus japonicus* (Aspidochirota: Stichopodidae) and *Cucumaria japonica* (Dendrochirota: Cucumariidae). Russ J Mar Biol 28(3):197–202.

Falugi C, Aluigi MG, Chiantore MC, Privitera D, Ramoino P, Gatti MA, Fabrizi A, Pinsino A, Matranga V. 2012. Toxicity of metal oxide nanoparticles in immune cells of the sea urchin. Mar Envir Res 76:114–121.

Fontaine AR, Hall BD. 1981. The haemocyte of the holothurians *Eupentacta quinquesemita*: Ultrastructure and maturation. Can J Zool 59:1884–1891.

Fontaine AR, P Lambert. 1977. The fine structure of the leucocytes of the holothurian, *Cucumaria miniata*. Can J Zool 55:1530–1544.

Frank P, Kustin K, Robinson WE, Linebaugh L, Hodgson KO. 1995. Nature and ligation of vanadium within whole blood cells and Henze solution from the tunicate *Ascidia ceratodes*, as investigated by using X-ray absorption spectrometry. Inorg Chem 34:5942–5949.

Gilbert BM, Avenant-Oldewage A. 2017. Trace element and metal sequestration in vitellaria and sclerites, and reactive oxygen intermediates in a freshwater monogenean, *Paradiplozoon ichthyoxanthon*. PLoS ONE 12(5): e0177558.

Gleeson RA, Aldric HC, White JF, Trapido-Rosenthal HG, Carr WES. 1993. Ionic and elemental analyses of olfactory sensillar lymph in the spiny lobster, *Panulirus argus*. Comp Bioch Physiol 105(A):29–34.

Gorshkov AN, Blinova MI, Pinaev GP. 2009. Ultrastructure of coelomic epithelium and coelomocytes of the starfish *Asterias rubens* L. in norm and after wounding. Cell Tissue Biol 3(5):477–490.

Grand A, Pratchett M, Rivera-Posada J. 2014. The Immune Response of *Acanthaster planci* to Oxbile Injections and Antibiotic Treatment. J Mar Biol. doi.org/10.1155/2014/769356

Grimmer, J. C and Holland, N. D. 1979. Haemal and Coelomic Circulatory Systems in the Arms and Pinnules of *Florometra serratissima* (Echinodermata: Crinoidea). Zoomorphologie 94:93-109.

Holland ND, Phillips JH, Giese AC. 1965. An Autoradiographic Investigation of Coelomocyte Production in the Purple Sea Urchin (*Strongylocentrous purpuratus*). Biol Bull 128(2):259–270.

Isaeva VV, Kletki V. 1994. Morfogeneze (Cells in Morphogenesis). Moscow: Nauka.

Johnson PT, Beesan RJ. 1966. In vitro studies on *Patiria mininata* (Brandt) Coelomocytes, with remarks on revolving cysts. Life Sci 5:1641–1666.

Johnson PT. 1969a. The coelomic elements of sea urchins (*Strongylocentrotus*). I. The normal coelomocytes; their morphology and dynamics in hanging drops. J Invertebr Pathol 13:25–41.

Johnson PT. 1969b. The coelomic elements of sea urchins (*Strongylocentrotus*) II. Cytochemistry of the Coelomocytes. Histochemie 17:213–231.

Kaneshiro E, Karp RD. 1980. The ultrastructure of coelomocytes of the sea star *Dermasterias imbricata*. Biol Bull 159:295–310.

Kanungo K. 1979. The Coelomocytes of Asteroid Echinoderms. In: Cheng TC. Ed. Invertebrate Blood. Cells and Serum Factors. Plenum, New York, pp. 7–40.

Kindred JE. 1921. Phagocytosis and clotting in the perivisceral fluid of *Arbacia*. Biol Bull 41:144–152.

Kindred JE. 1924. The cellular elements in the perivisceral fluid of echinoderms. Biol Bull 47:228-251.

Kieneke, A.; Ahlrichs, W. H.; Arbizu, P. M and Bartolomaeus, T. 2008. Ultrastructure of protonephridia in *Xenotrichula carolinensis syltensis* and *Chaetonotus maximus* (Gastrotricha: Chaetonotida): comparative evaluation of the gastrotrich excretory organs. Zoomorphology 127:1–20.

Kitade O. 2004. Comparison of symbiotic flagellate faunae between termites and a wood-feeding cockroach of the genus *Cryptocecus*. Microb Environ 19: 215–220.

Lavine MD, Strand MR. 2002. Insect hemocytes and their role in immunity. Insect Biochem Mol Biol 32(10):1295–1309.

Letourneau M, Lapraz F, Sharma A, Vanzo N, Waltzer L, Crozatier M. 2016. Drosophila hematopoiesis under normal conditions and in response to immune stress. FEBS Letters, 590(22): 4034-4051. doi: 10.1002/1873-3468.

Leys SP, Eerkes-MedranoDI. 2006. Feeding in a Calcareous Sponge: Particle Uptake by Pseudopodia. Biol Bull 211: 157-171.

Li Q, Li Y, Li H, Wang YN, Xu DH. 2010. Production, characterization and application of monoclonal antibody to spherulocytes: a subpopulation of coelomocytes of *Apostichopus japonicus*. Fish Shellfish Immunol, 29:832-838.

Liebman E. 1950. The leucocytes of *Arbacia punctulata*. Biol Bull 98:46–59.

Lin WY, Grant S, Beck G. 2007. Generation of monoclonal antibodies to coelomocytes of the purple sea urchin *Arbacia punctulata*: characterization and phenotyping. Develop Comp Immunol 31:465-475.

Manzo S, Schiavo S, Oliviero M, Toscano A, Ciaravolo M, Cirino P. 2017. Immune and reproductive system impairment in adult sea urchin exposed to nanosized ZnO via food. Sci Total Environ 599–600: 9–13

Martoja R, Martoja M. 1967. Initiation aux Techniques de l'Histologie Animale. Masson et Cie, Paris

Matranga V, Bonaventura R, Di Bella G. 2002. Hsp70 as a stress marker of sea urchin coelomocytes in short term cultures. Cell Mol Biol 48: 3453–59.

Matranga V, Pinsino A, Celi M, Natoli A, Bonaventura R, Schröder HC, Müller WEG. 2005. Monitoring chemical and physical stress using sea urchin immune cells. In: Matranga V (ed) Echinodermata. Springer, Heidelberg, p 85–110.

Matranga V, Toia G, Bonaventura R, Muller WEG. 2000. Cellular and biochemical responses to environmental and experimentally induced stress in sea urchin coelomocytes. Cell Stress Chap 5:158–165.

McCaughey C, Bodnar A. 2012. Investigating the Sea Urchin Immune System: Implications for Disease Resistance and Aging. J Young Invest 23(6):25–33.

Michibata H, Terada T, Anada N, Yamakawa K, Numakunai T. 1986. The accumulation and distribution of vanadium, iron, and manganese in some solitary ascidians. Biol Bull 171:672–681.

Michibata H. 1996. The Mechanism of Accumulation of Vanadium by Ascidians: Some Progress towards an Understanding of this Unusual Phenomenon. Zool Sci 13(4):489–502.

Minakhina S, Tan W, Steward R. 2011. JAK/STAT and the GATA factor Pannier control hemocyte maturation and differentiation in *Drosophila*. Develop Biol 352(2):308-16.

Nakahara Y, Kanamori Y, Kiuchi M, Kamimura M. 2010. Two Hemocyte Lineages Exist in Silkworm Larval Hematopoietic Organ. PLoS ONE 5(7): e11816.

Ni J, Tokuda G. 2013. Lignocellulose-degrading enzymes from termites and their symbiotic microbiota. Biotechnol Adv 31:838–50

Nielsen LF, Moe D, Kirkeby S, Garbarsch C. 1998. Sirius red and acid fuchsin staining mechanisms. Biotech Histochem 73(2):71–77.

Ohkuma M, Noda S, Hongoh Y, Nalepa CA, Inoue T. 2009. Inheritance and diversification of symbiotic trichonymphid flagellates from a common ancestor of termites and the cockroach *Cryptocercus*. Proc R Soc B 276: 239–245 doi:10.1098/rspb.2008.1094

Ohkuma, M. 2008. Symbioses of flagellates and prokaryotes in the gut of lower termites. Trends Microbiol 16, 345–352.

Palis J. 2014. Primitive and definitive erythropoiesis in mammals. Front Physiol 5(3):1–9.

Perveen N, Ahmad M. 2017. Toxicity of some insecticides to the haemocytes of giant honeybee, *Apis dorsata* F. under laboratory conditions. Saudi J Biol Sci 24: 1016–1022.

Pester M, Brune A. 2007. Hydrogen is the central free intermediate during lignocellulose degradation by termite gut symbionts. ISME J. 1:551–565.

Pirie PJS, Bell MV. 1984. The localization of inorganic elements, particularly vanadium and sulphur, in haemolymph from the ascidians *Ascidia mentula* (Müller) and *Ascidiella aspersa* (Miiller). J Exp Biol Ecol 74:187–194

Queiroz V, Custódio MR. 2015. Characterisation of the spherulocyte subpopulations in *Eucidaris tribuloides* (Cidaroida: Echinoidea). Ital J Zool 82(3):338-348.

Raghavachar A, Fleischer S, Frickhofen N, Heimpel H, Fleischer B. 1987. T lymphocyte control of human eosinophilic granulopoiesis. Clonal analysis in an idiopathic hypereosinophilic syndrome. J Immunol 139(11):3753-3758.

Ramírez-Gómez F, García-Arrarás JE. 2010. Echinoderm immunity. Inver Surv J 7:211–220.

Rebelo MdF, Figueiredo EdS, Mariante RM, Nóbrega A, de Barros CM, Allodi S. 2013. New Insights from the Oyster Crassostrea rhizophorae on Bivalve Circulating Hemocytes. PLoS ONE 8(2): e57384.

Romero A, Novoa B, Figueras A. 2016. Cell mediated immune response of the Mediterranean sea urchin *Paracentrotus lividus* after PAMPs stimulation. Develop Comp Immunol 62: 29–38.

Sato S, Burgess SB, McIlwain DL. 1994. Transcription and motoneuron size. J Neuroch 63:1609–1615.

Schmidt EE, Schibler U. 1995. Cell size regulation, a mechanism that controls cellular RNA accumulation: Consequences on the regulation of the ubiquitous transcription factors Oct1 and NF-Y and the liver-enriched transcription factor DBP. J Cell Biol 128:467–483.

Silva JRMC, Peck L. 2000. Induced in vitro phagocytosis of the Antarctic starfish *Odontaster validus* (Koehler, 1906) at 0 °C. Polar Biol 23(4):225–230.

Silva JRMC. 2013. Immunology in Sea Urchins. In: Lawrence JM (ed) Edible Sea Urchins: Biology and Ecology; Developments in Aquaculture and Fisheries Science. Elsevier Science, Amsterdam. p. 187–194.

Smith CL, Ghosh J, Buckley KM, Clow LA, Dheilly NM, Huag T, Henson JH, ChengMan Lun CL, Majeske AJ, Matranga V, Nair SV, Rast JP, Raftos DA, Roth M, Sacchi S, Schrankel CS, Stensvag K. 2010. Echinoderm immunity. In: Söderhäll K (ed) Invertebrate immunity. Landes Bioscience and Springer Science BusinessMedia, New York. p 260–301.

Smith LC, Rast JP, Brockton V, Terwilliger DP, Nair SV, Buckley KM, Majeske AJ. 2006. The sea urchin immune system. Inver Surv J 3:25–39.

Smith VJ. 1981. The Echinoderms. *In*: Ratcliffe NA, Rowley AF, (ed.). Invertebrate Blood Cells. Academic Press, New York. p 513–562.

Sohn DS, Kim KY, Lee WB, Kim DC. 1993. Eosinophilic granulopoiesis in human fetal liver. Anat Rec 235(3):453-60.

Stabili L, Pagliara P. 2015. The sea urchin *Paracentrotus lividus* immunological response to chemical pollution exposure: The case of Lindane. Chemosphere 134: 60–66.

Sugio M, Takeuchi K, Kutsuna J, Tadokoro R, Takahashi Y, Yoshida-Noro C, Tochinai S. 2008. Exploration of embryonic origins of germline stem cells and neoblasts in Enchytraeus japonensis. Gene Expr Patterns 8:227–236.

Sugio M, Yoshida-Noro C, Ozawa K, and Tochinai S. 2012. Stem cells in asexual reproduction of *Enchytraeus japonensis* (Oligochaeta, Annelid): Proliferation and migration of neoblasts. Dev Growth Differ 54: 439–450.

Taupin P. 2008. Electron microscopy of cell suspension. Annals of Microsc 8:19–21.

Tebbi CK, Mahmoud AA, Polmar S, Gross S. 1980. The role of eosinophils in granulopoiesis. I. Eosinophilia in neutropenic patients. J Pediat 96(3 Pt 2):575-581.

Thiele J, Timmer J, Jansen B, Zankovich R, Fischer R. 1990. Ultrastructure of neutrophilic granulopoiesis in the bone marrow of patients with chronic myeloid leukemia (CML). A morphometric study with special emphasis on azurophil (primary) and specific (secondary) granules. Virchows Arch B Cell Pathol Incl Mol Pathol 59(3):125-131.

Tullius TD, Gillum WO, Carlson RMK, Hodgson KO. 1980. Structural study of the vanadium complex in living ascidian blood cells by x-ray absorption spectroscopy. J Am Chem Soc 102(17):5670–5676.

van der Ploeg MJ, Handy RD, Waalewijn-Kool PL, van den Berg JH, Herrera Rivera ZE, Bovenschen J, Molleman B, Baveco JM, Tromp P, Peters RJ, Koopmans GF, Rietjens IM, van den Brink NW. 2014. Effects of silver nanoparticles (NM-300K) on *Lumbricus rubellus* earthworms and particle characterization in relevant test matrices including soil. Envir Toxic Chem 33(4):743–752.

Vethamany VG, Fung M. 1972. The fine structure of coelomocytes of the sea urchin, *Strongylocentrotus drobachiensis* (Muller O.F.). Can J Zool 50:77–81.

Vlisidou I, Wood W. 2015. Drosophila blood cells and their role in immune responses. FEBS J282: 1368–1382

Webster M, Witkin KL, Cohen-Fix O. 2009. Sizing up the nucleus: Nuclear shape, size, and nuclear-envelope assembly. J Cell Sci 122:1477–1486.

Weinstein PP. 2006. Morphological differentiation and function of the coelomocytes in the parasitic stages of *Nippostrongylus brasiliensis*. J Parasitol, 92(5):894-917.

Wells PG. 2013. Observing the entocommensal ciliate fauna of sea urchins, *Strongylocentrotus* spp.—an exercise that illustrates the wonders of symbiosis. Symbiosis 60:45–47.

Xing J, Yang HS, Chen MY. 2008. Morphological and ultrastructural characterization of the coelomocytes in *Apostichopus japonicus*. Aquat Biol 2:85–92.

Xu D, Sun P, Song W, Warren A. 2008. Studies on the new endocommensal ciliate, *Strombidium foissneri nov.sp*. (Ciliophora, Oligotrichida) from the intestine of the sea urchin *Hemicentrotus pulcherrimus* (Camarodonta, Echinoida). Denisia 23: 273–278.

Yoshimura T, Azuma JI, Tsunoda K, Takahashi M. 1993. Cellulose metabolism of the symbiotic protozoa in termite, *Coptotermes formosanus* Shiraki (Isoptera: Rhinotermitidae): I. Effect of the degree of polymerization of cellulose. Mokuzai Gakkaishi, 39, 221–226.

Figures and Captions

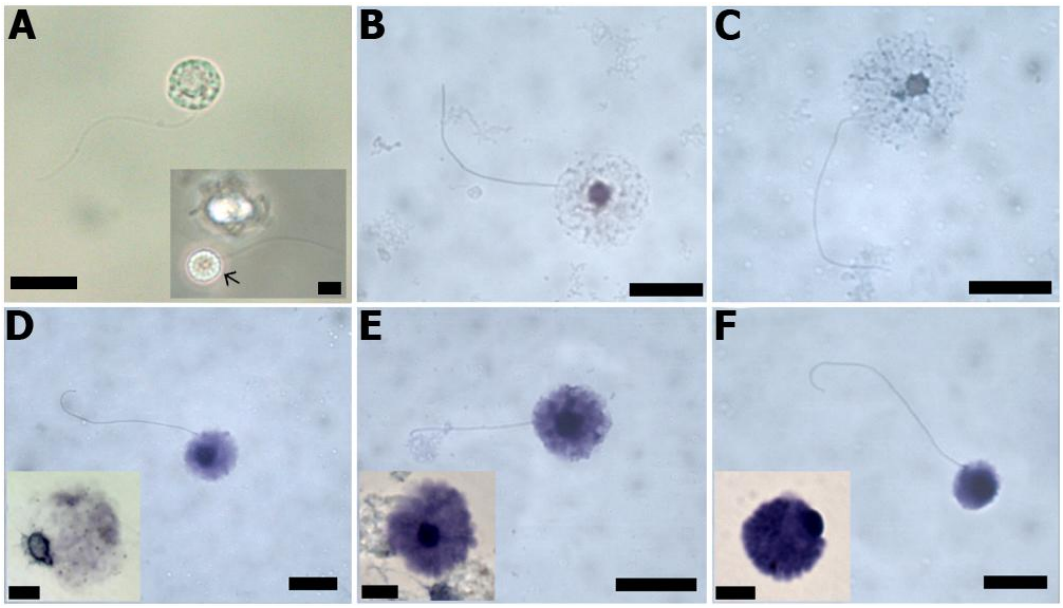

Figure 1 – Light microscopy of the vibratile cell of *Eucidaris tribuloides*. A – Live cell in light microscopy; A inset – Live cell (arrow) in phase-contrast microscopy, highlighting the cytoplasmic spherules; B-F – Fixed cytospun cells. D-F – Toluidine Blue; lower, medium and higher maturations stages respectively; D-F insets – Live cytospun cells in the same stage. B – Hematoxylin and Eosin; C – Mallory's Trichrome. Scale: 10 µm; A, D-F insets: 5 µm.

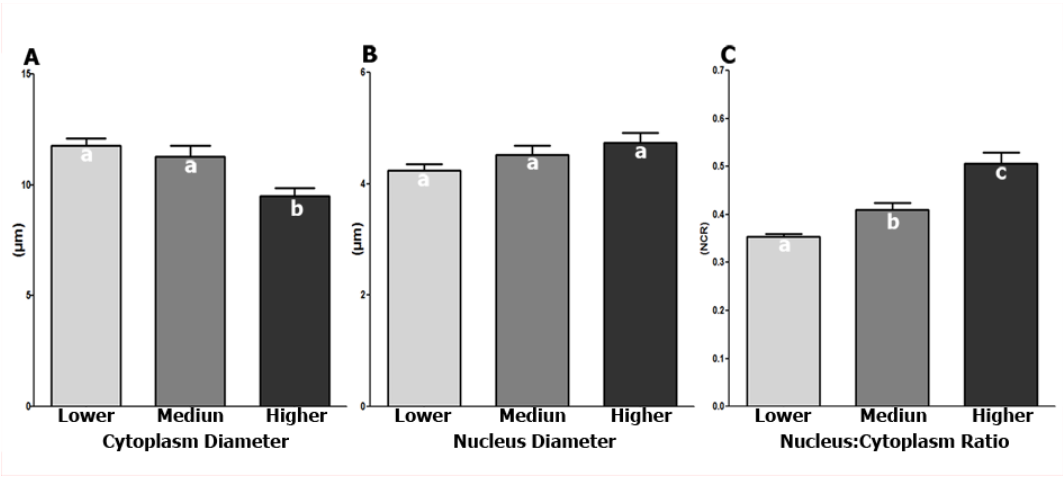

Figure 2 – Measurements of the vibratile cell of *Eucidaris tribuloides* according to its maturation level. A – Cytoplasm diameter; B – Nucleus diameter; C – Nucleus/ Cytoplasm Ratio (NCR). * Different letters have statistical significance.

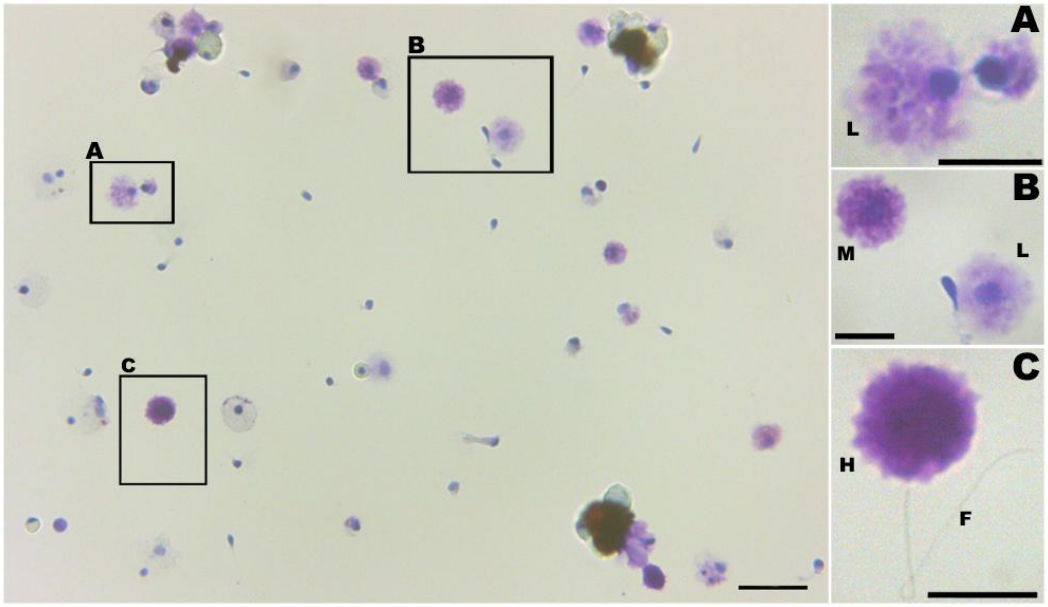

Figure 3 – Light microscopy of toluidine blue-stained vibratile cell of the *Eucidaris tribuloides* highlighting different maturation stages in the same area. A – Lower maturation stage; B – Lower and medium maturation stage; C – Higher maturation stage. Legend: F = Flagelum; H = higher maturation stage; L = lower maturation stage; M = medium maturation stage. Scale: Main board = 25 µm; Insets A-C = 10 µm.

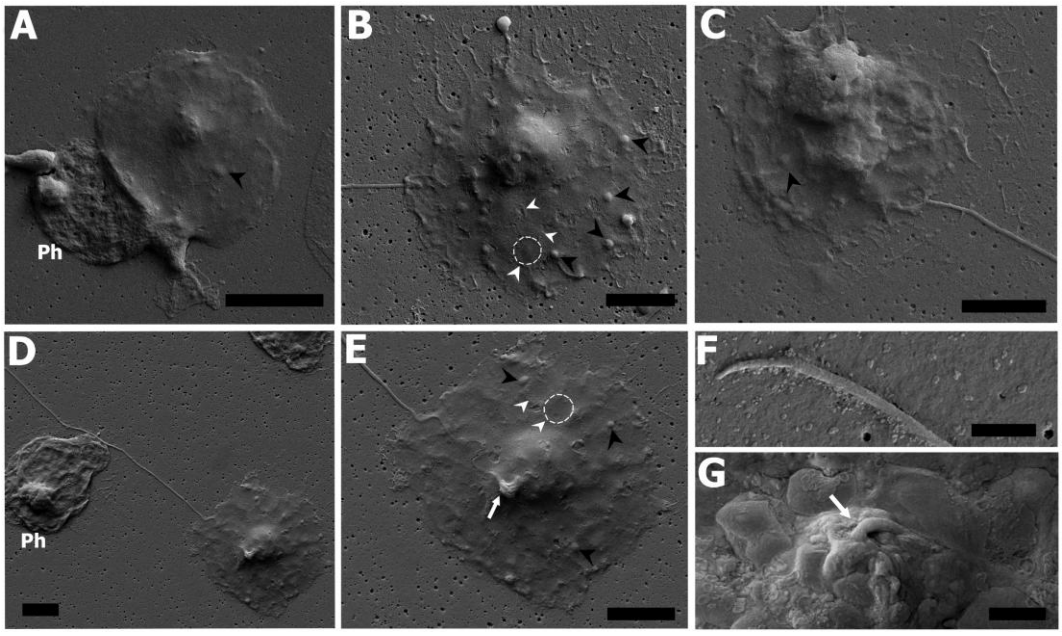

Figure 4 – Scanning electron microscopy of the vibratile cell of *Eucidaris tribuloides*. A-C – Maturation stages of vibratile cell (lower, medium and higher respectively); D – Overview of a medium maturation stage of the vibratile cell showing the flagellum and the cellular body; E – Cellular body highlighting the flagellum (arrow), the cytoplasmic spherules (dashed circle and white arrowhead) and the spherical masses (black arrowhead); F and G – Terminal portion and insertion site of the flagellum (arrow). Legend: Ph = Phagocytes; arrow = flagellum insertion; black arrowhead = spherical masses; dashed circle = boundary of the cytoplasmic spherule; white arrowhead = cytoplasmic spherules. Scale: A = 10 µm; B-E = 4 µm; F and G = 1µm.

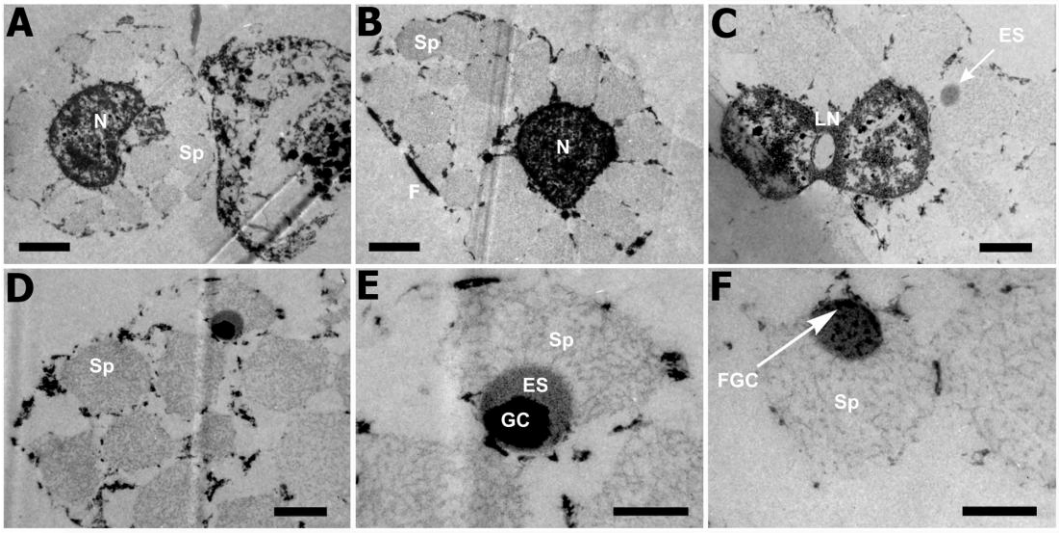

Figure 5 – Transmission Electron Microscopy of the vibratile cell of *Eucidaris tribuloides*. A and B – Whole cell showing nuclei and spherules; C – One lobed nuclei; D – Spherules in detail showing its irregular cotton-like material; E – One spherule with its irregular cotton-like material, electron-dense eccentric sphere, and the highly electron-dense granule core; F – Spherule with a forming granular core. Legend: ES = electron-dense eccentric sphere; F = flagellum; FGC = forming granule core; GC = granule core; LN = lobed nuclei; N = nuclei; Sp = spherule. Scale: A and B = 2 µm; C and D = 1 µm; E and F = 0.5 µm.

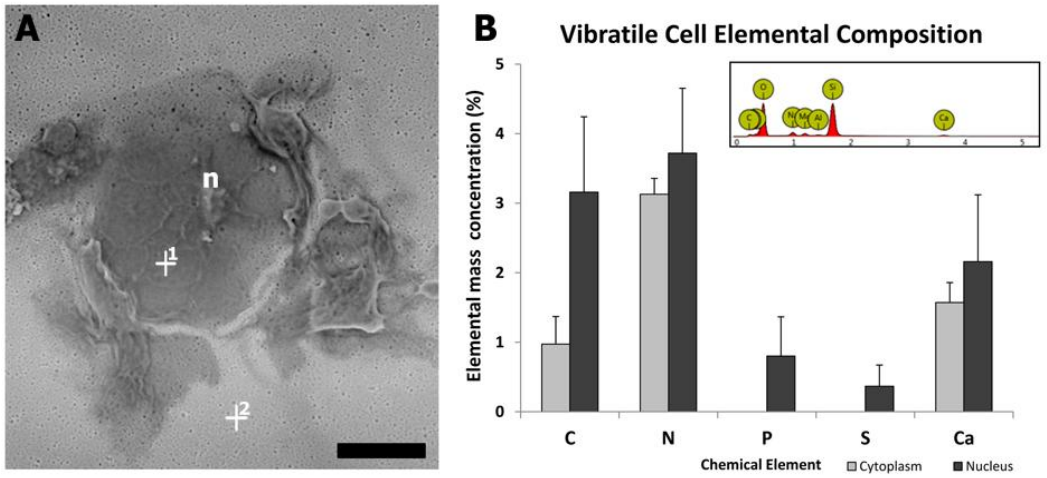

Figure 6 – Elemental concentration in the vibratile cell. A – Overview of vibratile cell in scanning electron microscope coupled to EDS; B – Elemental concentration in the cytoplasm (grey) and nucleus (black); Inset – EDS Spectrum for vibratile cell cytoplasm. Legend: 1 = cytoplasm; 2 = glass coverslip; n = nucleus. Scale: A = 10 µm.

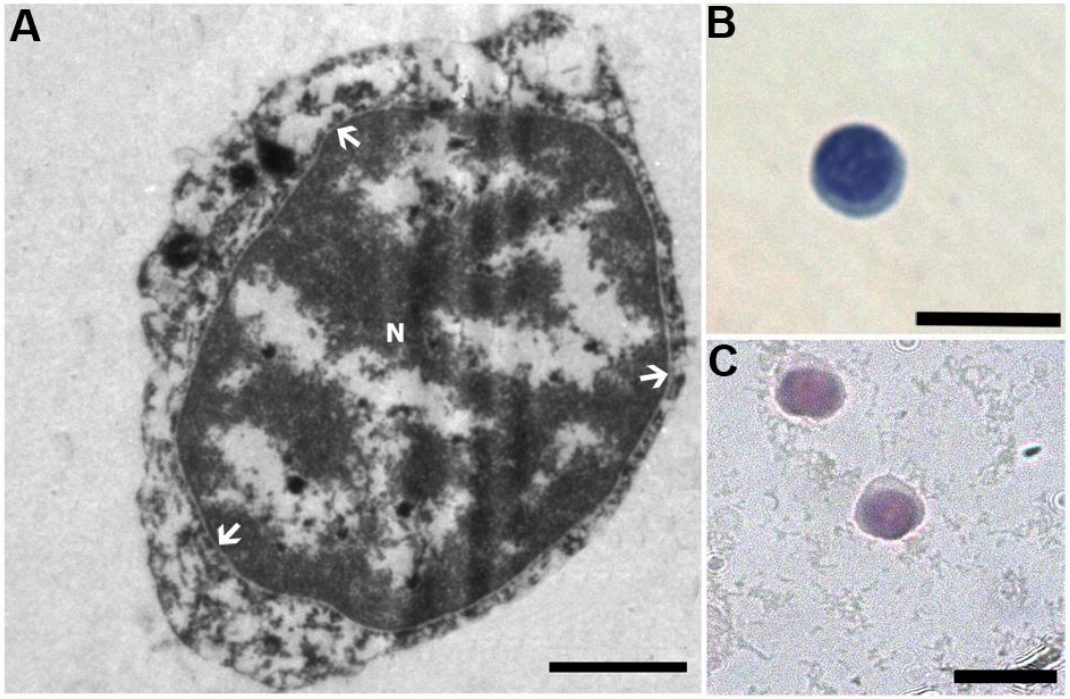

Figure 7 – Possible progenitor cell of *Eucidaris tribuloides*. A – Transmission electron microscopy; B and C – Light microscopy stained with Toluidine Blue and Hematoxylin and Eosin respectively. Legend: Arrowhead = nuclear membrane; N = Nuclei. Scale: A = 1 µm; B and C = 10 µm.

Capítulo 4

Isolamento e função fisiológica dos celomócitos de *Arbacia lixula* and *Lythechinus variegatus* (Echinoidea: Camarodonta).

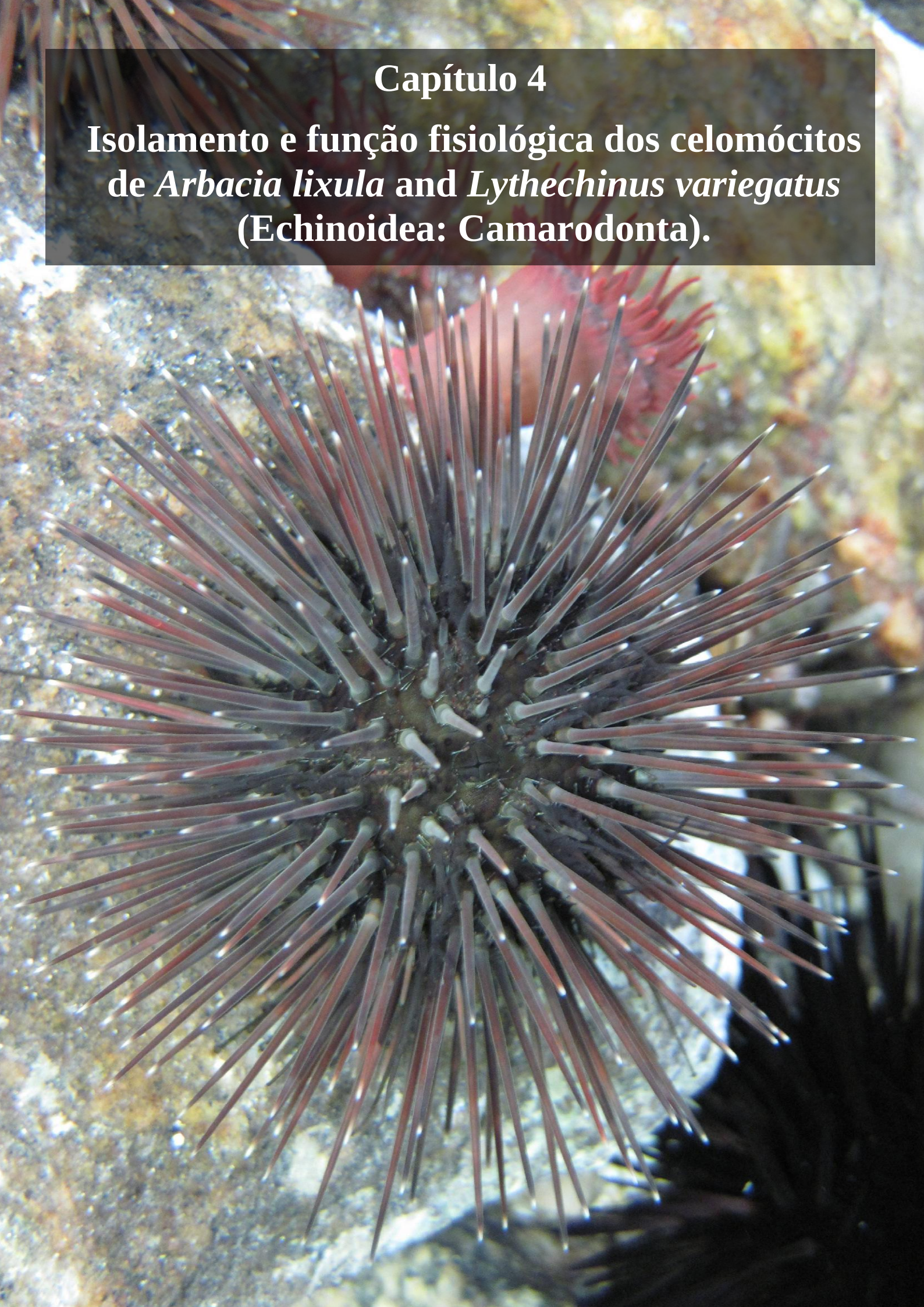

Justificativa

Embora os Echinoidea sejam o grupo mais bem estudado de equinodermos com relação às células celômicas, estes estudos frequemente utilizam a fração total de células, ou frações enriquecidas, contendo predominantemente um determinado tipo celular. Para os equinodermos, o isolamento dos celomócitos ainda não é uma realidade e mesmo técnicas mais sofisticadas, como por exemplo, a citometria de fluxo, não se mostraram eficientes. Aparentemente, o problema parece residir em dois grandes entraves: (I) a falta de marcadores específicos para cada tipo celular, e (II) a sobreposição das diferentes subpopulações de esferulócitos devido a similaridades de tamanhos e granulosidades peculiares do processo de maturação. No entanto, uma nova técnica de citometria, denominada de citometria de fluxo por imagem (CFI), se mostrou promissora para o estudo dos celomócitos dos equinodermos. Nesta técnica, além do registro do tamanho, granulosidade e fluorescência de cada partícula observada, uma foto também é tirada, propiciando a análise da morfologia. Com isso, esta técnica se mostrou bastante adequada para os celomócitos dos echinodermos, que têm sido tradicionalmente estudados por meio da morfologia. Assim, este capítulo traz os resultados das análises dos celomócitos de *Arbacia lixula* e *Lytechinus variegatus*, por meio da citometria de fluxo por imagem. *Gates* com as mesmas subpopulações celômicas isoladas foram obtidos pela primeira vez para duas espécies diferentes, além dos parâmetros utilizados para a obtenção destes *gates*. Adicionalmente, foi testado se esta técnica seria eficiente no monitoramento das condições fisiológicas dos organismos e para isso, avaliou-se a frequência das populações celomáticas de *Arbacia lixula* após a indução de uma infecção bacteriana, utilizando a bactéria *Escherichia colli*.

Comparative study of coelomocytes from *Arbacia lixula* and *Lythechinus variegatus*: cell characterization and evidence of physiological functions

Vinicius Queiroz[a, b, *], Sandra Marcia Muxel[a], Márcio R. Custódio[a, b]

To be subimitted to Journal Cytotechnology

[a] - Departamento de Fisiologia, Instituto de Biociências, Universidade de São Paulo, São Paulo, SP, Brazil

[b] - Centro de Biologia Marinha (NAP–CEBIMar), Universidade de São Paulo, São Paulo, Brazil

Abstract

Our study aimed to characterize coelomocytes of two sea urchin species, *Arbacia lixula*, and *Lytechinus variegatus*, as well as to study the physiological function of these cells during bacterial infection. An analysis of area and aspect ratio parameters, using imaging flow cytometry (IFC), allowed the identification of two main cell populations in the coelomic fluid: circular and elongated cells. A combination of this method with nucleus dye labeling using propidium iodide allowed the determination of gates containing isolated subpopulations of vibratile cells, red spherulocytes, and phagocytes in both species. Moreover, two different subpopulations of phagocytes (large and small) were distinguished. We observed an increase in the abundance of phagocytes and a decrease in that of spherulocytes and vibratile cells as a response to an *Escherichia coli* infection in *A. lixula*. Thus, as seen here, the use of IFC may facilitate coelomocyte studies, allowing functional characterization of large numbers of cells by employing simple but accurate experimental procedures, in addition to identifying specific gates for main subpopulations. Still, we provide the first experimental evidence about the function of vibratile cells, corroborating its physiological function

Keywords: Cytology, echinoderm immunity, invertebrate physiology, red spherulocyte, vibratile cell

[*] **Corresponding author**: V. Queiroz, Departamento de Fisiologia Geral, Instituto de Biociências, Universidade de São Paulo, Rua do Matão, nº 321, Cidade Universitária,

São Paulo (SP), Brazil. CEP: 05508-090. Tel: +55113091-7522. E-mail: vinicius_ufba@yahoo.com.br

INTRODUCTION

Echinoderms are marine deuterostome invertebrates characterized by their calcareous endoskeleton and remarkable pentamerous symmetry (Pawson 2007). They typically have six to eight main cell types in their coelomic fluid (Chia and Xing 1995). These cells, termed coelomocytes, are important for physiological functions such as regeneration (Garcia-Arraras et al. 2006), phagocytosis (Faria and Silva 2008), encapsulation of foreign matter (Canicatti and D'Ancona 1989), and clotting (Bertheussen and Seljelid 1978). Recent studies examined these cells at different levels, including morphology and ultrastructure (Deveci et al. 2015; Queiroz and Custódio 2015), physiological functions (Matranga and Bonaventura 2002; Arizza et al. 2007), biotechnological applications (Haug et al. 2002), and their potential use for bio-monitoring (Matranga et al. 2005).

Regardless of the research topic, two main approaches have been commonly employed in studies addressing echinoderm coelomocytes: use of samples containing all coelomic cell types or use of (semi-)purified populations (Haug et al. 2002; Dolmatova et al. 2003). For the latter, the most common method is based on standard protocols of centrifugation by density gradients using sucrose (Lindsay et al. 1965), Percoll (Smith et al. 1992), or Ficoll (Messer and Wardlaw 1979), among others (Arizza et al. 2007; Canicatti et al. 1990). However, these methods typically yield fractions with more than one cell type (Gerardi et al. 1990).

Recently, numerous attempts have been made to establish protocols for flow cytometry (Coteur et al. 2002; Xing et al. 2008). However, there are considerably few fluorescent markers for specific cell types of echinoderms (Lin et al. 2007; Liao and Fungmann 2017); therefore, most works used only structural parameters (side and forward scatter – Xing et al. 2008; Romero et al. 2016). In these studies, gates for specific cell populations could not be defined, and both methods only yielded enriched subpopulations (Arizza et al. 2007; Romero et al. 2016).

The main problem when working with flow cytometry is similar to that seen when using gradient methods: specific coelomocytes can undergo a sequence of

maturation stages (Chia and Xing 1995; Queiroz and Custódio 2015), and during this process, density, size, and/or granularity of different populations may overlap with that of other cell types. This restricts the separation of monotypic layers, in the case of density gradients, or the identification of gates containing isolated populations in cytometers (Romero et al. 2016).

In recent years, imaging flow cytometry (IFC) has been adopted in several studies on vertebrates (*e.g.* human cells and/or extracellular corpuscles – Basiji et al. 2007; Henery et al. 2008; Headland et al. 2014; Clark 2015) This method produces digital images of every single registered particle, which can then be analyzed in combination with the typical cytometry parameters to obtain additional data from the cell suspension. As stated by Barteneva et al. (2012) 'this method allows for the acquisition and identification of tens of thousands of cellular events based on their fluorescent and morphological parameters'. Traditional identification of coelomocytes based on their morphology can be considerably useful in studies on echinoderms (Smith 1991; Queiroz and Custódio 2015).

Regarding the understanding of the physiological function of echinoderm coelomocytes, sea urchin has been the most studied model (Smith et al., 2010; 2018). There are evidence, based on experimental studies, showing that phagocytes are involved in phagocytosis (Arizza et al. 2013), while red and colorless spherulocytes are involved in antibactericidal and cytotoxic activities respectively (Arizza et al. 2007; Coates et al. 2017). For vibratile cells, although the most accepted hypotheses have suggested their involvement in coelomic fluid circulation or clotting reactions (Cuénot, 1981; Johnsson, 1969), there is no experimental evidence.

Thus, in the present study, we addressed the coelomic cells of two sea urchin species: *Arbacia lixula* (AL) and *Lytechinus variegatus* (LV), in a comparative perspective. The DNA/nucleus dye propidium iodide (PI) and a correlation between area and aspect ratio parameters were used to produce gates containing isolated subpopulations in both species. Additionally, we applied IFC to investigate *in vivo* cellular responses of coelomocytes of AL to a bacterial infection with *Escherichia coli*. In addition to the response of phagocytes and red spherulocytes, we observed changes in the vibratile cells, corroborating its involvement in sea urchin immune response. Therefore, our results indicate that IFC can be used for characterizing coelomocytes and for investigating changes in the response of each cell type to physiological alterations.

MATERIAL AND METHODS

Study animals and immune cell collection

Two sea urchin species, one camarodont (LV) and one arbacioid (AL) were collected from the São Sebastião Channel, São Paulo State, Brazil, and transferred to the Instituto de Biociências – Universidade de São Paulo. Coelomic fluid of three respective individuals of each species was collected by inserting a needle into the peristomial membrane and aspirating the fluid into a syringe containing 1.5 mL of a fixation medium (2.5% glutaraldehyde) in an isosmotic anticoagulant solution (20 mM ethylenediamine tetraacetic acid, 460 mM sodium chloride, 7 mM sodium sulfate, 10 mM potassium chloride, 10 mM 4-(2-hydroxyethyl)-1-piperazineethanesulfonic acid, at pH 8.2 – Dunham and Weissman 1986). Equal volumes of coelomic fluid were collected, and the samples were stored at 4 °C for at least 6 h. After fixation, cell suspensions were centrifuged at 150 × g for 10 min using an Eppendorf 5804R centrifuge and the supernatant was removed; the cells were then resuspended using the anticoagulant solution. This procedure was repeated three times to remove the fixation medium. Cell density was counted using a Neubauer chamber and was adjusted to 1×10^7 cells/mL using the anticoagulant solution. Of this cell suspension, 50 µL was used for cytometric analyses. Additional samples were collected from other specimens (n = 9) as described above; however, immediately before cytometric analyses, cells were labeled using 1 µg/mL PI. In this additional analysis, only PI-positive particles were considered. To reduce differences regarding physiological competences and coelomic fluid volumes, 21 similar-sized specimens of AL (4-5 cm in diameter) were used for the infection experiments. All animals used in the experiments were kept at room temperature in seawater tanks for one week to allow acclimation, as described in Queiroz (2016).

Imaging flow cytometer data acquisition and analysis

Data acquisition was performed at the Central de Aquisição de Imagens e Microscopia of the Instituto de Biociências (CAIMI-IB) using an imaging flow cytometer (FlowSight, Amnis-Merck Millipore). Acquisition speed was set to ‘low’, and the highest resolution was used. Roughly 20,000 cells were acquired based on area (as pixels) and on the aspect ratio defined as the value of the minor axis divided by the

major cell axis on channel 1. The focused cells were gated using root mean squared (RMS) gradient, based on channel 1. Channels 1, 4, and 6 were used to analyze brightfield, PI labeling, and side scatter (SSC) parameters, respectively, using IDEAS software (Amnis-Merck Millipore). Cell debris and doublets were gated out based on area and aspect ratio features (indicated in Fig. 1). Singlet cells were gated to separate PI-positive cells, and subpopulations of coelomocytes were determined based on area vs. aspect ratio (Fig. 1). The width parameter was based on channel 1. Data on width and cell percentage are presented as means ± standard error of the mean. Differences in percentage means between treatments (PI^+ and no PI) or species were tested using a Student's two-tailed t-test at $p < 0.05$.

Bacterial culture and infection procedures

Escherichia coli (strain ATTC 11229) were cultured for 24 h before the experiments using LB nutrient broth (Sambrook and Russel, 2001) at 37 °C. The culture was collected after centrifugation at 5,000 × g for 15 min. The supernatant was removed, and *E. coli* were mixed with sterile-filtered (pore size 0.22 µm) natural seawater at a concentration of 1×10^9 cells/mL (Lee et al. 2001). Specimens of AL were injected through the peristome with 1 mL of *E. coli* (treatment group) or with the same volume of sterile natural seawater (control group) using a hypodermic needle (Lee et al. 2001). Before this experiment, the average cell density and coelomic fluid volume in the coelom of AL were determined as $8.7 \times 10^6 \pm 1.5 \times 10^6$ cells/mL and 6-7 mL per individual (n = 5), resulting in a final proportion of 15-20 bacteria per coelomocyte in the treatment group.

Experimental design

Twenty-one specimens of AL were assigned to one of three groups: the treatment group, which was injected with *E. coli* in sterile natural seawater (n = 9); the control group, which was injected with sterile-filtered natural seawater (n = 9); and the untreated group, which comprised the animals sampled before the start of the experiment (t_0) to compare the health status of the individuals (n = 3). All individuals of the control and treatment groups were injected at the beginning of the experiment (t_0), and at 24, 48, and 72 h, and the coelomic cells of three individuals were collected at the

same time of the day (10:00 h). Cells were fixated and analyzed as described above. Only PI-positive cells were considered in this analysis. Differences between means were tested using a Student's two-tailed t-test at $p < 0.05$.

RESULTS

Identifying coelomocyte populations

Using only the aspect ratio vs. area features, the coelomocytes were assigned to two major populations: circular cells ([C]; aspect ratio 0.78-1, area 100-900) and elongated cells ([E]; aspect ratio 0.2-0.6, area 100-900; Fig. 1). Within these two broad categories, most coelomocyte subpopulations present in the coelomic fluid, *i.e.* phagocytes, vibratile cells, and spherulocytes, were identified using IFC. In the circular population, two different groups were observed: the first group comprised small circular cells ([SC]; aspect ratio 0.78-1, area 100-200), and the second group comprised large circular cells ([LC]; aspect ratio 0.78-1, area 250-450). In the elongated population, only phagocytes were observed, which were subdivided into small elongated cells ([SE]; aspect ratio 0.2-0.6, area 100-300) and large elongated cells ([LE]; aspect ratio 0.2-0.6, area 300-900; Fig. 1). Cell populations in the intermediate region ([I]; aspect ratio 0.6-0.8, area 100-900) were heterogeneous as a mix of all subpopulations described above was observed in this gate.

Characteristics of coelomocytes based on IFC

Regardless of the species analyzed, morphology and width were considerably specific to each cell population, which facilitated coelomocyte recognition (Figs. 2 and 3; Table 1). Nevertheless, PI labeling was necessary to verify cell identification, mainly inside the SC gate. In the initial analyses, this area contained objects with contrasting morphologies in which the usual parameters (aspect ratio × area) could not be used for population separation. According to their granularity and opacity based on SSC characteristics, SC was divided into two subgroups: 'less complex' SC (SC_L) and 'complex' SC (SC_C; Fig. 2). To ensure that particles identified as SC_L were not in fact debris, the cells were labeled with PI, and further analyses were conducted. Labeled nuclei were only observed in SC_C, indicating that SC_L particles were debris (Fig. 3). Regarding other cell types, both unlabeled and PI-labeled cells provided very similar

results; however, to avoid potential errors, all descriptions were based exclusively on PI-labeled samples.

The SC were characterized as dark and visibly vacuolated coelomocytes (Fig. 2 and 3), while the LC subpopulation comprised large round cells with a central nucleus, granulous cytoplasm, and typically with a visible flagellum (*i.e.* vibratile cells – Fig. 2 and 3). SE comprised phagocytes with a peripheral nucleus and short cytoplasmic expansions (Fig. 2 and 3). LE were phagocytes with remarkable cytoplasmic expansions and with a subcentral nucleus, which was almost two-fold larger than that in SE (Fig. 2 and 3; Table 1). For each coelomic subpopulation, widths were very similar in both species (Table 1).

Coelomocyte frequency in different sea urchin species

The distribution of the main coelomic populations in gates C, I, and E, was very similar in both species, considering PI-labeled samples. However, there were some differences in the frequency of non-labeled coelomocytes (Table 1). Gate C comprised most cells (57.17 ± 1.83% in AL, and 59.44 ± 1.83% in LV) followed by E, which varied from 33.08 ± 0.88% in AL to 30.41 ± 1.53 in LV, and the less abundant intermediate cells, ranging from 9.33 ± 1.13% in AL to 9.74 ± 0.65 in LV (Table 1). The frequency of specific coelomocyte subpopulations in unlabeled samples differed from that in PI-labeled ones (Table 1). In *Arbacia lixula*, SC cells were the most abundant coelomocyte type in unlabeled samples, followed by SE and LC, while in the species LV, SE, LC and SC were respectively the most abundant cell types. LE cells were the most uncommon cell type in both species (Table 1). In contrast, in PI-labeled samples, LC were by far the most abundant coelomocytes (29.39 ± 0.79% in AL and 29.22 ± 0.85% in LV), followed by SC (11.77 ± 1.22% in AL and 8.09 ± 1.58% in LV; Table 1). LE were the third-most abundant cell type (7.05 ± 1.09% in AL, and 7.94 ± 0.63% in LV), and SE were the least abundant coelomocyte type (1.74% in AL, and 1.54% in LV). Except for SC, there were no significant differences between species (Table 1).

Experimental infection

Differences in coelomocyte frequencies of general and specific cell types were observed during the time of the experiment and between control and treatment groups,

mainly 48 and 72 h after *E. coli* injection (Fig. 4). In general, cell frequency in circular cells was lower in the treatment than in the control group (apart from SC after 24 h). However, a different pattern was observed regarding the frequencies of elongated coelomocytes, which showed an increase (Fig. 4). The frequency of circular cells in controls and untreated individuals was generally similar and differed significantly from treated individuals (Fig. 4).

The treatment decreased the frequency of circular cells over the course of the experiment (to about 15% after 24, 48, and 72 h) compared to the untreated group (Fig. 4A). Comparisons between control and treatment groups in the same period of time showed significant differences ($p < 0.05$) after 48 and 72 h (Fig. 4). The percentage of circular cells in the control group after 24 and 48 h was similar to that in the untreated group (at 0 h), but was reduced after 72 h. The same general pattern was observed in LC, the percentage of which decreased by nearly 20% in the treatment group, compared to the control group (at 48 h; Fig. 4B). In contrast, SC showed a different pattern: the treatment led to an increase in their abundance of almost 50% after 24 h, but to a reduction after 48 and 72 h, compared to the control (Fig. 4C).

Elongated cells were less abundant than circular cells at 0 h (Fig. 4A and 4D), and showed a distinct pattern in response to *E. coli* injections with higher abundance in the treatment than in the control group. The treatment promoted an increase in the abundance of elongated cells after 72 h (about 55%; Fig. 4D), of large elongated (LE) phagocytes after 48 h (about 40%; Fig. 4E), and smaller elongated cells after 72 h (about 80%; Fig. 4F). However, cell frequency in the gate I showed an increase in the treatment group after 48 h (about 15%), but a decrease after 72 h, compared to the control (Fig. 4G).

DISCUSSION

Coelomocyte populations

Flow cytometry has been used in some studies on coelomic cells of echinoderms, apart from crinoids and ophiuroids (Xing et al. 2008; Coteur et al. 2002; Fafandel et al. 2008). Echinoidea is the most extensively studied group, and this technique was used to measure DNA content (Fafandel et al. 2008), presence of neuroendocrine markers (Koros and Pulsford 1993), multixenobiotic resistance proteins (Marques-Santos et al.

2017), cytotoxic activity (Lin et al. 2001), and to generate of fluorescent markers (Lin et al. 2007), among other applications. Despite these different approaches, few studies succeeded in discriminating specific coelomocyte subpopulations.

Four main types of coelomocytes are typically recognized in echinoids, *i.e.* phagocytes, vibratile cells, and red and colorless spherulocytes (Chia and Xing 1995; Smith et al. 2018), but few studies using flow cytometry have identified coelomocytes other than phagocytes (vibratile cells – Doussantousse et al. 2011; red spherulocytes – Stabili and Pagliara, 2015). Using IFC, we identified most of the coelomocyte subpopulations described in sea urchins (*cf.* Fig. 2 and 3). The gate containing LC clearly comprised vibratile cells, which are the only flagellated coelomocytes in echinoids (*cf.* Fig. 2 and 3), and SC cells were similar to red spherulocytes. These were rather granular and showed darker coloration in the brightfield, probably due to echinochrome-A. However, no cells morphologically similar to colorless spherulocytes were discriminated.

Studies on live sea urchin phagocytes in suspension have reported petaloid and filopodial forms (Chia and Xing 1995). However, small phagocytes and discoidal and polygonal cells are typically observed after phagocytes attach and spread out on a flat surface (Edds 1993; Gross et al. 2000; Majeske et al. 2013). Cells morphologically similar to LE and SE observed using IFC were found in *Dermasterias imbricate* using scanning electron microscopy (Kaneshiro and Karp, 1980). Only one previous study successfully differentiated phagocytic subpopulations in echinoderms using conventional flow cytometry (Coteur et al. 2002). In the present study, two distinct phagocyte subpopulations were observed in two different species using IFC. The large phagocyte resembled the petaloid form of discoidal and polygonal phagocytes due to its bladder-like expansions (*cf.* Fig. 2 and 3). Indeed, SE cells matched the subpopulation described by Gross et al. (2000). However, specific phagocyte subpopulation can only be accurately identified based on cytoskeletal features, typically after spreading on a flat surface (Edds 1993; Majeske et al. 2013). Additional studies are needed to further elucidate these two phagocytic populations.

Data on cell type frequency and respective widths in the main gates (*viz.* C, E and I) followed the same pattern in both species, whereas the relative proportions of specific subpopulations differed markedly (Table 1). The LC and SC cells were more frequent in populations labeled with PI and gated for nucleated cells, compared to

unlabeled ones. In the latter, SC and SE populations were more frequent, probably due to false-positive detection of small debris as whole cells (as observed in SC_L cells in the initial analysis; *e.g.* Fig. 2). Therefore it is important to use PI-labeling or other nuclear markers to distinguish coelomocytes. Most previous studies referred to phagocytes as the most frequent coelomocyte (Faria and Silva 2008; Smith et al. 2006; 2010); however, this observation was not confirmed by our results. Numerous phagocytes were observed in the intermediate region. As highlighted in the echinoderm literature (Edds 1993; Eliseikina and Magarlamov 2002; Matranga et al. 2005), petaloid and filopodial cell morphology probably corresponds to different stages of the same cell type. Thus, the fast fixation method used here may have captured phagocytes in a transitional state and made them appear more rounded than elongated, which may have led to an underestimation of the actual proportion of this subpopulation.

Experimental infection

Immune challenges, by injections of either bacterial cells or purified bacterial factors (*e.g.* lipopolysaccharides or peptidoglycans), are useful to study immunological functions in invertebrates (Harshbarger and Heimpel 1968; Gätschenberger et al. 2013) including echinoderms (Yui and Bayne 1983; Ramírez-Gómez et al. 2010). In the present study, we simulated an infection by injecting live *E. coli* in the coelomic cavity of AL and observed coelomocyte population dynamics over 72 h. Studies assessing immune challenges in echinoderms over more than 24 h are rare (Kaneshiro and Karp 1980; Ptytycz and Seljelid 1993), and most studies involved the assessment of the first few hours after infection, typically only up to 48 h (Ptytycz and Seljelid 1993).

In the main cell gates (C and E), generally opposed trends in cell frequencies were observed in infected animals: the number of circular cells decreased, whereas elongated coelomocytes increased, compared to the control (*cf.* Fig. 4). In *Holothuria glaberrima* for instance, a similar pattern was observed in individuals stimulated with different pathogen-associated molecular patterns (PAMP) showing an increase in the number of phagocytes and a decrease in the number of type-1 spherulocytes (Ramírez-Gómez et al. 2010). In *Strongylocentrotus droebachiensis* and *S. purpuratus*, a remarkable initial decrease in cell frequency was observed in the first 6 h after infection, followed by an increase after 24 h (Yui and Bayne 1983; Ptytycz and Seljelid 1993).

In the present study, we observed a distinct change in the abundance of vibratile cells, red spherulocytes, and large and small phagocytes in AL, which can be interpreted as a physiological response to infection. Red spherulocytes have an antibacterial function (Coates 2017), and phagocytes can remove foreign particles, including bacteria (Smith et al. 2006). In contrast, there is no experimental evidence on vibratile cell function. However, some *in vitro* studies have pointed out that this cell population seems to be involved in defense mechanisms by degranulating during coagulation events (Johnson 1969a; 1969b; Bertheussen and Seljelid 1978). According to Johnsson (1969a), vibratile cells of *Strongylocentrotus* were able to 'cause temporary stasis of the coelomic fluid in areas of invasion by foreign liquid and other foreign material'. Smith et al. (2010) stated that 'clotting could be an important physiological response, functioning to block the loss of coelomic fluid, and to sequester pathogens and prevent their invasion throughout the body'. Furthermore, a recent study showed that lipopolysaccharides can elicit cell aggregation (Majeske et al. 2013). Therefore, we hypothesized that vibratile cells may be cooperating with other coelomocytes to maintain homeostasis in AL. Based on our results, the reduction of LC and SC cells (*i.e.* vibratile cells and red spherulocytes respectively) may be interpreted as a response in order to prevent the spreading and proliferation of bacteria. Vibratile cells could thus be involved in clotting reactions, possibly to immobilize pathogens (Johnson 1969a; 1969b; Bertheussen and Seljelid 1978) while red spherulocytes act antibiotically by releasing echinochrome-A (Coates et al. 2018). Subsequently, an increase in phagocytes (elongated cells) may be a strategy to cleanse the coelomic fluid of pathogens or foreign particles, a fact already observed in other species (Yui and Bayne 1983). This sequence might explain why the number of red spherulocytes and vibratile cells decreased in the first 24 h and then remained stable, whereas the number of phagocytes increased consistently.

Further interesting aspects can be seen in the intermediate region (*cf.* Fig. 4G). In this gate, a remarkable increase in cell frequency was observed in infected individuals, compared to the control. We suggest two hypotheses: first, these changes may be a natural phenomenon in the coelomic fluid as coelomocytes are able to modify their shape, as previously observed in spherulocytes and phagocytes (Smith et al. 2010; 2018); second, changes in proportions may be due to vibratile cells and red spherulocytes modifying their shapes by releasing their contents, and the recruitment of

circular and elongated cells during the inflammatory response. We found a remarkable decrease in the number of vibratile cells and red spherulocytes, and an increase in the number of phagocytes during the process. This is in line with the pattern observed in *H. glaberrima*, which showed similar changes in coelomocyte frequency after PAMP stimulation (Ramírez-Gómez et al. 2010). Accordingly, Ramírez-Gómez et al. (2010) suggest that lipopolysaccharides may elicit an immune response in echinoderms, thereby increasing the number of phagocytes and decreasing the number of spherulocytes.

The technique used in the present study seems to be suitable for both cell characterization and physiological investigation. Immediate coelomocyte fixation with 2.5% glutaraldehyde, a typical fixative for electron microscopy analyses, helped retain the flagellum of vibratile cells and prevented substantial changes in phagocyte shape (*cf.* Fig. 2 and 3), as previously reported (Kaneshiro and Karp 1980). However, the conspicuous morphology of red spherulocytes was not conserved. Instead, a small corpuscle was observed, which was considerably opaque due to the loss of pigments during fixation. This is supported by two observations: (I) most red spherulocytes observed using light microscopy (data not shown) presented the typical red coloration but appeared shrunken, and (II) the fixative solution turned reddish during the process, indicating that the cellular content of red spherulocytes partially leaked into the solution. Regarding phagocytes, it is possible that the three different subpopulations, *i.e.* discoidal, polygonal, and small phagocyte, show only two morphologies while in suspension in the physiological coelomic fluid and can only be differentiated after spreading on a flat surface. Moreover, the use of PI provided more reliable information as intact cells were differentiated from debris, and the noise was thus removed from the data.

Taken together, the use of IFC can provide fast and more accurate measurements to study the physiology of echinoderms (*e.g.* in studies on immune parameters and/or using coelomocytes as endpoint – Coteur et al. 2002; Stabili and Pagliara 2015; Wang et al. 2015; or on aquaculture – Wang et al. 2008; Shannon et al. 2015a; 2015b). This method can provide new insights in coelomocyte studies and has previously been applied in other phyla (Clark 2015; Erdbrugger and Lannigan 2016). With the present study, we provide, for the first time, parameters for IFC that can be used for diverse approaches as well as the first experimental evidence about vibratile cell function. This

is evidenced by our results on *A. lixula* coelomocyte subpopulation dynamics in response to experimental bacterial infection. We suggest the cooperation of different coelomocyte populations during infections. Vibratile cells and red spherulocytes may be involved in initial immobilization through clotting and neutralization, respectively, of foreign particles, whereas phagocytes are responsible for cleansing the coelomic cavity by phagocytosis. However, further studies on vibratile cells are needed, as a reliable morphological characterization and experimental assessments of their physiological functions are lacking. Still, it is necessary to know how the early cellular response in the coelomic cavity happens, which will certainly help to understand the real function of vibratile cells during foreign invasions.

ACKNOWLEDGMENTS

The authors thank Prof. Regina P. Markus, Prof. Pedro A. C. M. Fernandes, and the "Central de Aquisição de Imagens e Microscopia" (CAIMI) from the Instituto de Biociências of the Universidade de São Paulo for the use of the FlowSight Amnis (FAPESP 2014/20809-1).

FUNDING:

This study was supported by the Fundação de Amparo a Pesquisa do Estado de São Paulo-FAPESP (Grant number: 2015/21460-5 and 2018/14497-8) and Coordenação de Aperfeiçoamento de Pessoal de Nível Superior-CAPES.

REFERENCES

Arizza V, Giaramita F, Parrinello D, Cammarata M, Parrinello N. 2007. Cell cooperation in coelomocyte cytotoxic activity of *Paracentrotus lividus* coelomocytes. Comp. Biochem. Physiol. A: Mol. Integr. Physiol. 147: 389–394.

Barteneva NS, Fasler-Kan E, Vorobjev IA. 2012. Imaging Flow Cytometry: Coping with Heterogeneity in Biological Systems. J Histochem Cytochem 60(10) 723– 733

Basiji DA, Ortyn WE, Liang L, Venkatachalam V, Morrissey P. 2007. Cellular image analysis and imaging by flow cytometry. Clin Lab Med 27(3): 653–658.

Bertheussen K, Seljelid R. 1978. Echinoid phagocytes in vitro, Exp. Cell. Res. 111: 401–412.

Biophysical Research Communications 134:1319–1326. doi:10.1016/0006-291X(86)90394-3.

Borges JCS, Branco PC, Pressinotti LN, Silva JRMC. 2010. Intranuclear crystalloids of sea urchins as a biomarker for oil contamination. Polar Biol 33:843–849.

Canicatti C, D Jan, M Jangoux. 1990. Enrichment in different categories of *Holothuria polii* coelomocytes by centrifugation on Na-Metrizoate gradient. Boll Zool 57: 267-270.

Canicatti C, D'Ancona G. 1989. Cellular aspects of *Holothuria polii* immune response. J Invert Pathol 53:152-158.

Chao Y, Zhang T. 2011. Optimization of fixation methods for observation of bacterial cell morphology and surface ultrastructures by atomic force microscopy. Applied Microbiol Biotechnol 92:381–392.

Chia F, Xing J. 1995. Echinoderm coelomocytes, Zool. Stud. 35: 231–254.

Clark RT. 2015. Imaging flow cytometry enhances particle detection sensitivity for extracellular vesicle analysis. Nat Methods 12: 1-2.

Coteur G, DeBecker G, Warnau M, Jangoux M, Dubois P. 2002a. Differentiation of immune cells challenged by bacteria in the common European starfish, *Asterias rubens* (Echinodermata). Eur J Cell Biol 81:413-418.

Coteur G, Warnau M, Jangoux M, Dubois P. 2002b. Reactive oxygen species (ROS) production by amoebocytes of *Asterias rubens* (Echinodermata). Fish & Shellfish Immunol 12: 187–200.

Cuénot L. 1891. Etudes sur les sang et les glandes lymphatiques dans la sériee animale (2° partie: Invértebés). Arch. Zool. Exptl. Gén (Sér. 2), 9, 13-90, 365-475, 593-670.

Deveci R, Sener E, Izzetoglu S. 2015. Morphological and ultrastructural characterization of sea urchin immune cells, J. Morphol. 276: 583–588.

Dolmatova LS, Eliseykina, MG, Timchenko NF, Kovaleva AL, Shitkova OA. 2003. Generation of reactive oxygen species in the different fractions of the coelomocytes of holothurian *Eupentacta fraudatrix* in response to the thermostable toxin of *Yersinia pseudotuberculosis* in vitro. Chin J Limnol Oceanol 21 (4):128–134.

Doussantousse E, Pelletier E, Beaulieu L, Rainville L, Belzile C. 2011. Multixenobiotic resistance in coelomocytes from three echinoderm species. Aquat Biol 12: 81–96.

Dunham P, Weissman G. 1986. Aggregation of marine sponge cells induced by Ca pulses, Ca ionophores, and phorbol esters proceeds in the absence of external Ca. Biochemical and Biophysical Research Communications, 134(3):1319-1326.

Dybas L, Fankboner PV. 1986. Holothurian survival strategies: mechanisms for the maintenance of a bacteriostatic environment in the coelomic cavity of the sea cucumber, *Parastichopus californicus*. Dev Comp Immunol, 10(3):311-330.

Edds KT. 1993. Cell biology of echinoid coelomocytes: I. Diversity and characterization of cell types. J Invert Pathol 61:173-178.

Eliseikina MG, Magarlamov TY. 2002. Coelomocyte morphology in the Holothurians Apostichopus japonicus (Aspidochirota: Stichopodidae) and Cucumaria japonica (Dendrochirota: Cucumariidae). Russian Journal of Marine Biology, 28:197–202.

Erdbrugger U, Lannigan J. 2016. Analytical Challenges of Extracellular Vesicle Detection: A Comparison of Different Techniques. Cytometry Part A 89A: 123-134.

Fafandel M, Bihari N, Smodlaka M, Ravlic S. 2008. Hemocytes/coelomocytes DNA content in five marine invertebrates cell cycles and genome sizes. Biologia 63:730–736.

Faria MT, Silva JR. 2008. Innate immune response in the sea urchin *Echinometra lucunter* (Echinodermata), J. Invert. Pathol. 98 (2008) 58-62.

Fischer ER, Hansen BT, Nair V, Hoyt FH, Dorward DW. 2012. Scanning Electron Microscopy. Curr Protoc Microbiol 25:B:2B.2:2B.2.1–2B.2.47.

Garcia-Arraras JE, Schenk C, Rodrigues-Ramirez R, Torres II, Valentin G, Candelaria AG. 2006. Spherulocytes in the echinoderm *Holothuria glaberrima* and their involvement in intestinal regeneration, Dev. Dyn. 235: 3259-3267.

Gätschenberger H, Azzami K, Tautz J, Beier H (2013) Antibacterial Immune Competence of Honey Bees (Apis mellifera) Is Adapted to Different Life Stages and Environmental Risks. PLoS ONE 8(6): e66415. doi:10.1371/journal.pone.0066415

Gerardi P, Lassegues M, Canicatti C. 1990. Cellular distribution of sea urchin antibacterial activity. Biol Cell 70: 153–157

Gross PS, Clow LA, Smith LC. 2000. SpC3, the complement homologue from the purple sea urchin, *Strongyloncentrotus purpuratus*, is expressed in two subpopulations of the phagocytic coelomocytes. Immunogenetics 51:1034-1044.

Haug T, Kjuul AK, Styrvold OB, Sandsdalen E, Olsen ØM, Stensvåg K. 2002. Antibacterial activity in *Strongylocentrotus droebachiensis* (Echinoidea), *Cucumaria frondosa* (Holothuroidea), and *Asterias rubens* (Asteroidea). J Invert Pathol 81: 94–102.

Headland SE, Jones HR, D'as ASV, Perretti M, Norling LV. 2014. Cutting-Edge Analysis of Extracellular Microparticles using ImageStreamX Imaging Flow Cytometry. Sci Rep 4: 5237. DOI: 10.1038/srep05237

Henery S, George T, Hall B, Basiji D, Ortyn W, Morrissey P. 2008. Quantitative image based apoptotic index measurement using multispectral imaging flow cytometry: a comparison with standard photometric methods. Apoptosis. 13:1054–1063.

Horohov DW, Dunn PE. 1983. Phagocytosis and nodule formation by hemocytes of Manduca sexta larvae following injection of Pseudomonas aeruginosa. J Invertebr Pathol 41: 203–213

Horohov DW, Dunn PE. 1982. Phagocytosis and nodule formation by hemocytes of *Manduca sexta* larvae following injection of bacteria. Journal of Invertebrate Pathology, 40: 327-339.

Johnson PT. 1969a. The coelomic elements of sea urchins (*Strongylocentrotus*). I. The normal coelomocytes; their morphology and dynamics in hanging drops. J Invertebr Pathol 13:25–41.

Johnson PT. 1969b. The coelomic elements of the sea urchins (*Strongylocentratus*) III. In vitro reaction to bacteria. Journal of Invertebrate Pathology, 13: 42-62.

Kaneshiro ES, Karp RD. 1980. The ultrastructure of coelomocytes of the sea star *Dermasterias imbricata*. Biol Bull, 159:295±310.

Koltsova EA, Boguslavskaya LV, Maximov OV. 1981. On the functions of quinonoid pigment production in sea urchin embryos. Inter J Inver Repro 4:17–28.

Koros AMC, Pulsford A. 1993. Neuroendocrine Marker Expression on Sea Urchin Coelomocytes and Other immunoregulatory Parameters May be Used to Monitor Environmental Changes. Mar Envir Res 35: 137-140

Kudryavtsev IV, D'yachkov IS, Mogilenko DA, Sukhachev AN, Polevshchikov AV. 2016. The Functional Activity of Fractions of Coelomocytes of the Starfish *Asterias rubens* Linnaeus, 1758. Russ J Mar Biol 42(2): 158–165.

Lee YK, Soh BS, Wu JH. 2001. Quantitative assessment of phagocytic activity of hemocytes in the prawn, *Penaeus merguiensis*, by flow cytometric analysis. Cytometry A. 43: 82-85.

Li Q, Li Y, Li H, Wang YN, Xu DH. 2010. Production, characterization and application of monoclonal antibody to spherulocytes: A subpopulation of coelomocytes of *Apostichopus japonicas*. Fish Shellfish Immunol 29: 832– 838.

Liao WY, Fugmann SD. 2017. Lectins identify distinct populations of coelomocytes in *Strongylocentrotus purpuratus*. PloS one, 12(11), e0187987.

Lin W, Grant S, Beck G. 2007. Generation of monoclonal antibodies to coelomocytes of the purple sea urchin *Arbacia punctulata*: characterization and phenotyping. Dev Comp Immunol 31:465-475.

Lin WY, Zhang H, Beck G. 2001. Phylogeny of Natural Cytotoxicity: Cytotoxic Activity of Coelomocytes of the Purple Sea Urchin, *Arbacia punctulata*. J Exp Zool 290:741–750.

Lindsay J, RB Lyons, RL Bacon. 1965. Separation of sea urchin coelomocyte types by centrifugation. Am Zool 15: 645.

Majeske AJ, Bayne CJ, Smith LC. 2013. Aggregation of Sea Urchin Phagocytes Is Augmented In Vitro by Lipopolysaccharide. PLoS ONE 8(4): e61419. doi:10.1371/journal.pone.0061419

Marques-Santos LF, Hégaret H, Lima-Santos L, Queiroga FR, da Silva PM. 2017. ABCB1 and ABCC1-like transporters in immune system cells from sea urchins *Echinometra lucunter* and *Echinus esculentus* and oysters *Crassostrea gasar* and *Crassostrea gigas*. Fish and Shellfish Immunology, 70:195-203. doi: 10.1016/j.fsi.2017.09.014.

Matranga V, Bonaventura R, Di Bella G. 2002. Hsp70 as a stress marker of sea urchin coelomocytes in short term cultures. Cell Mol Biol 48: 3453–59.

Matranga V, Pinsino A, Celi M, Natoli A, Bonaventura R, Schröder HC, and Müller WEG 2005 Monitoring chemical and physical stress using sea urchin immune cells. In: Echinodermata, Ed. Matranga V. Springer, Heidelberg, 85–110.

Messer LI, Wardlaw AC. 1979. Separation of the coelomocytes of *Echinus esculentus* by density gradient centrifugation. Proceedings of the European Colloquium on Echinoderms/Brussels 3-8.

Pawson DL. 2007. Phylum Echinodermata, Zootaxa 1668: 749–764.

Pawson DL. 2007. Phylum Echinodermata. Zootaxa 1668:749–764.

Ptytycz B, Seljelid R. 1993. Bacterial clearance by the sea urchin *Strongylocentrotus droebrachiensis*. Developmental and Comparative Immunology, 17: 283-289.

Queiroz V, Custodio MR. 2015. Characterization of the spherulocyte subpopulations in *Eucidaris tribuloides* (Cidaroida: Echinoidea). Ital J Zool 82(3): 338-348.

Queiroz V. 2016. Opportunity makes the thief—observation of a sublethal predation event on an injured sea urchin. Mar Biodiv DOI 10.1007/s12526-016-0530-1.

Ramírez-Gómez, F., Aponte-Rivera, F., Méndez-Castaner, L., & García-Arrarás, J. E. 2010. Changes in holothurian coelomocyte populations following immune stimulation with different molecular patterns. Fish & shellfish immunology, 29(2), 175-185.

Romero A, Novoa B, Figueras A. 2016. Cell mediated immune response of the Mediterranean sea urchin *Paracentrotus lividus* after PAMPs stimulation. Dev Comp Immunol 62: 29–38.

Service M, Wardlaw AC. 1984. Echinochrome-A as a bactericidal substance in the coelomic fluid of *Echinus esculentus* (L.). Comp Biochem Physiol B Comp Biochem, 79:161–165

Shannon R, Blumenthal E, Mustafa A. 2015. Physiological and Immunological Responses in Giant California Sea Cucumbers (*Parastichopus californicus*) Exposed to Aquaculture-related Stress. Bioengin Biosci 3(4): 60-67.

Shannon R, Mustafa A. 2015. A Comparison of Stress Susceptibility of Sea Urchins and Sea Cucumbers in Aquaculture Conditions. Bioengin Biosci 3(6): 100-107.

Smith CL, RJ Britten, EH Davidson. 1992. SpCoel1: a sea urchin profilin gene expressed specifically in coelomocytes in response to injury. Mol. BioI. Cell 3: 403-414.

Smith LC, Ghosh J, Buckley KM, Clow LA, Dheilly NM, Huag T, Henson JH, ChengMan Lun CL, Majeske AJ, Matranga V, Nair SV, Rast JP, Raftos DA, Roth M, Sacchi S, Schrankel CS, Stensvag K. 2010. Echinoderm immunity. In: Söderhäll K, editor. Invertebrate immunity. New York, NY: Landes Bioscience and Springer Science BusinessMedia. pp. 260–301.

Smith LC, Rast JP, Brockton V, Terwilliger DP, Nair SV, Buckley KM, Majeske AJ. 2006. The sea urchin immune system. Inver Surv J 3:25–39.

Smith VJ. 1981. The Echinoderms. In: Ratcliffe NA, Rowley AF, editor. Invertebrate Blood Cells. New York: Academic Press. p 513–562.

Smith LC, Arizza V, Hudgell MAB, Barone G, Bodnar AG, Buckley KM, Furukawa R. 2018. Echinodermata: The Complex Immune System in Echinoderms. *In*: Advances in Comparative Immunology (pp. 409-501). Springer, Cham.

Stabili L, Pagliara P. 2015. The sea urchin *Paracentrotus lividus* immunological response to chemical pollution exposure: The case of lindane. Chemosphere 134: 60–66.

Wang F, Yang H, Gabr HR, Gao F. 2008. Immune condition of *Apostichopus japonicus* during aestivation. Aquaculture 285: 238–243.

Wang S, Li T, Xu L, LI L, Fan Y, Wei J. 2015. Immunopotentiating effect of small peptides on primary culture coelomocytes of sea cucumber, *Apostichopus japonicus*. J World Aquacult Soc. 46(3): 337-343.

Xing J, Yang HS, Chen MY. 2008. Morphological and ultrastructural characterization of the coelomocytes in *Apostichopus japonicus*. Aquat Biol 2:85–92.

Yui MA, Bayne CJ. Echinoderm immunology: bacterial clearance by the sea urchin Strongylocentrotur purpuratus. Biol Bull 1983;165:473–86.

Figures, Tables, and Captions

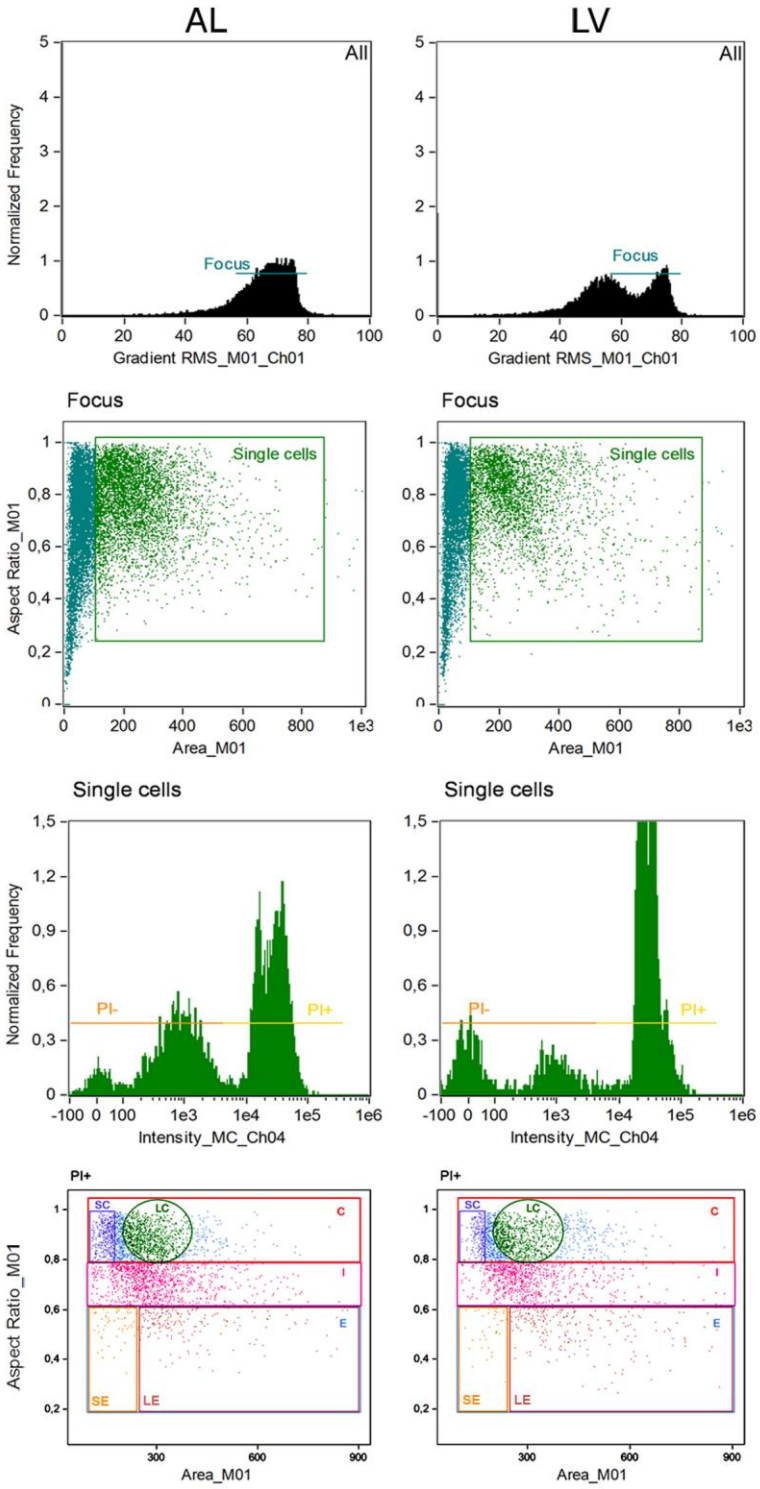

Figure 1 – Representative histogram of focused cells (line 1) gated based on RMS gradients of brightfield channels for *Arbacia lixula* (AL) and *Lytechinus variegatus* (LV). The single cell population (line 2) was determined in the focused cells (line 3) and was based on aspect ratio versus area parameters of the brightfield channel. The histogram of PI-labeled (PI^+) cells was based on the intensity of channel 4 and adjusted to gate subpopulations (line 4). Three main gates were assigned as indicated by circular (C), subdivided in small circular (SC) and large circular (LC); intermediate (I); and elongated (E), subdivided in small elongated (SE) and large elongated (LE).

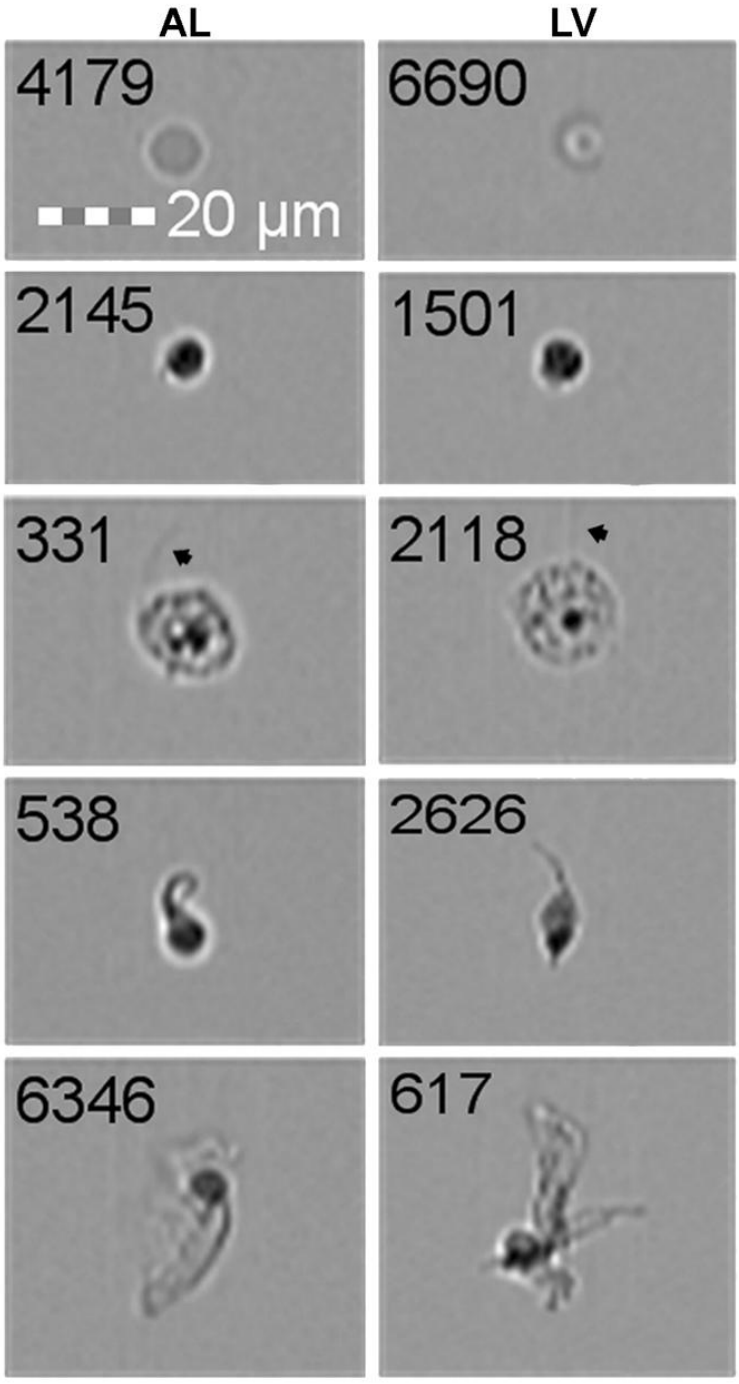

Figure 2 – Representative images of coelomocytes of *Arbacia lixula* (AL) and *Lytechinus variegatus* (LV) without propidium iodide labeling. Subpopulations of coelomocytes of single cells were based on aspect ratio, area, and granularity (SCC). Legend: small circular less (SCL), small circular complex (SCC), large circular (LC), small elongated (SE), and large elongated (LE), flagellum (black arrowhead). The number on each image indicates the record number.

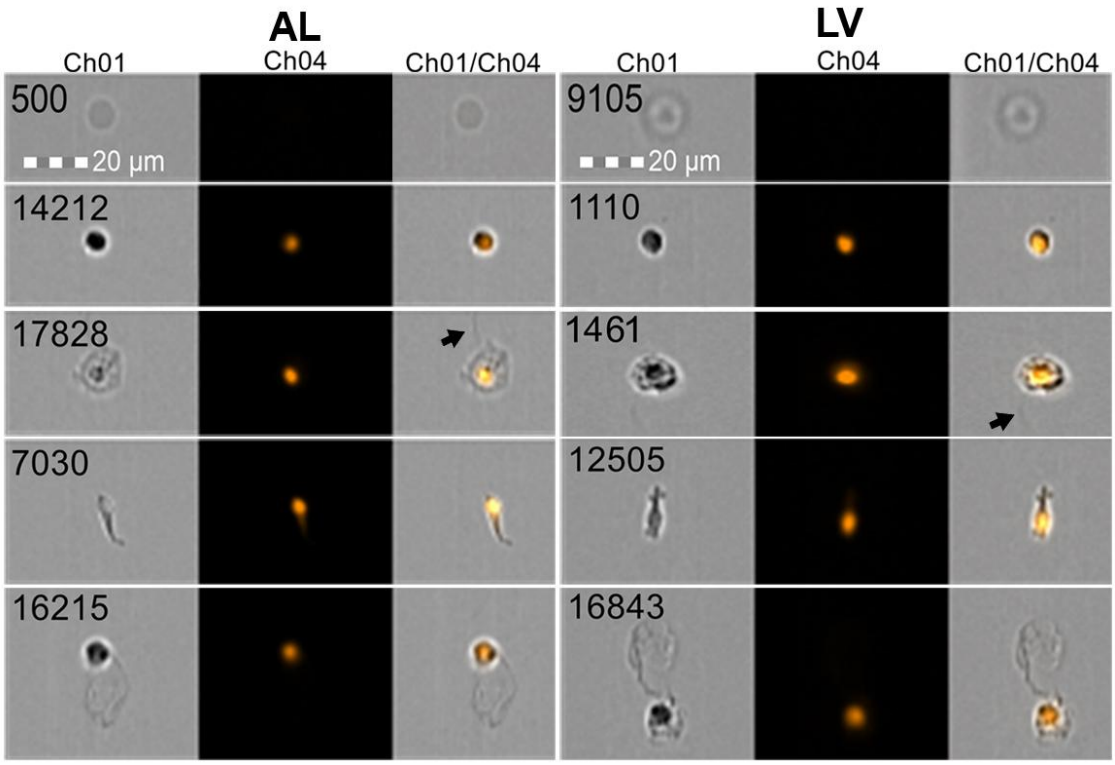

Figure 3 – Representative images of propidium iodide labeled (PI^+) coelomocytes of *Arbacia lixula* (AL) and *Lytechinus variegatus* (LV). From left to right: brightfield (channel 1 - gray), PI^+ fluorescence (channel 4 - orange), and merging of the fluorescence and brightfield channels. Legend: debris (Db), small circular (SC), large circular (LC), small elongated (SE), large elongated (LE), flagellum (black arrow). The number on each image indicates the record number.

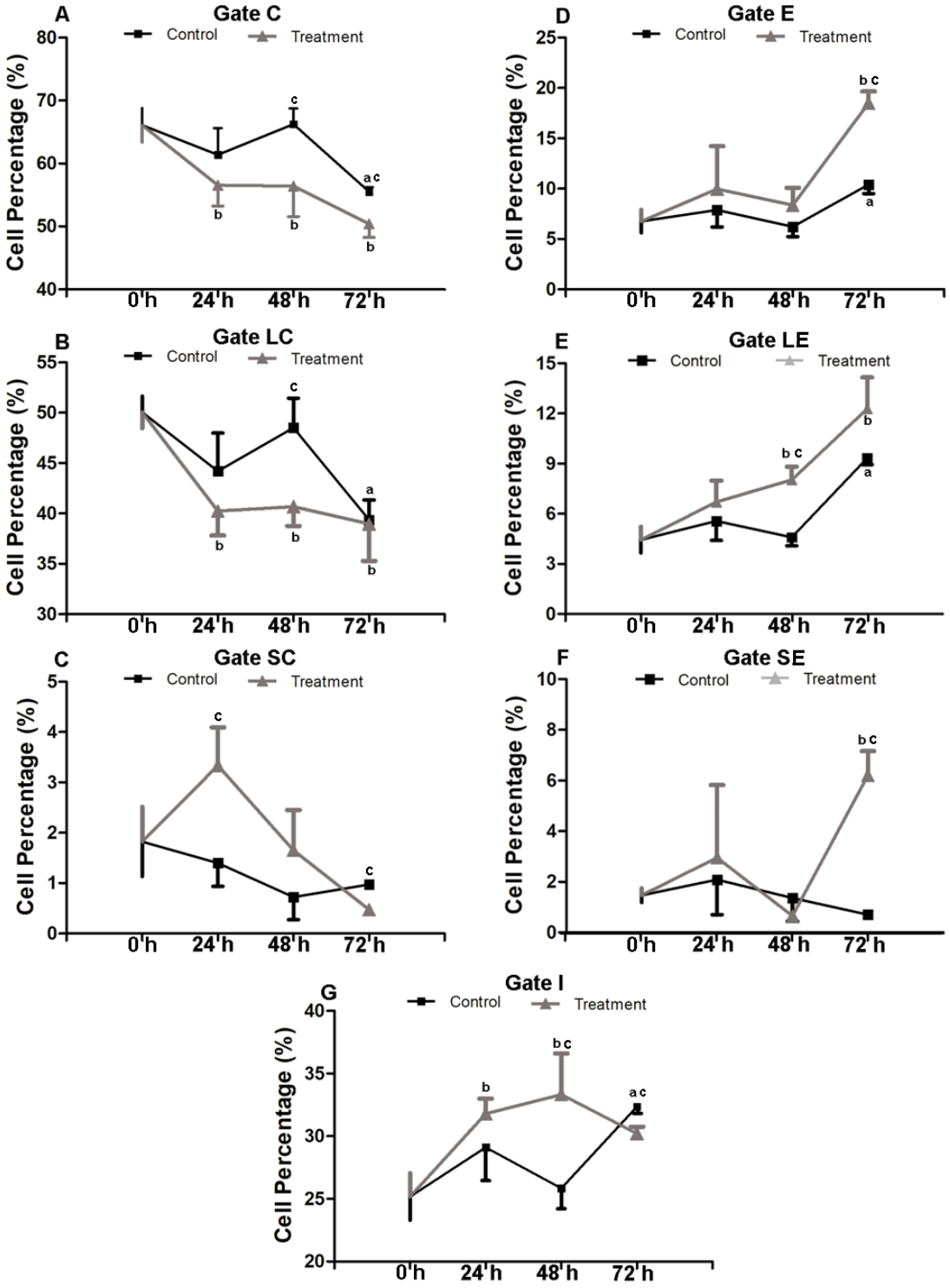

Fig. 4 – Coelomic cell dynamics of *Arbacia lixula* injected with *Escherichia coli*. A – Circular cells; B – Large circular cells; C – Small circular cells; D – Elongated cells; E – Large elongated cells; F – Small elongated cells; G – Intermediate cells. Legend: C = circular cells; LC = large circular; SC = small circular; E = Elongated; LE = large elongated; SE = small elongated; I = intermediate; letters indicate statistical significance (t-test at $p < 0.05$): a = comparison of different time points in control group to untreated animals (0 h); b = comparison of different time points in treatment group to untreated animals (0 h); c = comparison of treatment versus control group at the same time.

Table 1 – Percentage and width of coelomocytes measured by imaging flow cytometry in different sea urchin species with and without propidium iodide.

Species	Parameter	Treatment	C	SC	LC	E	SE	LE	I
AL	Percentage (%)	PI^+	57.17±1.83A*	11.77±1.22A*	29.39±0.79A*	33.08±0.88A*	1.74±0.07A*	7.05±1.09A*	9.33±1.13A*
		No PI	40.78±0.15a	23.73±2.66a	10.86±1.81a	23.76±0.75a	20.30±1.36a	3.46±0.64a	33.25±1.22a
	Width (µm)	PI^+	16.61±0.06	13.15±0.03	17.73±0.03	16.99±0.14	12.89±0.54	18.14±0.08	16.96±0.23
		No PI	14.31±0.25	12.14±0.03	19.5±0.02	13.85±0.19	11.98±0.02	19.5±0.02	15.74±0.05
LV	Percentage (%)	PI^+	59.44±1.83A*	8.09±1.58B*	29.22±0.85A*	30.41±1.53A*	1.54±0.15A*	7.94±0.63A*	9.74±0.65A*
		No PI	41.25±1.44a	12.12±0.01b	18.04±0.06b	29.05±0.99b	19.67±2.20a	9.38±1.43b	27.38±0.86b
	Width (µm)	PI^+	16.96±0.25	13.34±0.01	17.62±0.17	16.93±0.29	12.75±0.11	18.55±0.24	17.55±0.19
		No PI	16.27±0.38	11.58±0.03	18.76±0.16	15.08±0.29	11.77±0.06	20.41±0.22	16.09±0.25

AL = *Arbacia lixula*; LV = *Lytechinus variegatus*; PL = *Paracentrotus lividus*; PI^+ = Propidium iodide labeled cells; No PI = Unlabeled cells; C = Circular; I = Intermediate; E = Elongated; SC = Small circular; LC = Large circular; SE = Small elongated; LE = Large elongated. * = Asterisk indicates significant differences ($p > 0.05$) between treatments in the same species. Different letters indicate significant differences ($p > 0.05$) between species (upper case = PI^+; lower case = No PI).

Capítulo 5

Mecanismo de liberação de equinocromo-A pelo esferulócito vermelho de *Paracentrotus lividus*

Justificativa

Dentre os principais tipos celulares do fluido celômico dos ouriços regulares (*i.e.* fagócitos, células vibráteis e esferulócitos), os esferulócitos vermelhos são o segundo tipo mais bem estudado, perdendo apenas para os fagócitos. Para os esferulócitos vermelhos – uma célula preenchida com vesículas de cor avermelhada graças ao equinocromo-A, e com intenso movimento amebóide – muitas funções discrepantes já foram propostas. Contudo, atualmente é aceito que a atividade bactericida é a única (ou principal) função fisiológica desta célula. Embora exista uma quantidade considerável de informação acerca do seu papel nos ouriços, do composto responsável por essa atividade e de qual o mecanismo de ação dessa molécula, ainda existe uma lacuna importante acerca do funcionamento desta célula: o mecanismo de liberação do equinocromo. Neste contexto, o presente capítulo visa investigar o mecanismo pelo qual o esferulócito vermelho libera o equinocromo-A – a substância responsável pelo efeito bactericida – bem como a possibilidade da composição iônica do meio afetar o processo.

To degranulate, or not to degranulate, that's the question: mechanism of echinochrome release in the sea urchin red spherulocyte stimulated by lipopolysaccharide

Vinicius Queiroz[1, 2]*, Vincenzo Arizza[2], Mirella Vazzana[2] and Márcio R. Custódio[1]

To be submmited to the Journal Fish and Shellfish Immunology

1 – Departamento de Fisiologia Geral, Instituto de Biociências and Núcleo de Apoio à Pesquisa – Centro de Biologia Marinha (NAP–CEBIMar), Universidade de São Paulo, São Paulo, Brazil.

2 – Dipartimento Scienze e Tecnologie Biologiche Chimiche e Farmaceutiche (STEBICEF), Università degli Studi di Palermo, Palermo, Italy.

Abstract: Red spherulocytes, a coelomocyte with intense amoeboid movement, filled with reddish-colored vesicles due to the presence of the naphthoquinone pigment echinochrome-A (EA), are the second most well-studied subpopulation in sea urchin. It has been said to perform an antibacterial activity, by degranulating, when in contact with bacterial motifs such as lipopolysaccharides. However, empirical evidence about the mechanism by which red spherulocytes release their antibacterial content is lacking, and the hypothesis about its mechanisms are speculative. During experiments using lipopolysaccharide to test bacterial activity, we observed that red spherulocytes did not degranulate in the presence of this bacterial motif. Instead, this cell releases all its EA through a very different mechanism: the cell swelled until it burst, releasing all its content at once. In this context, we decide to investigate how the red spherulocyte release its content, and if the ionic composition of the extracellular fluid can affect the process. We observed that in addition to being a calcium-dependent process, EA release is also sodium-dependent, but it does not seem to need potassium. Taking into account that EA kills bacterial cells by chelating iron ions, this mechanism seems to be a more efficient way to fight bacterial invaders, since this mechanism can release the bactericidal compound in a fast way. Additionally, this might be a very efficient process to spread a substance (*i.e.* the EA) capable of activating the immune system, a function proposed in a recent study.

Keywords: Cell physiology, coelomocytes, degranulation**,** Echinodermata**,** *Paracentrotus lividus.*

Running title: Echinochrome release of red spherulocytes

***Corresponding author**: V. Queiroz, Departamento de Fisiologia Geral, Instituto de Biociências, Universidade de São Paulo, Rua do Matão, nº 321, Cidade Universitária, São Paulo (SP), Brazil. CEP: 05508-090. Tel: +55113091-7522. Email: vinicius_ufba@yahoo.com.br

INTRODUCTION

The class Echinoidea, which comprises organisms commonly known as sea urchins, sand dollars and heart urchins, is the most studied group of Echinodermata regarding the immune system (Smith et al., 2010; 2018). Coelomocytes, the term used to the free circulating cells in the coelomic fluid of the echinoderms, are the main immune effectors (Matranga et al., 2005), and usually divided into three main types. Phagocytes – which comprise three subpopulations (*i.e.* discoidal, polygonal and small phagocytes) – are the most extensively studied (Majeske et al., 2013; 2014), while the vibratile cell is the less known (Smith et al., 2006). Spherulocytes, cells filled with many cytoplasmic spherules, are the third cell type and may be divided into two subpopulations: colorless and red.

Red spherulocytes (RS) are the second most studied coelomocyte of regular urchins. This cell shows intense amoeboid movements in physiological conditions and is filled with a red compound, 6-ethyl-2,3,5,7,8-pentahydroxy-1,4-naphthoquinone, named echinochrome-A (EA) (Berdyshev et al., 2007). This compound was identified by Mac Munn (1883), and since then, many functions have been proposed to it, ranging from respiratory pigments (Mac Munn, 1885), excretion (Fox, 1953), photoreception (Yoshida, 1966), auxiliary in digestive processes (Pequignat, 1966), and algistat (Vevers, 1966).

The first steps toward the understanding of the real physiological function of EA in sea urchins, and consequently of the RS, were given approximately eighty years after the discovery of this molecule (Johnsson, 1969). According to this author, RS were involved in bactericidal activity by migrating toward the bacterial cells and releasing their echinochrome on them (Johnsson, 1969). Posteriorly, Wardlaw and Unkles (1978) observed that the extract of disrupted *Echinus esculentus* coelomocytes was able to kill one specific strain of *Pseudomonas*, a Gram-negative bacteria. A few years later, Service and Wardlaw (1985) observed that *E. esculentus* coelomocytes were effective not only against Gram-negative species but also against Gram-positive ones. The same authors, using purified EA, confirmed that this substance was involved with the bactericidal effect observed in the sea urchin coelomocytes (Service and Wardlaw, 1984). Later, Gerardi and coworkers (1990) confirmed that RS was responsible, using enriched fractions containing 98% of this cell (Gerardi et al., 1990). Lastly, Coates and coworkers (2018) discovered the molecular mechanism underlying the mode of action of the EA.

Despite all works addressing directly (Gerardi et al., 1990) or indirectly (Yui and Bayne, 1983) the physiological function of the RS, the mechanism by which this cell releases its content is still unknown. Although some authors have pointed out that RS degranulate (Smith, 2012; Arizza and Schillaci, 2016), this information seems to be quite speculative since there are no studies addressing this issue.

During experiments using the coelomocytes of *Paracentrotus lividus* and *Arbacia lixula*, we observed that in the presence of lipopolysaccharide (LPS), red spherulocytes did not release granules, *i.e.* they did not degranulate. Instead, the cell membrane breaks and all EA is released at once. Thus, in view of this new information, the aim of this study is to understand how the RS release the echinochrome and the factors affecting the process. In this context, we intend to answer three main questions: 1 – How do red spherulocytes release their echinochrome (process)? 2 – How does Echinochrome release occur (mechanism)? 3 – What factors may affect echinochrome-A release?

MATERIAL AND METHODS

Animals, bleeding procedure and cell collection

Sea urchin of the species *Paracentrotus lividus* and *Arbacia lixula* (n=5 for each one) were collected in the Gulf of Palermo (38°06.00′ N; 13°30.00′ E), Palermo, SW Italy. The coelomic fluid of both species was collected with a syringe preloaded with 0.5 ml of Tris-buffered saline with EDTA (TRIS-EDTA – 20 mM Tris, 500 mM NaCl, EDTA 70 mM, pH 7.5. Arizza et al., 2007; 2013). The syringe was inserted into the peristomial membrane and the same volume of coelomic fluid was withdrawn from each sea urchin separately. The cell density was adjusted to 10^6 cells/mL using a Neubauer chamber, and this solution was named stock solution (SS).

Mechanism of echinochrome release and the effect of medium composition on the process

To evaluate the mechanism by which the red spherulocyte release echinochrome, and if the ionic composition of the medium can affect the process, the behavior of red spherulocytes during incubation with lipopolysaccharide (LPS) was observed. Before each of the following procedures, 200 µL of the SS (2 x 10^5 cells/mL) were centrifuged (900 x g for 10 min at 4° C), and resuspended in 200 µL of a calcium-enriched Tris-buffered saline, containing Na^+ (TRIS-Na^+ – 500 mM NaCl, 20 mM Tris, 10 mM $CaCl_2$, pH 7.5) or K^+ (TRIS-K^+ – 500 mM KCl, 20 mM Tris, 10 mM $CaCl_2$, pH 7.5). The LPS solution (*Escherichia coli* 055:B5 – Sigma-Aldrich) was prepared in TRIS-Na^+ or TRIS-K^+ at a concentration of 5µg/µl (LPS-Na^+ or LPS-K^+, respectively). Cells were incubated with LPS at a final concentration of 1µg/µl (McCaughey and Bodnar, 2012) of LPS (4:1 cells suspension/LPS), in four different situations: (I) Cells in TRIS-Na^+ plus LPS-Na^+; (II) Cells in TRIS-K^+ plus LPS-K^+; and (III) Cells in TRIS-Na^+ plus LPS-K^+ or vice-versa. Controls consisted of cells incubated with the same solutions of the treatments, but with no LPS. The echinochrome release process was observed in both species, while cell counts were performed only in *P. lividus*. The analysis of the mechanism of echinochrome release was based on direct observations and time-lapse images of the cell behavior during incubation with LPS. The cells were observed every five minutes for 30 min, and the morphology and the number of red spherulocytes in 10 fields chosen randomly were recorded and compared with control

groups. Student t-tests were performed to analyze possible differences between groups, which were considered significant at a probability level of 0.05.

RESULTS

Mechanism of echinochrome release

In the TRIS-Na^+ solution, red spherulocytes showed an intense amoeboid morphology with an external irregular surface and remarkable spherules (Fig. 1A). When incubated in TRIS-Na^+ supplemented with LPS-Na^+, it is possible to see that the cells do not release granules individually. Instead, the cell burst and releases its content at once, with all process usually happening in a period ranging from five to fifteen minutes. The morphological changes during the process can be divided into two levels: subcellular, regarding the modifications in the cytoplasmic compartment; and cellular, regarding the changes in the cell as a whole. When the red spherulocyte comes into contact with LPS, the first set of changes happens at the subcellular level, with the spherule swelling. The process progresses to the cellular level only when the changes in the subcellular level are completed.

The process of echinochrome release starts immediately when the cells are exposed to LPS. It is possible to see individual spherules swelling and breaking inside the cytoplasm, but with no detectable change in cell size at this time (Fig. 1C-H). In this stage, during spherule disruption, the cell loses its granular aspect and the cytoplasm becomes apparently smooth and uniformly red (Fig. 1H and J). Changes in cell morphology start only after all cytoplasmic spherules have been broken. At this point, the cell starts to swell slowly (Fig. 1I-L) and acquire a round shape (Fig. 1L). At this moment, the cell membrane disrupts, releasing all its content at once, without observable granule release (Fig. 1M-P). This final step can be fast or slow. In the first, the cell burst and releases all its content at once, while in the second (Fig. 1) there is a membrane rupture and the content leaks slowly through the hole (Suppl. Material 1 Video). The process can be very fast in some cells, in which occurs the formation of membrane blebs, and it does not acquire the characteristic round shape before disruption, being completely deformed (Suppl. Material 2 Video). After releasing all echinochrome, it is still possible to observe the central to the subcentral nucleus and the cytoskeleton, and the cell shows a colorless aspect (Fig. 1P). Other cell types in the same preparations do not change their shape in the presence of LPS, only the RS.

Effect of medium composition on echinochrome release

The same process occurs for cells incubated in TRIS-Na^+ supplemented with LPS-Na^+. In control groups, the time of incubation did not affect the number of red spherulocytes, and quite similar values were observed at different times (99.6 ± 7.89 cells in 15 min; 100.0 ± 4.47 cells in 30 min. Fig. 2). On the other hand, there was a remarkable reduction in the number of red spherulocytes in all experimental groups when compared with the controls, and also between treatments (Fig. 2). Fifteen minutes after incubation there was a significant reduction (~ 73.1% - $p < 0.0001$) in red spherulocytes numbers (26.8% ± 11.17 cells), and this reduction was even higher (~ 96.6% - $p < 0.0001$), reaching a very low number (3.4 ± 2.07 cells) after 30 min when compared with respective controls (Fig. 2). Specifically, in this case, the time of incubation affected significantly the number of cells ($p < 0.0017$. Fig. 2).

Cells incubated with media other than TRIS-Na^+ plus LPS-Na^+ showed remarkable differences in their behavior and in the process of echinochrome release. Red spherulocytes suspended in TRIS-K^+ were very slow in their amoeboid movement (when the movement could be seen). After incubation with LPS-K^+, red spherulocytes showed the same slow movement than before, and the characteristic modifications of the echinochrome release process were not observed. Cell counts showed that the same pattern observed in control group (98.0 ± 9.69 cells in 15 min; 97.6 ± 4.77 cells in 30 min) was observed and in the treatment (102.6 ± 7.23 cells in 15 min; 97.2 ± 11.19 cells in 30 min), regardless of the time analyzed (Fig. 2), indicating that the red spherulocytes did not release their content.

In cells resuspended with one medium and incubated in LPS made in another one (TRIS-Na^+ plus LPS-K^+ or TRIS-K^+ plus LPS-Na^+), the results followed a third pattern. In TRIS-Na^+ plus LPS-K^+, the amoeboid movement of the red spherulocytes decreased when cells resuspended in TRIS-Na^+ received TRIS-K^+ with or without LPS. On the other hand, cells incubated with TRIS-K^+ plus LPS-Na^+, which were completely motionless at the beginning of the incubation, increased their amoeboid movement some minutes after have received TRIS-Na^+. However, the movement was very slow if compared with the controls.

Considering the release of echinochrome in these two situations, very few cells were observed suffering the characteristics change of the process. With TRIS-Na^+ plus LPS-K^+, the few cells observed releasing EA were seen just after LPS-K^+ addition and

stopped shortly after. In TRIS-K^+ plus LPS-Na^+, the RS spent considerable time to start to release its content. This suggests that both media affected, but not stopped, the process, and the cell counts corroborated this affirmation. For cells incubated in TRIS-Na^+ plus TRIS-K^+, the number of cells in the control group was similar to the other controls (101.8 ± 12.32 cells in 15 min; 102.8 ± 6.38 cells in 30 min), but there was a slight decrease (~ 20%) in the experimental group (77.8 ± 5.8 cells in 15 min; 81.4 ± 4.16 cells in 30 min). Cells incubated with TRIS-K^+ plus LPS-Na^+ followed exactly the same pattern with a similar values in the control (98.0 ± 4.35 cells in 15 min; 99.4 ± 6.95 cells in 30 min), and also a light decrease (~ 22%) in the treatment group (77 ± 5.43 cells in 15 min; 77.2 ± 7.08 cells in 30 min). The time of incubation did not affect the release of echinochrome (Fig. 2). We did not observe any effects of the ionic medium with or without LPS on any other cell population.

DISCUSSION

The RS is a remarkable echinoid coelomocyte that has long intrigued echinodermatologists. Although other non-immune functions have been postulated (Mac Munn, 1885; Fox, 1953; Pequignat, 1966; Vevers, 1966; Yoshida, 1966), nowadays it is well accepted that bactericidal activity is its only (or main) physiological function (Service M and Wardlaw, 1984; Gerardi et al., 1990). Its physiological function is already known (Johnson, 1969; Gerardi et al., 1990), as well as the chemical substance responsible by this activity (Service M and Wardlaw, 1984), and the mode of action of this molecule (Coates et al., 2018). However, there always was a gap in this sequence: how RS release their content (the process and the mechanism)? In the present study, we observed that RS release their content through a very unusual way, releasing all its content at once, after a set of morphological changes (subcellular and cellular), and that this process is Na^+-dependent but it seems not to depend on K^+.

Mechanism of Echinochrome release

Degranulation has been the term usually used to describe the mechanism by which RS release their echinochrome (Smith, 2005; Smith et al., 2006; 2010; Smith, 2012; Arizza and Schillaci, 2016), although the term *despherulation* may also be found in some studies (Holland et al., 1965; Chien et al., 1970; Johnson and Chapman, 1970). Degranulation can be characterized as a general term applied the release of granules, or

their content, through the rapid fusion of vesicles with the plasma membrane, regardless the specific mechanism that regulates the process (Henson, 1998; Alan et al., 2013; Kormelink et al., 2016). On the other hand, despherulation is the process of "*cell membrane breakdown and the escape of granules*" (Chia and Xing, 1996). To mammal cells (*e.g.* mast cells or basophils), the degranulation is already deeply detailed (Dvorak, 1991), and both the morphological changes during the granule release, the substances able of triggering the event and how these cells recovery from degranulation are known.

The process observed in the RS of *P. lividus* and *A. lixula* was completely different from the typical degranulation process described to mammal cells (Dvorak, 1991), and even for other invertebrates (Foley and Cheng, 1977). Whatever the term used to describe the mechanism by which RS releases echinochrome, the definitions allude to a more or less controlled (*i.e* degranulation or despherulation respectively) way of release granules. However, the most important point is that RS do not release granules. Instead, they inflate until the cell membrane rupture and all EA is liberated in a fast or slow way, but they were never observed releasing granules during the process. Similarly to the described to guinea pig basophils (Dvorak et al., 1981), the RS also suffers subcellular changes before cellular modifications begin. However, the similarities seem to stops there, because in the first model the basophils suffer a set of morphological changes to release the granules, while in the second does not degranulate. Another difference lies in the recovery process since guinea pig basophil recovers from the degranulation event (Dvorak et al., 1981; Dvorak, 1991), but RS seems to die after release echinochrome. During our *in vitro* observations, it was possible to see that the RS membrane seems to break in a drastic way, allowing the entrance of extracellular fluid, probably disturbing the cell homeostasis, and killing it. This assumption seems to be corroborated by studies conducted with *Strongylocentrotus purpuratus* and *A. lixula*, in which the number of RS in the coelomic fluid decreased considerably after Gram-negative bacteria injection (Yui and Bayne, 1983; Queiroz et al., in prep [*Chapter 4*]).

Many works dealing with RS have stated that this cell releases its content through degranulation. Nevertheless, the present work shows RS releasing EA by a completely different process. Even though, one question still remains unsolved: why to degranulate, or not to degranulate is so important? To answer this question, is it important to keep in mind two relevant information: (I) what is the function of the EA, and (II) what is the mechanism of action by which EA performs its function. As

described by Service and Wardlaw (1984), the bactericidal activity performed by the RS comes from the activity of the EA stored in the vesicles. Posteriorly, Coates and coworkers (2018) observed that echinochrome acts chelating free iron ions in solution in a ratio of 1:2 (echinochrome: iron), depriving bacteria of this metabolite. Such iron-chelating strategies seem to be widespread in the animal kingdom. Interleukin (IL-1, 6), hepcidin and lactoferrin are mammalian molecules known to decrease iron concentration during microbial infections (Van der Poll and Van Deventer, 1999; Michels et al., 2015; Slaats et al., 2016; Drago-Serrano et al., 2017). Even to echinoderms, the activity of iron-chelating molecules is not unheard of. Ferritin and IL-1α and ß-like molecules were effective in decrease iron concentration in the coelomic fluid of the sea star *Asteria forbesi* (Beck et al., 2002). However, the RS seems to be the first case in echinoderms of a cell specialized to deal primarily with bacterial infection through an iron-chelating strategy. In vertebrates, neutrophils and hepatocytes have an analogous function by releasing lactoferrin and hepcidin respectively (Zhang and Lachmann, 2000; Zhao et al., 2013).

Two main cell types will act in sea urchins to maintain the homeostasis during a bacterial infection: Red spherulocytes and phagocytes (Smith et al., 2010). The first coelomocyte will release the echinochrome-A as soon as the cell makes contact with the bacterial motifs (*e.g.* LPS), chelating the free iron and stopping the bacterial growth (Coates et al., 2018). Simultaneously, phagocytes will engulf bacterial cells, removing them from the coelomic fluid (Yui and Bayne, 1983). Taking into account the fact that bacterial cells can duplicate in 20 minutes (Creutziger et al., 2012), stoping bacterial growth seems to be an important step in the short-term, and the release of EA at once seems to be a very effective way to do it. When the cell "explodes", the EA diffuses very fast, chelating the iron in the vicinity of the cell. On the other hand, if the cell released EA granules, the time to diffusion would be much higher, which could make it difficult to neutralize bacterial growth. In addition to this, the mechanism of EA release observed here corroborates another putative physiological function of this compound: an immune stimulator. A recent study (Emerenciano, 2019) showed that the naphthoquinone pigment of *Staerechinus neumaieri* is able to modulate phagocyte activity, making these cells more active – higher motion and higher phagocytic capability. In this context, considering both physiological functions (*i.e.* iron-chelating and immune stimulator), EA releases in a fast way allowing its fast diffusion in the

coelomic fluid might be seen as a very effective way to stop bacterial growth and activate the immune system.

Effect of ionic composition of the medium on echinochrome release

Ionic composition inside and outside the cell is an important parameter in cell physiology. To the vertebrates, is it known that these molecules participate in the most varied physiological processes, ranging from size maintenance, cell signaling and immune responses (Clapham, 2007; Feske et al., 2015; Kay, 2017). In the mammal immune system, it is known that calcium is one of the most important ions (Vig and Kinet, 2009), but there is evidence that other ions (e.g. sodium and potassium) perform important immune functions (Eil et al., 2016; Wilck et al., 2019). In echinoderms, calcium has been known by many important functions related to coelomic fluid and coelomocytes (*i.e.* the immune system). For example, calcium is required to start/continue the clotting process (Boolotian and Giese, 1959), as well as to promote phagocytosis and cytotoxic activity (Arizza et al., 2007). Specifically to the RS, there is evidence that calcium is required for EA release (Coates et al., 2018). However, there is no information about possible functions related to sodium and potassium.

Exposition of RS to the ionophore Ionomycin triggered the release of EA from the cells, while cells treated with BAPTA, a chelator of calcium, did not release EA (Coates et al., 2018), corroborating the calcium-dependent mechanism of EA release. However, we observed that even in the presence of the appropriated stimuli and calcium (*i.e.* LPS and Ca^{2+}), the RS can not release its content. After 30 minutes, 96.6% of RS resuspended in TRIS-Na and incubated in LPS prepared in the same solution released their content, while RS resuspended in TRIS-K^+ and incubated in LPS-K did no release it (*Cf.* Fig. 2). Analysis using crossing solutions (*i.e.* TRIS-Na^+ plus LPS-K^+ or TRIS-K^+ plus LPS-Na^+), also corroborate the need for sodium to EA release. Echinochrome was released in these treatments, but in a very low percentage (~20% of the cells).

However, if there was sodium in both treatments, why was there a so low tax of echinochrome release? This can be explained by the dilution of sodium in both situations, and the qualitative observations corroborate that. In the first case, the process started just after LPS addition, while in the second case there was a delay in starting the process, but both stopped soon after beginning. The low concentration of Na, along with its dilution may explain these differences. In the first group, the addition of LPS in a

Na-rich solution started the process, promoting EA release in some cells, but the use of Na by the RS and its concomitant dissolution after the addition of LPS K^+ explain why the process starts and finishes in a short time. On the other hand, the RS of the second group (*i.e.* TRIS-K^+ plus LPS-Na^+) were in a solution without sodium until their mixture with the LPS-Na^+. At this moment, the cells made contact with the LPS and received a load of sodium, which was soon used to start the process of EA release, depleting the low Na-stock. This can explain why the morphological changes and EA release observed in this group were delayed and finished shortly after to start. Thus, in view of all information, we believe that the whole process of RS rupture is very likely caused by an osmotic shock, caused by the release of intracellular stores of ions and/or molecules in the cytoplasm. The increased osmotic pressure caused by these osmolytes would drive water to inside the cell, swelling and breaking it. However, this effect is restricted to the RS, since no other cell types in the same preparations showed any sign of alteration.

In summary, this study brings insights into the functioning of the RS. We provide data about an unexplored aspect of the RS physiology: the mechanism of EA release. Additionally, we also provide information about the effect ions other than calcium on the process. Based on an experimental approach by incubating sea urchin coelomic cells in a solution containing LPS and different ionic compositions, we are able to answer the three main questions that have driven this work. In the first question, that inquired about the process by which RS released the EA, we observed that this cell does not degranulate, as previously as supposed (Smith, 2005; Arizza and Schillaci, 2016). Instead, RS release EA in a completely different way: it explodes, releasing all content at once. Regarding the second question (how does Echinochrome release occur?), we observed a series of morphological changes, ranging from subcellular to cellular level, which results in EA release. The first step in the process is the rupture of all spherules inside the cytoplasm, without changes in cell size, followed by swelling and rupture of the cell membrane and EA release. The last important aspect was about which factors might modulate echinochrome-A release. We observed that in addition to being Ca-dependent, EA release is also Na-dependent, but potassium seems not to be involved.

Thus, even after these results which certainly fill important gaps in RS physiology, some questions remain unsolved. For example: Could other cell types influence red spherulocyte activity? Would RS show different response if it was

stimulated with bacterial cells? How is the molecular mechanism of EA release? Thus, these questions will drive our next steps into the understanding of RS physiology.

ACKNOWLEDGMENTS

This work was supported by FAPESP (Proc. 2015/21460-5 and 2018/14497-8) and Coordenação de Aperfeiçoamento de Pessoal de Nível Superior (CAPES).

REFERENCES

Alam R, Levi-Schaffer F, Koenderman L, Munitz A, Bickham UR, Malter JS, Anne M. 2013. Eosinophil Signal Transduction. (2013). Eosinophils in Health and Disease, 167–227.

Arizza V, Schillaci D. 2016. Echinoderm Antimicrobial Peptides: The Ancient Arms of the Deuterostome Innate Immune System. *In*: L. Ballarin, & M. Cammarata (Eds), Lessons in Immunity: From Single-cell Organisms to Mammals (pp. 159-176). Elsevier Inc.

Arizza V, Vazzana M, Schillaci D, Russo D, Giaramita FT, Parrinello N. 2013. Gender differences in the immune system activities of sea urchin *Paracentrotus lividus*. Comparative Biochemistry and Physiology Part A: Molecular & Integrative Physiology. 164 (3): 447-455.

Arizza V, Giaramita F, Parrinello D. 2007. Cell cooperation in coelomocyte cytotoxic activity of *Paracentrotus lividus* coelomocytes. Comp. Biochem. Physiol. A, 147:389-394.

Beck G, Ellis TW, Habicht GS, Schluter SF, Marchalonis JJ. 2002. Evolution of the acute phase response: iron release by echinoderm (*Asterias forbesi*) coelomocytes, and cloning of an echinoderm ferritin molecule. Developmental & Comparative Immunology, 26(1), 11–26. doi:10.1016/s0145-305x(01)00051-9

Berdyshev DV, Glazunov VP, Novikov VL. 2007. 7-Ethyl-2, 3, 5, 6, 8-pentahydroxy-1, 4-naphthoquinone (echinochrome A): A DFT study of the antioxidant mechanism. 1. Interaction of echinochrome A with hydroperoxyl radical. Russian Chemical Bulletin, 56(3): 413-429.

Chia FS, Xing J 1996. Echinoderm coelomocytes. Zoological Studies, 35: 231-254.

Boolootian RA, Giese AC. 1959. Clotting of echinoderm coelomic fluid. *Journal of Experimental Zoology, 140(2), 207–229.* doi:10.1002/jez.1401400203

Chien PK, Johnson PT, Holland ND, Chapman FA. 1970. The coelomic elements of sea urchins (*Strongylocentrotus*) — IV. Ultrastructure of the coelomocytes Protoplasma, 71 (1970), pp. 419-442.

Clapham DE. 2007. Calcium Signaling. Cell, 131(6), *1047–1058.*

Creutziger M, Schmidt M, Lenz P. 2012. Theoretical models for the regulation of DNA replication in fast-growing bacteria. New Journal of Physics, 14(9), 095016.

Coates CJ, McCulloch C, Betts J, Whalley T. 2018. Echinochrome A release by red spherule cells is an iron-withholding strategy of sea urchin innate immunity. Journal of innate immunity, 10(2): 119-130.

Drago-Serrano ME, Campos-Rodríguez R, Carrero JC, De la Garza M. 2017. Lactoferrin: balancing ups and downs of inflammation due to microbial infections. International journal of molecular sciences, 18(3), 501.

Dvorak AM. 1991. Blood Cell Biochemistry. 4. Basophil and mast cell degranulation and recovery (Vol. 4). Springer Science & Business Media.

Dvorak AM, Osage JE, Dvorak HF, Galli SJ. 198l, Surface membrane alterations in guinea pig basophils undergoing anaphylactic degranulation. A scanning electron microscopic study. Lab. Invest. 45:58-66.

Eil R, Vodnala S, Clever D. 2016. Ionic immune suppression within the tumor microenvironment limits T cell effector function. Nature 537, 539–543.

Emerenciano AK. 2019. Identificação do pigmento presente nos esferulócitos vermelhos do ouriço do mar antártico *Sterechinus neumayeri* (Meissner, 1900) e seu papel na modulação da resposta imune inata. Tese apresentada ao programa de pós-graduação de Biologia de Sistemas, do Instituto de Ciências Biomédicas da Universidade de São Paulo. 100 pp.

Feske S, Wulff H, Skolnik EY. 2015. Ion channels in innate and adaptive immunity. Annual review of immunology, 33, 291-353.

Foley DA, Cheng TC. 1977. Degranulation and other changes of molluscan granulocytes associated with phagocytosis. Journal of invertebrate pathology, 29(3), 321-325.

Fox DL. 1953. Animal Biochromes and Structural Colors. 1st Ed. Cambridge University Press. 459 pp.

Gerardi P, Lassegues M, Canicatti C. 1990. Cellular distribution of sea urchin antibacterial activity. Biology of the Cell, 70(3), 153-157.

Henson PM. 1998. Degranulation *In*: Delves PI, Roitt IMCE (Eds). Encyclopedia of Immunology (2° Edition) (1998). Academic Press, 736-738.

Holland ND, Phillips Jr JH, Giese AC. 1965. An autoradiographic investigation of coelomocyte production in the purple sea urchin (*Strongylocentrous purpuratus*). The Biological Bulletin, 128(2): 259-270.

Johnson PT, Chapman FA. 1970. Abnormal epithelial growth in sea urchin spines (*Strongylocentrotus franciscanus*). Journal of Invertebrate Pathology, 16(1), 116-122.

Johnson PT. 1969. The coelomic elements of sea urchins (Strongylocentrotus) III. In vitro reaction to bacteria. Journal of invertebrate pathology, 13(1): 42-62.

Kay AR. 2017. How Cells Can Control Their Size by Pumping Ions. Frontiers in Cell and Developmental Biology, 5. doi:10.3389/fcell.2017.00041

Kormelink TG, Arkesteijn GJ, van de Lest CH, Geerts WJ, Goerdayal SS, Altelaar MA, Wauben MH. 2016. Mast Cell Degranulation Is Accompanied by the Release of a Selective Subset of Extracellular Vesicles That Contain Mast Cell-Specific Proteases. The Journal of Immunology, 197(8), 3382-3392.

MacMunn CA. 1883. Studies in animal chromatology. Proceedings of the Birmingham Natural History and Philosophical Society, 3: 351-407.

MacMunn CA. 1885. On the chromatography of the blood of some invertebrates. Quart. Jour. Mic. Sci. 30: 51–96.

Majeske AJ, Bayne CJ, Smith LC 2013. Aggregation of Sea Urchin Phagocytes Is Augmented In Vitro by Lipopolysaccharide. PLoS ONE 8(4): e61419. https://doi.org/10.1371/journal.pone.0061419

Majeske AJ, Oren M, Sacchi S, Smith LC. 2014. Single sea urchin phagocytes express messages of a single sequence from the diverse Sp185/333 gene family in response to bacterial challenge. The Journal of Immunology, 193(11), 5678-5688.

Matranga V, Pinsino A, Celi M, Natoli A, Bonaventura R, Schröder HC, Müller WEG. 2005. Monitoring chemical and physical stress using sea urchin immune cells. In Echinodermata (pp. 85-110). Springer, Berlin, Heidelberg.

Michels K, Nemeth E, Ganz T, Mehrad B. 2015. Hepcidin and host defense against infectious diseases. PLoS pathogens, 11(8), e1004998.

Pequignat E. 1966. "Skin digestion" and epidermal adsorption in irregular and regular urchins and their probable relation to the outflow of spherule-coelomocytes. Nature, Lond. 210, 397-399.

Service M, Wardlaw AC. 1984. Echinochrome-A as a bactericidal substance in the coelomic fluid of *Echinus esculentus* (L.). Comp Biochem Physiol B Comp Biochem 1984; 79: 161–165

Service M, Wardlaw AC. 1985. Bactericidal activity of coelomic fluid of the sea urchin, Echinus esculentus, on different marine bacteria. Journal of the Marine Biological Association of the United Kingdom, 65(1), 133-139.

Slaats J, ten Oever J, van de Veerdonk FL, Netea MG. 2016. IL-1β/IL-6/CRP and IL-18/ferritin: distinct inflammatory programs in infections. PLoS pathogens, 12(12), e1005973.

Smith LC. 2005. Host responses to bacteria: Innate immunity in invertebrates. *In*: Ngai MJM, Henderson B, Ruby EG. (Eds). The Influence of Cooperative Bacteria on Animal Host Biology. Cambridge University Press. 425 pp.

Smith LC. 2012. Innate immune complexity in the purple sea urchin: diversity of the sp185/333 system. Frontiers in immunology, 3, 70.

Smith CL, Ghosh J, Buckley KM, Clow LA, Dheilly NM, Huag T, Henson JH, ChengMan Lun CL, Majeske AJ, Matranga V, Nair SV, Rast JP, Raftos DA, Roth M, Sacchi S, Schrankel CS, Stensvag K. 2010. Echinoderm immunity. *In*: Söderhäll K, editor. Invertebrate immunity. New York, NY: Landes Bioscience and Springer Science BusinessMedia. pp. 260–301.

Smith LC, Arizza V, Hudgell MAB, Barone G, Bodnar AG, Buckley KM, Furukawa R. 2018. Echinodermata: the complex immune system in echinoderms. *In*: Cooper L. (Ed). Advances in comparative immunology (pp. 409-501). Springer, Cham.

Smith LC, Rast JP, Brockton V, Terwilliger DP, Nair SV, Buckley KM, Majeske AJ. 2006. The sea urchin immune system. Invertebrate Survival Journal 3:25–39.

Van der Poll T, Van Deventer SJH. 1999. Interleukin-6 in Bacterial Infection and Sepsis: Innocent Bystander or Essential Mediator?. *In*: Vincent JL. (Eds). Yearbook of Intensive Care and Emergency Medicine 1999. Yearbook of Intensive Care and Emergency Medicine, vol 1999. Springer, Berlin, Heidelberg.

Vevers G. 1966. Physiology of Echinodermata. J Wiley, Interscience, New York, 267-275.

Vig M, Kinet JP. 2009. Calcium signaling in immune cells. Nat. Immunol. 10:21–27.

Wardlaw, A. C., & Unkles, S. E. (1978). Bactericidal activity of coelomic fluid from the sea urchin Echinus esculentus. Journal of Invertebrate Pathology, 32(1), 25-34.

Wilck N, Balogh A, Markó L, Bartolomaeus H, Müller DN. 2019. The role of sodium in modulating immune cell function. Nature Reviews Nephrology. doi:10.1038/s41581-019-0167-y

Yoshida M. 1966. Photosensitivity. *In*: Boolotian RA (Ed). Physiology of Echinodermata. Interscience Publishers, 435-464.

Yui MA, Bayne CJ. 1983. Echinoderm immunology: bacterial clearance by the sea urchin *Strongylocentrotur purpuratus*. Biol. Bull. 165: 473–86.

Zhang W, Lachmann PJ. 1996. Neutrophil lactoferrin release induced by IgA immune complexes can be mediated either by Fc alpha receptors or by complement receptors through different pathways. The Journal of Immunology, 156(7): 2599-2606.

Zhao N, Zhang AS, Enns CA. 2013. Iron regulation by hepcidin. The Journal of clinical investigation, 123(6), 2337-2343.

Figures and Captions

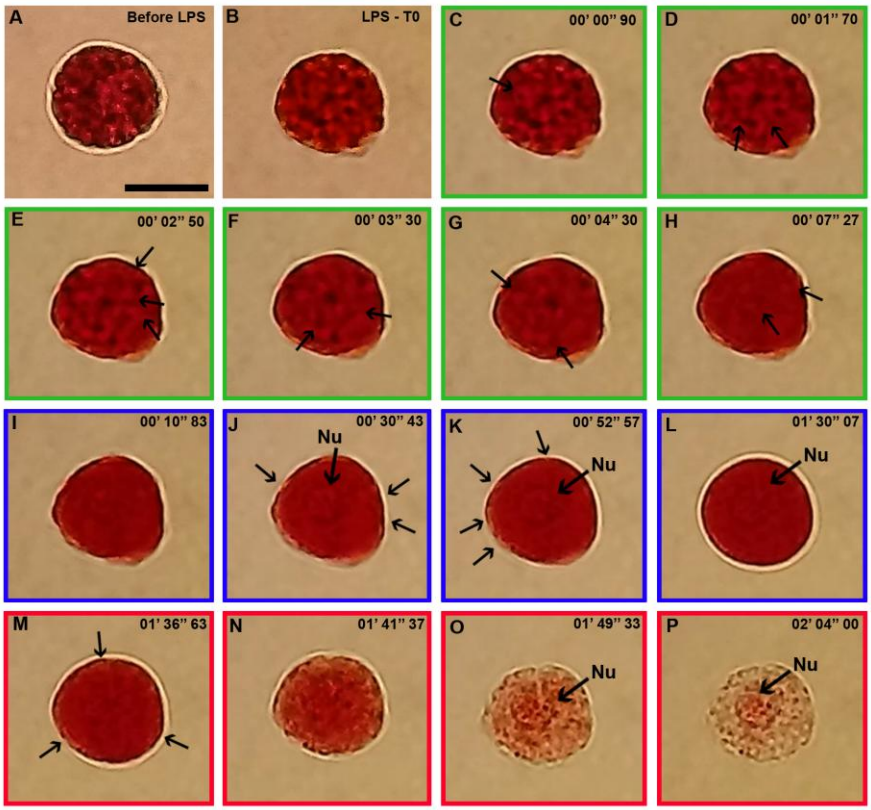

Figure 1 – Sequence of subcellular and cellular alterations preceding Echinochrome-A release in the red spherulocyte of *Paracentrotus lividus*. Green edge = subcellular stage; Blue edge = cellular stage (swelling); Red edge = cellular stage (echinochrome release). Scale = 10 µm. Legend: Black arrows = changes in red spherulocytes compared to the previous pictures; LPS = Lipopolysaccharide; Nu = nucleus.

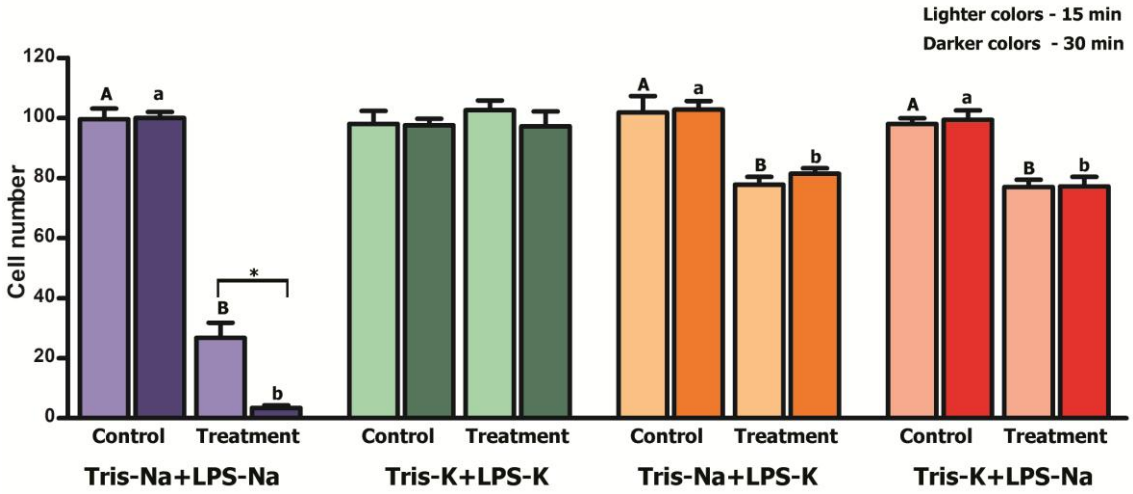

Figure 2 – Effect of the ionic composition on the number red spherulocytes in mixed coelomocyte population of *Paracentrotus lividus*. For each solution, distinct letters show significant differences in Student t-test between control and treatment ($p < 0.05$) at the same time; Asterisk (*) shows significant differences in Student t-test between times in the treatment group ($p < 0.05$). Legend: Lighter colors = 15 minutes; Darker colors = 30 min; Capital letters = 15 min; Small letters = 30 min.

Capítulo 6

O estado de saúde de ouriços-do-mar durante associações biológicas: um estudo de caso com *Echinometra lucunter* (Echinoidea)

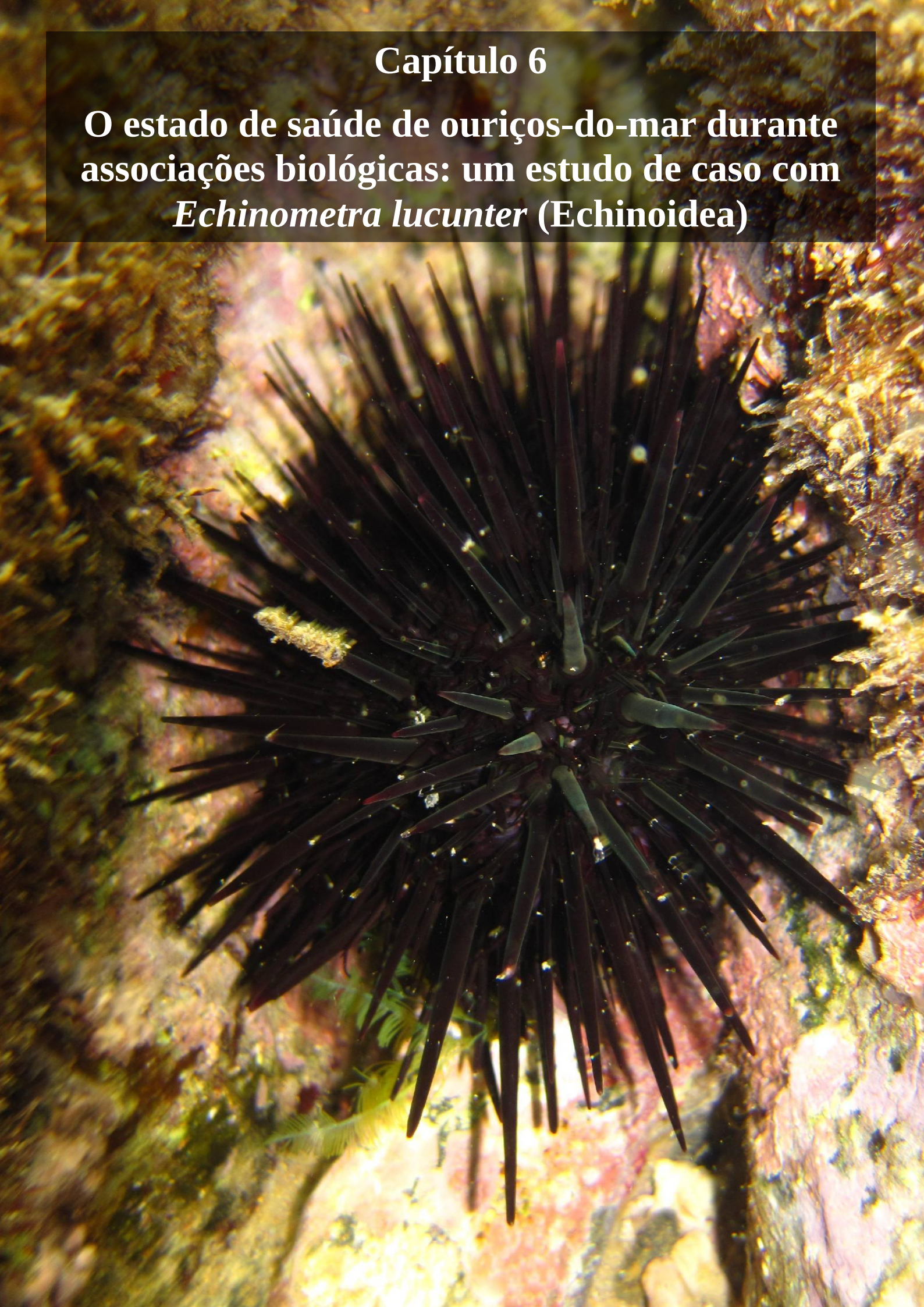

Justificativa

Os celomócitos de echinodermata, e em especial os da ordem Echinoidea, tem sido modelos de estudo interessantes, fornecendo evidencias para muitas áreas na biologia, variando de imunologia ao monitoramento ambiental. No entanto, o conhecimento acerca destas células, tanto em relação ao número total e proporção dos tipos presentes, também pode ser utilizado de maneira mais aplicada, como um indicativo de saúde nestes organismos. Um baixo número de fagócitos e principalmente um alto número de esferulócitos vermelhos têm sido relacionados a estresse em ouriços regulares. Assim, este capítulo traz um estudo de caso, relatando um caso raro de briozoário que foi encontrado sobre a carapaça de um ouriço vivo. Neste estudo, além das informações de cunho taxonômico, registramos alguns parâmetros fisiológicos do ouriço, no momento da retirada do briozoário e comparamos com organismos sadios coletados no mesmo momento.

Taxonomical and biological aspects of the epibiotic association between *Schizoporella errata* (Bryozoa) and the sea urchin *Echinometra lucunter*

Vinicius Queiroz

To be subimmited to the Turkish Journal of Zoology

Departamento de Fisiologia Geral, Instituto de Biociências and Núcleo de Apoio à Pesquisa – Centro de Biologia Marinha (NAP–CEBIMar), Universidade de São Paulo, São Paulo, Brazil. E-mail: vinicius_ufba@yahoo.com.br

Abstract: Although extremely well known for their epibiotic relationship with many living substrates, records of bryozoans settling on echinoderms are scarce. In the few recorded cases, approximately 70% of the hosts (basibionts) are cidaroid sea urchins and their primary spine seems to be the preferred place to bryozoan settlement. Here, an unprecedented epibiosis between a bryozoan and one non-cidaroid sea urchin is reported, in which the epibiont *Schizoporella errata* was found living on a living specimen of *Echinometra lucunter*. Additionally, the proportion of different coelomocytes in the coelomic fluid and the wound healing dynamics of the affected sea urchin and a control group of five healthy animals were observed. Only one colony of was found on the affected echinoid, and it presented 4.5-fold more red spherulocytes in the coelomic fluid than healthy specimens, as well as the careful removal of *S. errata*, revealed a previously wounded area underneath with advanced signs of healing, suggesting that the wound healing process had started before epibiont removal. Thus, the analyses of all the results presented here raise the possibility that maybe basibionts can be physiologically disturbed during epibiotic associations.

KEYWORDS: Coelomocytes, Echinodermata, echinoid, immune system, wound healing.

Short title: Epibiosis on *Echinometra lucunter*

***Correspondence:** V. Queiroz, Departamento de Fisiologia Geral, Sala 300, Instituto de Biociências, Universidade de São Paulo, Rua do Matão, nº 321, Cidade Universitária, São Paulo (SP), Brazil. CEP: 05508-090.

INTRODUCTION

Echinoderms are well known as hosts to a plethora of marine taxa, ranging from microorganisms to vertebrates (Barel & Kramers 1977), but records of epibiotic interactions are very rare (Wahl & Mark 1999). On the other hand, Bryozoans are one of the most common epibiotic organisms (Wahl & Mark 1999), usually living in association with live marine substrates, such as algae, mollusks (Taylor & Monks 1997), and vertebrates (Key *et al.* 1995). Even so, while bryozoans are widely recognized for their capability of living on these organisms, records of interactions with echinoderms are sporadic at best. Among the recorded echinoderm hosts, cidaroid sea urchins can be pointed as the most frequent basibionts for bryozoan settlement (Barel & Kramers 1977, Jangoux 1987, David *et al.* 2009, Sosa-Yañez *et al.* 2015). Works dealing with epibiotic interactions, including those involving bryozoans, have usually focused on taxonomic and/or ecological aspects (Taylor & Monks, 1997). There is, however, no studies addressing epibiont and/or basibiont physiological aspects during these associations.

In this context, the present work reports an unprecedented association between a cheilostome bryozoan and a non-cidaroid sea urchin. The epibiotic interaction between *Schizoporella errata* (Waters, 1878) and *Echinometra lucunter* (Linnaeus, 1758) is recorded here for the first time, in which the epibiont was found alive, living on the sea urchin test. Additionally, some physiological aspects of the host sea urchin, such as the proportion of coelomic cells and wound healing dynamics after epibiont removal are reported and compared with healthy individuals.

MATERIAL AND METHODS

Over forty specimens of *Echinometra lucunter* were collected by free diving in the winter, on July 2nd, 2016 at Praia Grande, São Sebastião, SE Brazil (23°49’24” S, 45°25’01” W) at a depth of 1.5-2 m. The cheilostome bryozoan *Schizoporella errata* was found attached to a single sea urchin. The affected echinoid and its epibiont were transported in 10L containers and transferred to an 80L aquarium at the Laboratório de Biologia Celular de Invertebrados Marinhos (IB-USP). Aquarium maintenance and physicochemical characteristics were adjusted according to Queiroz (2016). After a one-week acclimation period, the association was photographed and the bryozoan was carefully removed using a fine-pointed forceps. The colony was lifted up by the edges,

avoiding additional injuries to the echinoid. After removal, the colony was photographed, preserved in 70% ethanol and deposited in the Bryozoa Collection of the Museu de Zoologia da Universidade de São Paulo (MZSP 1311). Bryozoan identification was based on scanning electron microscopy (SEM), and measurements were made using the photographs, through ImageJ software.

Some basibiont physiological aspects (percentage of coelomic cells and wound healing process) were deliberately analyzed. Coelomic fluid (1 ml) of both the injured sea urchin and a control group (n=5 healthy sea urchins) was collected following standard methods (Queiroz & Custódio 2015) immediately before the colony removal. Shortly, a syringe needle preloaded with 1 ml of isosmotic anticoagulant solution was inserted into the peristomial membrane and the same volume of coelomic fluid was collected. The cell suspension was adjusted to 10^6 cell/mL, coelomocytes from each sea urchin were counted using a Neubauer chamber, and the proportion of main cell types (*i.e.* phagocytes (Pha), vibratile cells (VC), red and colorless spherulocytes (RS and CS)) was recorded. Additionally, the healing process was monitored for 10 days in the affected sea urchin and in the control group. For comparative purposes, injuries with a similar area were deliberately created on three healthy echinoids (control group) by removing some spines and scraping gently the denuded test with a surgical scalpel, simulating the situation found on the injured specimen. During this procedure, only the epidermis was removed, without damage to the calcareous structure.

RESULTS

The bryozoan *Schizoporella errata* was found encrusted on the test of the sea urchin *Echinometrta lucunter* (test diameter = 41 mm, Figure 1A and B). The encrusting colony was settled on a spineless area of 58.9 mm^2, and showed an oval and light convex outline, measuring 9.59 and 6.82 mm in the longest and shortest axis respectively (Figure 1C). The colored autozooids ranged from reddish-brown in the center of the colony to yellowish/cream in the periphery (Fig. 1B-E and 2B). Autozooid longer than wide, measuring 447.45 ± 73.77μm by 286 ± 58.66 μm (n = 20). Their shape ranged from squarish to hexagonal in the center to usually elongate in the periphery (Fig. 1D and E). Primary orifice broad, D-shaped anteriorly, and U-shaped in the posterior region (Fig. 1F-H). This orifice was 132.17 ± 7.65 long by 135.83 ± 7.65 μm wide (n=20). Single avicularia, close to the basolateral region of the primary orifice

(Fig. 1F and G). Autozooids bearing avicularia were more common in the center of the colony than in the periphery (Fig. 1D and H).

The coelomic fluid of the affected sea urchin collected immediately before colony removal showed no signs of foreign elements (*e.g* protozoan) and the cell density was only slightly smaller than in the healthy animals (7.83×10^6 and 7.86×10^6 cells/mL, respectively). In contrast, the proportion of all coelomic subpopulations in the affected sea urchin was different from the control group (Fig. 2). The percentage of phagocytes (59.7 ± 0.68 %) and vibratile cells (26.9 ± 1.39 %) in the control group was respectively 1.4 and 1.9-fold higher than in the affected animal (Pha = 42.8 %; VC = 14.3 %). On the other hand, red and colorless spherulocytes were 4.5 and 2.1-fold higher in the unhealthy organism (27.6 % and 15.2% respectively) than in healthy specimens (RS = 6.1 ± 0.93 %; 7.3 ± 1.02 %) (Fig. 2).

Except for the epibiont-affected area, the echinoid showed no further signs of injury as well as showed no classical symptoms of sickness (*e.g.* sluggish behavior, spine loss or tube feet unable to attach – Shimizu *et al.* 1995). Although the colony has been carefully removed by the edges without touching the central region of the wound, a piece of sea urchin test attached to the basal wall of the colony was accidentally extracted from the echinoid (Fig. 3A), which indicates a certain degree of structural weakening. After complete colony removal (Fig. 3B), a depression with a reddish smooth and apparently thick tissue layer on the test and a reddish-brown tissue around the injury were observed, indicating an intense inflammatory response. A more advanced state of wound healing was seen in the periphery of the damaged region (Fig. 3C). Three days after epibiont removal, the brownish tissue around the depression was no longer visible, the red color on the depression began to fade and the thickness of the red smooth layer began to decrease (Fig. 3D). In this stage, many copepods were seen crawling on the wound. Nine days after epibiont removal, the reddish-brown tissue around the depression and the red coloration on it had disappeared, revealing the calcareous structures (Fig. 3E). In health echinoids, the healing process differed in some details. Immediately after wound induction, it showed a whitish color due to the test and the freshly-extracted muscular and connective spine tissues (Fig. 2F). Three days later, red coloration on the wound was remarkable and differently from the injured urchin, which had no tissue around the wound, there was a thick layer of rotten tissue on all scraped region (Fig. 2G). After the sixth day, the intense red color began to fade and much of the rotten tissue had disappeared. Nine days after wound induction, the red-

colored region and the amount of rotten tissue on the wound were consistently smaller (Fig. 2H). Only after the twelfth day, the healing process seemed complete, with no tissue around the injury, similarly to the ninth day of the affected echinoid.

DISCUSSION

The bryozoan *Schizoporella errata* is recognized as a widely distributed exotic species, able to settle on any available substrate, including those originated from human activity (Micael *et al.* 2014). On the Brazilian coast, *S. errata* was recorded only in the Southeast region, specifically in the states of São Paulo (Morgado & Tanaka 2001) and Rio de Janeiro (Ramalho *et al.* 2011). Although Ignacio *et al*. (2010) had reported *S. errata* to Ilha Grande Bay, Marques *et al*. (2013) state that this record seems to be actually *S. pungens* Canu & Bassler, 1928. In fact, according to Tompsett *et al*. (2009), many worldwide records of *S. errata* are doubtful. The morphological and morphometric characteristics of the *S. errata* specimen found here compares fittingly with both the topotype and lectotype depicted by Tompsett *et al*. (2009).

Bryozoan epibiosis on echinoderms seems to be rather uncommon (Tab. I). Only twenty bryozoan species were already reported living on echinoderms, even whilst these hosts present most of the important traits to be adequate basibionts (Wahl & Mark 1999). While 73% are cidaroid sea urchins and primary spines seem to be the most frequent settlement area (Table I), sea cucumbers, sea stars, and ophiurans do not seem to be common hosts (Table I). Cidaroid sea urchins are well-known to have a primary spine with no epithelium. On the other hand, all body surfaces have a physiologically active tissue in non-cidaroid echinoids (and other echinoderms) (Märkel and Röser 1983). For non-cidaroid sea urchins, the epidermis could function as an additional means to prevent or at least hamper epibiotic settlements (Mckenzie & Grigolava 1996), added to the most common strategy, *viz.* pedicellariae (Campbell & Rainbow 1977). Thus, the lack of a physiologically inactive body surface area, such as molluscan shells and crustacean carapaces, may partially explain why it is so uncommon for non-cidaroid sea urchins to become basibionts, especially for bryozoans (Wahl & Mark 1999). Still, this can also help to understand why cidaroid echinoids seem to be the most common hosts to bryozoans.

In echinoderms, the circulating coelomocytes can be used as tools for accessing sea urchin health state in both natural and altered environments (Matranga *et al.* 2000)

as well as in diseased organisms (Jellett *et al.* 1988). The total cell count was similar between the affected and healthy individuals and fitted the number already observed for other healthy sea urchins (Coates et al. 2017). The percentage of specific subpopulations in the control group is also in accordance with the literature (Branco *et al.* 2013) indicating that they were really healthy. On the other hand, the high values of red spherulocytes found in the affected sea urchin fitted the pattern already recorded in impaired animals (Matranga *et al*. 2000, Branco *et al*, 2013).

Studies addressing regenerative capabilities in sea urchins usually analyze spine or tube feet (Bodnar and Coffman 2016), while test regeneration has been poorly studied (D'Andrea-Winslow *et al.* 2008). Here, the general healing pattern observed in healthy *E. lucunter* specimens was similar to that observed in *Lytechinus variegatus* (D'Andrea-Winslow *et al.* 2008). For both species, a reddish coloration was observed on the third day, which increased on the sixth day. For *L. variegatus*, healing is almost finished between 6-8 days (D'Andrea-Winslow *et al*. 2008), while this process spent more time (*i.e.* 12 days) in healthy *E. lucunter*. In contrast, the healing process in the affected *E. lucunter* seemed to be faster than in healthy individuals. The red coloration on the wound was observed just after colony removal and some regions in the periphery were already in an advanced healing stage (*Cf*. Fig. 2C). All dead tissue around the wound had disappeared on the third day as well as the red color on the wound begun to fade, and in the ninth day, the process was apparently complete. These data seem to suggest that in some instances, the healing process had already begun before colony removal.

In summary, for the first time, a bryozoan was found attached to a non-cidaroid sea urchin. Here, the species *Schizoporella errata* was found living in an unusual place: the test of a live *Echinometra lucunter*. Although there are many misidentifications related to *S. errata* records, the specimen studied here fits the morphological and morphometric parameters observed in the types recently analyzed. Still, even bryozoans being well known as epibionts on many groups, non-cidaroid sea urchins (and other echinoderms) do not seem to be the preferred hosts. Maybe this could be related to the presence of an epidermis covering all animals. Additionally, some biological/physiological aspects of the affected sea urchin were described. The data obtained from the control group fits the pattern found in literature, indicating that these individuals were really healthy. On the other hand, the high proportion of red spherulocytes and the intense red coloration on the wound of the affected sea urchin

were not consistent with undisturbed specimens. In fact, these data suggest that *Echinometra lucunter* seemed to be immunologically disturbed by this epibiotic association, although this cannot be directly attributed to the settlement of *S. errata*. Thus, even with no strong support about the epibiont effect on host physiology, one question becomes appropriate: can basibiont organisms be physiologically impaired during epibiotic interactions? The small number replicates analyzed do not allow answering it now. However, the data presented here show that this question deserves further attention in future studies.

ACKNOWLEDGMENTS

The author is indebted to Dr. Leandro M. Vieira for the identification of the bryozoan and Sheilla Schuindt (LME-IB/USP) for helping with SEM procedures. I am especially thankful to Dr. Marcio R. Custódio for his suggestions and criticism during manuscript preparation and to Daniel C. Cavallari for the English improvements. This study was supported by a doctoral grant (FAPESP Procs. 2015/ 21460-5 and 2018/14497-8).

REFERENCES

Barel, C. D., & Kramers, P. G. 1977. A survey of the echinoderm associates of the north-east Atlantic area. 2001. **Zoologische Verhandelingen 156**: 1–159.

Bodnar, A. G., & Coffman, J. A. 2016. Maintenance of somatic tissue regeneration with age in short- and long- lived species of sea urchins. **Aging cell,** 15(4): 778-787.

Branco, P. C., Borges, J. C. S., Santos, M. F., Jensch-Junior, B. E. & silva J. R. M. C. 2013. The impact of rising sea temperature on innate immune parameters in the tropical subtidal sea urchin *Lytechinus variegatus* and the intertidal sea urchin *Echinometra lucunter*. **Marine Environmental Research, 92**: 95–101.

Campbell, A. C. & Rainbow, P. S. 1977. The role of pedicellariae in preventing barnacle settlement on the sea-urchin test. **Marine Behaviour and Physiology, 4(4)**: 253–260.

Coates, C. J., McCulloch, C., Betts, J. & Whalley, T. 2018. Echinochrome a release by red spherule cells is an iron-withholding strategy of sea urchin innate immunity. **Journal of innate immunity**, 10(2): 119-130.

D'Andrea-Winslow, D. F. & Johnson, A. K. N. 2008. Bioelectromagnetic Energy Fields Accelerate Wound Healing and Activate Immune Cell Function. **Journal of Medical & Biological Sciences**, 2(1): 1-16

David, B., Stock, S. R., De Carlo, F., Heterier, V. & De Ridder, C. 2009. Microstructures of Antarctic cidaroid spines: Diversity of shapes and ectosymbiont attachments. **Marine Biology, 156**:1559–1572.

Gautier, V. 1959. Sur quelques cas d'epibioses: bryozoaires sur *Leptometra*. **Recueil des Travaux de la Station Marine d'Endoume 16(26)**:143–148.

Ignacio, B. L., Julio, L. M., Junqueira, A. O. R. & Ferreira-Silva, M. A. G. 2010. Bioinvasion in a Brazilian Bay: filling gaps in the knowledge of southwestern Atlantic biota. **Plos One, 5(9)**: 13065.

Jangoux, M. 1987. Diseases of Echinodermata. II. Agents metazoans (Mesozoa to Bryozoa). **Diseases of aquatic organisms, 2**:205–234.

Jellett, J. F., Wardlaw, A. C. & Scheibling, R. E. 1988. Experimental infection of the echinoid *Strongylocentrotus droebachiensis* with *Paramoeba invadens*: quantitative changes in the coelomic fluid. **Diseases of aquatic organisms, 4**:149–157.

Key, M. M., Jeffries, W. B. & Voris, H. K. 1995. Epizoic bryozoans, sea snakes, and other nektonic substrates. **Bulletin of Marine Science, 56**:462–474.

Märkel, K., & Röser, U. 1983. Calcite-resorption in the spine of the echinoid *Eucidaris tribuloides*. **Zoomorphology**, 103(1), 43–58. doi:10.1007/bf00312057

Matranga, V., Toia, G., Bonaventura, R. & Muller W. E. G. 2000. Cellular and biochemical responses to environmental and experimentally induced stress in sea urchin coelomocytes. **Cell Stress Chaperones, 5**: 158–165.

Mckenzie, J. D. & Grigolava, J. V. 1996. The echinoderm surface and its role in preventing microfouling. **Biofouling, 10**:261–272.

Micael, J., Marina, J. G., Costa, A. C. & Occhipinti-Ambrogi, A. 2014. The non-indigenous *Schizoporella errata* (Bryozoa: Cheilostomatida) introduced in the Azores Archipelago. **Marine Biodiversity Records, 7**(e133):1-6.

Morgado, E. H. & Tanaka M. O. 2001. The macrofauna associated with the bryozoan *Schizoporella errata* (Waters) in southeastern Brazil. **Scientia Marina, 65:** 173–181.

Mortensen, T. 1912. Report on the echinoderms collected by the Danmark-Expedition at northeast Greenland. **Meddelelser om Grønland, 45**:239-302.

Moyano, G. H. I. & Wendt, A. 1981. Bryozoa epizoos de *Psolus charcoti* Vaney, 1907 (Holothuroidea, Psolidae). **Instituto Antártico Chileno – Serie Cientifica, 27**:5-11.

Queiroz V. 2016. Opportunity makes the thief – Observation of a sublethal predation event on an injured sea urchin. **Marine Biodiversity 48(1): 153-154**

Queiroz, V. & Custódio M. R. 2015. Characterization of the spherulocyte subpopulations in *Eucidaris tribuloides* (Cidaroida: Echinoidea). **Italian Journal of Zoology, 82(3)**: 338–348.

Ramalho, L.V., Muricy, G. & Taylor. P. D. 2011. Taxonomic revision of some lepraliomorph cheilostome bryozoans (Bryozoa: Lepraliomorpha) from Rio de Janeiro State, Brazil. **Journal of Natural History, 45(13)**: 767-798.

Shimizu, M., Takaya, Y., Ohsaki, S. & Kawamata, K. 1995. Gross and histopathological signs of the spotting disease in the sea urchin *Strongylocentrotus intermedius*. **Fisheries Science, 61**: 608–613.

Sosa-Yañez, A., Vieira, L. M. & Solís-Marín, F. A. 2015. A new cheilostome bryozoan genus, *Abditoporella* (Hippoporidridae), from the eastern Pacific. **Zootaxa, 3994(2)**:275-282.

Taylor, P. D. & Monks N. 1997. A New Cheilostome Bryozoan Genus Pseudoplanktonic on Molluscs and Algae. **Invertebrate Biology, 116(1)**:39-51.

Tompsett, S., Porter J. & Taylor P. D. 2009. Taxonomy of the fouling cheilostome bryozoans, *Schizoporella unicornis*, (Johnston) and *Schizoporella errata* (Waters). **Journal of Natural History, 43(35-36)**: 2227-2243.

Wahl, M. & Mark, O. 1999. The predominantly facultative nature of epibiosis: experimental and observational evidence. **Marine Ecology Progress Series, 187**: 59–66.

Figures, Tables, and Captions

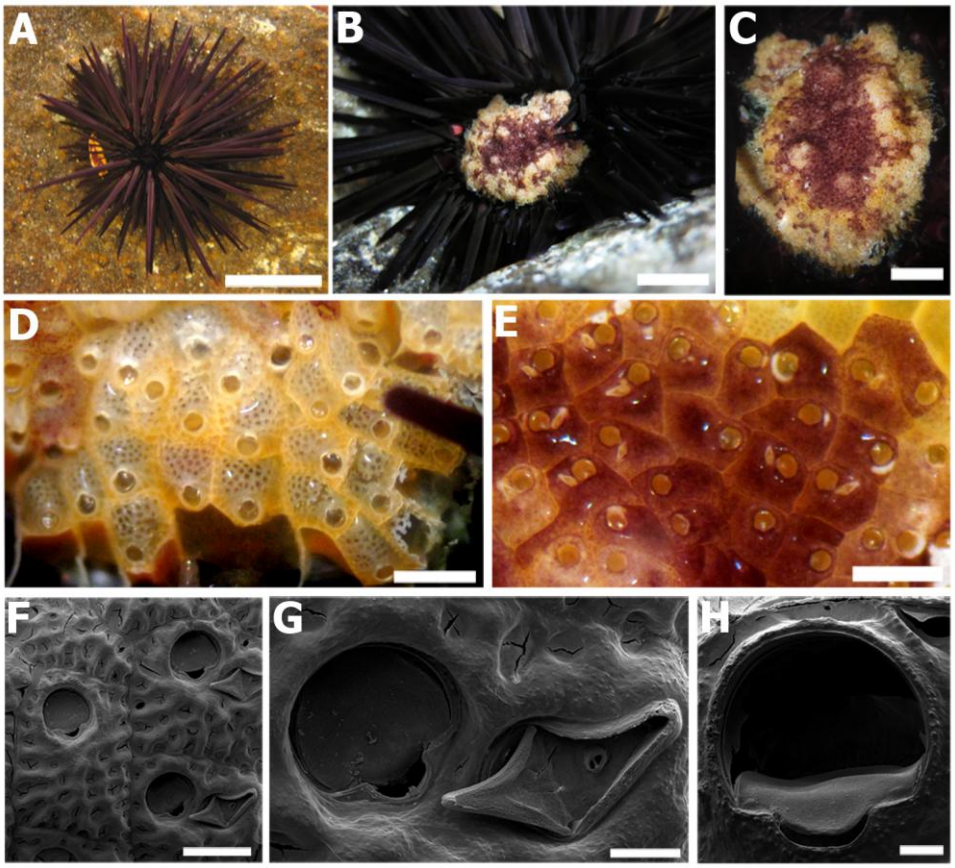

Figure 1 – *Schizoporella errata* on *Echinometra lucunter*: **A-E** – Live animals, **F-H** – Scanning electron microscopy. **A** – General view of the epibiotic relationship, **B** and **C** – Overview of bryozoans colony on sea urchin test, **D** – Autozooids on the periphery, **E** – Autozooids and avicularia in the center of the colony, **F** – Autozooids and avicularia in SEM analyses, **G** and **H** – primary orifice and avicularium in detail. Scale: A = 2.5 cm; B = 5mm; C = 2mm; D and E = 400 um; F =200um; G = 60 um; H = 20 um.

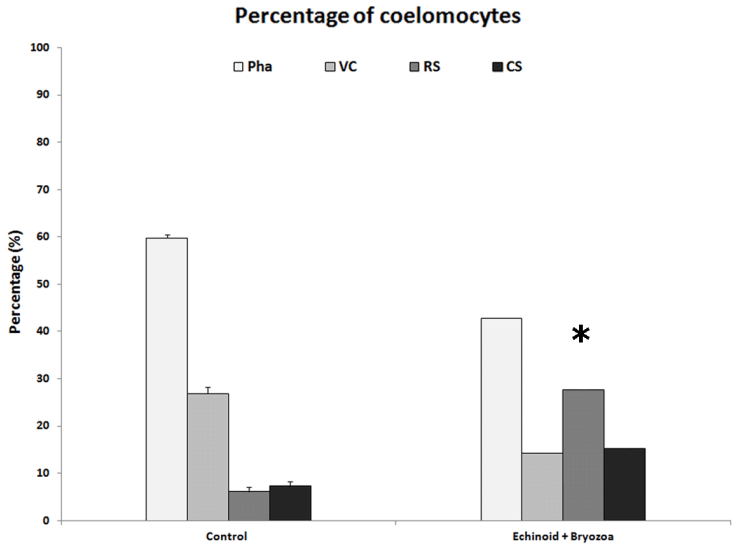

Figure 2 – Proportion of coelomocyte subpopulations in affected sea urchin and control group, after colony removal. (Pha, Phagocytes; VC, Vibratile Cell; RS, Red Spherulocyte; CS, Colorless Spherulocyte). * There is no standard deviation (SD) because these data are from only one individual.

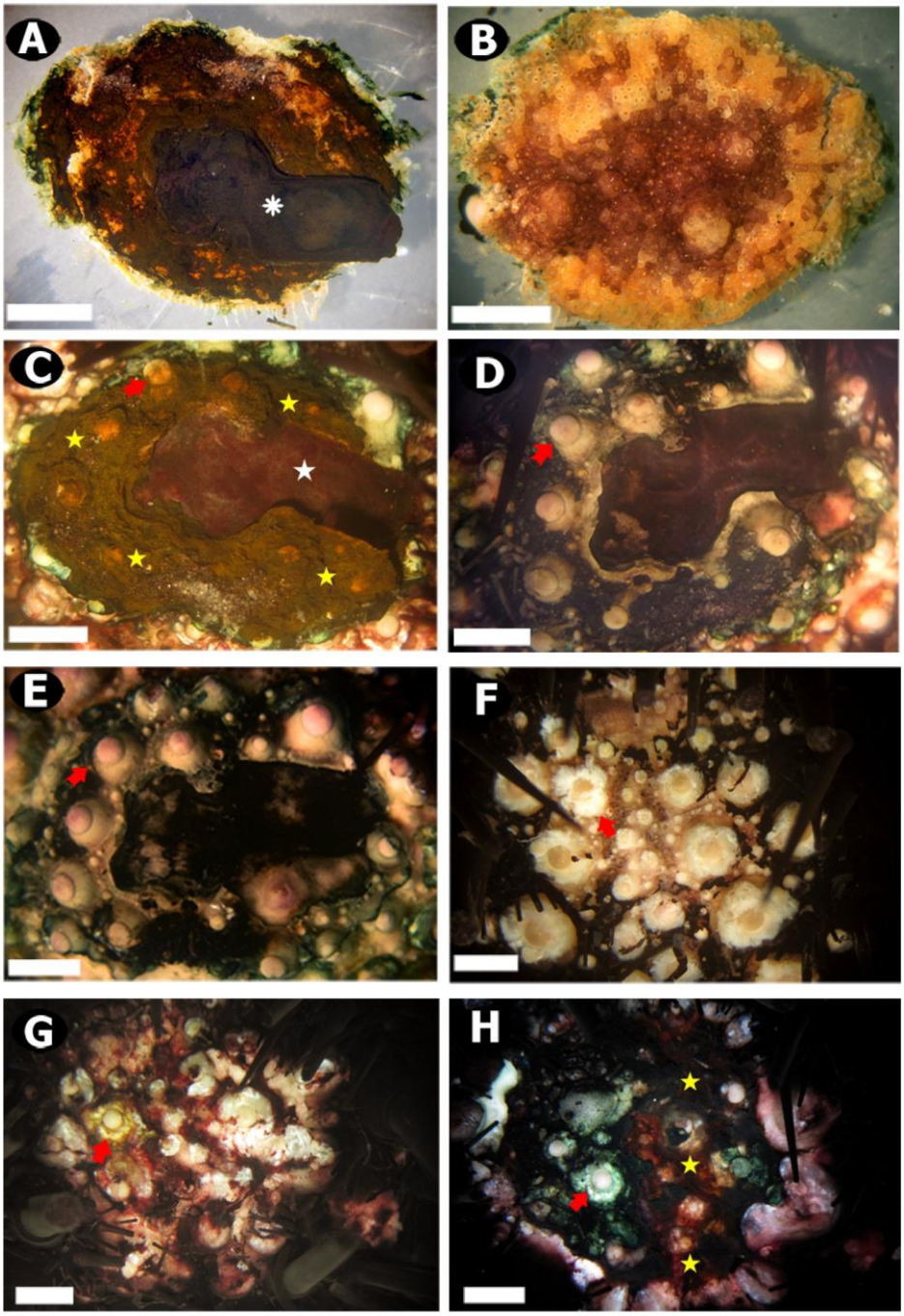

Figure 3 – Wound healing process in *Echinometra lucunter*. **A-B** – *Schizoporella errata* colony; **C-E** – Affected *Echinometra lucunter*; **F-H** – Healthy *Echinometra lucunter* (control group). **A** and **B** – Basal and anterior wall of the *Schizoporella errata* autozooids, respectively showing a piece of sea urchin test attached to them (*); **C** – Wound immediately after colony removal; **F** – Wound immediately after injury induction (control group); **D** and **G** – After three days; **E** and **H** – After nine days. (Asterisk, piece of sea urchin test on the basal wall of *Schizoporella errata*; White star, reddish depression on the test wound in the affected sea urchin; Yellow star, reddish-brown tissue; Red arrow, reference point). Scale: 3mm.

Table

Table I – Records of bryozoans living on echinoderm hosts.

Echinoderm host		Epibiotic Bryozoa		Place on host
Class	**Species**	**Order**	**Species**	
Cri	*Poliometra prolixa* [1, 2]	Cheilostomatida	*Eucratea loricata*	Cirri
	Leptometra phalangium [3]	Cheilostomatida	*Microporella ciliata*	Cirri and arms
			Smittina landsborovii	Arm (pinules)
			Buskea dichotoma	Cirri and arms
			Diaperoecia dorsalis	Cirri and arms
		Ctenostomatida	*Tubulipora liliacea*	Cirri and arms
			Disporella harmeri	Cirri and arms
Hol	*Psolus charcoti* [4]	Cheilostomatida	*Fenestrulina malusii*	Bivium
			Antarctothoa antarctica	Bivium
			Cellarinella watersi	Bivium
			Cellaria aurorae	Bivium
Ech	*Eucidaris thouarsii* [5]	Cheilostomatida	*Abditoporella dimorpha*	Primary spine; test of a dead animal
	Hesperocidaris asteriscus [5]			Primary spine
	Ctenocidaris perrieri [6]		*Chaperiopsis cervicornis* *Smittina obicullata*	Primary spine
	Ctenocidaris rugosa [6]		*Arachnopusia sp. 2*	Primary spine
	Ctenocidaris speciosa [6]		*Osthimosia sp. 1*	Primary spine
	Notocidaris platyacantha [6]		*Arachnopusia sp. 1*	Primary spine
	Notocidaris lanceolata [6]		*Micropora* sp. *Osthimosia* sp. 2	Primary spine
	Aporocidaris milleri [6]		*Osthimosia sp. 1*	Primary spine
	Echinometra lucunter [7]		***Schizoporella errata***	**Test (live host)**

Legend: **Cri** = Crinoidea; **Hol** = Holothuroidea; **Ech** = Echinoidea; **1** - Mortensen, 1912; **2** - Barel and Kramers, 1977; **3** – Gautier, 1959; **4** - Moyano & Wendt, 1981; 5 - Sosa-Yañez et al., 2015; **6** - David et al., 2009; **7** – **Present study.**

Considerações finais e perspectivas

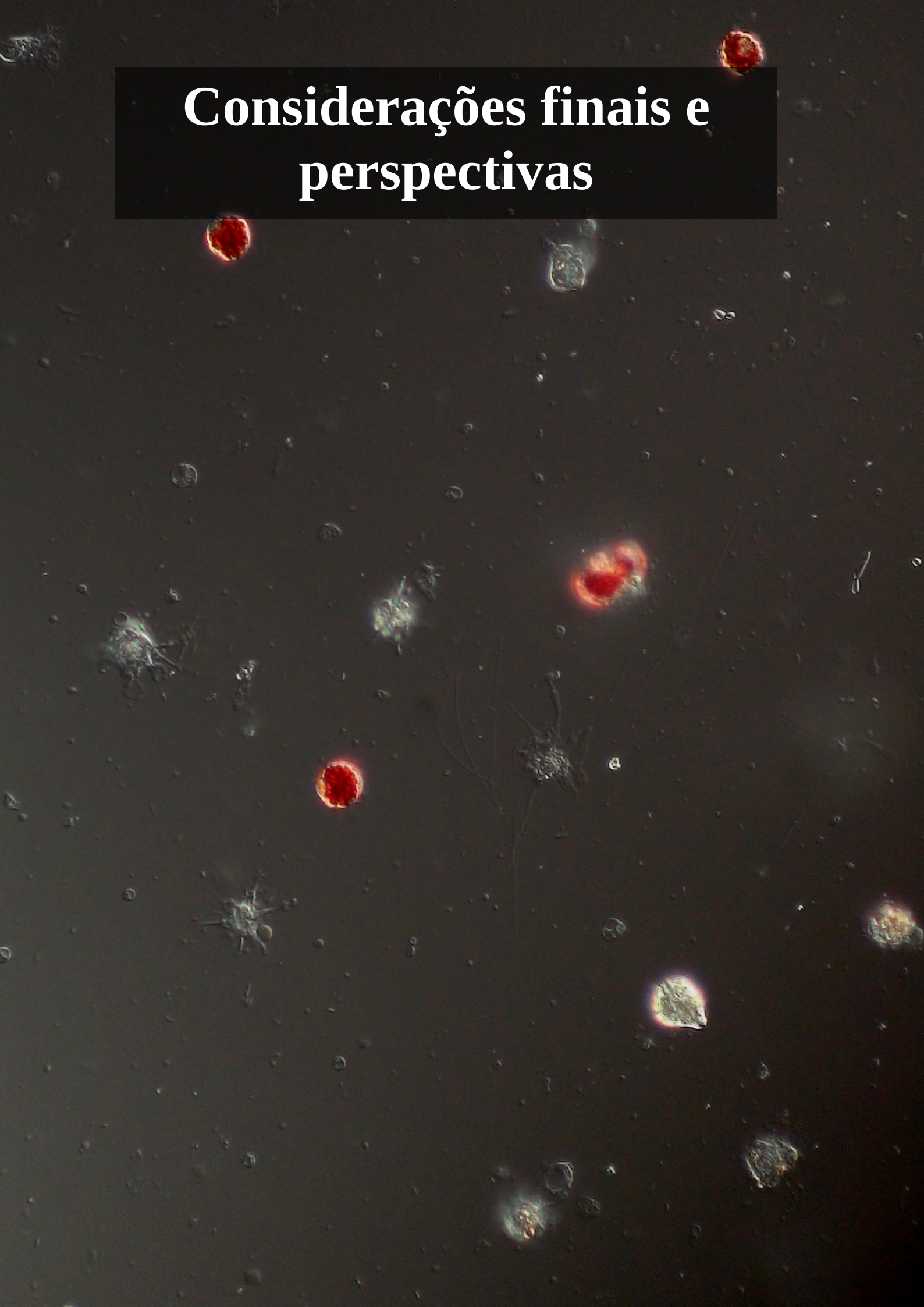

DIVERSIDADE DE CELOMÓCITOS EM ECHINOIDEA

A classe Echinoidea tem sido, sem sombra de dúvida, a mais estudada em Echinodermata com relação aos celomócitos e consequentemente é a que possui a maior quantidade de informação (Smith et al, 2006; 2010; 2018). No entanto, a diversidade dos tipos celulares tem sido subestimada. Este fato pode ser observado em alguns estudos/revisões, onde somente as células dos ouriços regulares têm sido consideradas (Karp and Cofaro, 1982; Cavey and Märkel, 1994). O presente estudo mostrou dois pontos importantes: (I) a diversidade de celomócitos nos ouriços irregulares é muito maior do que tem sido registrada na literatura corrente, principalmente em relação aos Clypeasteroida (bolacas-do-mar), onde somente para este grupo, cinco novos tipos de esferulócitos foram registrados; (II) mesmo para os tão bem estudados ouriços regulares, a diversidade de tipos celulares é maior do que a que tem sido pontuada. Além disso, embora o atual trabalho tenha sido restrito aos equinoides, é a primeira vez que um enfoque evolutivo é dado ao estudo dos celomócitos em Echinodermata, revelando padrões interessantes de distribuição das células, que parecem estar ligados às características fisiológicas das células. Por fim, a caracterização das células das espécies do gênero *Paracentrotus* trouxeram resultados interessantes, onde o esferulócito granular e a célula cristal foram observados em *P. gaimardi*, e para *P. lividus*, uma das espécies mais estudadas do mundo, um novo tipo celular também foi encontrado – o esferulócito granular. Isso nos mostra que mesmo para os ouriços regulares, os principais modelos de estudo em Echinodermata, a diversidade de tipos celulares ainda não é completamente entendida e merece ser revisitada.

MORFOLOGIA CELULAR E O ESTUDO DAS POPULAÇÕES CELÔMICAS EM ECHINODERMATA

Tradicionalmente em Echinodermata, e principalmente em Echinoidea, o estudo dos celomócitos tem se dado por meio de abordagens morfológicas, usando células vivas em suspensção ou microscopia eletrônica de transmissão (Johnson, 1979a; Chien et al., 1970), com pouquíssimos estudos se dispondo a utilizar preparações citoquímicas (Liebman, 1950; Johnson, 1979b). Para os pouquíssimos estudos citoquímicos, o método comumente empregado para aderir as células às lâminas (*i.e.*o espraiamento de células vivas) também tem se mostrado problemático, uma vez que o

mesmo tipo celular pode espraiar de maneiras diferentes, dificultando a identificação. Neste trabalho, também utilizamos uma abordagem morfológica, mas sob uma diferente pesrspectiva: uma abordagem integrativa (Queiroz & Custódio, 2015). Diferentes dos outros trabalhos, as abordagens utilizadas, foram consideradas conjuntamente, utilizando a informação de cada técnica de forma integrada. Para isso, abordamos a morfologia dos diferentes tipos celulares, utilizando várias técnicas diferentes (*e.g.* células vivas em suspensão, praparações citoquímicas, microscopia eletrônica de transmissão e varredura e espectroscopia de raios-X). Os dados oriundos destas técnicas possibilitaram não só uma caracterização morfológica mais acurada, como também a obtenção de dados relativos a outros aspectos, tais como a natureza química das inclusões citoplasmáticas e a descrição de um processo de maturação. Além disso, observamos que a utilização da citocentrifugação no preparo das lâminas para as análises citoquímicas e de microscopia de varredura foi um ponto positivo neste estudo. Esta técnica, que utiliza um princípio físico (*i.e.*a força de centrifugação) para aderir as células à lâmina, faz com que os diferentes tipos celulares apresentem sempre as mesmas características, propiciando a comparações entre diferentes equinoides (*e.g.* a célula vibrátil em *E. tribuloides* e em *C. subdepressus*). Com issso, este trabalho reforça a importancia de estudos morfológicos mais detalhados para o conhecimento das populações celulares, mostrando que dados interessantes podem ser obtidos com este tipo de abordagem.

ISOLAMENTO DAS FRAÇÕES CELULARES

A separação das diferentes subpopulações de celomócitos em Echinodermata há muito tem sido um grande problema (Chia & Xing, 1996). Trabalhos que buscam fracionar estas populações, se utilizam de centrifugação por gradientes de densidades que obtem subpopulações enriquecidas com variáveis níveis de pureza (Ariza et al., 2007; Kudryavtsev et al., 2016), mas não são capazes de produzir frações puras. Mesmo métodos mais sofisticados, como a citometria de fluxo, não tem produzido bons resultados (McCaughey & Bodnar, 2012; Kudryavtsev et al., 2016). O motivo disso talvez resida em dois principais fatos: a falta de marcadores celulares específicos, e a sobreposição de diferentes tipos por apresentarem características morfológicas (*e.g.* tamnho e granulosidade) similares (Chia & Xing, 1996; Queiroz & Cutódio, 2016). No entanto, o método utilizado aqui, a citometria de fluxo por imagem, se mostrou bastante

eficiente. Este método junta a possibilidade de observação da morfologia celular – o único critério confiável até o momento para a distinção dos tipos celulares – com a análise de uma enorme quantidade de células, o que propicia uma identificação acurada juntamente com a possibilidade da análise das condições fisiológicas. Além disso, pela primeira vez obteve-se um gate específico e replicável para a célula vibrátil, além de dados experimentais corroborando a sua participação na resposta imune.

FUNÇÃO FISIOLÓGICA DOS CELOMÓCITOS

Em Echinoidea, o nível de informação sobre a fisiologia dos celomócitos é bastante significativo (Smith et al, 2006; 2010; 2018). Sabe-se, por exemplo, do envolvimento dos fagócitos com as atividades de fagocitose, encapsulamento e rejeição de enxertos (Smith et al., 2006). Já os esferulócitos transparente e vermelho estão ligados à atividade citotóxica e bactericida respectivamente (Arizza et al., 2007; Coates et al., 2018). Para o último, muito detalhes são conhecidos, variando desde a função da célula, o composto responsável pela atividade bactericida e o modo de ação da molécula. No presente estudo, adicionamos informações sobre dois aspectos importantes do funcionamento do esferulócito vermelho: o mecanismo pelo qual a célula libera o equinocromo, e alguns dos fatores que afetam o processo. Para a célula vibrátil, especula-se seu envolvimento em movimentação do fluido celômico ou com funções imunes, mais especificamente coagulação. Para esta última célula, nosso estudo corrobora o seu envolvimento com o sistema imune, dadas as observações de dinâmica celular diferenciada após a infecção bacteriana. Para o esferulócito granular, nenhuma informação funcional foi obtida. No entanto esta célula é bastante similar, em morfologia e características citoquímicas, ao esferulócito acidofílico de *Holothuria tubulosa*, que tem sido relacionado com atividade citotóxica nesta espécie (Vazanna et al., 2018), sugerindo o envolvimento do esferulócito granular no processo. Para os esferulócitos dos ouriços irregulares, mesmo para as células similares às dos ouriços regulares, muito pouco é conhecido, e nada se sabe sobre os tipos novos observados aqui.

COOPERAÇÃO DOS CELOMÒCITOS DURANTE DESAFIOS IMUNES

Como mostrado no trabalho publicado por Arizza e colaboradores (2007), o esferulócito transparente parece ter sua atividade maximizada na presença de fagócitos, e o autor sugere que a atividade citotóxica deve ser modulada graças a algum composto liberado pelos fagócitos. No trabalho de Vazzana e colaboradores (2015), foi observado que durante a cicatrização em *Holothuria tubulosa* a diminuição do número de células progenitoras, 2,5 h após a injúria, foi seguinda por um aumento do número de esferulócitos. No nosso estudo observou-se uma aparente cooperação entre fagócitos, esferulócitos vermelhos e as células vibráteis. Trabalhos com este escopo, com evidências sobre os diferentes tipos celulares em uma dada situação experimental, se fazem necessários para o estudo das funções dos celomócitos. Assim como observado para o esferulócito transparente (Arizza et al., 2007), pode ser que a análise separada de um tipo celular específico não mostre a sua real função, visto que ele pode necessitar da atividade de outro tipo celular para exercer a sua função corretamente ou que ele coopere na função de outra subpopulação. Portanto, mais estudos analisando todos, ou muitas das subpopulações se fazer necessários para compreender a real função dos esferulócitos.

PERSPECTIVAS NO ESTUDO DOS CELOMÓCITOS DE ECHINODERMATA

Os novos dados encontrados neste trabalho respondem, ou pelo menos apontam o caminho a ser seguido, algumas das grandes questões envolvendo os celomócitos dos Echinodermata. Foi possível ver neste trabalho a diversidade de tipos de celomócitos em Echinoidea, estudados sob uma perspectiva evolutiva, juntamente com o estudo aprofundado das células celômicas de uma das espécies mais estudadas do mundo: *Paracentrotus lividus*. Além disso, apresentamos a caracterização morfológica detalhada da célula vibrátil, um dos celomócitos mais intrigantes nos equinodermos, juntamente com dados funcionais que corroboram a função imune desta célula. Por fim, analisamos o mecanismo de liberação de Echinochromo pelo esferulócito vermelho de *P. lividus*, alguns dos fatores que afetam o processo, e que esta célula pode ser utilizada como um bioindicador de estresse fisiológico em ouriços-do-mar.

Apesar de toda informação obtida neste trabalho, questões relevantes, tais como o conteúdo estocado pelos esferulócitos e pela célula vobrátil, a suas respectivas

funções fisiológicas bem como o seu local de origem ainda continuam sem respostas definitivas. Contudo, pelo menos para as duas primeiras questões, parece que os primeiros passos foram dados nesse trabalho. Observamos que os esferulócitos transparente e granular estocam mucopolissacarídeos e proteínas respectivamente, enquanto a célula vibrátil acumula glicosaminoglicanos. Para esta última célula também observamos que a quantidade de nitrogênio citoplasmático é pequena, corroborando a ideia de esférulas não são preenchidas com material proteico. Com relação às funções fisiológicas, observamos que a célula vibrátil de fato parece estar envolvida com resposta imune, (*i.e.* coagulação), enquanto o esferulócito granular pode estar relacionado com atividade citotóxica.

Por fim, os resultados alcançados aqui também levantam mais questionamentos, como por exemplo: 1 – Seriam os esferulócitos dos ouriços irregulares, células com diferentes morfologias e funções similares ou células morfológica e funcionalmente diferentes? 2 – Qual a função fisiológica dos esferulócitos dos ouriços irregulares? 3 – O que pode ter guiado a diversificação dos esferulócitos em Echinoidea? 4 – Qual a função fisiológica do esferulócito granular de *P. lividus*? 5 – Qual o mecanismo de ação da célula vibrátil? 6 – Quais os mecanismos moleculares envolvidos com a liberação do equinocromo dos esferulócitos vermelhos? 7 – Os esferulócitos vermelhos podem realmente ser utilizados como um indicador de saúde nos equinoides? 8 – Organismos basobiontes relamente podem alterar homeostase dos seus basobiontes? Assim, embora este trabalho tenha certamente contribuído para o entendimento da fisiologia dos Echinodermata, estas e outras perguntas ainda continiarão aguçando a curiosidade dos fisiólgos que trabalham com equinodermos.

REFERÊNCIAS

Ageenko VN, Kiselev KV, Odintsova NA. 2011. Expression of Pigment Cell-Specific Genes in the Ontogenesis of the Sea Urchin *Strongylocentrotus intermedius*. Evidence-Based Comp. Alter. Med., 2011: 9p.

Arikan H, Çiçek K. 2014. Haematology of amphibians and reptiles: a review. North-Western J. Zoo, 10(1):190-209.

Arizza V, Giaramita F, Parrinello D. 2007. Cell cooperation in coelomocyte cytotoxic activity of *Paracentrotus lividus* coelomocytes. Comp. Biochem. Physiol. A, 147:389-394.

Azwai SM, Abdouslam OE, Al-Bassam LS. 2007. Morphological characteristics of blood cells in clinically normal adult llamas (*Lama glama*). Veterinarski Arhiv 77(1):69-79.

Bachmann S, Goldschmid A. 1978. Fine structure of the axial complex of *Sphaerechinus granularis* (Lam.) (Echinodermata: Echinoidea). Cell Tissue Res 193:107–123.

Bookhout CG, Greenburg ND. 1940. Cell types and clotting reactions in the echinoid, *Mellita quinquiesperforata*. The Biological Bulletin, 79(2): 309-320.

Boolotian RA. 1966. Physiology of Echinodermata. Interscience Publishers, N.Y. 822p.

Cavey MJ, Märkel K. 1994. Echinoidea. *In*: Harrison, F. W. & Chia, F. S. (Eds.). Microscopic Anatomy of Invertebrates, Echinodermata (Vol. 14). Wiley-Liss. (pp. 345-400).

Chia F, Xing J. 1995. Echinoderm Coelomocytes. Zoological Studies 35(4):231-254.

Chien PK, Johnson PT, Holland ND, Chapman FA. 1970. The coelomic elements of sea urchins (*Strongylocentrotus*) IV. Ultrastructure of the coelomocytes. Protoplasma 71:419–442.

Coates CJ, McCulloch C, Betts J, Whalley T. 2018. Echinochrome A release by red spherule cells is an iron-withholding strategy of sea urchin innate immunity. Journal of innate immunity, 10(2): 119-130.

Coteur G, DeBecker G, Warnau M, Jangoux M, Dubois P. 2002. Differentiation of immune cells challenged by bacteria in the common European starfish, Asterias rubens (Echinodermata). European Journal of cell biology, 81(7), 413-418.

Edds KT. 1993. Cell biology of echinoid coelomocytes. Journal of Invertebrate Pathology 61:173–178. doi:10.1006/jipa.1993.1031

Falanga A, Marchetti M, Evangelista V. 2000. Polymorphonuclear leukocyte activation and hemostasis in patients with essential thrombocythemia and polycythemia vera. Blood, 96(13):4261-4266.

Fontaine AR, Hall BD. 1981. The haemocyte of the holothurians Eupentacta quinquesemita: ultrastructure and maturation. Can. J. Zool. 59: 1884-1891.

Frank U, Plickert G, Müller WA. 2004. Cnidarian Interstitial Cells: The Dawn of Stem Cell Research. *In:* Rinkevich B, Matranga V. (Eds). Stem Cells in Marine Organisms. 33-59.

Graham A, Richardson J. 2012. Developmental and evolutionary origins of the pharyngeal apparatus. Evodevo, 3(1), 24.

Johnson PT. 1969a. The coelomic elements of sea urchins (Strongylocentrotus). I. The normal coelomocytes; their morphology and dynamics in hanging drops. Journal of Invertebrate Pathology 13:25–41. doi:10.1016/0022-2011(69)90236-5.

Johnson PT. 1969b. The coelomic elements of sea urchins (Strongylocentrotus) II. Cytochemistry of the Coelomocytes. Histochemie 17:213–231. doi:10.1007/BF00309866.

Kaneshiro ES, Karp RD. 1980. The ultrastructure of coelomocytes of the sea star Dermasterias imbricate. Biol. Bull., 159: 295-310.

Karp RD, Coffaro KA. 1982. Cellular Defense Systems of the Echinodermata. *In*: Cohen N, Sigel MM. (Eds). Phylogeny and Ontogeny. Springer, Boston, MA.

Kawaguti S, Yaimasu T. 1954. Pigment cells in the perivisceral fluid of the Echinoidea. Biological Journal of Okayama University, 1: 249-264

Koltsova EA, Boguslavskaya LV, Maximov OV. 1981. On the functions of quinonoid pigment production in sea urchin embryos. Inter. J. Inver. Repro, 4:17–28.

Kroh A, Mooi R. 2019. World Echinoidea Database. Available from: http://www.marinespecies.org/echinoidea/aphia.php?p=browser&accepted=1&id[]=149854&id[]=510499#focus (accessed 04 December 2019)

Kudryavtsev IV, D'yachkov IS, Mogilenko DA, Sukhachev AN, Polevshchikov AV. 2016. The functional activity of fractions of coelomocytes of the starfish *Asterias rubens* Linnaeus, 1758. Russian Journal of Marine Biology, 42(2): 158-165.

Liebman E. 1950. The leucocytes of *Arbacia punctulata*. Biological Bulletin 98:46–59. doi:10.2307/1538598.

Maciel PO, Affonso EG, Boijink CL. 2011. *Myxobolus* sp. (Myxozoa) in the circulating blood of *Colossoma macropomum* (Osteichthyes, Characidae). Rev. Bras. Parasitol. Vet., Jaboticabal, 20(1):82-84.

Matranga, V, Pinsino A, Celi M, Natoli A, Bonaventura R, Schröder HC, Müller WE. 2005. Monitoring chemical and physical stress using sea urchin immune cells. Progress in Molecular and Subcellular Biology 39:85–110.

McCaughey C, Bodnar A. 2012. Investigating the Sea Urchin Immune System: Implications for Disease Resistance and Aging. J. Young Invest., 23(6):25-33.

Millott N. 1969. Injury and the axial organ of echinoids. Experientia 25:756.

Old JM, Huveneers C. 2006. Morphology of the blood cells from three species of Wobbegong sharks (*Orectolobus* species) on the east coast of New South Wales. Zoo Biol, 25(1):73-82.

Palis J. 2014. Primitive and definitive erythropoiesis in mammals. Fron. Phys, 5(3):1-9.

Pawson DL. 2007. Phylum Echinodermata. Zootaxa, 1668: 749-764.

Pisani D, Feuda R, Peterson KJ, Smith AB. 2012. Resolving phylogenetic signal from noise when divergence is rapid: A new look at the old problem of echinoderm class relationships. Molecular Phylogenetics and Evolution, 62(1): 27–34. doi:10.1016/j.ympev.2011.08.028

Queiroz V, Custódio MR. 2015. Characterization of the spherulocyte subpopulations in *Eucidaris tribuloides* (Cidaroida: Echinoidea). Italian Journal of Zoology, *82*(3): 338-348.

Ramírez-Gómez F, García-Arrarás JE (2010) Echinoderm immunity. ISJ, 7:211-220.

Reich A, Dunn C, Akasaka K, Wessel G. 2015. Phylogenomic Analyses of Echinodermata Support the Sister Groups of Asterozoa and Echinozoa. PLoS ONE 10(3): e0119627. doi:10.1371/ journal.pone.0119627

Sailasuta A, Satetasit J, Chutmongkonkul M (2011) Pathological Study of Blood Parasites in Rice Field Frogs, *Hoplobatrachus rugulosus* (Wiegmann, 1834). Vet. Med. Inter, 2011:1-5.

Service M, Wardlaw AC. 1984. Echinochrome A as bactericidal substance in the coelomic fluid of *Echinus Esculentus* (L.). Comp. Bioch. Phys, 79(B):161–165.

Smith CL, Ghosh J, Buckley KM, Clow LA, Dheilly NM, Huag T, Henson JH, ChengMan Lun CL, Majeske AJ, Matranga V, Nair SV, Rast JP, Raftos DA, Roth M, Sacchi S, Schrankel CS, Stensvag K. 2010. Echinoderm immunity. *In*: Söderhäll K, editor. Invertebrate immunity. New York, NY: Landes Bioscience and Springer Science BusinessMedia. pp. 260–301.

Smith LC, Arizza V, Hudgell MAB, Barone G, Bodnar AG, Buckley KM, Furukawa R. 2018. Echinodermata: the complex immune system in echinoderms. *In*: Cooper L. (Ed). Advances in comparative immunology (pp. 409-501). Springer, Cham.

Smith LC, Rast JP, Brockton V, Terwilliger DP, Nair SV, Buckley KM, Majeske AJ. 2006. The sea urchin immune system. Invertebrate Survival Journal 3:25–39.

Smith VJ 1981. The echinoderms. *In*: Ratcliffe NA, Rowley AF, (Eds). Invertebrate blood cells. New York, NY: Academic Press. 513–562.

Snyder GK, Sheafor BA. 1999. Red Blood Cells: Centerpiece in the Evolution of the Vertebrate Circulatory System. Amer. Zool., 39:189-198.

Tahseen Q. 2009. Coelomocytes: Biology and Possible Immune Functions in Invertebrates with Special Remarks on Nematodes. Inter. J. Zoo, 13 p.

Tavares-Dias M, Oliveira SR. 2009. A review of the blood coagulation system of fish. R. bras. Bioci., 7(2): 205-224.

Telford MJ, Lowe CJ, Cameron CB, Ortega-Martinez O, Aronowicz J, Oliveri P, 2014. Phylogenomic analysis of echinoderm class relationships supports Asterozoa. Proc Biol Sci. 281(1786), 20140479.

Vazzana M, Celi M, Chiaramonte M, Inguglia L, Russo D, Ferrantelli V, Arizza V. 2018. Cytotoxic activity of *Holothuria tubulosa* (Echinodermata) coelomocytes. Fish & shellfish immunology, 72: 334-341.

Vazzana M, Siragusa T, Arizza V, Buscaino G, Celi M. 2015. Cellular responses and HSP70 expression during wound healing in *Holothuria tubulosa* (Gmelin, 1788). Fish & shellfish immunology, 42(2): 306-315.

Vethamany VG, Fung M (1972) The fine structure of coelomocytes of the sea urchin, *Strongylocentrotus droebachiensis* (Muller O.F.). Can. J. Zool. 50:77-81.

Williams-III CR, Chapman GB, Blake AS. 2009. Ultrastructural study of the blood cells of the beluga whale, *Delphinapterus leucas*. J Morphol 209(1):97–110.

Xing K, Yang HS, Chen MY. 2008. Morphological and ultrastructural characterization of the coelomocytes in Apostichopus japonicus. Aquatic Biology, 2(1): 85-92.

Yang J, Zhang L, Yu C. 2013. Monocyte and macrophage differentiation: circulation inflammatory monocyte as a biomarker for inflammatory diseases. Biomark. Res., 2(1):1-9.

Ziegler A, Faber C, Bartolomaeus T. 2009. Comparative morphology of the axial complex and interdependence of internal organ systems in sea urchins (Echinodermata: Echinoidea). Front Zool, *6*(1): 10.

Zimmerman LM, Vogel LA, Bowden RM. 2010. Understanding the vertebrate immune system: insights from the reptilian perspective. J. Exp. Biol., 213(5):661-671.